Universiteit
Leiden
The Netherlands

New players in zebrafish caudal fin regeneration : differential requirement for protein-tyrosine phosphatases

Hale, A.J.M.

Citation
Hale, A. J. M. (2017, October 19). *New players in zebrafish caudal fin regeneration : differential requirement for protein-tyrosine phosphatases*. Retrieved from https://hdl.handle.net/1887/58874

Version:	Not Applicable (or Unknown)
License:	Licence agreement concerning inclusion of doctoral thesis in the Institutional Repository of the University of Leiden
Downloaded from:	https://hdl.handle.net/1887/58874

Note: To cite this publication please use the final published version (if applicable).

Cover Page

Universiteit Leiden

The following handle holds various files of this Leiden University dissertation:
http://hdl.handle.net/1887/58874

Author: Hale, A.J.M.
Title: New players in zebrafish caudal fin regeneration : differential requirement for protein-tyrosine phosphatases
Issue Date: 2017-10-19

New Players in Zebrafish Caudal Fin Regeneration:

Differential Requirement for Protein-Tyrosine Phosphatases

Alexander James Hale

ISBN 978-94-6233-733-6

Printed and lay-out by Gildeprint, Enschede

Cover design: The St. George's cross of England. The two horizontal ends represent regenerating zebrafish caudal fins.

New Players in Zebrafish Caudal Fin Regeneration:

Differential Requirement for Protein-Tyrosine Phosphatases

Proefschrift

Ter verkrijging van de graad van Doctor and de Universiteit Leiden, op gezag van Rector Magnificus Prof. Mr. Carel J. J. M. Stolker volgens besluit van het College voor Promoties te verdedigen op 19 oktober 2017
klokke 10:00 uur

door

Alexander James Hale
geboren te London borough of Hillingdon, United Kingdom, in 1990

Promotiecommissie

Promotores:

Prof. Dr. J. den Hertog – Hubrecht Institute, Utrecht, The Netherlands

Prof. Dr. H. P. Spaink

Overige leden:

Prof. Dr. G.P. van Wezel

Prof. Dr. A.H. Meijer

Prof. Dr. M.K. Richardson

Prof. Dr. J. Bakkers – Hubrecht Institute, Utrecht, The Netherlands

Dr. A.F. Hurlstone – University of Manchester, Manchester, United Kingdom

"A common fallacy in much of the adverse criticism to which science is subjected today is that it claims certainty, infallibility and complete emotional objectivity. It would be more nearly true to say that it is based upon wonder, adventure and hope."

- Sir Cyril N. Hinshelwood

For my Mum and Dad

CONTENTS

Chapter 1 – General Introduction 9

Chapter 2 – Recent Advances in Understanding the Role of Protein-Tyrosine Phosphatases in Development and Disease 23

Chapter 3 – Studying Protein-Tyrosine Phosphatases in Zebrafish 51

Chapter 4 – Impaired Caudal Fin-Fold Regeneration in Zebrafish Embryos Deficient for the Tumour Suppressor Pten 77

Chapter 5 – Differential Oxidation of Protein-Tyrosine Phosphatases during Zebrafish Caudal Fin Regeneration 105

Chapter 6 – An Essential Role for Shp2-MAPK Signalling During Zebrafish Embryo Caudal Fin-Fold Regeneration 149

Chapter 7 – The Function of Shp2a during Zebrafish Embryo Caudal Fin-Fold Regeneration is Independent from the Level of Shp2a Catalytic Activity 177

Chapter 8 – Summarizing Discussion 203

Appendix – Summary 218
– Nederlandse Samenvatting 222
– List of publications 226
– Curriculum vitae 227

Chapter 1

General Introduction

Alexander James Hale[1, 2]

1. Hubrecht Institute – KNAW and University Medical Center Utrecht, Utrecht, the Netherlands
2. Institute Biology Leiden, Leiden University, Leiden, the Netherlands

PROTEIN-TYROSINE PHOSPHATASES

Protein tyrosine phosphorylation is essential for the development and survival of eukaryotic organisms due to its role in regulating many cellular processes, including proliferation, differentiation, and migration (1). The frequency and duration of tyrosine phosphorylation of proteins is maintained by the antagonistic activities of protein-tyrosine kinases (PTKs) and protein-tyrosine phosphatases (PTPs) (2). Both inactivating and activating mutations of either PTKs or PTPs have been demonstrated to lead to aberrant tyrosine phosphorylation, which results in a plethora of developmental defects and diseases (3), highlighting the importance of balanced phospho-tyrosine signalling.

In humans, the PTP superfamily consists of 125 PTPs: 116 dephosphorylate phospho-tyrosine through a mechanism involving a conserved cysteine amino acid (4, 5), whereas the other 9 genes encode PTPs that dephosphorylate phospho-tyrosine through a distinct catalytic mechanism involving either aspartic acid or histidine (6, 7). The 116 cysteine-based PTPs are divided into three subgroups based on their structure and function: the classical PTPs, dual-specificity PTPs, and the low molecular weight PTPs. The classical PTPs are further subdivided into receptor and non-receptor PTPs. Each classical PTP has at least one catalytic domain containing the catalytic cysteine (in **bold**) within a conserved signature motif (I/V)H**C**XAGXXR(S/T)G (8). The catalytic PTP domain is associated with additional domains, such as Src homology 2 (SH2) containing domains in the classical PTP SHP2, or a C2 domain in the tumour suppressor phosphatase and tensin homolog (PTEN). The associated domains vary for each PTP and contribute to the specificity, regulation, and activity of the individual PTP (5).

Post-translational modifications (PTMs) of the PTP domain or the associated domains also often regulate the localisation and activity of the PTP. Some PTPs are activated by phosphorylation. For example, tyrosine phosphorylation of RPTPα, a receptor PTP, enables interaction with substrates (9). PTP1B, a cytoplasmic PTP, is activated by phosphorylation following growth factor stimulation of the insulin receptor (12). Most classical PTPs are inhibited by oxidation of the catalytic cysteine (13), examples include PTP1B (14), SHP2 (15), RPTPα (16), and RPTPε (17), a mechanism which will be subsequently described below. Other PTMs are specific to PTPs because these PTPs contain the appropriate domains. For example, the plasma membrane localisation of PTEN is due to lysine SUMOylation in its C2 domain (18). In addition to PTMs, catalytic

activity of cytoplasmic and receptor PTPs can be regulated through the formation of homo- and hetero-dimers (19–21).

As previously mentioned, the catalytic pocket in the PTP domain of classical PTPs is highly conserved, and provides a general catalytic mechanism (22). The conserved catalytic cysteine contains a sulphur atom, which is reactive due to being a thiolate anion with electrons to spare, allowing it to act as a nucleophile and mediate reactions with more positively charged atoms. As a result, the cysteine catalyses dephosphorylation through a two-step mechanism: first, the sulphur atom of the cysteine commences nucleophilic attack on the phosphorous atom (more positively charged than the sulphur atom) of the phospho-tyrosine residue of the substrate, creating a phospho-cysteine intermediate; second, hydrolysis of this intermediate releases the inorganic phosphate and returns the cysteine to a free and active state (15, 23, 24). Several residues in and around the catalytic site of the PTP are required for correct substrate dephosphorylation: the arginine in the catalytic pocket is required for substrate binding and stabilizing the phospho-cysteine intermediate; and an aspartic acid residue in the conserved WPD loop acts as a general acid and protonates the phenolic oxygen group on the phospho-tyrosine, cleaving the phosphate off the tyrosine residue of the substrate. The same aspartic acid residue subsequently acts as a general base, in consort with a conserved glutamic acid residue, to promote hydrolysis of the phospho-cysteine intermediate (24–26).

Classical PTPs exclusively dephosphorylate phospho-tyrosine residues due to a deep catalytic pocket, preventing the shorter phospho-serine and phospho-threonine residues from reaching the catalytic cysteine (27). In addition, the residues surrounding the catalytic cysteine ensure a low dissociation constant (pKa) for the catalytic pocket, conferring catalytic activity to the cysteine in its thiolate anion form. The nature of the cysteine's catalytic activity is such that it is also highly susceptible to oxidation by reactive oxygen species (ROS), which is why most PTPs are regulated by reversible oxidation-mediated inactivation.

ROS, such as hydrogen peroxide (H_2O_2), can reversibly oxidize the catalytic cysteines of PTPs. Mild oxidation results in conversion of the sulphur atom to sulphenic acid, inactivating the PTP as the sulphur atom on the cysteine now no longer has electrons to attack the phosphorous atom of the phospho-tyrosine substrate with (28, 29). Although this state is reversible, highly oxidizing environments can oxidize the sulphur atom to sulphinic acid, or sulphonic acid, permanently inactivating the PTP (30, 31). The catalytic cysteine protects itself from irreversible oxidation by rapidly forming a

disulphide bond with another nearby cysteine (32, 33) or a sulphenyl-amide ring with a nearby nitrogen atom (14). Both states are stable, making them resistant to further oxidation, and are readily reduced back to the catalytically active form of the PTP by endogenous glutathione and thioredoxin systems (17, 34–36).

The numerous PTMs enable precise and context dependent regulation of phosphotyrosine signalling. Therefore, this establishes PTPs as fundamentally essential signalling molecules. Functional analyses of PTPs in *Drosophila*, *C. elegans*, zebrafish, and mice over the last couple of decades has resulted in overwhelming evidence in support of this fact (reviewed in chapter 2).

REGENERATION

Extensive research over the last century has revealed that there are several forms of regeneration. Epimorphic regeneration is the complete replacement of lost tissue without scar formation. The process has been studied for well over a century (37), and its progress has fostered the field of regenerative medicine. Humans harbour the ability of epimorphic regeneration early in gestation, but unfortunately rapidly lose this ability with age (38). Adult humans are capable of another form of regeneration called compensatory growth, where lost tissue is replaced through hypertrophy (increase in cell size) or hyperplasia (increase in cell number) (39), but, as the name suggests, compensatory growth does not replace the original tissue that was lost. Examples of compensatory growth include when a kidney is removed and the remaining kidney grows to twice its normal size (40), or when lobes of the liver are removed and the remaining lobes grow in size to the original size of the liver. In these examples, a new kidney or new lobes of the liver are not formed, hence distinguishing compensatory growth from epimorphic regeneration. Compensatory growth has been observed in several more organs, including the thymus (41), the beta-cells of the pancreas (42), the heart (43), the spleen (44), and the cortex of the adrenal glands (45). The most recent practical advancements in the field of regenerative medicine have been delivered by leaps in tissue engineering, enabling the fabrication of tissue grafts for transplantation to replace the lost tissue and promoting integration of host vasculature (46). Alternatively, wound healing or compensatory growth are promoted by injection of (induced pluripotent) stem cells or immune modulation (47). However, the possibility of re-activating the ability of epimorphic regeneration is what inspired

the field of regenerative medicine, and fundamental research studies organisms that retain a lifelong capacity for epimorphic regeneration with the aim of improving our understanding of this process, and in the hope of discovering the mechanism required to instigate the process in human adults.

Several vertebrate animals, including salamanders, axolotls, and zebrafish, can fully regenerate organs and appendages (48). Zebrafish (*Danio rerio*) are the most studied and fully regenerate multiple organs after injury, including the heart, retina, pancreas, spinal cord, and caudal fin (49–51). In the last decade, major strides have been made in understanding zebrafish cardiac (52–55) and spinal cord (56–58) regeneration, which has been accompanied by advances in understanding bone (59–61) and blood vessel (62, 63) regeneration.

The zebrafish caudal fin is, by far, the most studied for several reasons: it is easily accessible in embryos and adults, it occurs rapidly, it is easily observable, and loss of the caudal fin does not impair the animal (64). Following amputation of the zebrafish caudal fin, regeneration proceeds sequentially through three distinct phases: wound healing, blastema formation, and regenerative outgrowth. This process completes within two-three weeks in adults, and within 72-96 hours in embryos (65). In the first step, nearby cells migrate to cover the wound and form an apical epidermal cap (66). No proliferation occurs during this step. In the second step, the apical epidermal cap signals for the dedifferentiation of cells to form a blastema (49, 50). The fate of the dedifferentiated cells is lineage restricted, and hence the proliferative cells of the blastema demonstrate a multipotent potential (67). In the third step, the cells of the blastema proliferate and re-differentiate to replace the lost tissue of the zebrafish caudal fin.

Many advances have been made in understanding the molecular mechanisms involved in regeneration. Immediately following amputation of the caudal fin of zebrafish embryos, termed the caudal fin-fold, a large increase in H_2O_2 is observed emanating from the wound margin and extending into the tissue (68). This production of H_2O_2 may be a crucial trigger for regeneration, as inhibiting the production of the H_2O_2 completely blocks regeneration (69, 70). The function of the H_2O_2 produced following caudal fin-fold amputation is not clear, but has been shown to recruit immune cells to the wound margin (68, 71). ROS are recognized as crucial second messenger molecules that, through the coordination of multiple intracellular signalling pathways, instigate appropriate cellular responses to stress (72–74). Furthermore, ROS have been demonstrated to regulate PTP activity in cancer (75), the migration of

cells (76), and insulin signalling and diabetes (77, 78). To date, many genes have been implicated in the regenerative process, including serine/threonine phosphatases (79, 80), and most up-regulated transcripts have a role in metabolism or signalling (81). Multiple signalling pathways have been experimentally validated by creating genetic knock-out or overexpression mutants. Signalling pathways shown to be essential for regeneration include fibroblast growth factor (82, 83), sonic hedgehog (84, 85), bone morphogenetic protein (86, 87), Wnt (88, 89), Notch (90–92), and phosphoinositide 3-kinase (PI3K) (93–95).

The signalling pathways often have a role in multiple aspects of the regeneration process and this is also reflected by the fluctuation of gene expression during different phases of the regenerative process (80), demonstrating a need for precise spatio-temporal regulation of multiple signalling pathways. The genes identified implicate almost every cellular process, such as mitosis, protein degradation, migration, and metabolic processes, highlighting the complexity of the molecular and cellular processes required for regeneration, and adding to the challenge of understanding this extremely complex process.

SCOPE OF THIS THESIS

The work described in this thesis aims to implicate PTPs as essential signalling molecules for the regeneration of the zebrafish embryo caudal fin-fold. The production of ROS immediately following zebrafish caudal fin-fold amputation likely stimulates many changes in protein activity and cell behaviour. We hypothesized that, due to the sensitivity of PTPs to oxidation, PTPs would become oxidized in response to caudal fin amputation. We further used *pten* and *ptpn11* knock-out zebrafish to demonstrate the importance of PTP activity in the process of regeneration.

Amputation of the zebrafish caudal fin hence represents an opportunity to study PTP oxidation *in vivo*, under physiologically relevant conditions. PTP oxidation by ROS has been extensively established through the treatment of PTPs in cells or *in vitro* with exogenous H_2O_2. However, the difficulty of measuring intracellular ROS concentrations has hindered ascertaining if PTPs become oxidized *in vivo* by endogenous ROS levels. By combining chemical modifications of reduced and reversibly oxidized thiols, the use of an antibody specific for irreversibly oxidized PTPs, and state-of-the art mass

spectrometry, we investigate the oxidation of PTPs in zebrafish tissue directly following amputation.

In addition, zebrafish embryos are powerful tools for delineating the specific role of proteins through the ability to create knock-outs and re-introduce mutant proteins. Their transparency enables easy imaging, and drug screens are easy to perform because they are oviparous. We used genetic *pten* and *ptpn11* knock-out zebrafish, deficient for Pten and Shp2 respectively, and by re-introducing mutant proteins that are catalytically inactive, unable to bind substrates, or have altered sensitivity to oxidation, we demonstrate the role of Pten and Shp2 in the regenerative process. Using inhibitors of the signalling pathways Pten and Shp2 are involved in, we shed light on the signalling roles of Pten and Shp2 during zebrafish caudal fin-fold regeneration.

OUTLINE OF THIS THESIS

Chapter 2 provides a review of the recent advances made to understand the role of PTPs in embryonic development. We provide an overview of developmental processes dependent on receptor and non-receptor PTPs in a variety of model organisms. We highlight the requirement for balanced phospho-tyrosine signalling and provide a few examples of diseases that result from mutations in PTPs.

Chapter 3 describes some of the methods used in the experiments within this thesis. We detail how the micro-injection of zebrafish embryos is performed to introduce mutant proteins. Moreover, we detail how the zebrafish embryonic caudal fin-fold amputations are performed, as well as how to prepare embryonic zebrafish tissue for detection of protein by immunoblotting. Additionally, we provide tips on crucial steps and alternatives.

Chapter 4 describes the importance of the tumour suppressor Pten in zebrafish caudal fin-fold regeneration. We show that *pten* knock-out zebrafish embryos do not regenerate their caudal fin-folds, and that regeneration is rescued by re-introducing wild-type Pten, but not catalytically inactive mutant Pten. Blastema formation occurs normally in the caudal fin-folds of Pten deficient zebrafish embryos, but proliferation during regenerative outgrowth is arrested. Zebrafish embryos deficient for Pten also display elevated Akt phosphorylation, and their regeneration is rescued when treated with the PI3K inhibitor LY294002.

Chapter 5 unveils differential oxidation of PTPs following amputation of adult zebrafish caudal fins. Adult wild-type zebrafish caudal fins were lysed in reducing or alkylating buffers to enable detection of all PTPs or the oxidized PTPs following amputation of the caudal fin respectively. Using an antibody specific for the conserved oxidized catalytic site of PTPs and identification by liquid chromatography mass spectrometry, we identified 33 PTPs in the zebrafish caudal fin and 8 were reversibly oxidized 40 minutes after caudal fin amputation. Zebrafish embryos deficient for functional Shp2, which is oxidized, do not regenerate, whilst zebrafish embryos deficient for RPTPα, which is not oxidized, regenerate normally.

Chapter 6 describes the importance of the PTP Shp2 in zebrafish caudal fin-fold regeneration, demonstrating that both catalytic activity and the SH2 domain of Shp2a are required for its function in caudal fin-fold regeneration. We show that *ptpn11* knock-out zebrafish embryos, lacking functional Shp2, do not regenerate their caudal fin-fold. Whereas expression of catalytically inactive Shp2a or a SH2 domain mutant of Shp2a did not rescue caudal fin-fold regeneration of *ptpn11* knock-out zebrafish embryos, expression of a C-terminal domain mutant of Shp2a did rescue caudal fin-fold regeneration. Compared to sibling zebrafish embryos expressing Shp2a, proliferation during regenerative outgrowth is arrested in *ptpn11* knock-out zebrafish embryos, despite normal blastema formation. Interestingly, zebrafish embryos deficient for Shp2 display reduced mitogen activated protein kinase (MAPK) phosphorylation, and inhibition of MAPK in wild-type zebrafish embryos also inhibits regeneration and arrests proliferation during regenerative outgrowth.

Chapter 7 covers structure and function analysis of Shp2a in zebrafish caudal fin-fold regeneration. We further assessed the role of Shp2a by mutating the back-door cysteines of Shp2a, which have previously been proposed to have a role in protecting the catalytic cysteine from irreversible oxidation-mediated inactivation. We show that the back-door cysteine mutants of Shp2a have reduced catalytic activity *in vitro* and experience enhanced oxidation in response to ROS in cells. Surprisingly, expressing the back-door cysteine mutants of Shp2a in *ptpn11* knock-out zebrafish embryos, lacking functional Shp2, rescued zebrafish caudal fin-fold regeneration. Considering the reduced catalytic activity of the back-door cysteine mutants of Shp2a, we also investigated the role the level of Shp2a catalytic activity has in its function in caudal fin-fold regeneration. Interestingly, expression of two known mutants of Shp2a with increased (D61G) or reduced (A462T) catalytic activity in *ptpn11* knock-out zebrafish embryos rescued caudal fin-fold regeneration to a similar extent. Collectively, our

results suggest that the level of Shp2a catalytic activity does not affect the function of Shp2a in the regenerative outgrowth of the caudal fin-fold.

Chapter 8 summarizes the discussions of **Chapters 4-7**, and proposes future research that will address the outstanding questions that results from the work described in this thesis. Finally, we provide some perspectives on the field of regeneration research and regenerative medicine.

REFERENCES

1. Hunter T (2009) Tyrosine phosphorylation: thirty years and counting. *Curr Opin Cell Biol* 21(2):140–146.
2. Hunter T (1995) Protein kinases and phosphatases: The Yin and Yang of protein phosphorylation and signaling. *Cell* 80(2):225–236.
3. Blume-Jensen P, Hunter T (2001) Oncogenic kinase signalling. *Nature* 411(6835):355–365.
4. Alonso A, Pulido R (2016) The extended human PTPome: A growing tyrosine phosphatase family. *FEBS J* 283(8):1404–1429.
5. Tonks NK (2013) Protein tyrosine phosphatases - From housekeeping enzymes to master regulators of signal transduction. *FEBS J* 280(2):346–378.
6. Rayapureddi JP, et al. (2003) Eyes absent represents a class of protein tyrosine phosphatases. *Nature* 426(6964):295–298.
7. Tootle TL, et al. (2003) The transcription factor Eyes absent is a protein tyrosine phosphatase. *Nature* 426(6964):299–302.
8. Fischer EH, Charbonneau H, Tonks NK (1991) Protein tyrosine phosphatases: a diverse family of intracellular and transmembrane enzymes. *Science* 253(5018):401–406.
9. den Hertog J, Tracy S, Hunter T (1994) Phosphorylation of receptor protein-tyrosine phosphatase alpha on Tyr789, a binding site for the SH3-SH2-SH3 adaptor protein GRB-2 in vivo. *EMBO J* 13(13):3020–3032.
10. Tracy S, van der Geer P, Hunter T (1995) The receptor-like protein-tyrosine phosphatase, RPTP alpha, is phosphorylated by protein kinase C on two serines close to the inner face of the plasma membrane. *J Biol Chem* 270(18):10587–10594.
11. Chen SC, Khanna RS, Bessette DC, Samayawardhena LA, Pallen CJ (2009) Protein tyrosine phosphatase-α complexes with the IGF-I receptor and undergoes IGF-I-stimulated tyrosine phosphorylation that mediates cell migration. *Am J Physiol - Cell Physiol* 297(1):C133 LP-C139.
12. Dadke S, Kusari A, Kusari J (2001) Phosphorylation and activation of protein tyrosine phosphatase (PTP) 1B by insulin receptor. *Mol Cell Biochem* 221(1–2):147–154.
13. Östman A, Frijhoff J, Sandin A, Böhmer F-D (2011) Regulation of protein tyrosine phosphatases by reversible oxidation. *J Biochem* 150(4):345–56.
14. Salmeen A, et al. (2003) Redox regulation of protein tyrosine phosphatase 1B involves a sulphenyl-amide intermediate. *Nature* 423(6941):769–773.
15. Meng TC, Fukada T, Tonks NK (2002) Reversible oxidation and inactivation of protein tyrosine phosphatases in vivo. *Mol Cell* 9(2). doi:10.1016/s1097-2765(02)00445-8.
16. Yang J, et al. (2007) Reversible oxidation of the membrane distal domain of receptor PTP alpha is mediated by a cyclic sulfenamide. *Biochemistry* 46(3). doi:10.1021/bi061546m.
17. Ostman A, et al. (2011) Regulation of protein tyrosine phosphatases by reversible oxidation. *J Biochem* 150(4):345–56.
18. Gonzalez-Santamaria J, et al. (2012) Regulation of the tumor suppressor PTEN by SUMO. *Cell Death Dis* 3:e393.
19. Toledano-Katchalski H, et al. (2003) Dimerization in vivo and inhibition of the nonreceptor form of protein tyrosine phosphatase epsilon. *Mol Cell Biol* 23(15):5460–5471.
20. Heinrich F, et al. (2015) The PTEN tumor suppressor forms homodimers in solution. *Structure* 23(10):1952–1957.
21. Jiang G, et al. (1999) Dimerization inhibits the activity of receptor-like protein-tyrosine phosphatase-α. *Nature* 401(6753):606–610.
22. Tonks NK, Neel BG (2001) Combinatorial control of the specificity of protein tyrosine phosphatases. *Curr Opin Cell Biol* 13(2):182–195.

23. Pot DA, Dixon JE (1992) A thousand and two protein tyrosine phosphatases. *Biochim Biophys Acta - Mol Cell Res* 1136(1):35–43.
24. Zhang ZY, Wang Y, Dixon JE (1994) Dissecting the catalytic mechanism of protein-tyrosine phosphatases. *Proc Natl Acad Sci U S A* 91(5):1624–1627.
25. Zhang ZY, Maclean D, McNamara DJ, Sawyer TK, Dixon JE (1994) Protein tyrosine phosphatase substrate specificity: size and phosphotyrosine positioning requirements in peptide substrates. *Biochemistry* 33(8):2285–2290.
26. Lohse DL, Denu JM, Santoro N, Dixon JE (1997) Roles of aspartic acid-181 and serine-222 in intermediate formation and hydrolysis of the mammalian protein-tyrosine-phosphatase PTP1. *Biochemistry* 36(15):4568–4575.
27. Barford D, Flint AJ, Tonks NK (1994) Crystal structure of human protein tyrosine phosphatase 1B. *Science* 263(5152):1397–1404.
28. Klomsiri C, Karplus PA, Poole LB (2011) Cysteine-based redox switches in enzymes. *Antioxid Redox Signal* 14(6):1065–77.
29. Groen A, et al. (2005) Differential oxidation of protein-tyrosine phosphatases. *J Biol Chem* 280(11):10298–304. Epub 2004 Dec 28.
30. Lo Conte M, Carroll KS (2013) The Chemistry of Thiol Oxidation and Detection. *Oxidative Stress Redox Regul*:1–42.
31. Lo Conte M, Carroll KS (2013) The redox biochemistry of protein sulfenylation and sulfinylation. *J Biol Chem* 288(37):26480–26488.
32. Sone M, Kishigami S, Yoshihisa T, Ito K (1997) Roles of disulfide bonds in bacterial alkaline phosphatase. *J Biol Chem* 272(10):6174–6178.
33. Cumming RC, et al. (2004) Protein disulfide bond formation in the cytoplasm during oxidative stress. *J Biol Chem* 279(21):21749–21758.
34. Dagnell M, et al. (2013) Selective activation of oxidized PTP1B by the thioredoxin system modulates PDGF-beta receptor tyrosine kinase signaling. *Proc Natl Acad Sci U S A* 110(33):13398–13403.
35. Lee SR, et al. (2002) Reversible inactivation of the tumor suppressor PTEN by H2O2. *J Biol Chem* 277:20336–20342.
36. Chen CY, Willard D, Rudolph J (2009) Redox regulation of SH2-domain-containing protein tyrosine phosphatases by two backdoor cysteines. *Biochemistry* 48(6):1399–1409.
37. MORGAN TH (1901) REGENERATION AND LIABILITY TO INJURY. *Science (80-)* 14(346):235 LP-248.
38. Gurtner GC, Werner S, Barrandon Y, Longaker MT (2008) Wound repair and regeneration. *Nature* 453(7193):314–321.
39. Wilt F Growth. *Britannica*. Available at: https://www.britannica.com/science/growth-biology [Accessed May 7, 2017].
40. Malt RA (1969) Compensatory growth of the kidney. *N Engl J Med* 280(26):1446–1459.
41. Marmorston-Gottesman J, Jaffe HL (1925) COMPENSATORY HYPERTROPHY OF THE THYMUS GLAND IN THE RAT. *J Exp Med* 42(3):413–418.
42. Bonner-Weir S, Deery D, Leahy JL, Weir GC (1989) Compensatory growth of pancreatic beta-cells in adult rats after short-term glucose infusion. *Diabetes* 38(1):49–53.
43. Drenckhahn J-D, et al. (2008) Compensatory Growth of Healthy Cardiac Cells in the Presence of Diseased Cells Restores Tissue Homeostasis during Heart Development. *Dev Cell* 15(4):521–533.
44. CAMERON GR, RHEE KS (1959) Compensatory hypertrophy of the spleen: a study of splenic growth. *J Pathol Bacteriol* 78:335–349.
45. Baddour JA, Sousounis K, Tsonis PA (2012) Organ repair and regeneration: an overview. *Birth Defects Res C Embryo Today* 96(1):1–29.

46. Vacanti JP, Langer R (1999) Tissue engineering: the design and fabrication of living replacement devices for surgical reconstruction and transplantation. *Lancet* 354:SI32-I34.
47. Mao AS, Mooney DJ (2015) Regenerative medicine: Current therapies and future directions. *Proc Natl Acad Sci* 112(47):14452–14459.
48. Tanaka E, Reddien PW (2011) The cellular basis for animal regeneration. *Dev Cell* 21(1):172–185.
49. Poss KD, Keating MT, Nechiporuk A (2003) Tales of regeneration in zebrafish. *Dev Dyn* 226(2):202–210.
50. Pfefferli C, Jaźwińska A (2015) The art of fin regeneration in zebrafish. *Regeneration* 2(2):72–83.
51. Moss JB, et al. (2009) Regeneration of the pancreas in adult zebrafish. *Diabetes* 58(8):1844–1851.
52. Bakkers J (2011) Zebrafish as a model to study cardiac development and human cardiac disease. *Cardiovasc Res* 91(2):279–288.
53. Wu C-C, et al. (2017) Spatially Resolved Genome-wide Transcriptional Profiling Identifies BMP Signaling as Essential Regulator of Zebrafish Cardiomyocyte Regeneration. *Dev Cell* 36(1):36–49.
54. Jopling C, et al. (2010) Zebrafish heart regeneration occurs by cardiomyocyte dedifferentiation and proliferation. *Nature* 464(7288):606–609.
55. Poss KD, Wilson LG, Keating MT (2002) Heart regeneration in zebrafish. *Science* 298(5601):2188–2190.
56. Hui SP, Dutta A, Ghosh S (2010) Cellular response after crush injury in adult zebrafish spinal cord. *Dev Dyn* 239(11):2962–2979.
57. Strand NS, et al. (2016) Wnt/β-catenin signaling promotes regeneration after adult zebrafish spinal cord injury. *Biochem Biophys Res Commun* 477(4):952–956.
58. Ghosh S, Hui SP (2016) Regeneration of Zebrafish CNS: Adult Neurogenesis. *Neural Plast* 2016:5815439.
59. Stewart S, Gomez AW, Armstrong BE, Henner A, Stankunas K (2014) Sequential and opposing activities of Wnt and BMP coordinate zebrafish bone regeneration. *Cell Rep* 6(3). doi:10.1016/j.celrep.2014.01.010.
60. Geurtzen K, et al. (2014) Mature osteoblasts dedifferentiate in response to traumatic bone injury in the zebrafish fin and skull. *Development* 141(11):2225–2234.
61. Knopf F, et al. (2011) Bone regenerates via dedifferentiation of osteoblasts in the zebrafish fin. *Dev Cell* 20(5):713–724.
62. Thorimbert V, et al. (2015) Bone morphogenetic protein signaling promotes morphogenesis of blood vessels, wound epidermis, and actinotrichia during fin regeneration in zebrafish. *FASEB J* 29(10):4299–4312.
63. Huang CC, Lawson ND, Weinstein BM, Johnson SL (2003) reg6 is required for branching morphogenesis during blood vessel regeneration in zebrafish caudal fins. *Dev Biol* 264(1):263–274.
64. Akimenko M-A, Mari-Beffa M, Becerra J, Geraudie J (2003) Old questions, new tools, and some answers to the mystery of fin regeneration. *Dev Dyn* 226(2):190–201.
65. Kawakami A, Fukazawa T, Takeda H (2004) Early fin primordia of zebrafish larvae regenerate by a similar growth control mechanism with adult regeneration. *Dev Dyn* 231(4):693–9.
66. Poleo G, Brown CW, Laforest L, Akimenko MA (2001) Cell proliferation and movement during early fin regeneration in zebrafish. *Dev Dyn* 221(4):380–390.
67. Tu S, Johnson SL (2011) Fate restriction in the growing and regenerating zebrafish fin. *Dev Cell* 20(5):725–732.

68. Niethammer P, Grabher C, Look a T, Mitchison TJ (2009) A tissue-scale gradient of hydrogen peroxide mediates rapid wound detection in zebrafish. *Nature* 459(7249):996–9.

69. Love NR, et al. (2013) Amputation-induced reactive oxygen species are required for successful Xenopus tadpole tail regeneration. *Nat Cell Biol* 15(2):222–8. doi: 10.1038/ncb2659. Epub 2013 Jan 13.

70. Yoo SK, Freisinger CM, LeBert DC, Huttenlocher A (2012) Early redox, Src family kinase, and calcium signaling integrate wound responses and tissue regeneration in zebrafish. *J Cell Biol* 199(2):225–34. doi: 10.1083/jcb.201203154. Epub 2012 Oct.

71. Pase L, et al. (2012) Neutrophil-delivered myeloperoxidase dampens the hydrogen peroxide burst after tissue wounding in zebrafish. *Curr Biol* 22(19):1818–1824.

72. Finkel T (2011) Signal transduction by reactive oxygen species. *J Cell Biol* 194(1):7–15.

73. Ray PD, Huang BW, Tsuji Y (2012) Reactive oxygen species (ROS) homeostasis and redox regulation in cellular signaling. *Cell Signal* 24(5):981–90. doi: 10.1016/j.cellsig.2012.01.008. Epub 2.

74. Thannickal VJ, Fanburg BL (2000) Reactive oxygen species in cell signaling. *Am J Physiol Lung Cell Mol Physiol* 279(6):L1005-28.

75. Liou M-Y, Storz P (2010) *Reactive oxygen species in cancer* doi:10.3109/10715761003667554. Reactive.

76. Frijhoff J, Dagnell M, Godfrey R, Ostman A (2014) Regulation of protein tyrosine phosphatase oxidation in cell adhesion and migration. *Antioxid Redox Signal* 20(13):1994–2010.

77. Meng TC, Buckley DA, Galic S, Tiganis T, Tonks NK (2004) Regulation of insulin signaling through reversible oxidation of the protein-tyrosine phosphatases TC45 and PTP1B. *J Biol Chem* 279(36):37716–37725.

78. Gurzov EN, et al. (2014) Hepatic oxidative stress promotes insulin-STAT-5 signaling and obesity by inactivating protein tyrosine phosphatase N2. *Cell Metab* 20(1):85–102.

79. Padhi BK, et al. (2004) Screen for genes differentially expressed during regeneration of the zebrafish caudal fin. *Dev Dyn* 231(3):527–541.

80. Saxena S, et al. (2012) Proteomic Analysis of Zebrafish Caudal Fin Regeneration. *Mol Cell Proteomics* 11(6):M111.014118-M111.014118.

81. Yoshinari N, Ishida T, Kudo A, Kawakami A (2009) Gene expression and functional analysis of zebrafish larval fin fold regeneration. *Dev Biol* 325(1):71–81.

82. Wills AA, Kidd AR, Lepilina A, Poss KD (2008) Fgfs control homeostatic regeneration in adult zebrafish fins. *Development* 135(18):3063–3070.

83. Poss KD, et al. (2000) Roles for Fgf signaling during zebrafish fin regeneration. *Dev Biol* 222(2):347–58.

84. Quint E, et al. (2002) Bone patterning is altered in the regenerating zebrafish caudal fin after ectopic expression of sonic hedgehog and bmp2b or exposure to cyclopamine. *Proc Natl Acad Sci U S A* 99(13):8713–8718.

85. Singh B, et al. (2015) Hedgehog Signaling during Appendage Development and Regeneration. *Genes (Basel)* 6(2):417–435.

86. Smith a., Avaron F, Guay D, Padhi BK, Akimenko M a. (2006) Inhibition of BMP signaling during zebrafish fin regeneration disrupts fin growth and scleroblasts differentiation and function. *Dev Biol* 299(2):438–54. Epub 2006 Aug 10.

87. Christen B, Rodrigues AM, Monasterio MB, Roig CF, Izpisua Belmonte JC (2012) Transient downregulation of Bmp signalling induces extra limbs in vertebrates. *Development* 139(14):2557–2565.

88. Wehner D, et al. (2014) Wnt/β-catenin signaling defines organizing centers that orchestrate growth and differentiation of the regenerating zebrafish caudal fin. *Cell Rep* 6(3):467–481.

89. Kawakami Y, et al. (2006) Wnt/β-catenin signaling regulates vertebrate limb regeneration. *Genes Dev* (858):3232–3237.

90. Münch J, González-Rajal A, de la Pompa JL (2013) Notch regulates blastema proliferation and prevents differentiation during adult zebrafish fin regeneration. *Development* 140(7):1402–11.

91. Grotek B, Wehner D, Weidinger G (2013) Notch signaling coordinates cellular proliferation with differentiation during zebrafish fin regeneration. *Development* 140(7):1412–23. doi: 10.1242/dev.087452. Epub 2013 Mar 5.

92. Kametani Y, Chi NC, Stainier DYR, Takada S (2015) Notch signaling regulates venous arterialization during zebrafish fin regeneration. *Genes to Cells* 20(5). doi:10.1111/gtc.12234.

93. Nakatani Y, Nishidate M, Fujita M, Kawakami A, Kudo A (2008) Migration of mesenchymal cell fated to blastema is necessary for fish fin regeneration. *Dev Growth Differ* 50(2):71–83.

94. Hirose K, Shiomi T, Hozumi S, Kikuchi Y (2014) Mechanistic target of rapamycin complex 1 signaling regulates cell proliferation, cell survival, and differentiation in regenerating zebrafish fins. *BMC Dev Biol* 14:42.

95. Rojas-Muñoz A, et al. (2009) ErbB2 and ErbB3 regulate amputation-induced proliferation and migration during vertebrate regeneration. *Dev Biol* 327(1):177–190.

Chapter 2

Recent Advances in Understanding the Role of Protein-Tyrosine Phosphatases in Development and Disease

Alexander J. Hale[1,2,*], Eline ter Steege[1,*] and Jeroen den Hertog[1,2]

1. Hubrecht Institute – KNAW and University Medical Center Utrecht, Utrecht, the Netherlands
2. Institute Biology Leiden, Leiden University, Leiden, the Netherlands
** These authors contributed equally*

SUMMARY

Protein-tyrosine phosphatases (PTPs) remove phosphate groups from tyrosine residues, and thereby propagate or inhibit signal transduction, and hence influence cellular processes such as cell proliferation and differentiation. The importance of tightly controlled PTP activity is reflected by the numerous mechanisms employed by the cell to control PTP activity, including a variety of post-translational modifications, and restricted subcellular localization. This review highlights the strides made in the last decade and discusses the important role of PTPs in key aspects of embryonic development: the regulation of stem cell self-renewal and differentiation, gastrulation and somitogenesis during early embryonic development, osteogenesis, and angiogenesis. The tentative importance of PTPs in these processes is highlighted by the diseases that present upon aberrant activity.

1. INTRODUCTION

The Hubrecht Institute has a long history of signal transduction research and how signalling affects developmental biology and stem cells. More than a quarter of a century ago, den Hertog cloned genes encoding PTPs and ever since, the function of PTPs in development and disease has been studied at the Hubrecht Institute. Recent progress in our understanding of PTP function resulting from research at the Hubrecht and elsewhere will be discussed here.

The phosphorylation and de-phosphorylation of proteins is an essential mechanism by which cellular signalling is regulated. Proteins are phosphorylated on tyrosine residues by protein-tyrosine kinases (PTKs) and de-phosphorylated by protein-tyrosine phosphatases (PTPs). PTPs have demonstrated to be important regulators of fundamental cellular processes, including proliferation, differentiation, and cell-cell adhesion.

Since the purification of the first PTP, PTP1B, in 1988 (1), 125 PTPs have been identified in the human genome, constituting an enzyme superfamily divided into three groups: the classical PTPs, dual-specificity PTPs, and the low molecular weight PTPs (2, 3). The classical PTPs are further subdivided into receptor and non-receptor PTPs (**Table 1** and **Fig. 1**). Each PTP holds one or two catalytic domains with a conserved signature motif (I/V)H**C**XAGXXR(S/T)G containing the catalytic cysteine (in **bold**) essential for catalysing the removal of a phosphate group from a phospho-tyrosine residue. The domains associated with the catalytic domains of PTPs are diverse and contribute to their specificity, regulation, and activity (3). PTPs are often regulated by post-translational modifications, including phosphorylation and oxidation. For example, RPTPα and SHP2 are activated by phosphorylation of two serine residues and a tyrosine residue respectively (4). Most classical PTPs are inhibited by reversible oxidation of the cysteine residue in the catalytic site, and the unique micro-environment of the catalytic site determines the sensitivity of each PTP to oxidation-mediated inhibition (5). The activity of RPTPs is also regulated by dimerization, where activation or inactivation is determined by the exact orientation of the dimer. In addition, post-translational modifications alter the status of the RPTP dimer, and thereby influence catalytic activity (4).

In the last decades, research has revealed an important role for PTPs in development. Moreover, mutations in PTPs, which lead to aberrant PTP activity, result in disease or contribute to disease progression. This review will focus on the recent advances in understanding the role of PTPs in stem cell self-renewal and differentiation, gastrulation and somitogenesis during early embryonic development, osteogenesis, and angiogenesis. Finally, disease phenotypes correlated with mutations in PTPs will be discussed.

Table. 1. List of classical protein-tyrosine phosphatases divided into receptor PTPs and non-receptor, cytoplasmic, PTPs. Human (*Homo sapiens*), Mouse (*Mus musculus*), and Zebrafish (*Danio rerio*) orthologues are listed.

	Human		Mouse		Zebrafish	
	GENE	PROTEIN	*Gene*	PROTEIN	*gene*	Protein
Cytoplasmic	*PTPN1*	PTP1B	*Ptpn1*	PTP1B	*ptpn1*	Ptp1b
	PTPN2	TC-PTP	*Ptpn2*	TC-PTP	*ptpn2a*	Tc-ptpa
					ptpn2b	Tc-ptpb
	PTPN3	PTPH1	*Ptpn3*	PTPH1	*ptpn3*	Ptp-h1
	PTPN4	PTP-MEG1	*Ptpn4*	PTP-MEG1	*ptpn4a*	Meg1a
					ptpn4b	Meg1b
	PTPN5	STEP	*Ptpn5*	STEP	*ptpn5*	Step
	PTPN6	SHP1	*Ptpn6*	SHP1	*ptpn6*	Shp1
	PTPN7	HE-PTP	*Ptpn7*	HE-PTP	*ptpn7*	He-ptp
	PTPN9	PTP-MEG2	*Ptpn9*	PTP-MEG2	*ptpn9a*	Meg2a
					ptpn9b	Meg2b
	PTPN11	SHP2	*Ptpn11*	SHP2	*ptpn11a*	Shp2a
					ptpn11b	Shp2b
	PTPN12	PTP-PEST	*Ptpn12*	PTP-PEST	*ptpn12*	Pest
	PTPN13	PTP-BAS	*Ptpn13*	PTP-BAS	*ptpn13*	Ptp-bas
	PTPN14	PTPD2/PEZ	*Ptpn14*	PTPD2/PEZ	*ptpn14*	Pez
	PTPN18	PTP-HSCF	*Ptpn18*	PTP-HSCF	*ptpn18*	Ptp-hscf
	PTPN20	PTPN20	*Ptpn20*	PTPN20	*ptpn20*	Ptpn20
	PTPN21	PTP-D1	*Ptpn21*	PTP-D1	*ptpn21*	Ptp-d1
	PTPN22	LYP	*Ptpn22*	LYP	*ptpn22*	Lyp
	PTPN23	HD-PTP	*Ptpn23*	HD-PTP	*ptpn23a*	Hd-ptpa
					ptpn23b	Hd-ptpb
Receptor	*PTPRC*	CD45	*Ptprc*	CD45	*ptprc*	Cd45
	PTPRM	RPTPμ	*Ptprm*	RPTPμ	*ptprm*	Rptpμ
	PTPRK	RPTPκ	*Ptprk*	RPTPκ	*ptprk*	Rptpκ
	PTPRT	RPTPρ	*Ptprt*	RPTPρ	*ptprt*	Rptpρ
	PTPRU	RPTPʎ	*Ptpru*	RPTPʎ	*ptprua*	RptpʎaRptpʎb
					ptprub	
	PTPRF	LAR	*Ptprf*	LAR	*ptprfa*	LARa
					ptprfb	LARb
	PTPRS	RPTPσ	*Ptprs*	RPTPσ	*ptprsa*	Rptpσa
					ptprsb	Rptpσb
	PTPRD	RPTPδ	*Ptprd*	RPTPδ	*ptprda*	Rptpδa
					ptprdb	Rptpδb
	PTPRB	RPTPβ	*Ptprb*	RPTPβ	*ptprb*	Rptpβ
	PTPRJ	DEP-1	*Ptprj*	DEP-1	*ptprja*	Dep-1a
					ptprjb	Dep-1b
	PTPRH	SAP1	*Ptprh*	SAP1	*ptprh*	Sap1
	PTPRO	RPTPO	*Ptpro*	RPTPO	*ptpro*	Rptpo
	PTPRQ	RPTPQ/PTPS31	*Ptpro*	RPTPQ/PTPS31	*ptprq*	Rptpq
	PTPRA	RPTPα	*Ptpra*	RPTPα	*ptpra*	Rptpα
	PTPRE	RPTPε	*Ptpre*	RPTPε	*ptprea*	Rptpεa
					ptpreb	Rptpεb
	PTPRZ	RPTPζ	*Ptprz*	RPTPζ	*ptprza*	Rptpζa
					ptprzb	Rptpζb
	PTPRG	RPTPγ	*Ptprg*	RPTPγ	*ptprga*	Rptpγa
					ptprgb	Rptpγb
	PTPRR	PC-PTP	*Ptprr*	PC-PTP	*ptprr*	Rptpr
	PTPRN	IA2	*Ptprn*	IA2	*ptprna*	Rptpna
					ptprnb	Rptpnb
	PTPRN2	IA2β	*Ptprn2*	IA2β	*ptprn2*	Rptpn2

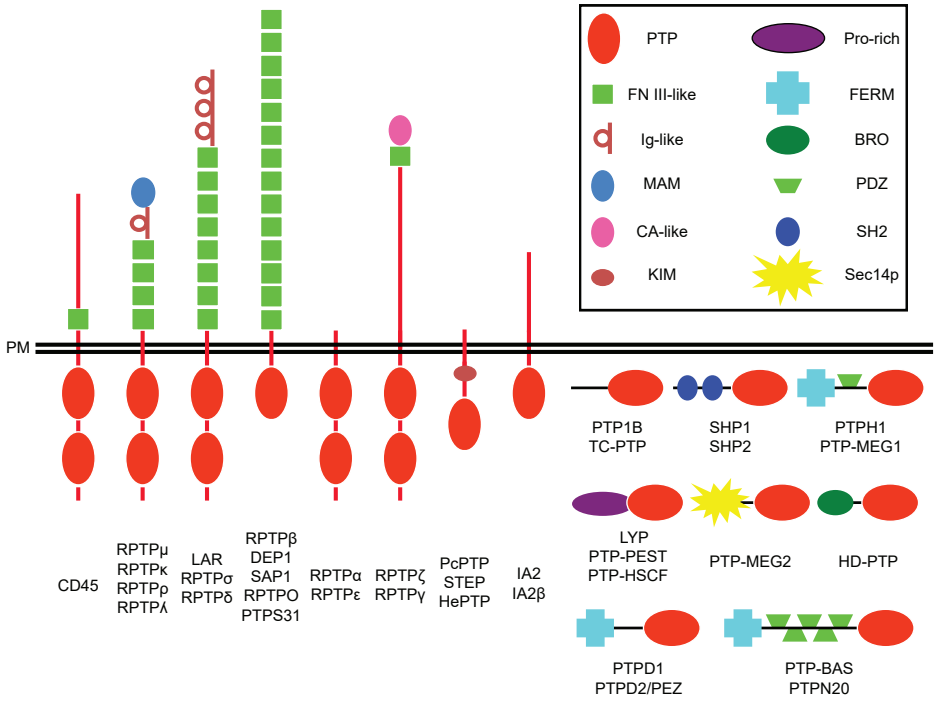

Fig. 1. Family of classical protein-tyrosine phosphatases divided into receptor PTPs and non-receptor, cytoplasmic, PTPs. PTPs are clustered based on their functional domains, indicated in the boxed legend (top right).

2. PTPS IN THE REGULATION OF STEM CELL SELF-RENEWAL AND DIFFERENTIATION

Stem cells are able to proliferate and maintain their pluripotent capacity by self-renewal, and are at the origin of all cell types. In response to key stimuli, stem cells forfeit their pluripotency and differentiate into tissue specific cell lineages. PTPs are involved in the regulation of stem cell fate via various signalling pathways (reviewed in (6)). Here, we will discuss the importance of PTP regulation in stem cell fate and differentiation during development.

2.1 Embryonic stem cells

Several PTPs have been found to be important in determining embryonic stem cell (ESC) fate. SHP2, a cytoplasmic PTP encoded by the *PTPN11* gene and containing two SRC homology 2 (SH2) domains, is required in the initial stages of mouse and human

embryonic development for the differentiation of ESCs into the three germ layers (7, 8). In mice, it has been reported that SHP2 promotes ESC differentiation into hemangioblasts, multipotent precursor cells that differentiate into cells of the hematopoietic cell lineage and endothelial cells (8). SHP2 has a crucial role in adipogenesis, as SHP2 deficiency supresses differentiation of ESCs to adipocytes (9), and of pre-adipocytes to adipocytes (10).

Phosphatase and Tensin Homolog (PTEN) belongs to the PTP superfamily and is a dual specificity phosphatase with roles in cell motility, metabolism, and polarity (11). PTEN negatively regulates AKT, a major instigator of cellular processes such as proliferation, migration, and cell survival. PTEN de-phosphorylation of phosphatidylinositol 3,4,5-triphosphate (PIP3) to phosphatidylinositol 4,5-bisphosphate (PIP2) inhibits the phosphorylation cascade that activates AKT. Knockdown of PTEN in human ESCs results in increased proliferation, survival, and self-renewal. In addition, ESC differentiation into neuro-ectoderm, rather than cells of the other germ layers, increases (12). This indicates that PTEN is not solely important for ESC growth, but is also required for proper differentiation of ESCs into all three lineages.

Protein-tyrosine phosphatase 1B (PTP1B), encoded by the *PTPN1* gene, has an important role in determining the mesendodermal fate of ESCs. Overexpression of PTP1B results in ESC differentiation towards a mesendodermal fate, whilst PTP1B knockdown leads to differentiation towards a neuro-ectodermal fate (13).

2.2 Hematopoietic stem cells

PTPs are important for the regulation of hematopoietic stem cells (HSCs). SHP2 is essential for the maintenance of the HSC pool and differentiation into lineages of the hematopoietic system. Loss of *Ptpn11* in the HSCs of mice leads to loss of almost all HSCs and progenitors of hematopoietic cell lineages, and mortality within 6 to 8 weeks post birth (14). Whilst knockdown of SHP2 in human $CD34^+$ cells results in reduced proliferation and differentiation into hematopoietic cell lineages *in vivo,* gain-of-function mutations in SHP2 result in aberrant differentiation and proliferation profiles of HSCs (15–18).

In contrast, T-cell PTP (TC-PTP), encoded by *PTPN2* and so named because it was originally cloned from T-cells and is highly expressed in cells of the hematopoietic system, negatively regulates HSC self-renewal and differentiation. Knockout of *Ptpn2* or pharmacological inhibition of TC-PTP increases the number of stem and progenitor cells in mice (19). RPTPσ, encoded by *PTPRS*, also negatively regulates HSC self-renewal

because transplanting *Ptprs*$^{-/-}$ bone marrow cells in mice increases HSC regeneration (20).

2.3 Neuronal stem cells

In addition to ESCs and HSCs, SHP2 is vital to the proliferation and self-renewal of neuronal stem cells (NSCs), neuronal migration, and neurite outgrowth. SHP2 deficient NSCs have severely decreased neuron and oligodendrocyte differentiation, and mice suffer postnatal lethality (21, 22). In contrast, neurite outgrowth is negatively suppressed by RPTPσ, since neurite outgrowth is enhanced in RPTPσ deficient neurons (23).

2.4 Mesenchymal stem cells

Leukocyte common antigen-related RPTP (LAR), RPTPQ, and SHP1, encoded by *PTPRF*, *PTPRQ*, and *PTPN6* respectively, are all involved in differentiation of mesenchymal stem cells (MSCs) into adipocytes. Knockdown of LAR increases adipogenesis, whereas overexpression of LAR decreases adipogenic differentiation (24). Similarly, RPTPQ overexpression decreases MSC differentiation into adipocytes (25).

Like LAR and RPTPQ, SHP1 negatively regulates MSC differentiation into adipocytes. SHP1 modulates Wnt/β-catenin signalling to express transcription factors needed for differentiation of MSCs into osteoblasts, shifting the balance between adipogenesis and osteogenesis in favour of MSC differentiation to an osteoblast fate (26). SHP1 deficient mice therefore have increased adipogenic markers and decreased osteogenic markers, accompanied by an increase in adipose tissue and a reduction in bone mass.

3. ROLE OF PTPS IN GASTRULATION AND SOMITOGENESIS DURING EARLY EMBRYONIC DEVELOPMENT

During early embryonic development, gastrulation is the process where the single-layered blastula is reorganized to form the three primary germ layers: endoderm, ectoderm, and mesoderm, that will eventually give rise to all organs. Gastrulation starts with emboly, the process where a layer of cells migrates and converges into the interior of the embryo forming an underlying layer. Following emboly, cells extend along one axis and converge (narrow) along a perpendicular axis in convergence and extension (C&E) movements. Epiboly, the thinning and spreading of cell layers, mostly

of ectoderm, that will finally cover the whole embryo, occurs in parallel (27). After gastrulation, the ectoderm will form the epidermis and nervous system, and the endoderm the epithelium of the digestive system, organs associated with this system, and the respiratory system. The mesodermal layer will give rise to somites on either side of the neural tube, which will eventually give rise to blood and blood vessels, the skeletomuscular system, connective tissue, and internal organs (28). A substantial number of PTPs have been identified as important regulators of development. The exact timing when each PTP acts, and on which signalling pathways, for normal development to occur still needs to be mapped. Here, we provide an overview of the recent research investigating the role of PTPs in early embryonic development.

3.1 Cytoplasmic PTPs

PTEN is undoubtedly important to normal development as *Pten* knockout mice suffer early embryonic lethality (29–31). Zebrafish contain two *pten* genes, *ptena* and *ptenb*, that are both highly homologous to human *PTEN*. Zebrafish deficient for both Ptena and Ptenb are embryonic lethal by 5-7 days post fertilization. Pten deficient zebrafish are characterized by smaller eyes that are set wider apart, a shortened body axis, an enlarged head, and heart oedema (32). Increased Akt phosphorylation, which enhances proliferation and cell survival, in Pten deficient zebrafish is the underlying cause of their phenotype, as treatment with a PI3K inhibitor can rescue the abnormalities. Further studies in mice demonstrated that PTEN is important for the formation of the anterior-posterior axis, by regulating migration of anterior visceral endoderm. Mouse embryos lacking PTEN in the epiblast demonstrate defects in migration of the embryonic layers, suggesting an important role for PTEN in migration of endoderm and mesoderm after gastrulation (33).

Overexpression of Ptp1b in zebrafish induces lethal defects in gastrulation and somitogenesis (34). Later studies in *Drosophila* emphasized the importance of correct tyrosine phosphorylation of proteins in early embryonic development. Lack of PTP61F, the *Drosophila* gene that encodes both the PTP1B and TC-PTP orthologues, results in reduced fecundity and life span. Reducing PTP61F expression by RNAi results in eye overgrowth and thickened and deformed veins in the wings, and overexpression of PTP61F impairs growth (35). PTP1B and TC-PTP regulate insulin receptor (IR) signalling in non-redundant and distinct ways. Importantly, whereas loss of PTP1B results in enhanced MAPK signal transduction, loss of TC-PTP does not affect insulin stimulated MAPK signalling in mouse embryonic fibroblasts (36–38). Of note is that MAPK signal

transduction induced by other ligands, such as tumor necrosis factor (TNF), is enhanced by loss of TC-PTP. In *Drosophila*, PTP61F acts as a negative regulator of MAPK signal transduction (39), suggesting a similar role as PTP1B. However, further research is needed to determine if the observed phenotype in *Drosophila* is due to aberrations in MAPK signalling, and hence that the defects can be ascribed to the orthologue of PTP1B, TC-PTP or both.

PTP-PEST, encoded by the *PTPN12* gene, is a phosphatase containing PEST-sequences, and is mostly expressed by cells of the hematopoietic system. Gastrulation occurs normally in PTP-PEST deficient mouse embryos, however after E9.5 several developmental defects such as growth retardation, a smaller cardiac region, caudal development arrest, and disrupted somite formation are observed. These mice also lack the formation of a fetal liver and reach embryonic lethality between E9.5 – E10.5. The precise role of PTP-PEST in embryonic development needs to be elucidated, but these results imply that PTP-PEST is more important in later embryonic development (40). As PTP1B appears to affect early embryonic development, and that PTP-PEST appears to affect later stages, there is evidence that specific PTPs may regulate distinct stages of embryonic development.

In early mouse development, SHP2 deficiency leads to embryonic lethality due to aberrant ERK signalling causing increased apoptosis in trophoblast stem cells (41). Similarly, Shp2 deficient zebrafish are embryonic lethal at 6-7 days post fertilization and display a reduced body axis, heart and eye oedema, and craniofacial defects (42).

3.2 Receptor PTPs

The *C. elegans* orthologue of the mammalian RPTP, LAR, has two isoforms, PTP-3A and PTP-3B, and loss-of-function results in mild, but lethal, gastrulation defects (43, 44). Mutations in Syndecan-1 (SDN-1), a heparin sulphate proteoglycan with which members of the LAR family interact, lead to movement and egg-laying defects, and low levels of lethality. As mutations in both PTP-3B and SDN-1 result in severe defects during gastrulation and arrested embryogenesis during epiboly, PTP-3B and SDN-1 likely have overlapping functions during early embryonic development (44). PTP-3B likely acts in Wnt signalling during embryonic development as knockdown of the Wnt ligand LIN-44 in PTP-3B mutants resulted in no synergistic phenotypes. Ongoing research aims to explore the mechanism by which SDN-1, PTP-3B, and LIN-44 affect gastrulation.

In early mouse embryogenesis, knockout of *Ptprs* and *Ptprf* leads to urogenital and craniofacial defects, such as smaller lower jaws, cleft palates, and no nasal capsules, resulting in a phenotype similar to Pierre-Robin Sequence (45, 46). This phenotype in RPTPσ and LAR deficient mice is thought to be due to decreased proliferation of mandibular cells and defective patterning of mandibular bone and cartilage, as a result of altered regulation of the BMP and Wnt signalling pathways (46).

In *Drosophila* a potential orthologue of the human stomach-associated SAP1 PTP, PTP52F, has an essential role in the transition from larva to pupa, as mutations lead to mortality at the post pupal stage (47).

In Zebrafish, Rptpα, Rptpε, Ptp-bas, and Ptpn20 are all essential for gastrulation. Knockdown of these four PTPs in zebrafish embryos induces phenotypes that correlate with defects in C&E movements and epiboly cell migration, formation of oedemas around the yolk and heart upon Rptpα knockdown, and a shortened body axis upon both Rptpα and Rptpε knockdown (6, 48). Rptpα and Rptpε, encoded by *ptpra* and *ptpre* respectively, act upstream of kinases Fyn and Yes, activating RhoA, which in turn activates Rock, ultimately resulting in cell polarization. In contrast, Ptpn20 and Ptp-bas, encoded by *ptpn20* and *ptpn13* respectively, signal to reduce RhoA activity. This balance of positive and negative regulation of RhoA is essential for cell polarization, which in turn determines proper C&E movements and epiboly cell migration.

4. PTPS IN BONE FORMATION

Osteoblasts and osteoclasts are important cells in the maintenance of bone matrix, and have opposing activities to constantly remodel bone. Osteoblasts form a specialized unit of connected cells, called the osteon, which synthesize essential cross-linked collagen and a calcium- and phosphate-based mineral, called hydroxyapatite, for the formation and mineralization of bone in a process known as osteogenesis (49). Osteoclasts, multi-nucleated cells formed through the fusion of monocyte-macrophage precursor cells, digest bone in the process known as bone resorption. Differentiation of precursor cells into osteoclasts is regulated by receptor activator of nuclear factor kappa-B ligand (RANKL) and macrophage colony-stimulating factor (M-CSF) (50). When attached to bone, osteoclasts form adhesion structures called podosomes, which are densely packed into a ring referred to as the sealing zone. Osteoclasts then release acid and collagenase to demineralise and degrade the bone matrix. The podosome

core is composed of filamentous actin and its formation is regulated by a multi-protein branching machinery that consists of cortactin, Wiskott-Aldrich syndrome protein (WASP), WASP interacting protein (WIP), and the Arp2/3 complex. When integrins from osteoclasts bind to ligands in the bone, they recruit proteins involved in podosome dynamic and organization, such as PYK2 and SRC (50, 51). Knockout of *Csk* in mice leads to osteopetrosis, i.e. increased bone density, due to reduced bone resorption (52), underpinning the importance of well regulated SRC activity during bone formation.

4.1 Cytoplasmic PTPs

In 1995, Ari Elson discovered a cytoplasmic form of PTPε encoded by the *PTPRE* gene (53), which is referred to as cyt-PTPε and plays an important role in osteogenesis. Lack of cyt-PTPε increases the trabecular bone mass of young adult female mice, as a consequence of reduced bone resorption. cyt-PTPε deficient mice show reduced numbers of osteoclasts in contact with bone, but no reduction in total osteoclast number, suggesting impaired functioning of osteoclasts (54, 55). In addition, podosomes have a perturbed internal structure, cellular organization, and reduced stablity, presumably because of dysregulated SRC, PYK2, RHO, and RAC activity, which are involved in integrin signalling pathways required for podosome formation. cyt-PTPε is activated by SRC following integrin signalling and maintains SRC activity via a positive feedback loop (56, 57). Since RPTPα is closely related tot PTPε, it has been suggested that RPTPα performs a similar role in osteoclast function. However, mice lacking RPTPα do not show any changes in bone mass, function of osteoclasts, or podosome organization and function (54).

PTP-PEST is associated with SRC, PYK2, proline-serine-threonine phosphatase-interacting protein (PSTPIP), and WASP in podosomes. PTP-PEST dephosphorylates SRC at Y527, allowing SRC-mediated phosphorylation and activation of WASP and Cortactin, ultimately resulting in formation of the sealing zone (58, 59). PTP-PEST also regulates osteoclast function through dephosphorylation of PYK2, leading to PYK2 inactivation and reduced osteclast activity, followed by re-organization of the sealing zone (60). Furthermore, monocyte-macrophage fusion, required for oseoclast formation, is dependent on delicate PTP-PEST controlled PYK2 phosphorylation; both PYK2 hyperphosphorylation, as a result of PTP-PEST deficiency, and PYK2 inhibition lead to a fusion defect (61). PTP-PEST also has an important role in osteoblasts because PTP-PEST increases differentiation of pre-osteoblasts to osteoblasts and has been shown to decrease osteoblast migration *in vitro*, by inactivating the GTPase Dynamin (62).

SHP2 deficient mice suffer such severe impairment of osteogenesis that they develop osteopetrotic bones and develop cartilage abnormalities (63, 64). However, how SHP2 regulates osteogenesis in mice is under debate. Bauler *et al.* suggest that osteogenesis is impaired in SHP2 deficient mice as a result of a lack of AKT activation required for the proliferation and survival of osteoclast precursor cells (63). In contrast, Zhou *et al.* demonstrate that SHP2 deletion has little effect on the proliferation and survival of osteoclast precursor cells in the presence of M-CSF and RANKL, and instead propose that SHP2 is important in pre-osteoclast fusion by responding to RANKL signaling (64). Whichever pathway SHP2 acts on, it is likely in response to, or in an effort to regulate, SRC activity.

4.2 Receptor PTPs

RPTPO, encoded by the *PTPRO* gene, is an osteoclast transmembrane PTP and mainly expressed in hematopoietic cells, such as B-lymphocytes, osteoclasts, and their precursor cells. RPTPO has been demonstrated to be important for the differentiation and activity of osteoclast-like cells derived from a lymphoblast cell line (65), and likely regulates osteoclast activity, migration, and survival through a SRC-dependent manner (66, 67). Overexpression of RPTPO maintains increased osteoclast activity as a result of reduced apoptosis, whereas knockdown, or overexpression of inactive RPTPO leads to increased apoptosis and reduced osteoclast actvity (67). Furthermore, overexpression of RPTPO in osteoclast-like cells decreases bone density and mass in young adult male mice due to increased bone resorption (68). This is in stark contrast to the effect of knocking-out the aforementioned cyt-*Ptpε* in female mice. Since overexpression of RPTPO or knockout of cyt-*Ptpε* results in the same phenotype in male or female mice respectively, it could be that sex-dependent hormone signalling in osteoclasts is affected by the activity of each PTP and that both converge on the same pathway. In parallel to activation of SRC, RPTPO also increases the bone resoprtion activity of osteoclasts independently of SRC by inactivating EPHA4, a negative regulator of osteoclast activity (69).

5. PTPS IN ANGIOGENESIS

Blood vessel formation is regulated by VEGF mediated signalling through the VEGF tyrosine kinase receptor family, consisting of VEGF receptor (VEGFR) 1, 2 and 3, of

which VEGFR2 mediates the major actions. Stimulation with VEGF activates VEGFR2 signalling that induces VE-Cadherin tyrosine phosphorylation (70). Hence, it comes as no surprise that PTPs have a critical role in angiogenesis. New blood vessels are formed by sprouting of endothelial tip cells from pre-existing blood vessels towards an angiogenic stimulus, such as VEGF. Tip cells contain filopodia that have many VEGFR2 receptors to 'sense' the VEGF gradient and migrate towards the source of this gradient. The stalk cells that are positioned next to tip cells proliferate upon tip cell movement, causing the blood vessel to elongate. This vessel-branching model of tip cell migration and stalk cell proliferation is under the control of NOTCH signalling. The permeability and stability of blood vessels is regulated by intercellular junctions, and vascular endothelial (VE)-Cadherin is the major determinant of blood vessel wall integrity, changing the activity or presence of VE-Cadherin at cell-cell contacts will affect the permeability and stability of the blood vessel walls. Loss of VE-Cadherin, therefore, does not lead to inhibition of angiogenesis, but to defects in vessel remodelling and cell-cell junction integrity (71).

5.1 Cytoplasmic PTPs

PTP1B overexpression in endothelial cells inhibits VEGF mediated phosphorylation of VEGFR2 and reduces VE-Cadherin tyrosine phosphorylation, resulting in reduced proliferation and migration, stabilized cell-cell contacts between endothelial cells, and disrupted angiogenesis (72, 73). PTP1B knockout primary mouse endothelial cells display enhanced VEGF induced MAPK and VEGFR2 phosphorylation, and PTP1B deficient mice and leptin deficient obese mice (ob/ob mice), in which PTP1B is inhibited, demonstrate enhanced angiogenesis (73, 74). Hence, PTP1B negatively regulates angiogenesis, and recent research implicates PTP1B in a Calpain-dependent negative feedback mechanism of VEGF induced angiogenesis (75). Yet, it remains to be determined if PTP1B acts on VEGFR2 directly.

In contrast to PTP1B, PTP-PEST positively regulates angiogenesis by stimulating endothelial cell migration and vascular development. Loss of *Ptpn12* in mice leads to a reduced number of endothelial cells in the aorta and yolk sac, fewer, but larger vessels, and mortality between E9.5 and E10.5 (40). Moreover, when PTP-PEST deficiency is limited exclusively to endothelial cells, these cells show a decreased adhesion to collagen and fibronectin, and reduced migration, with the resulting perturbation in angiogenesis leading to embryonic lethality (76). PTP-PEST has been shown *in vitro* to

contribute to integrin-mediated adhesion and migration of endothelial cells, through the dephosphorylation of CAS, Paxillin, and PYK2.

Zebrafish deficient for Ptena and Ptenb, alongside elevated phospho-Akt levels, have upregulated levels of Vegfaa, and subsequently demonstrate hyper-vascularization (77). It is the lipid phosphatase activity of Pten, rather than the protein phosphatase activity, and proper spatial expression of Pten that are essential for regulation of angiogenesis and the development of blood vessels in zebrafish. Pten mutated at lysine 13 to an arginine has enhanced plasma membrane localization in mammalian and zebrafish cells, and rescues the hyper-vascularization phenotype (78, 79). However, stalled intersegmental vessels are observed during development when this Pten mutant is expressed in wild-type zebrafish embryos, suggesting that sufficient, and not excess, membrane localized Pten is required for proper angiogenesis. In mice, PTEN is important for the regulation of stalk cell proliferation, and NOTCH induced PTEN expression results in cell cycle arrest, and hence proper formation of blood vessels (80). Overexpression of PTEN reduces endothelial cell proliferation and vascular density, and aberrant angiogenesis is observed when PTEN activity is reduced (81), suggesting a fine balance of PTEN activity is required for proper blood vessel formation. One of the limitations to understanding the exact role of PTEN in angiogenesis during normal embryonic development is that knowledge pertaining to angiogenesis has mostly been inferred from tumour angiogenesis. Tumours often exhibit enhanced angiogenesis but, also, PTEN is a tumour suppressor gene that is often mutated in tumours (82–84). It is therefore difficult to appreciate the role of PTEN in angiogenesis. Nevertheless, it is evident from studies to date that PTEN has a crucial role in angiogenesis and is a factor that ensures proper blood vessel development.

5.2 Receptor PTPs

Mice deficient for RPTPβ, also known as vascular endothelial PTP (VE-PTP) because it is exclusively expressed in endothelial cells, display severe vascular remodelling defects, and reach mortality by E10. The mice are not able to form a hierarchical branched vascular network, indicating that RPTPβ is not necessary at the initial stages of blood vessel formation, but for the maintenance of blood vessels. In addition, RPTPβ deficient mice have defects in heart formation (85, 86). RPTPβ, encoded by the *PTPRB* gene, maintains blood vessels by binding VE-Cadherin and ensuring optimal VE-Cadherin function, and thereby endothelial cell-cell adhesion. Furthermore, RPTPβ cooperates with integrins and RAS to induce endothelial cell spreading and migra-

tion. In the presence of fibronectin, RPTPβ promotes the formation of filopodia and lamellipodia, and induces cell migration. These effects are abolished when SRC family kinases are inhibited, suggesting that integrin-induced activation of SRC family kinase signalling is important for RPTPβ induced endothelial cell spreading and migration (87). VEGF stimulation induces dissociation of RPTPβ from VE-Cadherin, and, due to the loss of endothelial cell-cell adhesion, results in increased cell layer permeability and diapedesis of leukocytes (88, 89). Although proximity ligation assays suggested a direct association of RPTPβ with VEGFR2 (90), the mechanism is proposed to be mediated by PYK2 activation of RPTPβ substrates. Substrate binding to RPTPβ would then induce a conformational change resulting in detachment of the extracellular domain of RPTPβ from VE-Cadherin (91). RPTPβ is also implicated in orchestrating vessel remodelling independent of VE-Cadherin via TIE-2, a receptor tyrosine kinase that functions downstream of vascular growth factor Angiopoietin. When RPTPβ is inhibited, TIE-2 dissociates and is activated, driving endothelial cell proliferation, and stabilizing endothelial cell-cell junctions (92, 93). Since TIE-2 also determines blood vessel size, its activity is restricted by RPTPβ to ensure proper blood vessel formation and size (92). Interestingly, the stimulation of VE-Cadherin by active RPTPβ and the activation of TIE-2 upon RPTPβ inhibition, is a feedback mechanism that ensures endothelial cell-cell integrity: active RPTPβ inhibits TIE-2 and stimulates endothelial cell-cell adhesion via VE-Cadherin, whereas inactive RPTPβ cannot activate VE-Cadherin, but endothelial cell-cell adhesions are still stabilised by the now active TIE-2 (93).

Density Enhanced PTP (DEP-1), also known as CD148, is a glycoprotein encoded by *PTPRJ*, and found at the cell surface. It is closely related to RPTPO, RPTPQ and RPTPβ, and consists of a single PTP domain and an extracellular domain consisting of fibronectin III repeats (**Fig. 1**). DEP-1 deficient mice have impaired VEGF induced formation of functional capillaries, and the capillaries that do form are shorter and less dense (94). This results in a phenotype, similar to PTP-PEST deficient mice, characterized by impaired angiogenesis, enlarged vessel formation, disruption of branching and vascular remodelling, and embryonic lethality by E11.5 (95). DEP-1, encoded by the *PTPRJ* gene, functions to maintain endothelial cell permeability by activating SRC in response to VEGF, and SRC subsequently phosphorylates Cortactin and VE-Cadherin (94, 96, 97). Depletion of DEP-1 leads to a reduction of VEGF induced phosphorylation of VE-Cadherin, thus maintaining cell-cell junction integrity, and to decreased Cortactin phosphorylation, resulting in impaired vascular branching and invasion of endothelial cells. Interestingly, increasing DEP-1 activity, using a bivalent antibody, also

impairs endothelial cell proliferation and angiogenesis (98). And consistent with this, overexpression of DEP-1 inhibits proliferation, migration, and formation of capillary-like structures of primary endothelial cells (99). In addition, DEP-1 overexpression promotes VEGF induced cell layer permeability in cultured human umbilical vein endothelial cells (HUVECs) (97). Taken together, these studies confirm the importance of regulating DEP-1 activity for angiogenesis.

6. PTPS IN DISEASE

Recent and ongoing research continues to highlight the importance of PTPs in development, and it is therefore not surprising that PTPs contribute to a plethora of human diseases and disorders (100, 101). For some PTPs it is still unclear what their role is in disease. *PTPN22*, for example, has been implicated in type 1 diabetes (T1DM) and breast cancer, but little follow up work has been done and mutations in *PTPN22* are even predicted to be over-represented in breast cancer (102–105). PTPs are often considered the guardians of kinase driven phosphorylation cascades, and loss-of-function is fittingly associated with enhanced signal transduction, as observed in many cancers (106). However, there are numerous examples where PTP activity is not inhibiting, and is required to stimulate signal transduction and promote cellular responses. Of 21 RPTPs, 20 are mutated in multiple cancers and RPTPs more often experience a gene amplification rather than a gene loss (107). However, as the most common mechanism of genetic modification of RPTPs is mutation, further research will have to be done to determine if these are activating or silencing mutations, or rather neutral mutations acquired during the tumorigenic process. Both too little or too much PTP activity may lead to disease, and the role of each PTP, whether it is limiting signalling or promoting signalling, may very well be context (i.e. cell type) dependent. For example, a gain-of-function mutation in SHP2 is found in juvenile myelomonocytic leukemia (JMML) patients (108), but in hepatocellular carcinogenesis SHP2 acts as a tumour suppressor (109).

6.1 SHP2 (PTPN11)

A large number of mutations, activating and inactivating, have been identified in SHP2 in association with human disease (110). Mutations in SHP2 that increase or decrease its catalytic activity are associated with Noonan syndrome (NS) and Noonan syndrome

with multiple lentigenes (NS-ML, formerly LEOPARD syndrome), respectively. Individuals with NS and NS-ML have characteristic cranio-facial abnormalities, heart defects, short stature, and an increased risk of developing JMML. Interestingly, NS is caused by mutations in SHP2 that activate SHP2 catalytic activity (e.g. D61G), whereas NS-ML is caused by mutations in SHP2 that strongly reduce catalytic activity (e.g. A461T). Recently, it was demonstrated that the NS-ML SHP2 mutants Y279C, A461T, G464A, T468M, R498L, Q506P, and Q510E do indeed have impaired catalytic activity but also display structural properties typical of activating mutations, which could explain the similar symptoms presented by individuals with NS and NS-ML (111, 112). The SHP2 mutant proteins from NS and NS-ML patients appear to have an increased tendency to adopt an open conformation and interact longer with scaffolding adaptors, prolonging substrate turnover, and thereby compensate for the reduced phosphatase activity (111, 112). The exact mechanism by which mutated SHP2 induces NS and NS-ML is poorly understood, but aberrant ERK phosphorylation and signalling is a likely consequence of unbalanced SHP2 activity. Enhanced SHP2 activity is associated with systemic lupus erythematosus and, recently, Wang et al. (2016) demonstrated that inhibition of SHP2 reduced the autoimmune response thought to underlie the disease. SHP2 inhibition normalized ERK/MAPK signalling and reduced proliferation of cultured human lupus T cells. In contrast, mutations in SHP2 that lead to a loss-of-function result in a myeloproliferative disorder, because of enhanced proliferation and decreased apoptosis of hematopoietic stem cells (18). This may be because of pro-inflammatory cytokines, secreted by monocytes recruited to the stem cell micro-environment of SHP2 deficient hematopoietic stem cells, having detrimental effects on the homeostasis of the hematopoietic stem cell population (114).

6.2 PTP1B (PTPN1) and RPTPσ (PTPRS)

Type 2 diabetes (T2DM) is associated with mutations in *PTPN1* and *PTPRS*. Negative regulation of insulin receptor (IR) signalling by PTP1B is well established (reviewed by (115)), and *Ptpn1* knockout mice fed a high fat diet are resistant to weight gain compared to control mice (116). PTP1B deficiency also increases insulin sensitivity and glucose uptake in insulin receptor substrate-2 (IRS-2) deficient mice, suggesting PTP1B inhibits IR signalling by acting on or downstream of IRS-2 (117). Indeed, PTP1B depletion improves insulin sensitivity and glucose tolerance, as well as decreasing the occurrence of diabetes development, in mice deficient for IR and IRS-1 (118). However, mice lacking PTP1B also display an accentuated pro-inflammatory response and

compromised macrophage viability (119), indicating care should be taken in ongoing clinical trials. Variations in the *PTPRS* gene are associated with T2DM development (120), and, similar to PTP1B, RPTPσ deficient mice have a reduced body mass and increased insulin sensitivity (121).

6.3 TC-PTP (PTPN2)

Development of T1DM is associated with mutations in *PTPN2*, which negatively regulates IR signalling in concurrence with PTP1B. Lack of TC-PTP leads to multiple cellular defects related to T1DM, including increased β-cell apoptosis, altered β-cell function, and decreased self-antigen tolerance due to increased T-cell receptor signalling and dysregulation of FOXP3 T-regulatory cells (103, 104). Mutations in *PTPN2* also influence susceptibility to Crohn's disease (CD) (122–124). CD development is driven by epithelial barrier defects and a dysfunctional immune response, and TC-PTP plays a role in preserving the epithelial barrier function by regulating the inflammatory response (125, 126). In addition, TC-PTP deficiency leads to impaired autophagosome formation, resulting in defective bacterial clearance of intestinal cells and increased apoptosis in intestinal epithelial cells (127). Moreover, mutations in *PTPN2* lead to aberrant T-cell dysfunction, and consequently increased intestinal inflammation and dysbiosis (microbial imbalance) (128). Both autophagy and T-cell dysfunctions are also found in CD patients, implicating TC-PTP.

6.4 PTEN (PTEN)

Mutations in *PTEN* cause PTEN hamartoma tumour syndromes (PHTS), rare inherited syndromes characterized by hamartomas in tissues originating from all three germ layers. PHTS encompasses four distinct syndromes: Proteus syndrome, Proteus-like syndrome, Cowden syndrome, and Bannayan-Riley-Ruvalcaba syndrome, of which Cowden syndrome is the most prevalent (129). PHTS are consistent with mutant zebrafish lacking three of four pten alleles, that develop hemangiosarcomas (130). Not only the lipid phosphatase activity of PTEN, which suppresses Akt activity, but also the protein phosphatase activity of PTEN, important in cell cycle arrest and inhibition of cell invasion, has been shown to have a tumour suppressive function (131). Loss-of-function mutations in *PTEN*, which lead to increased AKT activation, IR signalling, and thus insulin sensitivity, are also associated with an increase in adiposity and obesity (132). Constitutive AKT activation also corresponds with the development of autism spectrum disorders (ASDs), extensively reviewed in other publications (133–135). ASDs

are neurodevelopmental disorders characterized by communication deficits, impaired social interactions, and restricted and repetitive behaviour. PTEN is involved by influencing different cellular processes, for example deletion of *Pten* in the hippocampal adult neural stem cells of mice results in an increased proliferation and differentiation of these stem cells, leading to depletion of the stem cell pool, and development of hypertrophied neurons. These mice display seizure activity, macrocephaly, and impairments in social interactions (136).

7. CONCLUSION AND FUTURE PERSPECTIVES

In conclusion, PTPs have diverse roles in various biological processes, as represented schematically in **Fig. 2**. This schematic is not comprehensive and future research on the role of PTPs in development will undoubtedly lead to the inclusion of more PTPs and more developmental processes. Nevertheless, it is evident that PTPs have crucial roles in various developmental processes and, as a result, also in disease. Because PTPs have a pivotal role in disease and because they regulate protein-tyrosine phosphorylation enzymatically, PTPs are now being considered as drug targets. The major concern regarding the development of PTP inhibitors is selectivity because the PTP catalytic site is highly conserved and it is therefore challenging to develop inhibitors that target the catalytic site of just one specific PTP. In addition, the catalytic site is positively charged, and heavily charged molecules that may target such a site do not easily cross the cell membrane. For this reason, and in the hope to gain specificity, attempts are being made to develop inhibitors that do not target the conserved catalytic site directly, but instead less conserved allosteric sites.

Various non-specific PTP1B inhibitors have been developed (137, 138), and one of the latest, anti-sense oligonucleotide ISIS-113715, looks promising as it increases insulin sensitivity and adiponectin concentrations in monkeys (139). In 2014 the lab of Nick Tonks tested a novel allosteric inhibitor of PTP1B, MSI-1436, which does not target the catalytic site but instead the C-terminus of PTP1B (140). MSI-1436 traps PTP1B in an inactive state, and its effectiveness was demonstrated in a mouse model of HER2 driven breast tumourigenesis, where it inhibited HER2 signalling and abrogated metastasis.

In contrast to the large number of PTP1B inhibitors, there are only a few SHP2 inhibitors. In recent years, SHP2 inhibitors have been developed that block prolife-

ration of patient derived hematopoietic progenitor cells expressing the E67K or the D61Y mutation, and leukemic cells and mouse myeloid progenitor cells that carry the E76K mutation (141–143). Since D61G is the most common mutation in NS, it should be determined whether these compounds also work for NS patients with the D61G, and other SHP2 mutations. Recently, a highly potent and selective allosteric inhibitor for SHP2 (SHP099) has been developed which inhibits proliferation and differentiation in mouse tumours, and in human cancer cells *in vitro* driven by mutated receptor tyrosine kinases (144).

Taken together, the great strides made in the last decade in fundamental and translational research to understand the function and importance of PTPs, and to target them in an attempt to cure disease, have left a bright future for research and the well-being of patients alike. With more research to elucidate the function and regulation of PTPs, and development of drugs that target PTPs, PTP inhibitors may soon appear in the clinic.

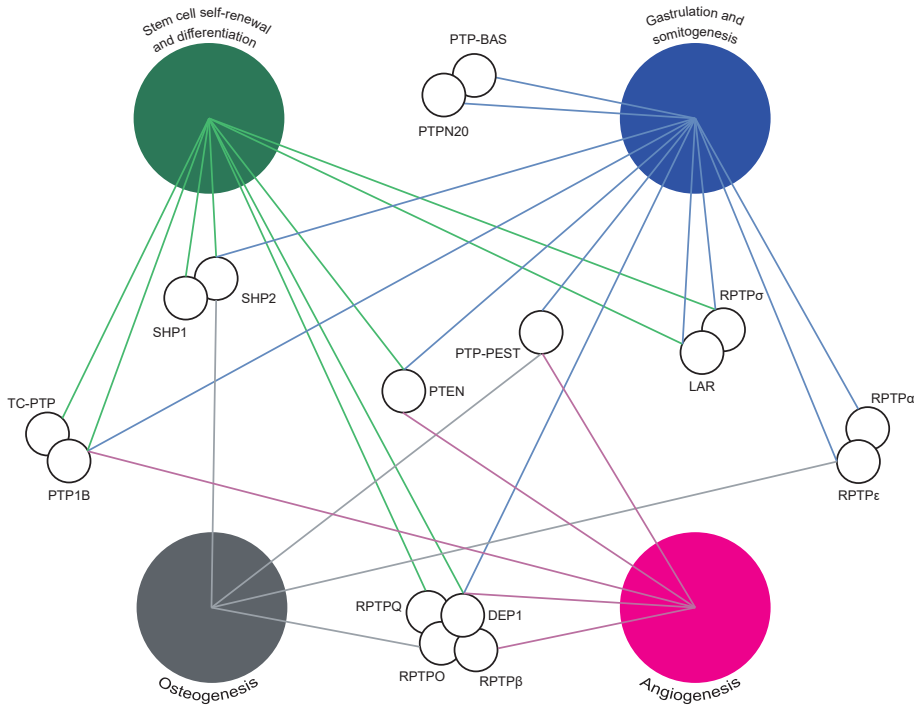

Fig. 2. Protein-tyrosine phosphatases are involved in key aspects of development. Big circles represent developmental processes and small circles are individual PTPs. Lines indicate involvement of the PTP in particular developmental processes. PTPs are clustered based on similar overall architecture.

REFERENCES

1. Tonks NK, Diltz CD, Fischer EH (1988) Characterization of the major protein-tyrosine-phosphatases of human placenta. *J Biol Chem* 263(14):6731–6737.
2. Alonso A, Pulido R (2016) The extended human PTPome: A growing tyrosine phosphatase family. *FEBS J* 283(8):1404–1429.
3. Tonks NK (2013) Protein tyrosine phosphatases - From housekeeping enzymes to master regulators of signal transduction. *FEBS J* 280(2):346–378.
4. den Hertog J, Östman A, Böhmer FD (2008) Protein tyrosine phosphatases: regulatory mechanisms. *Febs J* 275(5):831–847.
5. Östman A, Frijhoff J, Sandin A, Böhmer F-D (2011) Regulation of protein tyrosine phosphatases by reversible oxidation. *J Biochem* 150(4):345–56.
6. van Eekelen M, Runtuwene V, Overvoorde J, den Hertog J (2010) RPTPalpha and PTPepsilon signaling via Fyn/Yes and RhoA is essential for zebrafish convergence and extension cell movements during gastrulation. *Dev Biol* 340(2):626–639.
7. Wu D, et al. (2009) A conserved mechanism for control of human and mouse embryonic stem cell pluripotency and differentiation by Shp2 tyrosine phosphatase. *PLoS One* 4(3):e4914.
8. Chan RJ, Johnson SA, Li Y, Yoder MC, Feng GS (2003) A definitive role of Shp-2 tyrosine phosphatase in mediating embryonic stem cell differentiation and hematopoiesis. *Blood* 102(6):2074–2080.
9. He Z, et al. (2013) Nonreceptor tyrosine phosphatase Shp2 promotes adipogenesis through inhibition of p38 MAP kinase. *Proc Natl Acad Sci U S A* 110(1):79–88.
10. Tao J, Zheng L, Meng M, Li Y, Lu Z (2016) Shp2 suppresses the adipogenic differentiation of preadipocyte 3T3-L1 cells at an early stage. *Cell Death Discov* 2:16051.
11. Song MS, Salmena L, Pandolfi PP (2012) The functions and regulation of the PTEN tumour suppressor. *Nat Rev Mol Cell Biol* 13(5):283–296.
12. Alva JA, Lee GE, Escobar EE, Pyle AD (2011) Phosphatase and Tensin Homolog Regulates the Pluripotent State and Lineage Fate Choice in Human Embryonic Stem Cells. *Stem Cells* 29(12):1952–1962.
13. Matulka K, et al. (2013) PTP1B is an effector of activin signaling and regulates neural specification of embryonic stem cells. *Cell Stem Cell* 13(6):706–719.
14. Chan G, et al. (2011) Essential role for Ptpn11 in survival of hematopoietic stem and progenitor cells. *Blood* 117(16):4253–4261.
15. Chan G, et al. (2009) Leukemogenic Ptpn11 causes fatal myeloproliferative disorder via cell-autonomous effects on multiple stages of hematopoiesis. *Blood* 113(18):4414–4424.
16. Dong L, et al. (2016) Leukaemogenic effects of Ptpn11 activating mutations in the stem cell microenvironment. *Nature* 539(7628):304–308.
17. Li L, et al. (2012) A critical role for SHP2 in STAT5 activation and growth factor – mediated proliferation , survival , and differentiation of human CD34 ƨ cells. *Blood* 118(6):1504–1515.
18. Xu D, et al. (2010) A germline gain-of-function mutation in Ptpn11 (Shp-2) phosphatase induces myeloproliferative disease by aberrant activation of hematopoietic stem cells. *Blood* 116(18):3611–3621.
19. Bourdeau A, Trop S, Doody KM, Dumont DJ, Tremblay ML (2013) Inhibition of T cell protein tyrosine phosphatase enhances interleukin-18-dependent hematopoietic stem cell expansion. *Stem Cells* 31(2):293–304.
20. Quarmyne M, et al. (2015) Protein tyrosine phosphatase – σ regulates hematopoietic stem cell – repopulating capacity. 125(1):177–182.

21. Ke Y, et al. (2007) Deletion of Shp2 in the brain leads to defective proliferation and differentiation in neural stem cells and early postnatal lethality. *Mol Cell Biol* 27(19):6706–6717.
22. Huang Y-S, et al. (2012) Involvement of SHP2 in focal adhesion, migration and differentiation of neural stem cells. *Brain Dev* 34(8):674–684.
23. Kirkham DL, et al. (2006) Neural stem cells from protein tyrosine phosphatase sigma knockout mice generate an altered neuronal phenotype in culture. *BMC Neurosci* 7:50.
24. Kim W-K, et al. (2009) Regulation of adipogenic differentiation by LAR tyrosine phosphatase in human mesenchymal stem cells and 3T3-L1 preadipocytes. *J Cell Sci* 122(22):4160–4167.
25. Jung H, et al. (2009) Involvement of PTP-RQ in differentiation during adipogenesis of human mesenchymal stem cells. *Biochem Biophys Res Commun* 383(2):252–257.
26. Jiang M, et al. (2016) SHP1 Regulates Bone Mass by Directing Mesenchymal Stem Cell Differentiation. *Cell Rep* 16(3):769–780.
27. Solnica-Krezel L, Sepich DS (2012) Gastrulation: Making and Shaping Germ Layers. *Annu Rev Cell Dev Biol* 28:687–717.
28. Kiecker C, Bates T, Bell E (2016) Molecular specification of germ layers in vertebrate embryos. *Cell Mol Life Sci* 73(5):923–947.
29. Cristofano AD, Pesce B, Cordon-Cardo C, Pandolfi PP (1998) Pten is essential for embryonic development and tumour suppression. *Nat Genet* 19(4):348–355.
30. Suzuki A, et al. (1998) High cancer susceptibility and embryonic lethality associated with mutation of the PTEN tumor suppressor gene in mice. *Curr Biol* 8(21):1169–1178.
31. Stambolic V, et al. (1998) Negative regulation of PKB/Akt-dependent cell survival by the tumor suppressor PTEN. *Cell* 95(1):29–39.
32. Faucherre A, Taylor GS, Overvoorde J, Dixon JE, den Hertog J (2008) Zebrafish pten genes have overlapping and non-redundant functions in tumorigenesis and embryonic development. *Oncogene* 27(8):1079–1086.
33. Bloomekatz J, Grego-Bessa J, Migeotte I, Anderson K V. (2012) Pten regulates collective cell migration during specification of the anterior-posterior axis of the mouse embryo. *Dev Biol* 364(2):192–201.
34. Van Der Sar AM, De Fockert J, Betist M, Živković D, Den Hertog J (1999) Pleiotropic effects of zebrafish protein-tyrosine phosphatase-1B on early embryonic development. *Int J Dev Biol* 43(8):785–794.
35. Buszard BJ, et al. (2013) The nucleus- and endoplasmic reticulum-targeted forms of protein tyrosine phosphatase 61F regulate Drosophila growth, life span, and fecundity. *Mol Cell Biol* 33(7):1345–1356.
36. Galic S, et al. (2005) Coordinated Regulation of Insulin Signaling by the Protein Tyrosine Phosphatases PTP1B and TCPTP. *Mol Cell Biol* 25(2):819–829.
37. van Vliet C, et al. (2005) Selective regulation of tumor necrosis factor-induced Erk signaling by Src family kinases and the T cell protein tyrosine phosphatase. *Nat Immunol* 6(3):253–260.
38. Blanquart C, Karouri SE, Issad T (2010) Protein tyrosine phosphatase-1B and T-cell protein tyrosine phosphatase regulate IGF-2-induced MCF-7 cell migration. *Biochem Biophys Res Commun* 392(1):83–88.
39. Tchankouo-Nguetcheu S, et al. (2014) Negative regulation of MAP kinase signaling in Drosophila by Ptp61F/PTP1B. *Mol Genet Genomics* 289(5):795–806.
40. Sirois J, et al. (2006) Essential function of PTP-PEST during mouse embryonic vascularization, mesenchyme formation, neurogenesis and early liver development. *Mech Dev* 123(12):869–880.

41. Yang W, et al. (2006) An Shp2/SFK/Ras/Erk signaling pathway controls trophoblast stem cell survival. *Dev Cell* 10(3):317–327.
42. Bonetti M, et al. (2014) Distinct and overlapping functions of ptpn11 genes in zebrafish development. *PLoS One* 9(4):e94884.
43. Harrington RJ, Gutch MJ, Hengartner MO, Tonks NK, Chisholm AD (2002) The C. elegans LAR-like receptor tyrosine phosphatase PTP-3 and the VAB-1 Eph receptor tyrosine kinase have partly redundant functions in morphogenesis. *Development* 129(9):2141–2153.
44. Hartin SN, Hudson ML, Yingling C, Ackley BD (2015) A synthetic lethal screen identifies a role for lin-44/Wnt in C. elegans embryogenesis. *PLoS One* 10(5):e0121397.
45. Uetani N, et al. (2009) Maturation of ureter-bladder connection in mice is controlled by LAR family receptor protein tyrosine phosphatases. *J Clin Invest* 119(4):924–935.
46. Stewart K, Uetani N, Hendriks W, Tremblay ML, Bouchard M (2013) Inactivation of LAR family phosphatase genes Ptprs and Ptprf causes craniofacial malformations resembling Pierre-Robin sequence. *Development* 140(16):3413–22.
47. Santhanam A, Liang SY, Chen DY, Chen GC, Meng TC (2013) Midgut-enriched receptor protein tyrosine phosphatase PTP52F is required for Drosophila development during larva-pupa transition. *FEBS J* 280(2):476–488.
48. van Eekelen M, Runtuwene V, Masselink W, den Hertog J (2012) Pair-wise regulation of convergence and extension cell movements by four phosphatases via RhoA. *PLoS One* 7(4):e35913.
49. Fratzl P, Weinkamer R (2007) Nature's hierarchical materials. *Prog Mater Sci* 52(8):1263–1334.
50. Mellis DJ, Itzstein C, Helfrich MH, Crockett JC (2011) The skeleton: A multi-functional complex organ. The role of key signalling pathways in osteoclast differentiation and in bone resorption. *J Endocrinol* 211(2):131–143.
51. Georgess D, Machuca-gayet I, Blangy A, Jurdic P (2014) Podosome organization drives osteoclast- mediated bone resorption. 8(3):192–204.
52. Marzia M, et al. (2000) Decreased c-Src Expression Enhances Osteoblast Differentiation and Bone Formation. *J Cell Biol* 151(2):311–320.
53. Elson A, Leder P (1995) Identification of a cytoplasmic, phorbol ester-inducible isoform of protein tyrosine phosphatase epsilon. *Proc Natl Acad Sci U S A* 92(26):12235–12239.
54. Finkelshtein E, et al. (2014) Protein tyrosine phosphatases epsilon and alpha perform nonredundant roles in osteoclasts. *Mol Biol Cell* 25(11):1808–1818.
55. Chiusaroli R, et al. (2004) Tyrosine Phosphatase Epsilon Is a Positive Regulator of Osteoclast Function in Vitro and In Vivo. *Mol Biol Cell* 15:234–244.
56. Granot-Attas S, Luxenburg C, Finkelshtein E, Elson A (2009) Protein Tyrosine Phosphatase Epsilon Regulates Integrin-mediated Podosome Stability in Osteoclasts by Activating Src. *Mol Biol Cell* 20(20):4324–4334.
57. Levy-Apter E, et al. (2014) Adaptor protein GRB2 promotes Src tyrosine kinase activation and podosomal organization by protein-tyrosine phosphatase ε in osteoclasts. *J Biol Chem* 289(52):36048–36058.
58. Chellaiah MA, Kuppuswamy D, Lasky L, Linder S (2007) Phosphorylation of a Wiscott-Aldrich syndrome protein-associated signal complex is critical in osteoclast bone resorption. *J Biol Chem* 282(13):10104–10116.
59. Chellaiah MA, Schaller MD (2009) Activation of Src kinase by protein-tyrosine phosphatase-PEST in osteoclasts: Comparative analysis of the effects of bisphosphonate and protein-tyrosine phosphatase inhibitor on Src activation in vitro. *J Cell Physiol* 220(2):382–393.
60. Eleniste PP, Du L, Shivanna M, Bruzzaniti A (2012) Dynamin and PTP-PEST cooperatively regulate Pyk2 dephosphorylation in osteoclasts. *Int J Biochem Cell Biol* 44(5):790–800.

61. Rhee I, Davidson D, Souza CM, Vacher J, Veillette A (2013) Macrophage fusion is controlled by the cytoplasmic protein tyrosine phosphatase PTP-PEST/PTPN12. *Mol Cell Biol* 33(12):2458–69.
62. Eleniste PP, Huang S, Wayakanon K, Largura HW, Bruzzaniti A (2014) Osteoblast differentiation and migration are regulated by dynamin GTPase activity. *Int J Biochem Cell Biol* 46(1):9–18.
63. Bauler TJ, et al. (2011) Development of severe skeletal defects in induced SHP-2-deficient adult mice: a model of skeletal malformation in humans with SHP-2 mutations. *Dis Model Mech* 4(2):228–239.
64. Zhou Y, et al. (2015) SHP2 regulates osteoclastogenesis by promoting preosteoclast fusion. *FASEB J* 29(5):1635–1645.
65. Amoui M, Suhr S-M, Baylink DJ, Lau K-HW (2004) An osteoclastic protein-tyrosine phosphatase may play a role in differentiation and activity of human monocytic U-937 cell-derived, osteoclast-like cells. *Am J Physiol Cell Physiol* 287(4):874–884.
66. Lau KHW, et al. (2006) An osteoclastic protein-tyrosine phosphatase is a potential positive regulator of the c-Src protein-tyrosine kinase activity: A mediator of osteoclast activity. *J Cell Biochem* 97(5):940–955.
67. Amoui M, Sheng MHC, Chen ST, Baylink DJ, Lau KHW (2007) A transmembrane osteoclastic protein-tyrosine phosphatase regulates osteoclast activity in part by promoting osteoclast survival through c-Src-dependent activation of NFκB and JNK2. *Arch Biochem Biophys* 463(1):47–59.
68. Sheng MHC, et al. (2009) Targeted transgenic expression of an osteoclastic transmembrane protein-tyrosine phosphatase in cells of osteoclastic lineage increases bone resorption and bone loss in male young adult mice. *J Biol Chem* 284(17):11531–11545.
69. Lau KHW, Amoui M, Stiffel V, Chen ST, Sheng MHC (2015) An Osteoclastic Transmembrane Protein-Tyrosine Phosphatase Enhances Osteoclast Activity in Part by Dephosphorylating EphA4 in Osteoclasts. *J Cell Biochem* 116(8):1785–1796.
70. Esser S, Lampugnani MG, Corada M, Dejana E, Risau W (1998) Vascular endothelial growth factor induces VE-cadherin tyrosine phosphorylation in endothelial cells. *J Cell Sci* 111(13):1853–1865.
71. Carmeliet P, Jain RK (2011) Molecular Mechanisms and and clinical applications of angiogenesis. *Nature* 473(7347):298–307.
72. Nakamura Y, et al. (2008) Role of protein tyrosine phosphatase 1B in vascular endothelial growth factor signaling and cell-cell adhesions in endothelial cells. *Circ Res* 102(10):1182–1191.
73. Lanahan AA, et al. (2014) PTP1B is a physiologic regulator of vascular endothelial growth factor signaling in endothelial cells. *Circulation* 130(11):902–909.
74. Zhang J, et al. (2015) Protein tyrosine phosphatase 1B impairs diabetic wound healing through vascular endothelial growth factor receptor 2 dephosphorylation. *Arterioscler Thromb Vasc Biol* 35(1):163–174.
75. Zhang Y, Li Q, Youn JY, Cai H (2017) Protein Phosphotyrosine Phosphatase 1B (PTP1B) in Calpain-dependent Feedback Regulation of Vascular Endothelial Growth Factor Receptor (VEGFR2) in Endothelial Cells. *J Biol Chem* 292(2):407–416.
76. Souza CM, et al. (2012) The phosphatase PTP-PEST/PTPN12 regulates endothelial cell migration and adhesion, but not permeability, and controls vascular development and embryonic viability. *J Biol Chem* 287(51):43180–43190.
77. Choorapoikayil S, Weijts B, Kers R, de Bruin A, den Hertog J (2013) Loss of Pten promotes angiogenesis and enhanced vegfaa expression in zebrafish. *Dis Model Mech* 6(5):1159–1166.

78. Stumpf M, Blokzijl-Franke S, den Hertog J (2016) Fine-Tuning of Pten Localization and Phosphatase Activity Is Essential for Zebrafish Angiogenesis. *PLoS One* 11(5):e0154771.

79. Stumpf M, Den Hertog J (2016) Differential requirement for pten lipid and protein phosphatase activity during zebrafish embryonic development. *PLoS One* 11(2):e0148508.

80. Phng LK, Gerhardt H (2009) Angiogenesis: A Team Effort Coordinated by Notch. *Dev Cell* 16(2):196–208.

81. Serra H, et al. (2015) PTEN mediates Notch-dependent stalk cell arrest in angiogenesis. *Nat Commun* 6:7935.

82. Fang J, Ding M, Yang L, Liu L-Z, Jiang B-H (2007) PI3K/PTEN/AKT signaling regulates prostate tumor angiogenesis. *Cell Signal* 19(12):2487–2497.

83. Ma J, et al. (2009) PTEN regulate angiogenesis through PI3K/Akt/VEGF signaling pathway in human pancreatic cancer cells. *Mol Cell Biochem* 331(1–2):161–171.

84. Tian T, et al. (2010) PTEN regulates angiogenesis and VEGF expression through phosphatase-dependent and -independent mechanisms in HepG2 cells. *Carcinogenesis* 31(7):1211–1219.

85. Bäumer S, et al. (2006) Vascular endothelial cell–specific phosphotyrosine phosphatase (VE-PTP) activity is required for blood vessel development. *Blood* 107(12):4754–4762.

86. Dominguez MG, et al. (2007) Vascular endothelial tyrosine phosphatase (VE-PTP)-null mice undergo vasculogenesis but die embryonically because of defects in angiogenesis. *Proc Natl Acad Sci U S A* 104(9):3243–3248.

87. Mori M, et al. (2010) Promotion of cell spreading and migration by Vascular Endothelial-Protein Tyrosine Phosphatase (VE-PTP) in cooperation with integrins. *J Cell Physiol* 224(1):195–204.

88. Nottebaum AF, et al. (2008) VE-PTP maintains the endothelial barrier via plakoglobin and becomes dissociated from VE-cadherin by leukocytes and by VEGF. *J Exp Med* 205(12):2929–2945.

89. Broermann A, et al. (2011) Dissociation of VE-PTP from VE-cadherin is required for leukocyte extravasation and for VEGF-induced vascular permeability in vivo. *J Exp Med* 208(12):2393–2401.

90. Mellberg S, et al. (2009) Transcriptional profiling reveals a critical role for tyrosine phosphatase VE-PTP in regulation of VEGFR2 activity and endothelial cell morphogenesis. *FASEB J* 23(5):1490–1502.

91. Vockel M, Vestweber D (2013) How T cells trigger the dissociation of the endothelial receptor phosphatase VE-PTP from VE-cadherin. *Blood* 122(14):2512–2522.

92. Winderlich M, et al. (2009) VE-PTP controls blood vessel development by balancing Tie-2 activity. *J Cell Biol* 185(4):657–671.

93. Frye M, et al. (2015) Interfering with VE-PTP stabilizes endothelial junctions in vivo via Tie-2 in the absence of VE-cadherin. *J Exp Med* 214(2):1–21.

94. Fournier P, Dussault S, Fusco A, Rivard A, Royal I (2016) Tyrosine Phosphatase PTPRJ/DEP-1 Is an Essential Promoter of Vascular Permeability, Angiogenesis, and Tumor Progression. *Cancer Res* 76(17):5080–5091.

95. Takahashi T, et al. (2003) A mutant receptor tyrosine phosphatase, CD148, causes defects in vascular development. *Mol Cell Biol* 23(5):1817–1831.

96. Spring K, Lapointe L, Caron C, Langlois S, Royal I (2014) Phosphorylation of DEP-1/PTPRJ on threonine 1318 regulates Src activation and endothelial cell permeability induced by vascular endothelial growth factor. *Cell Signal* 26(6):1283–1293.

97. Spring K, et al. (2012) Tyrosine phosphorylation of DEP-1 / CD148 as a mechanism controlling Src kinase activation , endothelial cell permeability , invasion and capillary formation. *Blood* 120(13):2745–2756.

98. Takahashi T, et al. (2006) A monoclonal antibody against CD148, a receptor-like tyrosine phosphatase, inhibits endothelial cell growth and angiogenesis. *Blood* 108(4):1234–1243.
99. Brunner PM, et al. (2011) Density enhanced phosphatase-1 (DEP-1) downregulates urokinase receptor (uPAR) surface expression in confluent endothelial cells. *Blood* 1(15):4154–4161.
100. Hendriks WJAJ, et al. (2013) Protein tyrosine phosphatases in health and disease. *FEBS J* 280(2):708–30.
101. Hendriks WJAJ, Pulido R (2013) Protein tyrosine phosphatase variants in human hereditary disorders and disease susceptibilities. *Biochim Biophys Acta - Mol Basis Dis* 1832(10):1673–1696.
102. Qu H, Tessier M-C, Hudson TJ, Polychronakos C (2005) Confirmation of the association of the R620W polymorphism in the protein tyrosine phosphatase PTPN22 with type 1 diabetes in a family based study. *J Med Genet* 42(3):266–270.
103. Sharp RC, Abdulrahim M, Naser ES, Naser SA (2015) Genetic Variations of PTPN2 and PTPN22: Role in the Pathogenesis of Type 1 Diabetes and Crohn's Disease. *Front Cell Infect Microbiol* 5:95.
104. Cerosaletti K, Buckner JH (2012) Protein tyrosine phosphatases and type 1 diabetes: genetic and functional implications of PTPN2 and PTPN22. *Rev Diabet Stud* 9(4):188–200.
105. Muzny DM, et al. (2012) Comprehensive molecular portraits of human breast tumours. *Nature* 487(7407):61–70.
106. Östman A, Hellberg C, Böhmer FD (2006) Protein-tyrosine phosphatases and cancer. *Nat Rev Cancer* 6(4):307–320.
107. Du Y, Grandis JR (2015) Receptor-type protein tyrosine phosphatases in cancer. *Chin J Cancer* 34(2):61–69.
108. Loh ML, et al. (2003) Somatic mutations in PTPN11 implicate the protein tyrosine phosphatase SHP-2 in leukemogenesis. *Blood* 103(6):2325–2332.
109. Bard-Chapeau EA, et al. (2011) PTPN11/Shp2 Acts as a Tumor Suppressor in Hepatocellular Carcinogenesis. *Cancer Cell* 19(5):629–639.
110. Tajan M, de Rocca Serra A, Valet P, Edouard T, Yart A (2015) SHP2 sails from physiology to pathology. *Eur J Med Genet* 58(10):509–525.
111. Yu ZH, et al. (2014) Molecular basis of gain-of-function LEOPARD syndrome-associated SHP2 mutations. *Biochemistry* 53(25):4136–4151.
112. Yu ZH, et al. (2013) Structural and mechanistic insights into LEOPARD syndrome-associated SHP2 mutations. *J Biol Chem* 288(15):10472–10482.
113. Wang J, et al. (2016) Inhibition of SHP2 ameliorates the pathogenesis of systemic lupus erythematosus. *J Clin Invest* 126(6):2077–2092.
114. Dong L, et al. (2016) Leukaemogenic effects of Ptpn11 activating mutations in the stem cell microenvironment. *Nature*:1–17.
115. Bakke J, Haj FG (2015) Protein-tyrosine phosphatase 1B substrates and metabolic regulation. *Semin Cell Dev Biol* 37:58–65.
116. Elchebly M, et al. (1999) Increased insulin sensitivity and obesity resistance in mice lacking the protein tyrosine phosphatase-1B gene. *Science* 283(5407):1544–1548.
117. Xue B, et al. (2007) Protein-tyrosine phosphatase 1B deficiency reduces insulin resistance and the diabetic phenotype in mice with polygenic insulin resistance. *J Biol Chem* 282(33):23829–23840.
118. González-Rodríguez Á, et al. (2010) Inhibition of PTP1B restores IRS1-mediated hepatic insulin signaling in IRS2-deficient mice. *Diabetes* 59(3):588–599.

119. Través PG, et al. (2014) Pivotal role of protein tyrosine phosphatase 1B (PTP1B) in the macrophage response to pro-inflammatory and anti-inflammatory challenge. *Cell Death Dis* 5(3):e1125.

120. Långberg E-C, Gu HF, Nordman S, Efendic S, Ostenson C-G (2007) Genetic variation in receptor protein tyrosine phosphatase sigma is associated with type 2 diabetes in Swedish Caucasians. *Eur J Endocrinol* 157(4):459–64.

121. Chagnon MJ, et al. (2006) Altered glucose homeostasis in mice lacking the receptor protein tyrosine phosphatase sigma. *Can J Physiol Pharmacol* 84(7):755–763.

122. Franke A, et al. (2010) Genome-wide meta-analysis increases to 71 the number of confirmed Crohn's disease susceptibility loci. *Nat Genet* 42(12):1118–1125.

123. Glas J, et al. (2012) PTPN2 gene variants are associated with susceptibility to both Crohn's disease and ulcerative colitis supporting a common genetic disease background. *PLoS One* 7(3):e33682.

124. Marcil V, et al. (2013) Association between the PTPN2 gene and Crohn's disease: dissection of potential causal variants. *Inflamm Bowel Dis* 19(6):1149–1155.

125. Scharl M, et al. (2009) Protection of Epithelial Barrier Function by the Crohn's Disease Associated Gene Protein Tyrosine Phosphatase N2. *Gastroenterology* 137(6):2030–2040.

126. McCole DF (2012) Regulation of epithelial barrier function by the inflammatory bowel disease candidate gene, PTPN2. *Ann N Y Acad Sci* 1257(1):108–114.

127. Scharl M, et al. (2012) Protein tyrosine phosphatase nonreceptor type 2 regulates autophagosome formation in human intestinal cells. *Inflamm Bowel Dis* 18(7):1287–1302.

128. Spalinger MR, et al. (2015) PTPN2 controls differentiation of $CD4^+$ T cells and limits intestinal inflammation and intestinal dysbiosis. *Mucosal Immunol* 8(4):918–929.

129. Blumenthal GM, Dennis P (2008) PTEN hamartoma tumor syndromes. *Eur J Hum Genet* 16(11):1289–300.

130. Choorapoikayil S, Kuiper R V, de Bruin A, den Hertog J (2012) Haploinsufficiency of the genes encoding the tumor suppressor Pten predisposes zebrafish to hemangiosarcoma. *Dis Model Mech* 5:241–247.

131. Hollander MC, Blumenthal GM, Dennis P (2011) PTEN loss in the continuum of common cancers, rare syndromes and mouse models. *Nat Rev Cancer* 11(4):289–301.

132. Pal A, et al. (2012) Mutations as a Cause of Constitutive Insulin Sensitivity and Obesity. *N Engl J Med* 367(11):1002–1011.

133. Zhou J, Parada LF (2012) PTEN signaling in autism spectrum disorders. *Curr Opin Neurobiol* 22(5):873–879.

134. Lv JW, Cheng TL, Qiu ZL, Zhou WH (2013) Role of the PTEN signaling pathway in autism spectrum disorder. *Neurosci Bull* 29(6):773–778.

135. Tilot AK, II TWF, Eng C (2015) Balancing Proliferation and Connectivity in PTEN-associated Autism Spectrum Disorder. *Neurotherapeutics* 12(3):609–619.

136. Amiri A, et al. (2012) Pten deletion in adult hippocampal neural stem/progenitor cells causes cellular abnormalities and alters neurogenesis. *J Neurosci* 32(17):5880–5890.

137. Tamrakar AK, Maurya CK, Rai AK (2014) PTP1B inhibitors for type 2 diabetes treatment: a patent review (2011 – 2014). *Expert Opin Ther Pat* 24(10):1101–1115.

138. Barr AJ (2010) Protein tyrosine phosphatases as drug targets: strategies and challenges of inhibitor development. *Future Med Chem* 2(10):1563–1576.

139. Swarbrick MM, et al. (2009) Inhibition of Protein Tyrosine Phosphatase-1B with Antisense Oligonucleotides Improves Insulin Sensitivity and Increases Adiponectin Concentrations in Monkeys. *Endocrinology* 150(4):1670–1679.

140. Krishnan N, et al. (2014) Targeting the disordered C-terminus of PTP1B with an allosteric inhibitor. *Nat Chem Biol* 10(7):558–566.

141. Yu B, et al. (2013) Targeting protein tyrosine phosphatase SHP2 for the treatment of PTPN11-associated malignancies. *Mol Cancer Ther* 12(9):1738–48.

142. Zhang X, et al. (2010) Salicylic acid based small molecule inhibitor for the oncogenic src homology-2 domain containing protein tyrosine phosphatase-2 (SHP2). *J Med Chem* 53(6):2482–2493.

143. Liu W, et al. (2013) Identification of Cryptotanshinone as an Inhibitor of Oncogenic Protein Tyrosine Phosphatase SHP2 (PTPN11). *J Med Chem* 56(18):7212–7221.

144. Chen Y-NP, et al. (2016) Allosteric inhibition of SHP2 phosphatase inhibits cancers driven by receptor tyrosine kinases. *Nature* 535(7610):148–52.

Chapter 3

Studying Protein-Tyrosine Phosphatases in Zebrafish

Alexander James Hale[1,2] and Jeroen den Hertog[1,2]

1. Hubrecht Institute-KNAW and University Medical Center Utrecht, The Netherlands
2. Institute of Biology Leiden, Leiden University, The Netherlands

SUMMARY

Protein-tyrosine phosphatases (PTPs) are a large family of signal transduction regulators that have an essential role in normal development and physiology. Aberrant activation or inactivation of PTPs is at the basis of many human diseases. The zebrafish, *Danio rerio,* is being used extensively to model major aspects of development and disease as well as the mechanism of regeneration of limbs and vital organs, and most classical PTPs have been identified in zebrafish. Zebrafish is an excellent model system for biomedical research because the genome is sequenced, zebrafish produce a large number of offspring, the eggs develop outside the mother and are transparent, facilitating intravital imaging, and transgenesis and (site-directed) mutagenesis are feasible. Together, these traits make zebrafish amenable for the analysis of gene and protein function. In this chapter we cover three manipulations of zebrafish embryos that we have used to study the effects of PTPs in development, regeneration and biochemistry. Micro-injection at the one-cell stage is at the basis of many zebrafish experiments and is described first. This is followed by a description for measuring regeneration of the zebrafish embryo caudal fin-fold, a powerful and robust physiological assay. Finally, the considerable but manageable troubleshooting of several complications associated with preparing zebrafish embryos for immunoblotting is explained. Overall, this chapter provides detailed protocols for manipulating zebrafish embryo samples with a compilation of tips collected through extensive experience from the zebrafish research community.

1. INTRODUCTION

Protein-tyrosine phosphatases (PTPs) are a large family of signal transduction regulators, determining rate and duration of phosphotyrosine (pTyr) phosphorylation cascades [1]. Disruption of PTP activity leads to aberrant pTyr signalling and is at the basis of many human diseases [2]. Much is already known of the mechanisms PTPs employ to regulate signal transduction [3] and the regulation of their dephosphorylating activity [4-6]. Yet, a full appreciation of the importance of temporal and spatial control of PTP activity is best acquired *in vivo*. Model organisms used to acquire such insights include the invertebrates *Drosophila* [7] and *C. elegans* [8] and the vertebrates *Danio rerio* [9], mouse [10] and rat [11].

The zebrafish *Danio rerio* is being used extensively to model major aspects of development [12] and diseases including cancer [13,14], metabolic disease [15-17] and cardiovascular disease [18]. Zebrafish are even used to study the mechanism of regeneration of limbs and vital organs [19,20]. Evidently, zebrafish studies are a key aspect of translational research and are enabling advancements in human health [21]. Zebrafish are oviparous, provide up to 200 embryos per mating pair per week and develop within 5 days, with most organs forming within 48 hours. Many existing genetic mutants are available from stock centres (Zebrafish International Resource Center in Eugene, USA, and European Zebrafish Resource Center in Karlsruhe, Germany) and mutagenesis is highly feasible using optimized transcription activator-like effector nucleases (TALENs) [22] or the combination of Clustered Regularly Interspaced Short Palindromic Repeats (CRISPR) with the CRISPR associated protein (CAS) [23-25]. Transient over-expression or stable transgenesis can readily be achieved through micro-injection of synthetic messenger RNA (RNA) or plasmid DNA respectively at the one-cell stage [26]. In addition, mutagenesis-based gene inactivation is carried out using reagents such as N-ethyl-N-nitrosourea (ENU) to generate random single nucleotide mutations [27].

Zebrafish embryos are transparent, allowing for easy analysis of developmental progression and defects as well as disease phenotypes. Intravital imaging of fluorescent markers expressed in a tissue- or cell type-specific manner provides a powerful tool for studying developmental processes. This has been taken advantage of extensively to study angiogenesis [28], lymphangiogenesis [29], convergence and extension cell movements during development [30] and even to capture embryonic development in 3D [31,32]. Intravital imaging of fusion proteins facilitates the analysis of protein

localization, protein-protein interactions and function in a whole organism *in vivo*. In addition, several techniques are now being refined and will augment the advantages of zebrafish as an experimental system. These include proteomics analysis of zebrafish embryos using mass-spectrometry following selection by immunoprecipitation [33-35], analysis of the plasma proteome following blood collection [36] and derivation of cell lines from single embryos [37].

Finally, the relative simplicity of adding compounds to either the water of the adults or the medium of the embryos, combined with the possibility for large sample number and rapid reproducibility has led to several bioactive compounds screens [18,38]. Notably, combining knock-outs or embryos with transient over-expression with timed drug treatments provides an unparalleled opportunity to pin-point the exact temporal role of proteins *in vivo*.

An important experimental consideration is that the zebrafish genome was duplicated early in evolution [39,40]. Whilst some of the duplicated chromosomes were lost, the duplicated genes that remain may have complementary or diverging expression patterns and exhibit redundant or complementary functions. Therefore, gene duplications may complicate the creation of knock-out mutants by requiring two redundant genes to be targeted. The translational value is another essential consideration when choosing an experimental system and the reason the zebrafish is regularly used to model disease is in part due to 84% of human genes associated with a disease having a zebrafish counterpart [41].

All classical PTPs, except *ptpn7*, *ptpn12* and *ptpn14*, have been identified in the zebrafish genome and 14 are duplicated [42]. Van Eekelen et al. 2010 also characterize expression duration and localization using *in situ* hybridization, identifying that some of the duplicated PTP pairs have divergent expression patterns, indicative of diverging functions. A good example of the complexity arisen from PTP duplication is that of *ptpn11*, encoding the Shp2 protein. Bonetti et al. 2014 demonstrate that zebrafish *ptpn11a* and *ptpn11b* encode highly homologous proteins, Shp2a and Shp2b respectively. Yet, whilst *ptpn11a*$^{-/-}$ mutants have severe developmental defects and are embryonic lethal, *ptpn11b*$^{-/-}$ mutants show no obvious developmental defects. This difference may suggest that Shp2a and Shp2b proteins are functionally distinct. Shp2b does have a function in development, because *ptpn11a*$^{-/-}$ *ptpn11b*$^{-/-}$ mutants exhibit a slightly more severe phenotype than *ptpn11a*$^{-/-}$ mutants. Furthermore, severe developmental defects displayed by *ptpn11a*$^{-/-}$ *ptpn11b*$^{-/-}$ double mutant embryos are rescued by transient over-expression of either Shp2a or Shp2b, demonstrating functional similarity

of Shp2a and Shp2b proteins. The expression patterns of *ptpn11a* and *ptpn11b* are distinct; *ptpn11a* is constitutively expressed at a high level throughout development, whereas *ptpn11b* expression is at a relatively low level during early development and increases steadily through later stages. Hence, we conclude that the difference in expression patterns of *ptpn11a* and *ptpn11b*, rather than an intrinsic difference in protein function of Shp2a and Shp2b is at the basis of the difference in function of *ptpn11a* and *ptpn11b* during development [43]. The accompanied complexity of gene duplication can be used to extensively delineate gene function and the advantages of zebrafish as an experimental system make it ideal for elucidating the intricate function and regulation of PTPs *in vivo*. Hence, zebrafish are often used to understand the role of PTPs in signalling in development [44-47] and, lately more, in disease [34].

2. MATERIALS

All solutions are prepared in double-distilled, deionized MilliQ filtered water (resistivity of 18MΩ cm at 25°C).

2.1 Micro-injection

1. Brightfield/Nomarski optics stereo-microscope (e.g. Leica MZ9.5)
2. Micromanipulator (World Precision Instruments)
3. Pneumatic microinjector (Picopump PV830, World Precision Instruments)
4. Nitrogen (N_2) gas
5. Glass capillaries: Outer diameter 1mm, Inner diameter 0.78mm, length 100mm (Harvard Apparatus)
6. 0.01mm micrometre slide (e.g. TS-M1 from www.labshops.com)
7. 10µl microloader pipette tips (Eppendorf)
8. 0.5% Phenol red (Sigma)
9. Thermomixer (Eppendorf)
10. E3 medium: 5mM NaCl, 0.17mM KCl, 0.33mM $CaCl_2$, 0.33mM $MgSO_4$
11. 0.05% Methylene blue (Sigma)
12. Micropipette puller P97 (Sutter Instruments)
13. Putty or tape
14. Slanted lane mould (TU-1, Adaptive Science Tools)
15. Plastic 15cm plate (Corning)

16. Plastic 10cm plate (Corning)
17. Ultra Pure agarose (Invitrogen)
18. 70% ethanol
19. Mineral Oil (Sigma)

2.2 Regeneration assay

1. Stereo-microscope (e.g. Leica MDG17)
2. Brightfield/Nomarski optics stereo-microscope with camera function (e.g. Leica M165FC with Leica DFC420C camera)
3. 0.4% MS222: 0.4% ethyl 3-aminobenzoate methanesulfonate salt (MS222), 1M Tris-HCl pH7.5
4. Stainless steel surgical blade (Swann-Morton no.11)
5. Plastic Pasteur pipette
6. Glass Pasteur pipette
7. Plastic 10cm dish (Corning)
8. Plastic multi-well plates (Corning)
9. 10µl microloader pipette tips (Eppendorf)
10. E3 medium: 5mM NaCl, 0.17mM KCl, 0.33mM $CaCl_2$, 0.33mM $MgSO_4$.

2.3 Tissue lysis for protein extraction

1. 1.5ml tubes (Eppendorf)
2. Mini-pestle (to fit in the 1.5ml tubes)
3. 1ml syringe (BD Biosciences)
4. 0.2-0.8mm needles (BD Biosciences)
5. Sonicator (e.g. Diagenode Bioruptor Standard)
6. Degassed lysis buffer: 25mM (4-(2-hydroxyethyl)-1-piperazineethanesulfonic acid (HEPES) pH 7.4, 150mM NaCl, 0.25% deoxycholate, 1% triton X-100, 10mM $MgCl_2$, 1mM Ethylenediaminetetraacetic acid (EDTA), 10% glycerol
7. RIPA buffer: 25mM Tris-HCl pH7.6, 150mM NaCl, 1% NP-40, 1% sodium deoxycholate, 0.1% sodium dodecyl sulphate
8. Ginzburg fish Ringers buffer: 111.2mM NaCl, 3.35mM KCl, 2.38mM $NaHCO_3$.
9. Liquid nitrogen (N_2)
10. Thermomixer (Eppendorf)
11. Cold centrifuge (e.g. SciQuip 1-15PK)
12. Protease inhibitors Aprotinin, and Leupeptin (both 1mg/ml)

13. Phosphatase inhibitors Sodium Fluoride (0.5M), beta-Glycerophosphate (1M), and Sodium Orthovanadate (200mM)
14. 70% ethanol
15. 2x Laemmli sample buffer: 2% β-mercaptoethanol, 20% glycerol, 0.125M Tris-HCl pH6.8, 4% sodium dodecyl sulphate, (a pinch) bromophenol blue

3. METHODS

The underlying principle of the protocols and notes that follow is that zebrafish embryos are a living organism, useful for analysing phenotypes, but can also be considered a compact factory of cells malleable to existing molecular techniques. All procedures involving zebrafish described were approved by the local animal experiments committee and performed according to local guidelines and policies in compliance with national and European law. Zebrafish maintenance and breeding were performed following published protocols [48].

An absolute must for the genetic manipulation of zebrafish is the skill to microinject at the one-cell stage. This will be covered first (section 3.1) and following this a plethora of manipulations are available. Here, a description for measuring regeneration of the zebrafish embryo caudal fin-fold, a powerful and robust physiological assay, will be described (section 3.2). Also, the method of lysing zebrafish tissue for protein extraction to perform SDS-PAGE and immunoblotting will be detailed (section 3.3), which requires considerable but manageable troubleshooting due to the complications that arise from obtaining a homogenous zebrafish cell lysate and lack of antibodies that recognize the zebrafish orthologue.

In section 3.1 we cover the use of micro-injection for introduction of alien genetic material into an organism, which began in 1971 when it was used to introduce DNA into xenopus oocytes [49]. Since then the technique has been adapted for micro-injection of zebrafish embryos at the one-cell stage and early mouse blastocysts for transgenesis [50,51] and cells in culture [52]. A detailed video protocol for micro-injection of zebrafish embryos can be found on Jove entitled “Microinjection of zebrafish embryos to analyse gene function” [53]. Needles for holding and injecting RNA or DNA are made using a glass capillary micropipette puller, which contains a heating filament that slowly melts the glass and as the two halves separate the tip is stretched to the

correct diameter. Each machine model will need to be calibrated according to the manufacturer's instructions before use.

RNA micro-injection leads to efficient, and usually high, expression within several hours and will be described below, though the reader can consider all uses of "RNA" interchangeable with "DNA". The only significant factor when micro-injecting DNA is that accuracy needs to be high to ensure that the DNA ends up in the cell. For this reason, significant effort is made to align embryos properly in the micro-injection plate to improve accuracy of injecting directly into the cell. Micro-injection is a technique that develops and improves with experience. It is easy to learn but difficult to teach as a lot is based on a singular coordinated movement of fingers moving the needle into the embryo and feet ejecting the RNA or DNA, and this is a "comfortable" feeling once mastered. For example, it takes practice to be able to estimate just how much of the needle needs to be shortened once mounted; there is no way to measure this. Practice is essential, and once the technique is acquired the individual tends to improve without any further guidance.

In section 3.2 a zebrafish embryo caudal fin-fold regeneration assay is described. Some urodeles and teleosts are capable of epimorphic regeneration, perfect or near-perfect replacement of lost tissue, throughout their lifetime [54]. Zebrafish are capable of regenerating multiple tissues, including fins, the brain, retina, spinal cord and heart [19]. Zebrafish are therefore an excellent model to study and understand the mechanism of epimorphic regeneration. The results that emerge from such research may pave the way to enabling adult mammal organs to regenerate, most of which are currently limited to inflammation and formation of a collagen-rich connective tissue scar following injury [55]. Adult zebrafish caudal fin regeneration takes 10-12 days to complete. In comparison, embryo caudal fin-folds only take three days, making the embryonic regeneration assay an efficient and reproducible technique. A previously established zebrafish embryo caudal fin-fold regeneration model [56] was adapted to amputate at 2 days post fertilization and regeneration is then completed by three days post amputation (5 days post fertilization).

Importantly, as regeneration rate is higher in embryos, wound healing is also more rapid. For this reason, it is paramount that a picture of the amputated caudal fin-fold be taken as soon as possible to capture the wound margin as accurately as possible. Another consideration with a zebrafish embryo caudal fin-fold regeneration assay is that changes in regeneration rate could also be due to changes in rate of embryonic development. It's ideal to compare amputated embryos with same stage

uncut embryos and, therefore a picture of an uncut embryo is taken at the same time as the embryo with the wound margin. This technique can easily be combined with micro-injection of RNA or DNA or drug treatments.

Section 3.3 describes tissue lysis of whole zebrafish embryos for extraction of protein. Zebrafish embryos, up to 6 days, can be considered tissue extracts for applying molecular techniques. Thus, the method remains the same regardless of age but becomes more laborious with older, more defined tissue. Preparation of zebrafish embryos for SDS-PAGE requires de-yolking, and then lysis buffer is applied before the sample is homogenized. A general method can be found on the ZFIN database [57] but we have developed our own lysis buffers and homogenization techniques for specific uses of the protein extract and this will be explained in detail below.

Zebrafish embryos have a yolk sac, providing nutrients for growth until day 6 when the embryos can eat particle food [58]. This yolk sac contains a high concentration of vitellogenin, a phospholipo-glycoprotein composed of multiple subunits, the most predominant two at around 150kDa and 80kDa. Unfortunately, the yolk proteins interfere with detection of specific proteins by immunoblotting, presumably due to the high expression levels of the yolk proteins. Particularly detection of specific proteins of similar sizes as the yolk proteins is problematic. This interference can be largely reduced by de-yolking embryos using Ginzburg fish ringers solution [59]. After de-yolking, lysis buffer is applied. We use one of two lysis buffers, each has advantages and disadvantages. Whereas RIPA lysis buffer is fast and provides high yield, the presence of SDS may disrupt delicate protein-protein interactions. In comparison, degassed lysis buffer will yield less protein but the absence of SDS protects delicate protein-protein interactions, which is useful if intending to perform co-immunoprecipitation. Following the choice of lysis buffer there are three options for homogenization. The least challenging, but also the least effective in terms of yield, is using a mini-pestle to crush the embryo in the 1.5ml tube containing lysis buffer. A higher yield can be obtained by using a syringe and needle to aspirate and push the tissue through a small (<0.4mm) needle opening (shearing). Complications arise with larger tissue (e.g. adult zebrafish fin clips and embryos approaching 5 days post fertilization) which may clog the needle. Though laborious, this complication can be resolved by first choosing an appropriately sized (>0.6mm) needle for the dense tissue extract and repeating homogenization with a smaller needle afterwards. The final alternative is to use a sonicator, which works well on embryos up to 4 days old but may take considerably longer on defined tissue such as adult zebrafish fin-clips.

Following successful lysis of zebrafish tissue, the lysate can be loaded onto an SDS-PAGE gel following a standard protocol. The only exception is that a protein concentration assay (e.g. Biorad Bradford assay) is not performed on zebrafish embryos because the sample is less pure than from cells and there is an abundance of yolk protein which will skew the estimation. Instead protein level is correlated with the number of embryos per unit volume of lysis buffer used. A standard protocol for immunoblotting can also be applied. A far greater problem is the sheer lack of antibodies that recognize the zebrafish protein homologues. It is not uncommon that when the zebrafish and mammalian homologues share a high percentage amino acid sequence similarity, the antibody raised against the mammalian homologue does not bind the zebrafish homologue. Even when the epitope sequence is conserved the antibody doesn't necessarily work for the zebrafish homologue; sometimes the antibody will simply not bind anything but more often the problem is increased non-specific binding (including sequestration of the antibody by the yolk protein). This antibody issue may be partially circumvented by raising an antibody against the purified target zebrafish protein. Though, functionality of these antibodies is not necessarily guaranteed and should be tested thoroughly for validation. Also of note is that these antibodies don't always have the same efficiency on endogenous proteins in zebrafish embryos. Hopefully, with time, a range of antibodies produced and validated by different labs will become available on the commercial market. Some are already available at the Zebrafish International Resource Centre (ZIRC).

3.1 Micro-injection

1. Dissolve ultra-pure agarose in E3 medium with 0.01% methylene blue to prepare a 2% agarose solution.
2. Pour 2% agarose into a plastic 10cm dish and gradually apply the plastic lane mould onto the surface of the agarose. Leave new micro-injection plate (**Fig. 1**) to set (*see* **Note 1**).

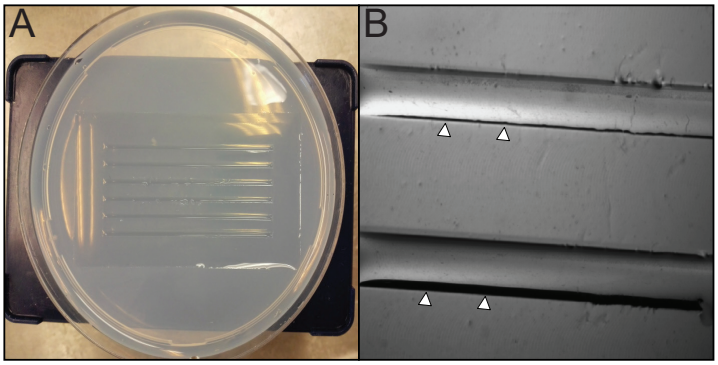

Fig. 1. Example of a micro-injection plate made of 2% agarose (**A**) and higher magnification showing the grooves with the bevelled edge (arrow heads) on the bottom side (**B**).

3. Remove the mould and pour E3 medium with 0.01% methylene blue to cover the surface. Store at 4°C (*see* **Note 2**).
4. Prepare RNA by diluting as required in a mixture of MilliQ water and 0.5% phenol red (*see* **Note 3**).
5. Heat RNA for 5-10mins at 65°C and 1150rpm in a thermomixer (*see* **Note 4**). Keep RNA on ice.
6. Switch on pneumatic microinjector and open the N_2 gas valve. The "regulator" pressure should not exceed 30psi.
7. Wipe base of stereo-microscope with 70% ethanol and adjust lamp brightness as desired.
8. Place needle under stereo-microscope and use the micrometre slide to determine the point at which the needle tip width is equal to 20µm. Use tweezers to remove the excess of the needle that extends beyond this point.
9. Use microloader pipette tips to transfer 1-2µl of RNA into the cut needle.
10. Position micromanipulator and mount needle half way up the shaft of the pressure dispenser.
11. Position needle tip in a small dish of mineral oil and check pneumatic microinjector is set to "gated".
12. In "gated" mode apply pressure to the foot pump for 1-2sec. to eject some RNA solution (*see* **Note 5**).
13. Switch pneumatic microinjector to "timed," switch the "range" to "100ms" and the "period" to maximum "2.0" so that duration of ejection is 200ms. Now, a single push of the foot pump will eject a single drop of RNA.

14. Press down on foot pump to eject a single drop of RNA into the mineral oil. Use the micrometre slide to measure size of droplet (*see* **Note 6**).
15. Adjust droplet size to 1nl by first reducing the duration of ejection. Lower the "period" slightly and repeat step 15. If droplet size is still too small when duration of ejection is 70ms ("period" is "0.70"), use the tweezers to remove more of the needle tip and repeat adjustment with "period" (*see* **Note 7**). Once a droplet of 1nl is obtained rest the needle in mineral oil.
16. Collect fresh fertilized embryos in a plastic 10cm dish with E3 medium. From this point on you have ~30mins before the single cell of the embryo divides. Work fast (*see* **Note 8**).
17. Transfer embryos to the lanes in the microinjection plate using a plastic Pasteur pipette (*see* **Note 9**).
18. Under the stereo-microscope the single cell of the embryo will be clearly visible. Position embryo such that the cell is at the top (*see* **Note 10**).
19. Use micromanipulator to adjust needle position and penetrate through the chorion and into the cell of the embryo. Almost simultaneously, press the foot pump to eject some RNA into the cell and withdraw the needle (*see* **Note 11**).
20. Move to the next embryo and repeat the micro-injection until the desired number of embryos has been micro-injected.
21. When finished use a plastic Pasteur pipette and E3 medium with 0.01% methylene blue to rinse the embryos into a plastic 10cm dish with fresh E3 medium with 0.01% methylene blue. Incubate at 28.5°C (*see* **Note 12**).
22. Discard needle in sharps bin and remaining embryos in designated waste bin. Close the N_2 gas valve, switch pneumatic microinjector to "gated" again and use foot pump to eject remaining N_2 gas. Switch off pneumatic microinjector and stereo-microscope light.

If injecting RNA encoding a fluorescent protein, a standard fluorescence microscope with appropriate filter can be used to visually assess success rate. It is common for protein expression to vary between embryos (**Fig. 2**) as each embryo is micro-injected in a slightly different position and embryos have varying rates of protein synthesis, depending on health and developmental stage. Practice micro-injections using mRNA encoding Green Fluorescent Protein (GFP) is convenient for evaluation of success rate. The technique is considered "mastered" once a success rate of 95% or higher is reached.

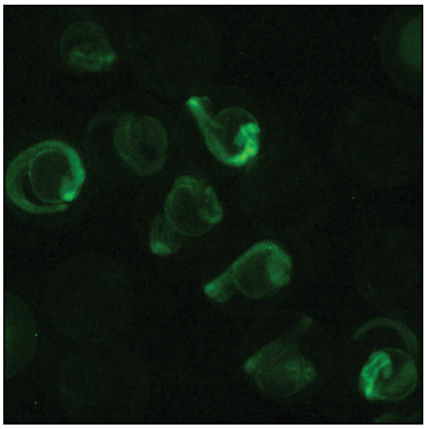

Fig. 2. 24 hours post fertilization zebrafish embryos, still in their chorion, displaying variation in GFP protein expression between embryos following micro-injection of GFP RNA.

RNA or DNA injection into the cell at the one-cell stage of zebrafish should lead to expression in all subsequent daughter cells, but mosaicism is frequently observed. If RNA is micro-injected at a late one-cell stage or whilst the first cell division is in progress mosaicism in the form of patchy expression, with only small clusters of cells translating the RNA, may arise (**Fig. 3A**). When RNA is micro-injected accurately there may be considerably less mosaicism but it will still be present (**Fig. 3B**). Depending on the purpose of the experiment, the presence of mosaicism can offer some advantages in that a comparison can be made, for example, between the same population of cells expressing the micro-injected protein and those without in the same embryo.

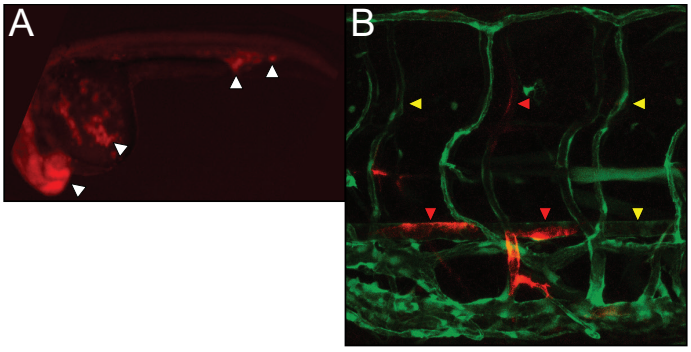

Fig. 3. Examples of non-ubiquitous expression following micro-injection of RNA. (**A**) Example of patchy expression from RNA micro-injection. An embryo micro-injected with RNA encoding wild-type human Pten tagged with mCherry is imaged at 2dpf. Mosaic mCherry expression is found in a few clusters of cells scattered around the body of the embryo (arrow heads), suggesting RNA was not micro-injected at the one-cell stage. (**B**) Example of mosaic expression in the trunk of an embryo at five days post fertilization. A transgenic embryo expressing *flt4:mCit* to mark the vasculature, shown in green, is micro-injected with plasmid DNA encoding *prox1a:KalTA4,UAS:tagRFP*, shown in red, at the one-cell stage. Despite accurate micro-injection only some vessels express RFP (red arrow heads), demonstrating mosaicism. Yellow arrow heads show similar vessels without RFP expression for comparison.

3.2 Regeneration assay

1. Dechorionate embryos using tweezers
2. Anaesthetise embryos by transferring to 0.1% MS222 in E3 medium with 0.01% methylene blue for 2-4mins (*see* **Note 13**).
3. Place the lid of a 10cm plastic dish over the light source of a stereo-microscope (*see* **Note 14**).
4. Transfer one embryo at a time to surface of plastic lid in a droplet of 0.1% MS222 in E3 medium with 0.01% methylene blue using a plastic Pasteur pipette (*see* **Note 15**).
5. Use a stainless steel surgical blade to amputate the caudal fin-fold of the zebrafish embryo immediately distal to the notochord under the stereo-microscope (*see* **Note 16**).
6. Use a glass Pasteur pipette to transfer embryo to fresh 0.1% MS222 in E3 medium with 0.01% methylene blue (*see* **Note 17**).
7. Capture wound margin of amputated zebrafish embryo caudal fin-fold using a stereo-microscope (Leica M165FC) with an attached camera (Leica DFC420C) (*see* **Note 18**).
8. Wash embryo in fresh E3 medium.
9. Use a glass Pasteur pipette to transfer embryo to a well in a multi-well plate containing fresh E3 medium with 0.01% methylene blue (*see* **Note 19**).
10. Repeat steps 4-9 until multi-well plates of both amputated and uncut controls are filled. Incubate embryos at 28.5°C for 3 days (*see* **Note 20**).
11. Prepare 0.2% MS222 in E3 medium by mixing half volume 0.4% MS222 and half volume E3 medium. Use a plastic Pasteur pipette to add 3-4 droplets of 0.2% MS222 in E3 medium to each well.
12. Use a glass Pasteur pipette to transfer one embryo per time to a 10cm plate containing fresh 0.1% MS222 in E3 medium with 0.01% methylene blue.
13. Capture size of zebrafish embryo caudal fin-fold using a stereo-microscope (e.g. Leica M165FC) with an attached camera (e.g. Leica DFC420C) (*see* **Note 21**).
14. Repeat steps 12-13 until all embryos of multi-well plates for both amputated and uncut controls have been imaged.

The images captured at 2 and 5 days post fertilization are of uncut controls and amputated embryos (**Fig. 4**). The change in zebrafish embryo caudal fin-fold length after three days is calculated by subtracting the length of the fin-fold from the tip of the

notochord at day five from that at day two for each embryo. This is easily quantified using the measure tool in ImageJ and the difference calculated is a measure of regenerative outgrowth.

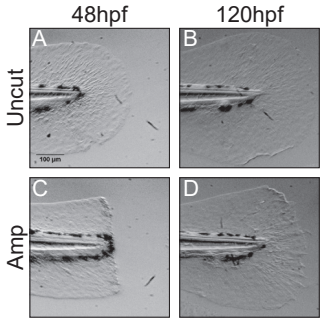

Fig. 4. Brightfield images of the caudal fin-fold of zebrafish embryos. Fin-fold margins are captured at 48 hours post fertilization (**A**, **C**), and again at 5 days post fertilization (**B**, **D**), of uncut controls (**A**, **B**) and embryos amputated adjacent to the notochord (**C**, **D**). Scale bar is equivalent for all panels.

3.3 Tissue lysis for protein extraction

1. Dechorionate embryos using tweezers (*see* **Note 22**).
2. Transfer embryos to a 1.5ml tube, 96-well plate or similar. Remove as much system water or E3 medium as possible.
3. Prepare Ginzburg fish Ringers solution by adding protease and phosphatase inhibitors (10µl/ml Sodium Fluoride, 5µl/ml beta-Glycerophosphate, 5µl/ml Sodium Orthovanadate, 1µl/ml Aprotinin, 1µl/ml Leupeptin) and add sufficient volume to the embryos to allow repeated pipetting with a P200 tip (~600µm wide).
4. Repeatedly pipette up and down in a gentle steady motion or invert regularly. Do not create air bubbles. Alternatively, place multiple embryos in a well of a 6-well plate filled with Ginzburg fish Ringers solution and place plate on a thermomixer set to 28.5°C and 400-800rpm for 30-45mins (*see* **Note 23**).
5. Wash de-yolked embryos with fresh Ginzburg fish Ringers solution and transfer to chosen vessel (1.5ml tube or 96-well plate)
6. Centrifuge briefly at 4°C to collect embryos at bottom of tube or well.
7. Aspirate Ginzburg fish Ringers solution and snap-freeze embryos in liquid nitrogen (*see* **Note 24**).
8. Defrost frozen tissue on ice.
9. Prepare chosen lysis buffer by adding protease and phosphatase inhibitors (10µl/ml Sodium Fluoride, 5µl/ml beta-Glycerophosphate, 5µl/ml Sodium Orthovanadate, 1µl/ml Aprotinin, 1µl/ml Leupeptin) and add volume according to age:

Tissue age	Volume lysis buffer
<24hpf	1µl /embryo
24-48hpf	1-2µl /embryo
48-96hpf	2-5µl /embryo
>96hpf	>5µl /embryo
Adult fin clips	>10µl

Next, there are three homogenization options available for proceeding with tissue lysis; the steps required for homogenization using a mini-pestle (A), a syringe and needle (B), or sonication (C), are described below.

A. Mini-pestle homogenization (1.5ml tubes only):

10A. Quickly, with the tissue still frozen, start applying pressure using a mini-pestle that fits in a 1.5ml tube (*see* **Note 25**).

11A. Withdraw pestle and use a pipette to wash head of pestle to maximize amount of lysate collected.

12A. Clean pestle by rinsing with 70% ethanol followed by water and repeat steps 10-11 for each sample.

13A. Rest on ice.

B. Syringe and needle homogenization:

10B. Wait for tissue to defrost in lysis buffer.

11B. Attach a sterile needle, width 0.2-0.8mm, to a 1ml syringe. No larger than 0.2mm is highly recommended for 24hpf.

12B. Aspirate and dispense suspension repeatedly until tissue has been completely sheared (*see* **Note 26**).

13B. Rest on ice.

C. Sonication homogenization:

10C. Wait for tissue to defrost in lysis buffer.

11C. Incubate on ice for 30mins

12C. Sonicate at “high” intensity for 15mins. with a repeated cycle of 30sec. ON, followed by 30sec. OFF.

13C. Rest on ice.

14. Once homogenized with chosen method centrifuge samples at 14,000xrpm and 4°C for 20mins.
15. Transfer supernatant to a fresh tube or plate and discard the pellet. Can store supernatant at -80°C at this point if required.
16. Mix equal volume lysate and 2x laemmli buffer.
17. Boil samples for 5-10mins (*see* **Note 27**).
18. Store at -20°C or continue loading samples onto an SDS gel.

Please note that there are many variations on the de-yolking and homogenization procedures. For example, de-yolking can be carried out after mini-pestle homogenization by centrifuging lysate and re-suspending the pellet in Ginzburg fish Ringers solution. The sample is then centrifuged again to remove the Ginzburg fish Ringers solution and re-suspended in 1x sample buffer (created by mixing equal volumes of chosen lysis buffer and 2x laemmli buffer). This way the de-yolking procedure is more convenient but a possible consequence is greater variation in protein concentration between samples as some lysed protein may have been lost in the multiple centrifugations where supernatants are discarded. Another alternative is to only disrupt the integrity of the embryos a little using mini-pestle homogenization and follow that with sonication to achieve more efficient lysis. One's choice will be determined by a combination of purpose for the lysate, embryo age and, ultimately, experience.

Preparation of zebrafish embryo lysates requires more diligence than for cell lysates. This is partly due to the high protein content compared to cultured cells, resulting in the bands being "fatter" and more "smiley" (**Fig. 5**). This can also cause protein bands to run slightly slower, but offsets size estimation by no more than 5kDa.

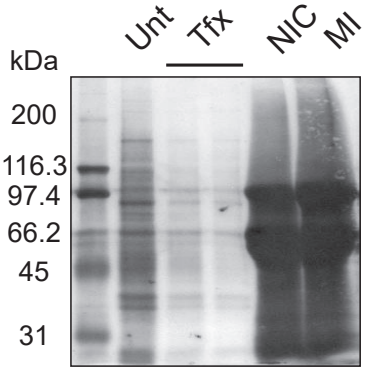

Fig. 5. Coomassie stain of PVDF membrane showing differences between HEK293T cells lysed with RIPA buffer (lanes 2-4) and zebrafish embryos lysed with RIPA buffer and subjected to mini-pestle homogenization (lanes 5 and 6). A typical experiment comparing non-transfected (Unt) and transfected (Tfx) HEK 293T cells with non-injected control (NIC) and micro-injected (MI) zebrafish embryo samples (7.5 embryo equivalents per lane). Lane 1 contains a molecular weight marker.

The right combination of de-yolking, lysis buffer and homogenization optimizes the result. For example, embryos can be lysed in RIPA buffer prepared for SDS-PAGE using mini-pestle homogenization without dechorionating and de-yolking (**Fig. 6A**). But when embryos are dechorionated, de-yolked, lysed using degassed lysis buffer and prepared for SDS-PAGE using mini-pestle homogenization the result is less yield but almost as clean as that obtained from pure cell lysate (**Fig. 6B**). Then again, **Fig. 6B** clearly shows that de-yolking can lead to unequal protein concentration between samples, as a result of both the lysate that remains on the head of the pestle and the centrifugation step required.

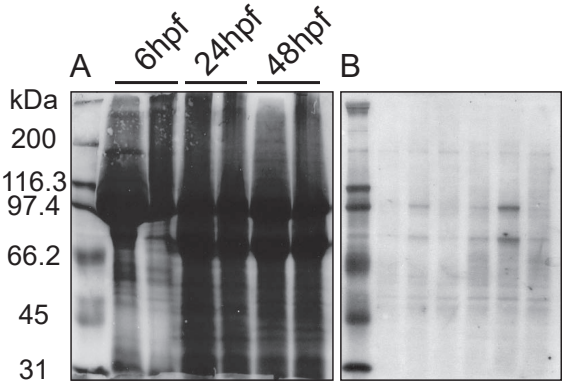

Fig. 6. Coomassie stains of PVDF membranes containing zebrafish embryo samples. (**A**) Samples, not dechorionated or de-yolked, lysed in RIPA buffer and subjected to mini-pestle homogenization (5 embryo equivalents per lane). Zebrafish embryos were lysed at 6, 24 and 48 hours post fertilization (hpf). Notice how "fat" and "smiley" the bands are. (**B**) Samples after dechorionating, de-yolking,lysis in degassed lysis buffer and subjected to mini-pestle homogenization (1 embryo per lane). Zebrafish embryos were lysed at 48hpf. Notice that the protein content is considerably less, but that the lysate profile is more "clean" and similar to that of the cell lysates seen in figure 5. A typical experiment with six different conditions is depicted. Lane 1 in (**A**) and (**B**) contains a molecular weight marker.

4. NOTES

1. The plastic mould is embossed with ramps with a 45° bevelled side (**Fig. 1B**). This aids micro-injection as the embryo will be pushed into the corner of the lane, allowing the needle to more easily penetrate the chorion and yolk or cell.
2. The agarose microinjection plates will keep for 1-2 weeks, after which moulds will begin to grow and the borders of the lanes begin to soften and break. The moulds do not interfere with the embryos as long as the embryos are washed afterwards but the breaks in the lanes can inconvenience injections.
3. In general, not more than 500pg of RNA is injected in zebrafish embryos (this is achieved using 1nl of RNA at 500ng/µl). The phenol red is only used as a dye to observe successful injection (once competent this aid is no longer required) and 1µl for every 15µl is more than sufficient.
4. Heating the RNA removes secondary structures such as hair-pin loops. This ensures that most of the RNA injected is available for translation and ultimately increases the efficiency of micro-injection. This step is not necessary if injecting DNA.
5. This action removes air bubbles from the RNA. The RNA is now under pressure. If "hold" pressure is too great the RNA will now begin to leak from the needle tip, adjust if necessary.
6. Calibration of the RNA droplet to 1nl is measured using a 0.01mm micrometre slide. Briefly, according to $V = 4/3\pi r^3$, a droplet of 1nl has a radius of 62µm and the diameter is hence 124µm. The micrometre slide has divisions of 10µm; meaning 1nl is equivalent to 12 divisions. The needle width is measured to approximately 20µm wide prior to mounting and the width of each new needle then needs to be adjusted to create a 1nl droplet using the micrometre slide to calibrate.
7. Duration of ejection MUST NOT be <70ms ("period" not <0.70) as this results in ejection of unreliable droplet size with repeated injections. If needle tip is shortened by too much a new needle will have to be prepared. Resting the needle tip in mineral oil avoids RNA drying up and forming a plaque that blocks the ejection of RNA. If, despite best efforts, the needle does become blocked there are two options; switch the pneumatic pump back to "gated" and try to flush the plaque off, or if the duration of ejection is still set relatively high (>100ms for example) remove the tip of the needle with the tweezers and re-calibrate droplet size using the micrometre slide and reducing the duration of ejection by lowering the "period."

8. If too much time is lost and RNA is micro-injected at the two-cell stage, the mosaicism that arises will be considerable (**Fig. 3A**).
9. Under the stereo-microscope the lanes will be clearly visible. Use a truncated microloader pipette tip to position embryos in the lanes. At this point it is prudent to eject a single RNA droplet and check it is still 1nl on the micrometre slide. It is good to do this before every round of micro-injecting as well in case the yolk from the embryos micro-injected in the previous round has blocked the needle and causes <1nl to be ejected in subsequent rounds of micro-injecting.
10. Brightfield is usually sufficient for identifying the cell and micro-injecting but Nomarski optics can be used to improve contrast between the yolk and the transparent cell of the zebrafish embryo.
11. This movement is extremely fluid such that it's one move, once competent a rate of >50 embryos per minute is achievable. If the cell is missed and instead the RNA is deposited into the yolk of the embryo then continue. During development most of the RNA from the yolk will be taken up into the cell. Especially when learning the technique the first few times it is easier to aim right under the cell, providing a wider target area, as the RNA will be taken up within minutes following injection through cytoplasmic streaming. If injecting DNA be aware that DNA is a considerably larger molecule and is therefore barely taken up through cytoplasmic streaming!
12. If development needs to be accelerated or decelerated for any reason then incubate at maximum 31°C (faster development) or minimum 21.5°C (slower development), respectively.
13. MS222 is sensitive to light and loses potency with time. For this reason, I often wrap the plastic dish with 0.1% MS222 in E3 medium 0.01% methylene blue in aluminium foil when intending to amputate many embryos.
14. Preferably cut on the lid so the rim does not obstruct the motion of incision. The plastic will not break. A Leica MDG17 is preferable for the amputations as the small base provides free vertical movement of the arm when performing amputations.
15. In parallel I usually transfer an uncut control embryo to the plastic 10cm dish with fresh 0.1% MS222 in E3 medium with 0.01% methylene blue mentioned in step 6.
16. The main focus area for improvement in this technique is accuracy to perform the amputation as close to the notochord as possible without damaging the notochord. The notochord does not regenerate, hence if nicked or amputated the embryo will die. Also, avoiding tearing of the fin-fold tissue by pulling the surgical blade away from wound margin is desirable to simplify the analysis of regenerative

outgrowth. The optimal incision motion is made using downward pressure to sever the zebrafish embryo caudal fin-fold tissue and not slicing towards you, as this can create a pulling force on the fin-fold tissue and lead to a sheared fin-fold instead of a clean cut.

17. Preferably use a glass Pasteur pipette from this point forward as the amputated zebrafish embryo caudal fin-fold readily sticks to plastic, causing damage to the caudal fin-fold.
18. Use microloader pipette tips to position embryo with the posterior end flat on the bottom of the plastic dish. Nomarski optics can be used to improve contrast of the transparent caudal fin-fold of the zebrafish embryo. For comparing different embryos it's paramount to use the same zoom settings on the stereo-microscope. Using the above-mentioned Leica set-up there is enough space to take a picture of both the amputated embryo and the uncut control in the same image.
19. Smaller than a 24-well plate is not recommended as the embryos have insufficient space to grow.
20. By performing the assay this way each uncut control is near enough at the same developmental stage as the amputated embryos and changes in embryonic growth rate can be accounted for.
21. The caudal fin-fold of 5dpf zebrafish embryos is substantially bigger than at 2dpf. Hence, each zebrafish embryo for both amputated and uncut controls requires a separate image.
22. The chorion contains maternal DNA and proteins, this need to be removed for accurate estimation of embryonic protein content.
23. The temperature is simply set to a comfortable temperature in which the embryo will survive. If using a 1.5ml tube or multi-well plate it is easy to look under a standard stereo-microscope to check how much of the yolk has dissociated from the embryo.
24. If not de-yolking, any excess system water or E3 medium can be removed from adult zebrafish fin-clips or embryos respectively and directly subjected to snap-freezing in liquid nitrogen. By snap-freezing the tissue becomes more brittle, increasing homogenization efficiency. Can store tissue at this point at -80°C.
25. Accompany a firm up-down motion with a gentle rotation for maximum efficiency. The tissue will shear. When removing the pestle some buffer or tissue may adhere to the head.

26. Creating air bubbles is practically unavoidable with this method but if the appropriate needle is used the tissue will be better sheared than it would have been with a mini-pestle. A small amount of suspension is always lost in the tip of the syringe which cannot be dispensed.
27. This removes quaternary and tertiary structures of proteins. Take into consideration that, after preparation with sample buffer and boiling, the sample may be very viscous, especially if little lysis buffer is used for many embryos. Upon such an occurrence, the sample usually needs to be diluted with more sample buffer for accurate loading to be feasible. It is therefore very important to follow the guidelines set out in step 9 to avoid this complication.

ACKNOWLEDGEMENTS

I would like to make a special mention of Miriam Stumpf who optimized sonication of zebrafish embryos in our lab and was kind enough to share her expertise. Also, I thank Jelte Sikkens and Andreas van Impel for providing figures 3A and 3B respectively. I am grateful to all my colleagues, both within the den Hertog group and in the wider field of zebrafish research, for sharing their experiences with me and helping to make this chapter as comprehensive as possible with contributions from experts in zebrafish research.

REFERENCES

1. Tonks NK (2006) Protein tyrosine phosphatases: from genes, to function, to disease. Nature reviews Molecular cell biology 7 (11):833-846. doi:10.1038/nrm2039
2. Hendriks WJ, Elson A, Harroch S, Pulido R, Stoker A, den Hertog J (2013) Protein tyrosine phosphatases in health and disease. The FEBS journal 280 (2):708-730. doi:10.1111/febs.12000
3. Tonks NK (2013) Protein tyrosine phosphatases--from housekeeping enzymes to master regulators of signal transduction. The FEBS journal 280 (2):346-378. doi:10.1111/febs.12077
4. Andersen JN, Mortensen OH, Peters GH, Drake PG, Iversen LF, Olsen OH, Jansen PG, Andersen HS, Tonks NK, Moller NP (2001) Structural and evolutionary relationships among protein tyrosine phosphatase domains. Mol Cell Biol 21 (21):7117-7136. doi:10.1128/MCB.21.21.7117-7136.2001
5. Chiarugi P, Cirri P (2003) Redox regulation of protein tyrosine phosphatases during receptor tyrosine kinase signal transduction. Trends in Biochemical Sciences 28 (9). doi:10.1016/s0968-0004(03)00174-9
6. den Hertog J, Groen A, van der Wijk T (2005) Redox regulation of protein-tyro sine phosphatases. Archives of Biochemistry and Biophysics 434 (1). doi:10.1016/j.aab.2004.05.024
7. Zinn K (1993) Drosophila protein tyrosine phosphatases. Seminars in cell biology 4 (6):397-401
8. Gutch MJ, Flint AJ, Keller J, Tonks NK, Hengartner MO (1998) The Caenorhabditis elegans SH2 domain-containing protein tyrosine phosphatase PTP-2 participates in signal transduction during oogenesis and vulval development. Genes & development 12 (4):571-585
9. van der Sar AM, de Fockert J, Betist M, Zivkovic D, den Hertog J (1999) Pleiotropic effects of zebrafish protein-tyrosine phosphatase-1B on early embryonic development. Int J Dev Biol 43 (8):785-794.
10. Revuelta-Cervantes J, Mayoral R, Miranda S, Gonzalez-Rodriguez A, Fernandez M, Martin-Sanz P, Valverde AM (2011) Protein Tyrosine Phosphatase 1B (PTP1B) Deficiency Accelerates Hepatic Regeneration in Mice. American Journal of Pathology 178 (4):1591-1604. doi:10.1016/j.ajpath.2010.12.020
11. Zabolotny JM, Bence-Hanulec KK, Stricker-Krongrad A, Haj F, Wang YP, Minokoshi Y, Kim YB, Elmquist JK, Tartaglia LA, Kahn BB, Neel BG (2002) PTP1B regulates leptin signal transduction in vivo. Developmental Cell 2 (4):489-495. doi:10.1016/s1534-5807(02)00148-x
12. Haffter P, Granato M, Brand M, Mullins MC, Hammerschmidt M, Kane DA, Odenthal J, vanEeden FJM, Jiang YJ, Heisenberg CP, Kelsh RN, FurutaniSeiki M, Vogelsang E, Beuchle D, Schach U, Fabian C, NussleinVolhard C (1996) The identification of genes with unique and essential functions in the development of the zebrafish, Danio rerio. Development 123:1-36
13. Feitsma H, Cuppen E (2008) Zebrafish as a cancer model. Molecular cancer research : MCR 6 (5):685-694. doi:10.1158/1541-7786.MCR-07-2167
14. Blackburn JS, Langenau DM (2014) Zebrafish as a model to assess cancer heterogeneity, progression and relapse. Disease models & mechanisms 7 (7):755-762. doi:10.1242/dmm.015842
15. Seth A, Stemple DL, Barroso I (2013) The emerging use of zebrafish to model metabolic disease. Disease models & mechanisms 6 (5):1080-1088. doi:10.1242/dmm.011346
16. Intine RV, Olsen AS, Sarras MP, Jr. (2013) A zebrafish model of diabetes mellitus and metabolic memory. J Vis Exp (72):e50232. doi:10.3791/50232

17. Vliegenthart AD, Tucker CS, Del Pozo J, Dear JW (2014) Zebrafish as model organisms for studying drug-induced liver injury. British journal of clinical pharmacology 78 (6):1217-1227. doi:10.1111/bcp.12408

18. Peterson RT, Link BA, Dowling JE, Schreiber SL (2000) Small molecule developmental screens reveal the logic and timing of vertebrate development. Proceedings of the National Academy of Sciences of the United States of America 97 (24):12965-12969. doi:10.1073/pnas.97.24.12965

19. Gemberling M, Bailey TJ, Hyde DR, Poss KD (2013) The zebrafish as a model for complex tissue regeneration. Trends Genet 5 (13):00113-00113

20. Goessling W, North TE (2014) Repairing quite swimmingly: advances in regenerative medicine using zebrafish. Disease models & mechanisms 7 (7):769-776. doi:10.1242/dmm.016352

21. Phillips JB, Westerfield M (2014) Zebrafish models in translational research: tipping the scales toward advancements in human health. Disease models & mechanisms 7 (7):739-743. doi:10.1242/dmm.015545

22. Sun N, Zhao H (2013) Transcription activator-like effector nucleases (TALENs): a highly efficient and versatile tool for genome editing. Biotechnology and bioengineering 110 (7):1811-1821. doi:10.1002/bit.24890

23. Irion U, Krauss J, Nusslein-Volhard C (2014) Precise and efficient genome editing in zebrafish using the CRISPR/Cas9 system. Development 141 (24):4827-4830. doi:10.1242/dev.115584

24. Jao LE, Wente SR, Chen W (2013) Efficient multiplex biallelic zebrafish genome editing using a CRISPR nuclease system. Proceedings of the National Academy of Sciences of the United States of America 110 (34):13904-13909. doi:10.1073/pnas.1308335110

25. Hwang WY, Fu Y, Reyon D, Maeder ML, Tsai SQ, Sander JD, Peterson RT, Yeh JR, Joung JK (2013) Efficient genome editing in zebrafish using a CRISPR-Cas system. Nature biotechnology 31 (3):227-229. doi:10.1038/nbt.2501

26. Holder N, Xu Q (1999) Microinjection of DNA, RNA, and protein into the fertilized zebrafish egg for analysis of gene function. Methods Mol Biol 97:487-490. doi:10.1385/1-59259-270-8:487

27. de Bruijn E, Cuppen E, Feitsma H (2009) Highly Efficient ENU Mutagenesis in Zebrafish. Methods Mol Biol 546:3-12. doi:10.1007/978-1-60327-977-2_1

28. Lawson ND, Weinstein BM (2002) In vivo imaging of embryonic vascular development using transgenic zebrafish. Dev Biol 248 (2):307-318

29. van Impel A, Schulte-Merker S (2014) A fisheye view on lymphangiogenesis. Advances in anatomy, embryology, and cell biology 214:153-165. doi:10.1007/978-3-7091-1646-3_12

30. van Eekelen M, Runtuwene V, Overvoorde J, den Hertog J (2010) RPTPalpha and PTPepsilon signaling via Fyn/Yes and RhoA is essential for zebrafish convergence and extension cell movements during gastrulation. Dev Biol 340 (2):626-639. doi:10.1016/j.ydbio.2010.02.026

31. Keller PJ, Schmidt AD, Wittbrodt J, Stelzer EH (2008) Reconstruction of zebrafish early embryonic development by scanned light sheet microscopy. Science 322 (5904):1065-1069. doi:10.1126/science.1162493

32. Schmid B, Shah G, Scherf N, Weber M, Thierbach K, Campos CP, Roeder I, Aanstad P, Huisken J (2013) High-speed panoramic light-sheet microscopy reveals global endodermal cell dynamics. Nature communications 4:2207. doi:10.1038/ncomms3207

33. Paardekooper Overman J, Preisinger C, Prummel K, Bonetti M, Giansanti P, Heck A, den Hertog J (2014) Phosphoproteomics-mediated identification of Fer kinase as a target of mutant Shp2 in Noonan and LEOPARD syndrome. PLoS ONE 9 (9):e106682. doi:10.1371/journal.pone.0106682

34. Paardekooper Overman J, Yi JS, Bonetti M, Soulsby M, Preisinger C, Stokes MP, Hui L, Silva JC, Overvoorde J, Giansanti P, Heck AJ, Kontaridis MI, den Hertog J, Bennett AM (2014) PZR coordinates Shp2 Noonan and LEOPARD syndrome signaling in zebrafish and mice. Mol Cell Biol 34 (15):2874-2889. doi:10.1128/MCB.00135-14

35. Lemeer S, Jopling C, Gouw J, Mohammed S, Heck AJ, Slijper M, den Hertog J (2008) Comparative phosphoproteomics of zebrafish Fyn/Yes morpholino knockdown embryos. Molecular & cellular proteomics : MCP 7 (11):2176-2187. doi:10.1074/mcp.M800081-MCP200

36. Babaei F, Ramalingam R, Tavendale A, Liang Y, Yan LS, Ajuh P, Cheng SH, Lam YW (2013) Novel blood collection method allows plasma proteome analysis from single zebrafish. Journal of proteome research 12 (4):1580-1590. doi:10.1021/pr3009226

37. Choorapoikayil S, Overvoorde J, den Hertog J (2013) Deriving cell lines from zebrafish embryos and tumors. Zebrafish 10 (3):316-325. doi:10.1089/zeb.2013.0866

38. den Hertog J (2005) Chemical genetics: Drug screens in Zebrafish. Bioscience reports 25 (5-6):289-297. doi:10.1007/s10540-005-2891-8

39. Meyer A, Schartl M (1999) Gene and genome duplications in vertebrates: the one-to-four (-to-eight in fish) rule and the evolution of novel gene functions. Current opinion in cell biology 11 (6):699-704

40. Woods IG, Kelly PD, Chu F, Ngo-Hazelett P, Yan YL, Huang H, Postlethwait JH, Talbot WS (2000) A comparative map of the zebrafish genome. Genome research 10 (12):1903-1914

41. Howe K, Clark MD, Torroja CF, Torrance J, Berthelot C, Muffato M, Collins JE, Humphray S, McLaren K, Matthews L, McLaren S, Sealy I, Caccamo M, Churcher C, Scott C, Barrett JC, Koch R, Rauch GJ, White S, Chow W, Kilian B, Quintais LT, Guerra-Assuncao JA, Zhou Y, Gu Y, Yen J, Vogel JH, Eyre T, Redmond S, Banerjee R, Chi J, Fu B, Langley E, Maguire SF, Laird GK, Lloyd D, Kenyon E, Donaldson S, Sehra H, Almeida-King J, Loveland J, Trevanion S, Jones M, Quail M, Willey D, Hunt A, Burton J, Sims S, McLay K, Plumb B, Davis J, Clee C, Oliver K, Clark R, Riddle C, Elliot D, Threadgold G, Harden G, Ware D, Begum S, Mortimore B, Kerry G, Heath P, Phillimore B, Tracey A, Corby N, Dunn M, Johnson C, Wood J, Clark S, Pelan S, Griffiths G, Smith M, Glithero R, Howden P, Barker N, Lloyd C, Stevens C, Harley J, Holt K, Panagiotidis G, Lovell J, Beasley H, Henderson C, Gordon D, Auger K, Wright D, Collins J, Raisen C, Dyer L, Leung K, Robertson L, Ambridge K, Leongamornlert D, McGuire S, Gilderthorp R, Griffiths C, Manthravadi D, Nichol S, Barker G, Whitehead S, Kay M, Brown J, Murnane C, Gray E, Humphries M, Sycamore N, Barker D, Saunders D, Wallis J, Babbage A, Hammond S, Mashreghi-Mohammadi M, Barr L, Martin S, Wray P, Ellington A, Matthews N, Ellwood M, Woodmansey R, Clark G, Cooper J, Tromans A, Grafham D, Skuce C, Pandian R, Andrews R, Harrison E, Kimberley A, Garnett J, Fosker N, Hall R, Garner P, Kelly D, Bird C, Palmer S, Gehring I, Berger A, Dooley CM, Ersan-Urun Z, Eser C, Geiger H, Geisler M, Karotki L, Kirn A, Konantz J, Konantz M, Oberlander M, Rudolph-Geiger S, Teucke M, Lanz C, Raddatz G, Osoegawa K, Zhu B, Rapp A, Widaa S, Langford C, Yang F, Schuster SC, Carter NP, Harrow J, Ning Z, Herrero J, Searle SM, Enright A, Geisler R, Plasterk RH, Lee C, Westerfield M, de Jong PJ, Zon LI, Postlethwait JH, Nusslein-Volhard C, Hubbard TJ, Roest Crollius H, Rogers J, Stemple DL (2013) The zebrafish reference genome sequence and its relationship to the human genome. Nature 496 (7446):498-503. doi:10.1038/nature12111

42. van Eekelen M, Overvoorde J, van Rooijen C, den Hertog J (2010) Identification and expression of the family of classical protein-tyrosine phosphatases in zebrafish. PLoS ONE 5 (9):e12573. doi:10.1371/journal.pone.0012573

43. Bonetti M, Rodriguez-Martinez V, Paardekooper Overman J, Overvoorde J, van Eekelen M, Jopling C, Hertog J (2014) Distinct and overlapping functions of ptpn11 genes in Zebrafish development. PLoS ONE 9 (4):e94884. doi:10.1371/journal.pone.0094884

44. Liao WH, Cheng CH, Hung KS, Chiu WT, Chen GD, Hwang PP, Hwang SP, Kuan YS, Huang CJ (2013) Protein tyrosine phosphatase receptor type O (Ptpro) regulates cerebellar

formation during zebrafish development through modulating Fgf signaling. Cellular and molecular life sciences : CMLS 70 (13):2367-2381. doi:10.1007/s00018-013-1259-7

45. van Eekelen M, Runtuwene V, Masselink W, den Hertog J (2012) Pair-wise regulation of convergence and extension cell movements by four phosphatases via RhoA. PLoS ONE 7 (4):e35913. doi:10.1371/journal.pone.0035913
46. Hayashi M, Majumdar A, Li X, Adler J, Sun Z, Vertuani S, Hellberg C, Mellberg S, Koch S, Dimberg A, Koh GY, Dejana E, Belting HG, Affolter M, Thurston G, Holmgren L, Vestweber D, Claesson-Welsh L (2013) VE-PTP regulates VEGFR2 activity in stalk cells to establish endothelial cell polarity and lumen formation. Nature communications 4:1672. doi:10.1038/ncomms2683
47. Wyatt L, Wadham C, Crocker LA, Lardelli M, Khew-Goodall Y (2007) The protein tyrosine phosphatase Pez regulates TGFbeta, epithelial-mesenchymal transition, and organ development. J Cell Biol 178 (7):1223-1235. doi:10.1083/jcb.200705035
48. Kimmel CB, Ballard WW, Kimmel SR, Ullmann B, Schilling TF (1995) STAGES OF EMBRYONIC-DEVELOPMENT OF THE ZEBRAFISH. Developmental Dynamics 203 (3):253-310
49. Gurdon JB, Lane CD, Woodland HR, Marbaix G (1971) Use of frog eggs and oocytes for the study of messenger RNA and its translation in living cells. Nature 233 (5316):177-182
50. Kola I, Sumarsono SH (1995) Microinjection of in vitro transcribed RNA and antisense oligonucleotides in mouse oocytes and early embryos to study the gain- and loss-of-function of genes. Methods Mol Biol 37:135-149. doi:10.1385/0-89603-288-4:135
51. Gordon JW, Scangos GA, Plotkin DJ, Barbosa JA, Ruddle FH (1980) Genetic transformation of mouse embryos by microinjection of purified DNA. Proceedings of the National Academy of Sciences of the United States of America 77 (12):7380-7384
52. Graessmann M, Graessmann A (1983) Microinjection of tissue culture cells. Methods in enzymology 101:482-492
53. Rosen JN, Sweeney MF, Mably JD (2009) Microinjection of zebrafish embryos to analyze gene function. J Vis Exp (25). doi:10.3791/1115
54. Agrawal V, Johnson SA, Reing J, Zhang L, Tottey S, Wang G, Hirschi KK, Braunhut S, Gudas LJ, Badylak SF (2010) Epimorphic regeneration approach to tissue replacement in adult mammals. Proc Natl Acad Sci U S A 107 (8):3351-3355. doi: 3310.1073/pnas.0905851106. Epub 0905852009 Dec 0905851104.
55. Poss KD, Keating MT, Nechiporuk A (2003) Tales of regeneration in zebrafish. Dev Dyn 226 (2):202-210.
56. Kawakami A, Fukazawa T, Takeda H (2004) Early fin primordia of zebrafish larvae regenerate by a similar growth control mechanism with adult regeneration. Dev Dyn 231 (4):693-699.
57. Bradford Y, Conlin T, Dunn N, Fashena D, Frazer K, Howe DG, Knight J, Mani P, Martin R, Moxon SA, Paddock H, Pich C, Ramachandran S, Ruef BJ, Ruzicka L, Bauer Schaper H, Schaper K, Shao X, Singer A, Sprague J, Sprunger B, Van Slyke C, Westerfield M (2011) ZFIN: enhancements and updates to the Zebrafish Model Organism Database. Nucleic acids research 39 (Database issue):D822-829. doi:10.1093/nar/gkq1077
58. Kimmel CB, Ballard WW, Kimmel SR, Ullmann B, Schilling TF (1995) Stages of embryonic development of the zebrafish. Developmental dynamics : an official publication of the American Association of Anatomists 203 (3):253-310. doi:10.1002/aja.1002030302
59. Westerfield M (2000) The zebrafish book. A guide for the laboratory use of zebrafish (Danio rerio). 4th edn. Univ. of Oregon Press, Eugene

Chapter 4

Impaired Caudal Fin-Fold Regeneration in Zebrafish Embryos Deficient for the Tumour Tuppressor Pten

Alexander James Hale[1,2], Ali Kiai[1],
Jelte Sikkens[1], and Jeroen den Hertog[1,2]

1. Hubrecht Institute – KNAW and University Medical Center Utrecht, Utrecht, the Netherlands
2. Institute Biology Leiden, Leiden University, Leiden, the Netherlands

ABSTRACT

Zebrafish are able to completely regrow their caudal fin-folds after amputation. Following injury, wound healing occurs, followed by the formation of a blastema, that produces cells to replace the lost tissue in the final phase of regenerative outgrowth. Here we show that surprisingly, the phosphatase and tumour suppressor Pten, an antagonist of PI3K signalling, is required for zebrafish embryo caudal fin-fold regeneration. We found that homozygous knock-out mutant (*ptena*$^{-/-}$*ptenb*$^{-/-}$) zebrafish embryos, lacking functional Pten, did not regenerate their caudal fin-folds. AKT phosphorylation was enhanced, which is consistent with the function of Pten. Re-expression of Pten, but not catalytically inactive mutant Pten-C124S, rescued regeneration, as did pharmacological inhibition of PI3K. Blastema formation, determined by *in situ* hybridization for the blastema marker *junbb*, was induced normally upon caudal fin-fold amputation of *ptena*$^{-/-}$*ptenb*$^{-/-}$ zebrafish embryos. Whole-mount immunohistochemistry using specific markers indicated that proliferation was arrested in zebrafish embryos lacking functional Pten, and that apoptosis was enhanced. Together, these results suggest a critical role for Pten by limiting PI3K signalling during the regenerative outgrowth phase of zebrafish embryo caudal fin-fold regeneration.

INTRODUCTION

Zebrafish (*Danio rerio*) fully regenerate multiple organs after injury, including the heart, retina, spinal cord, and caudal fin, in a process termed epimorphic regeneration (Pfefferli & Jaźwińska, 2015; Poss, Keating, & Nechiporuk, 2003). In broad terms, regeneration of the zebrafish caudal fin proceeds sequentially through three distinct phases: wound healing, blastema formation, and regenerative outgrowth. Adult zebrafish regenerate their caudal fin-folds within two weeks, whilst zebrafish embryos regenerate their caudal fin-folds within 72 hours (Kawakami, Fukazawa, & Takeda, 2004). The mechanism of embryonic caudal fin-fold regeneration is the same as adult caudal fin regeneration. Following injury, nearby cells migrate to cover the wound and form an apical epidermal cap that is essential to initiate blastema formation and regenerative outgrowth (Poleo, Brown, Laforest, & Akimenko, 2001). To date, many genes have been implicated in the regenerative process (Padhi et al., 2004) and multiple signalling pathways have been validated to be essential for regeneration, including fibroblast growth factor, sonic hedgehog, bone morphogenetic protein, Wnt, and Notch (Gemberling, Bailey, Hyde, & Poss, 2013).

Phosphatase and Tensin Homologue (PTEN) is one of the most frequently mutated tumor suppressor genes and has a central role in cell signalling. PTEN is a protein-tyrosine phosphatase and lipid phosphatase with selectivity for the 3-position of phosphatidylinositol-(3,4,5)-trisphosphate (PIP3) and hence, PTEN is an antagonist of phosphoinositide-3-kinase (PI3K). Activation of PI3K leads to attraction of AKT (also known as PKB) to the plasma membrane and subsequently to phosphorylation of AKT on threonine 308 and serine 473 to activate it (Burgering & Coffer, 1995). The importance of PI3K signalling is highlighted by activated AKT (p-AKT) interacting with and stimulating many factors presiding over various cellular processes. Notably, p-AKT promotes cell cycle progression to drive cell proliferation, and enhances cell survival by inhibiting pro-apoptotic transcription factors (Vara et al., 2004). Elevated p-AKT has been reported in regenerating caudal fins of medaka (*Oryzias latipes*), and inhibition of PI3K activity using the inhibitor LY294002, inhibits medaka, as well as adult caudal fin and embryonic zebrafish caudal fin-fold regeneration (Nakatani, Nishidate, Fujita, Kawakami, & Kudo, 2008; Rojas-Muñoz et al., 2009). Inhibition of downstream mechanistic target of rapamycin (mTOR) signalling with rapamycin also inhibits regeneration (Hirose, Shiomi, Hozumi, & Kikuchi, 2014). These studies highlight the importance of PI3K signalling in regeneration. However, the role of PTEN in zebrafish caudal fin

regeneration has not been addressed. It is evident that PI3K inhibition attenuates regeneration and hence, one would expect that PTEN inhibition has the opposite effect, and enhances regeneration.

To date, the only implication of PTEN in regeneration has been limited to the promotion of central nervous system (CNS) axon regeneration. Various mouse PTEN knockdown or conditional knock-outs have been generated that show enhanced axon regeneration (Liu et al., 2010; Ohtake, Hayat, & Li, 2015). Also *C. elegans* mutants of *daf-18*, the PTEN homologue in *C. elegans*, display improved axon regeneration through enhanced mTOR signalling (Byrne et al., 2014). These studies investigated axon regeneration following crushing or axotomy, and suggest that PTEN plays a role in regeneration by limiting regenerative outgrowth of axons. However, axon connections are predominantly rescued by compensatory sprouting from spared neural fibres, and true regenerative outgrowth of injured axons rarely occurs in the adult mouse CNS (He, 2010). Hence, the importance of PTEN in regeneration remains to be determined.

To investigate the role of Pten in the regeneration of whole tissue and to test if *pten* knock-out mutants have enhanced regeneration, we tested the regenerative capacity of caudal fin-folds of zebrafish embryos lacking functional Pten (*i.e.* mutants homozygous for nonsense mutations in both *ptena* and *ptenb*) (Faucherre, Taylor, Overvoorde, Dixon, & Hertog, 2008). Surprisingly, we found that the caudal fin-fold of *ptena*$^{-/-}$*ptenb*$^{-/-}$ zebrafish embryos did not regenerate. AKT phosphorylation was elevated in amputated caudal fin-folds of *ptena*$^{-/-}$*ptenb*$^{-/-}$ zebrafish embryos and inhibition of excess PI3K activity restored regeneration. Blastema formation following amputation occurred normally. However, compared to siblings, cell proliferation was arrested and apoptosis enhanced close to the site of amputation.

MATERIALS AND METHODS

Zebrafish husbandry

All procedures involving experimental animals were approved by the local animal experiments committee (Koninklijke Nederlandse Akademie van Weterschappen-Dierexperimenten commissie KNAW-DEC protocol HI12.0701) and performed according to local guidelines and policies in compliance with national and European law. The *ptena*$^{+/-}$*ptenb*$^{-/-}$ and *ptena*$^{-/-}$ *ptenb*$^{+/-}$ zebrafish lines in the Tuebingen Long fin (TL) background were previously created by target-selected gene inactivation (TSGI), and

both *ptena*^{hu1864} and *ptenb*^{hu1435} alleles result from non-sense mutations that lead to a premature stop codon upstream of the catalytic cysteine, Cys124 (Faucherre et al., 2008). Adult *ptena*$^{+/-}$*ptenb*$^{-/-}$ and *ptena*$^{-/-}$*ptenb*$^{+/-}$ zebrafish were in-crossed to generate *ptena*$^{-/-}$*ptenb*$^{-/-}$ zebrafish embryos for all experiments. Zebrafish were raised and maintained as described by Westerfield (Westerfield, 2000) under a 14 hours light/ 10 hours dark cycle at 28.5°C.

mRNA synthesis and micro-injections

The constructs pCS2+-zfPtenb-mCherry, pCS2+-zfPtena-mCherry, pCS2+-hPTEN-mCherry, and pCS2+-zfPtenb-C124S-mCherry were obtained as described (Faucherre et al., 2008). Sense messenger RNA (mRNA) synthesis and micro-injection into one-cell stage zebrafish embryos was performed as described (Stumpf & Den Hertog, 2016).

Caudal fin-fold amputation

Zebrafish embryos were amputated as previously described (Hale & den Hertog, 2016), amputations were performed at 2 days post fertilisation (dpf) for all experiments. Regeneration was allowed to proceed until analysis at 3 days post amputation (dpa) or fixation at either 1dpa or 2dpa. LY294002 hydrochloride (Sigma) was administered directly following recovery of amputated zebrafish embryos in E3 medium. Whole zebrafish embryos were lysed for genotyping or fixed in 4% PFA, in PBS, either 3hpa for *in situ* hybridization, or at 1dpa and 2dpa for immunohistochemistry.

In situ hybridization

In situ hybridizations were performed as previously described (Thisse, Thisse, Schilling, & Postlethwait, 1993), using *junbb* and *and1* digoxigenin-UTP-labelled anti-sense riboprobes. Parts of *junbb* and *and1* were amplified from zebrafish cDNA using specific primers (Table S1) and the resulting PCR products were cloned into vectors and used as DNA templates for synthesis of riboprobes. Digoxigenin-UTP-labelled anti-sense riboprobes were synthesized from *and1* plasmid DNA, or *junbb* PCR product, produced using *fwd: TACACGACGCTGAACGCATA* and *rev: TAATACGACTCACTATAGGTGTCCGTTCTCTTCCGTCC*. Caudal fin-folds of zebrafish embryos were severed and mounted in 70% glycerol in PBS for imaging on a Zeiss Axioskop 2 Mot Plus microscope with either a Plan-NEOFLUAR 10x/0.30 or 20x/0.50 objective. The rest of the zebrafish embryo was lysed for genotyping.

Immunohistochemistry

Zebrafish embryos fixed in 4% PFA were washed in PBS 0.1% Tween-20 and antigen retrieval performed depending on the antibody used: ice-cold acetone for 20mins for PCNA; ice-cold methanol for 20mins for activated Caspase-3 (Sorrells, Toruno, Stewart, & Jette, 2013); and 10mM Tris, 1mM EDTA, pH 9.0 for p-AKT (Ser473) (van der Velden et al., 2011). Whole zebrafish embryos were incubated overnight at 4°C in mouse anti-PCNA (1:200, #M0879; DAKO Agilent Pathology Solutions), rabbit anti-activated Caspase-3 (1:200, #9661 Cell Signaling Technology), or rabbit anti–p-AKT (Ser473) (1:50; #4060; Cell Signaling Technology). Secondary antibodies conjugated to Cy5 goat anti-mouse or goat anti-rabbit IgG were used 1:500 and 1:200 respectively (#115-175-146 and #111-175-144; Jackson ImmunoResearch). Nuclei were shown by DAPI (4',6-diamidino-2-phenylindole) staining. Caudal fin-folds of zebrafish embryos were mounted for imaging in 70% glycerol in PBS, and the rest of the zebrafish embryo was lysed for genotyping. Z-stacks (6µm step size) of the caudal fin-fold were acquired for every zebrafish embryo with a Leica Sp8 confocal microscope. ImageJ software (http://rsb.info.nih.gov./ij/) was used to generate maximum intensity (z) projections and merge channels. Quantification was performed on the original z-projections (1024 x 1024px, 300dpi) following rolling ball background subtraction with an average from 50px. Particles were counted for activated Caspase-3 following a black and white thresholding of 121-255 and using a size restriction of 0.000009-0.000144inch^2. Mean intensity of p-AKT was measured from the wound margin inwards using an ROI with dimensions equivalent to h: 1.58µm (475px) and w: 0.78µm (235px) for uncut zebrafish embryos and w: 0.45µm (135px) for amputated zebrafish embryos.

Genotyping

All zebrafish embryos that were used in these assays were genotyped to establish *ptena* and/or *ptenb* status. To this end, genomic zebrafish DNA was extracted through lysis of zebrafish embryos in 100µg/ml proteinase K (Sigma) diluted in SZL buffer (50mM KCl, 2.5mM MgCl, 10mM Tris pH 8.3, 0.005% NP40, 0.005% Tween-20, and 10% 0.1% Gelatine). Lysis was performed by incubating at 60°C for 1 hour, followed by 95°C for 15 minutes in a thermal cycler (BioRad T100). Primers of *ptena* and *ptenb*, containing the non-sense mutations of the *ptena*^{hu1864} and *ptenb*^{hu1435} alleles (Table S1), were mixed with genomic zebrafish DNA and Kompetitive Allele Specific PCR (KASP) master mix (LGC Group). Amplification was carried out according to the manufacturer's

instructions and the resulting PCR products were analysed in a PHERAstar microplate reader (BMG LABTECH). Klustercaller software was used to identify the mutations.

Statistics

For analysis of caudal fin-fold lengths, histograms of whole data sets were examined to determine non-normal distribution of the data. Statistical analysis of unequal variances was obtained through a Kruskall-Wallis test. Differences between different experimental conditions were assessed for significance using a Mann-Whitney U test. Differences were considered significant when $p<0.001$, and if they satisfied a confidence interval of 99% in a Monte Carlo exact test. All tests for regenerating caudal fin-folds were performed in SPSS (IBM). For analysis of immunohistochemistry measurements, differences between different experimental condition were assessed for significance using a Mann-Whitney U test with a confidence level set to 95%. All tests for immunohistochemistry measurements were performed in GraphPad Prism (GraphPad Software). Differences were considered significant when $p<0.05$.

RESULTS

Pten catalytic activity is required for zebrafish embryo caudal fin-fold regeneration

To address the role of Pten in regeneration, we first investigated whether zebrafish embryos regenerate their caudal fin-fold in the absence of functional Pten protein. Zebrafish carry two *pten* genes: *ptena* and *ptenb*, encoding Pten proteins that are functionally redundant (Faucherre et al., 2008). Zebrafish carrying a single wild-type (WT) *pten* allele (*ptena*$^{+/-}$*ptenb*$^{-/-}$ or *ptena*$^{-/-}$*ptenb*$^{+/-}$) show no detectable defects during development or as adults, and they are viable and fertile, but are predisposed to the development of hemangiosarcomas (Choorapoikayil, Kuiper, de Bruin, & den Hertog, 2012). In-crossing adult *ptena*$^{+/-}$*ptenb*$^{-/-}$ zebrafish produces *ptena*$^{-/-}$*ptenb*$^{-/-}$ zebrafish embryos and their sibling controls, *ptena*$^{+/-}$*ptenb*$^{-/-}$ and *ptena*$^{+/+}$*ptenb*$^{-/-}$, that resemble wild-type zebrafish embryos for experimentation. Homozygous knock-out mutant zebrafish embryos (*ptena*$^{-/-}$*ptenb*$^{-/-}$) develop severe abnormalities during development and are embryonic lethal after 6 dpf. This is consistent with mouse PTEN knock-outs that are not viable either (Cristofano et al., 1998). The developmental abnormalities of Pten deficient zebrafish embryos are apparent from 3dpf onwards and are characte-

rized by heart oedema, curvature and swelling of the body axis, cranial deformations, and vascular hyper-branching (Choorapoikayil, Weijts, Kers, de Bruin, & den Hertog, 2013). To investigate if Pten protein is required for caudal fin-fold regeneration, the caudal fin-folds of zebrafish embryos were amputated immediately posterior to the notochord at 2dpf and allowed to regenerate for 3 days. Representative pictures of regenerating fin-folds at 3dpa and the fin-folds of uncut controls are depicted (**Fig. 1A**). Caudal fin-fold lengths were determined and are presented as percentage caudal fin-fold growth, normalized to uncut controls of *ptena*$^{+/+}$*ptenb*$^{-/-}$ zebrafish embryos (**Fig. 1B** and S1B). In contrast to their siblings, *ptena*$^{-/-}$*ptenb*$^{-/-}$ zebrafish embryos displayed severely impaired regeneration. We also observe that the shape of the amputated caudal fin-fold of *ptena*$^{-/-}$*ptenb*$^{-/-}$ zebrafish embryos was more rectangular compared to the rounded caudal fin-folds of their siblings. Fin-fold growth in uncut controls was indistinguishable between *ptena*$^{-/-}$*ptenb*$^{-/-}$ zebrafish embryos and siblings (**Fig. S1B**).

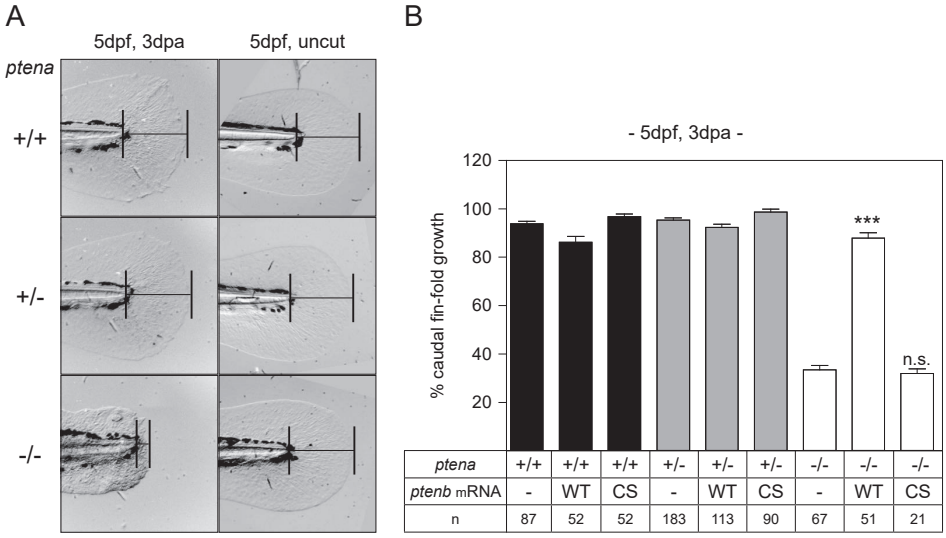

Fig. 1. Impaired caudal fin-fold regeneration in Pten deficient embryos. (**A**) Embryos from a *ptena*$^{+/-}$*ptenb*$^{-/-}$ in-cross were micro-injected at the one-cell stage with synthetic mRNA encoding WT Ptenb (WT), catalytically inactive Ptenb-C124S (CS), or were not injected (-). At 2dpf the caudal fin-fold was amputated and regeneration was assessed at 3dpa (i.e. 5dpf, 3dpa), equivalent uncut controls were included (i.e. 5dpf, uncut). All embryos were genotyped. Representative images of non-injected embryo caudal fin-folds are shown, and of WT Ptenb or Ptenb-C124S-injected embryos in **Fig. S1**. (**B**) The means of caudal fin-fold growth following amputation are depicted relative to caudal fin-fold growth of uncut *ptena*$^{+/+}$*ptenb*$^{-/-}$ controls. Means of micro-injected amputated *ptena*$^{-/-}$*ptenb*$^{-/-}$ embryos were compared to non-injected amputated *ptena*$^{-/-}$*ptenb*$^{-/-}$ embryos. Significance: *** p<0.001; n.s. not significant; error bars indicate standard error of the mean. Data pooled from multiple experiments.

To confirm that the absence of functional Pten is responsible for the lack of zebrafish embryo caudal fin-fold regeneration, one-cell stage zebrafish embryos from a *ptena*$^{+/-}$ *ptenb*$^{-/-}$ in-cross were micro-injected with mRNA encoding either WT Ptenb, or catalytically inactive Ptenb-C124S (Myers et al., 1998). These Ptenb proteins are tagged with C-terminal mCherry and only positively fluorescent zebrafish embryos, expressing the Pten-mCherry fusion proteins, had their caudal fin-folds amputated and regeneration documented. WT Ptenb rescued caudal fin-fold regeneration in *ptena*$^{-/-}$*ptenb*$^{-/-}$ zebrafish embryos, whereas expression of the catalytically inactive Ptenb-C124S had no effect on caudal fin-fold regeneration compared to non-injected controls (-) (**Fig. 1, S1A**).

To test whether Ptena and Ptenb proteins are indeed functionally redundant in caudal fin-fold regeneration, we repeated the experiment using *ptena*$^{-/-}$*ptenb*$^{-/-}$ zebrafish embryos obtained from in-crossing adult *ptena*$^{-/-}$*ptenb*$^{+/-}$ zebrafish. Again, *ptena*$^{-/-}$ *ptenb*$^{-/-}$ zebrafish embryos displayed severely impaired caudal fin-fold regeneration, and siblings carrying one or two WT *ptenb* alleles regenerated normally, like zebrafish embryos carrying one or two WT *ptena* alleles (*cf.* **Fig. 1A** and **S2A**). To further show that Ptena and Ptenb are functionally redundant in caudal fin-fold regeneration, *ptena*$^{-/-}$*ptenb*$^{-/-}$ zebrafish embryos were micro-injected with mRNA encoding WT Ptena. In addition, as Pten is highly conserved amongst species (Stumpf, Choorapoikayil, & den Hertog, 2015), we tested whether human PTEN could also fulfil the functions of zebrafish Pten in rescuing caudal fin-fold regeneration by micro-injecting mRNA encoding human WT PTEN. Both zebrafish Ptena and Ptenb, as well as human PTEN rescued caudal fin-fold regeneration (**Fig. 2**). In conclusion, Pten catalytic activity is required for regeneration of the zebrafish embryo caudal fin-fold.

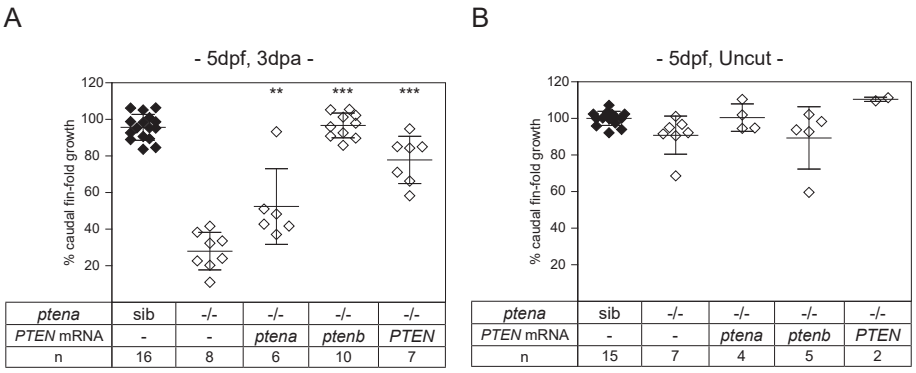

ptena	sib	-/-	-/-	-/-	-/-
PTEN mRNA	-	-	*ptena*	*ptenb*	*PTEN*
n	16	8	6	10	7

ptena	sib	-/-	-/-	-/-	-/-
PTEN mRNA	-	-	*ptena*	*ptenb*	*PTEN*
n	15	7	4	5	2

Fig. 2. Expression of zebrafish Pten, or human PTEN rescues caudal fin-fold regeneration in Pten deficient embryos. (**A**) Embryos from a *ptena*$^{+/-}$*ptenb*$^{-/-}$ in-cross were micro-injected at the one-cell stage with synthetic mRNA encoding zebrafish WT Ptena, zebrafish WT Ptenb, or human WT PTEN, or were not injected (-). At 2dpf the caudal fin-fold was amputated and regeneration was assessed at 3dpa (i.e. 5dpf, 3dpa), equivalent uncut controls (i.e. 5dpf, uncut) are shown in (**B**). All embryos were genotyped. The caudal fin length measurements of *ptena*$^{+/+}$*ptenb*$^{-/-}$ and *ptena*$^{+/-}$*ptenb*$^{-/-}$ embryos were pooled and represented above as "sib" for both amputated and uncut embryos. The means of caudal fin-fold growth following amputation are depicted relative to caudal fin-fold growth of uncut "sib" controls. Means of micro-injected amputated *ptena*$^{-/-}$*ptenb*$^{-/-}$ embryos were compared to non-injected amputated *ptena*$^{-/-}$*ptenb*$^{-/-}$ embryos. Significance: *** $p<0.001$; ** $p<0.01$; error bars indicate standard deviation.

Elevated PI3K signalling blocks caudal fin-fold regeneration in Pten deficient zebrafish embryos

PTEN loss, resulting in enhanced PI3K signal transduction, leads to hyper-active AKT (Stambolic et al., 1998). To confirm that this is also the case in our *ptena*$^{-/-}$*ptenb*$^{-/-}$ zebrafish embryos, we performed whole-mount immunohistochemistry for p-AKT (p-S473). At both 3dpf and 4dpf *ptena*$^{-/-}$*ptenb*$^{-/-}$ zebrafish embryos displayed elevated p-AKT levels compared to siblings with a more pronounced effect following fin-fold amputation (**Fig. 3, S3**).

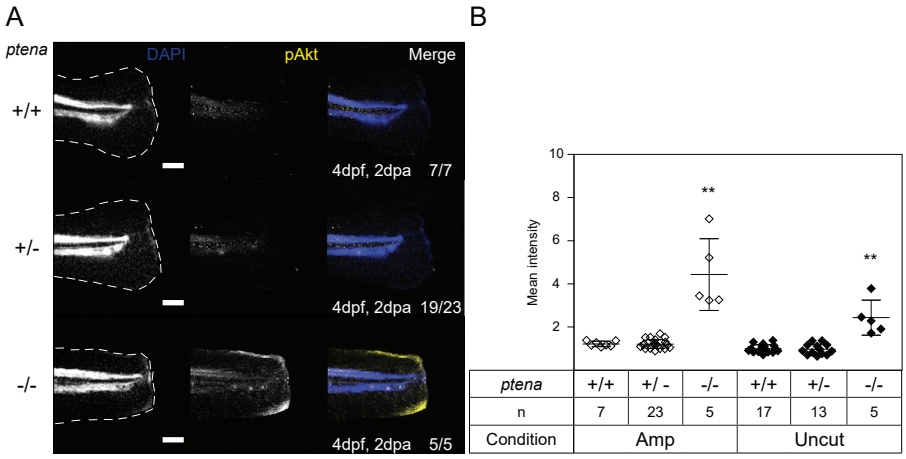

Fig. 3. Elevated p-AKT in the caudal fin-folds of Pten deficient embryos by 4dpf. (**A**) Caudal fin-folds of embryos from a *ptena*$^{+/-}$*ptenb*$^{-/-}$ in-cross were amputated and fixed at 2dpa (i.e. 4dpf, 2dpa) and subjected to whole-mount immunohistochemistry using a p-AKT-specific antibody (p-S473) (yellow). The embryos were counterstained with DAPI (blue). Representative images of amputated embryo caudal fin-folds are shown and in the left panels the edge of the fin-fold is indicated with a dashed line. Number of embryos showing similar patterns/ total number of embryos analysed is indicated in the bottom right corner. The scale bar represents 100µm. (**B**) p-AKT was quantified by mean intensity of the region between the notochord and the edge of the caudal fin-fold. Equivalent uncut controls were also quantified (representative pictures depicted in **Fig. S3A**). Means within amputated or uncut groups are compared to *ptena*$^{+/+}$*ptenb*$^{-/-}$ embryos. Significance: ** p<0.01; error bars represent standard deviation.

We hypothesized that the observed hyper-activation of AKT in Pten deficient zebrafish embryos causes impaired regeneration. If this is the case, then restoring p-AKT levels, by inhibiting over-active PI3K, should rescue regeneration in Pten deficient mutants. To test this hypothesis, the caudal fin-folds of zebrafish embryos obtained from a *ptena*$^{+/-}$*ptenb*$^{-/-}$ in-cross were amputated at 2dpf and allowed to regenerate for 3 days in the presence or absence of the PI3K inhibitor LY294002. Treatment of *ptena*$^{-/-}$*ptenb*$^{-/-}$ zebrafish embryos with LY294002 resulted in caudal fin-fold regeneration comparable with regeneration in siblings (**Fig. 4**). Uncut controls showed that LY294002 treatment by itself does not have any detrimental effects on caudal fin-fold growth. These results demonstrate that Pten-mediated modulation of PI3K activity is required for normal caudal fin-fold regeneration.

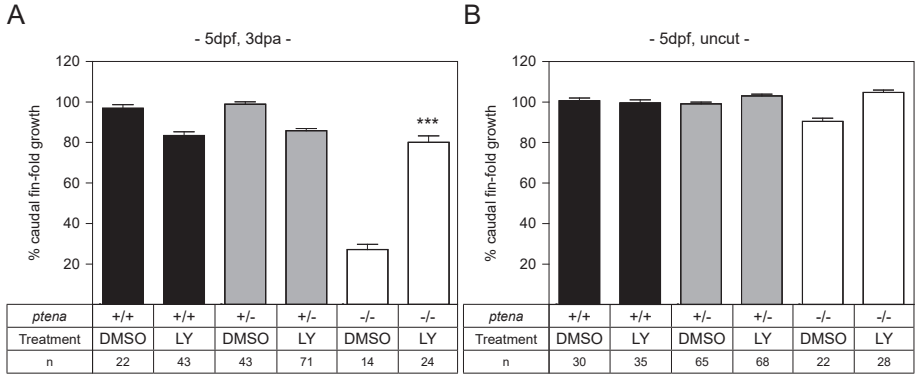

ptena	+/+	+/+	+/-	+/-	-/-	-/-
Treatment	DMSO	LY	DMSO	LY	DMSO	LY
n	22	43	43	71	14	24

ptena	+/+	+/+	+/-	+/-	-/-	-/-
Treatment	DMSO	LY	DMSO	LY	DMSO	LY
n	30	35	65	68	22	28

Fig. 4. Inhibition of PI3K rescues impaired caudal fin-fold regeneration in Pten deficient embryos. (**A**) At 2dpf the caudal fin-fold of embryos from a *ptena*$^{+/-}$*ptenb*$^{-/-}$ in-cross was amputated and incubated with 10µM LY294002, or 1% DMSO. Regeneration was assessed at 3dpa (i.e. 5dpf, 3dpa). (**B**) Equivalent uncut controls treated with LY294002, or 1% DMSO from 2dpf onwards were included (i.e. 5dpf, uncut). All embryos were genotyped. Regeneration was quantified by measuring the distance from the tip of the notochord to the edge of the caudal fin-fold. The means of caudal fin-fold growth are depicted relative to caudal fin-fold growth of DMSO treated uncut *ptena*$^{+/+}$*ptenb*$^{-/-}$ controls. Mean of LY294002 treated amputated *ptena*$^{-/-}$*ptenb*$^{-/-}$ embryos is compared to DMSO treated amputated *ptena*$^{-/-}$*ptenb*$^{-/-}$ embryos. The number of embryos is indicated (n). Significance: *** p<0.001; error bars indicate standard error of the mean. Data pooled from multiple experiments.

Normal blastema formation in zebrafish embryos deficient for Pten

We further characterised the *ptena*$^{-/-}$*ptenb*$^{-/-}$ mutants by assessing regeneration at two distinct stages: blastema formation and regenerative outgrowth. Amputated zebrafish embryos obtained from a *ptena*$^{+/-}$*ptenb*$^{-/-}$ in-cross were fixed at 3 hours post-amputation (hpa) and subjected to *in situ* hybridization for detection of *junbb* and *and1* transcription, both of which have previously been shown to be upregulated in the blastema (Thorimbert et al., 2015; Yoshinari, Ishida, Kudo, & Kawakami, 2009). *Junbb* was clearly induced by amputation of the caudal fin-fold, and *ptena*$^{-/-}$*ptenb*$^{-/-}$ mutant zebrafish embryos expressed *junbb* to a similar extent as their siblings (**Fig. 5**). There was no obvious difference in *and1* expression between *ptena*$^{-/-}$*ptenb*$^{-/-}$ zebrafish embryos and their siblings. However, *and1* expression was already high in uncut controls and was not enhanced in amputated zebrafish embryos, suggesting that *and1* expression is not a good marker for blastema formation in zebrafish embryos (**Fig. S4**). Nevertheless, *junbb* expression indicated that blastema formation was normal in Pten deficient zebrafish embryos.

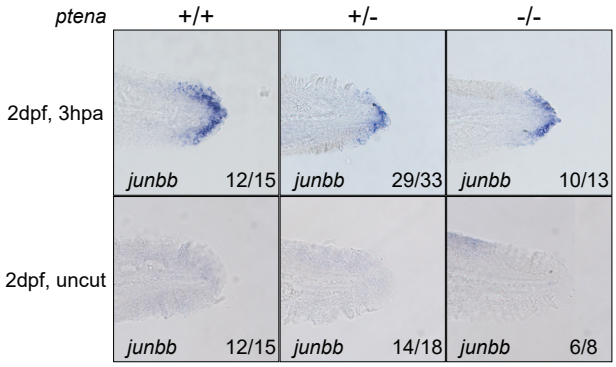

Fig. 5. Blastema is formed normally in Pten deficient embryos. At 2dpf the caudal fin-fold of embryos from a *ptena*$^{+/-}$*ptenb*$^{-/-}$ in-cross was amputated and allowed to regenerate. Embryos were fixed at 3hpa, or equivalent for uncut controls, and subjected to hybridization for *junbb*. Representative images of embryo caudal fin-folds are shown, and the number of embryos showing similar patterns/ total number of embryos analysed is indicated in the bottom right corner of each panel.

Arrested proliferation and enhanced apoptosis in regenerating caudal fin-fold of Pten deficient zebrafish embryos

Proliferation is upregulated during regenerative outgrowth to generate the cells required to form and replace the lost tissue (Kawakami et al., 2004; Poss et al., 2003), and apoptosis is also enhanced and may be required for successful regeneration to proceed (Gauron et al., 2013). Considering that PI3K signalling promotes cell proliferation and enhances cell survival, we analysed both during the regenerative outgrowth stage. Zebrafish embryos obtained from a *ptena*$^{+/-}$*ptenb*$^{-/-}$ in-cross were fixed at 1dpa or 2dpa and subjected to whole-mount immunohistochemistry for detection of proliferating cell nuclear antigen (PCNA) expression. PCNA immunofluorescence was high in amputated caudal fin-folds of siblings (**Fig. 6**), but remained low in uncut controls (**Fig. S5A, B**). At 1dpa PCNA immunofluorescence was found concentrated between the amputation plane and the wound margin at the edge of the caudal fin-fold, and there was no apparent difference between Pten deficient zebrafish embryos and their siblings (**Fig. S5C**). By 2dpa however, PCNA immunofluorescence was dispersed at the edge of the amputated caudal fin-fold of *ptena*$^{-/-}$*ptenb*$^{-/-}$ zebrafish embryos, whereas in siblings, that regenerated normally, PCNA immunofluorescence remained concentrated between the amputation plane and the wound margin (**Fig. 6**). Because PCNA positive cells were predominantly concentrated in the regenerating caudal fin-fold of siblings, which was absent in *ptena*$^{-/-}$*ptenb*$^{-/-}$ zebrafish embryos, quantification of PCNA staining was not meaningful. Nevertheless, from the representative images in **Fig. 6** it

is evident that proliferation was severely impaired in *ptena*$^{-/-}$*ptenb*$^{-/-}$ zebrafish embryos at 2dpa.

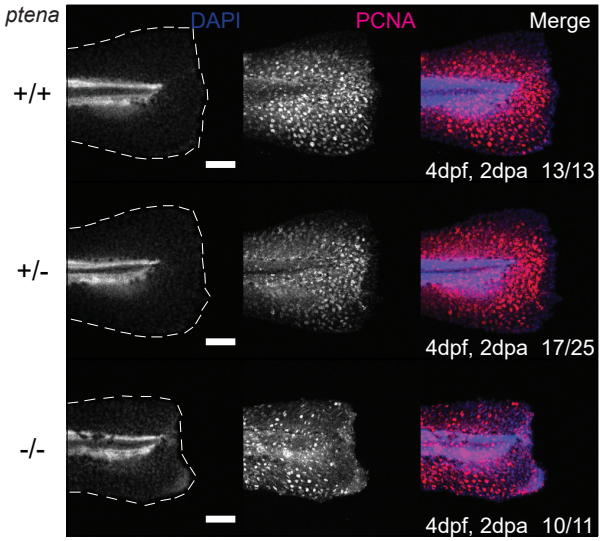

Fig. 6. Arrested proliferation at the edge of the amputated caudal fin-fold of Pten deficient embryos by 2dpa. At 2dpf the caudal fin-fold of embryos from a *ptena*$^{+/-}$*ptenb*$^{-/-}$ in-cross was amputated and allowed to regenerate. Embryos were fixed at 2dpa (i.e. 4dpf, 2dpa) and subjected to whole-mount immunohistochemistry using an antibody specific for the cell proliferation marker PCNA (red). The embryos were counterstained with DAPI (blue). Maximum intensity projection images were taken of the caudal fin-folds and all embryos were genotyped. Representative images of amputated embryo caudal fin-folds are shown, and in the left panels the edge of the fin-fold is indicated with a dashed line. The number of embryos showing similar patterns/ total number of embryos analysed is indicated in the bottom right corner of the right panels. The scale bar represents 100µm. Representative pictures of equivalent uncut controls are depicted in **Fig. S5A**.

We used whole-mount immunohistochemistry with an activated caspase-3-specific antibody to assess apoptosis. At both 1dpa and at 2dpa activated Caspase-3 is enhanced in *ptena*$^{-/-}$*ptenb*$^{-/-}$ zebrafish embryos compared to siblings (**Fig. 7, S6**). Representative images of caudal fin-folds of live zebrafish embryos stained with acridine orange, for cells undergoing apoptosis (Tucker & Lardelli, 2007), confirmed that *ptena*$^{-/-}$*ptenb*$^{-/-}$ zebrafish embryos experienced enhanced apoptosis compared to siblings (**Fig. S7**). Taken together, the lack of regeneration in *ptena*$^{-/-}$*ptenb*$^{-/-}$ zebrafish embryos is likely due to arrested proliferation and enhanced apoptosis.

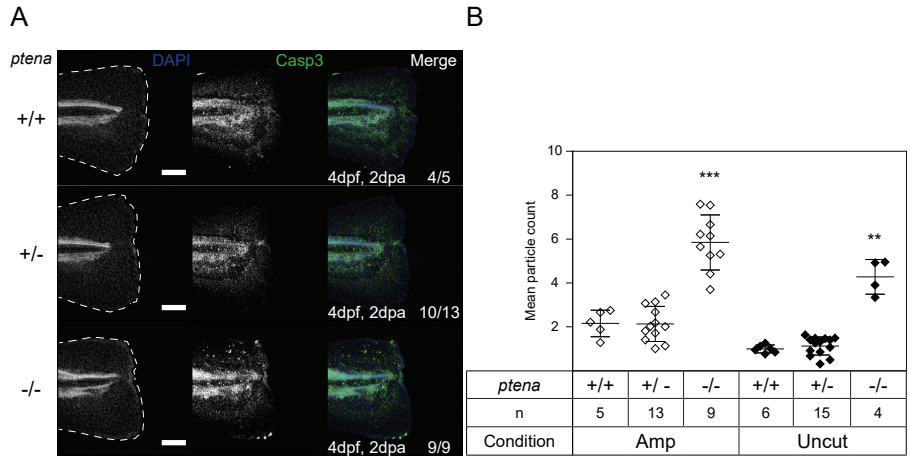

Fig. 7. Enhanced apoptosis in the caudal fin-folds of Pten deficient embryos by 4dpf. (**A**) Embryos from a *ptena*$^{+/-}$*ptenb*$^{-/-}$ in-cross were amputated and fixed at 2dpa (i.e. 4dpf, 2dpa) and subjected to whole-mount immunohistochemistry using an antibody specific for the apoptosis marker activated Caspase-3 (green). The embryos were counterstained with DAPI (blue). Representative images of amputated embryo caudal fin-folds are shown, and in the left panels the edge of the fin-fold is indicated with a dashed line. Number of embryos showing similar patterns/ total number of embryos analysed is indicated in the bottom right corner. The scale bar represents 100µm. (**B**) Caspase-3 immunofluorescence was quantified by mean particle count of the caudal fin-fold. Equivalent uncut controls were also quantified (representative pictures depicted in **Fig. S6A**). Means within amputated or uncut groups were compared to *ptena*$^{+/+}$*ptenb*$^{-/-}$ embryos. Significance: ** $p<0.01$; * $p<0.05$; error bars represent standard deviation.

DISCUSSION

Our results demonstrate a critical role for Pten in zebrafish embryo caudal fin-fold regeneration. Zebrafish embryos lacking functional Pten (*ptena*$^{-/-}$*ptenb*$^{-/-}$) do not regenerate their caudal fin-folds following amputation (**Fig. 1**). We propose that the increased p-AKT levels in *ptena*$^{-/-}$*ptenb*$^{-/-}$ zebrafish embryos (**Fig. 3, S3**) inhibit caudal fin-fold regeneration, which is consistent with our experiments to restore caudal fin-fold regeneration by balancing the increased PI3K signalling, by either re-expressing WT Ptenb (**Fig. 1B, S1A**), or inhibiting excess PI3K activity with LY294002 (**Fig. 4**). Although we cannot exclude that the inability of *ptena*$^{-/-}$*ptenb*$^{-/-}$ zebrafish embryos to regenerate their caudal fin-folds is secondary to developmental abnormalities, the lack of caudal fin-fold regeneration at 1 dpa (3 dpf), when no morphological abnormalities are present, suggests this is unlikely. Furthermore, the rescue of caudal fin-fold regeneration by treatment with LY294002, specifically during regenerative outgrowth, strongly suggests that Pten has a specific role during caudal fin-fold regeneration.

Normally, fin amputation induces three sequential steps to replace the lost fin: wound healing, blastema formation and regenerative outgrowth. Following wound healing, an apical epidermal cap is produced that signals for the formation of the blastema, and, thus, successful blastema formation is indicative of successful wound healing. *Junbb* expression is maintained well into the initial stage of regenerative outgrowth (Ishida, Nakajima, Kudo, & Kawakami, 2010), indicating that *junbb* is a definitive blastema marker. We show that the amputated caudal fin-folds of *ptena*$^{-/-}$*ptenb*$^{-/-}$ zebrafish embryos express *junbb*, like their siblings (**Fig. 5**), indicating that both wound healing and blastema formation occur normally in the absence of Pten. Whereas inhibition of PI3K with LY294002 has been shown to prevent blastema formation (Nakatani et al., 2008), our results demonstrate that excess PI3K activity is not detrimental to blastema formation.

Regenerative outgrowth is characterized by proliferation and differentiation of cells to replace the lost tissue. Whilst cells of amputated *ptena*$^{-/-}$*ptenb*$^{-/-}$ zebrafish embryo caudal fin-folds initially proliferate as normal (**Fig. S5C**), by 2dpa proliferation is arrested compared to siblings (**Fig. 6**). This result is surprising as it is well demonstrated that PTEN loss leads to increased proliferation (Shaw & Cantley, 2006). However, this response occurs in tumour cells, whereas the cells of developing *ptena*$^{-/-}$*ptenb*$^{-/-}$ zebrafish embryos are otherwise normal. Oncogenes expressed in normal healthy cells induce senescence (Gorgoulis & Halazonetis, 2010), and hyper-active AKT has been shown to do the same in mouse embryonic- and human-fibroblasts (Astle et al., 2012; Chen et al., 2005). Moreover, T-cell senescence occurs in some immunodeficient patients with germline gain-of-function mutations in PI3K (Lucas et al., 2014). Therefore, elevated p-AKT in our *ptena*$^{-/-}$*ptenb*$^{-/-}$ zebrafish embryos (**Fig. 3, S3**) may induce senescence that results in proliferation arrest by 2dpa.

Activated Caspase-3 positive cells are increased in caudal fin-folds of *ptena*$^{-/-}$*ptenb*$^{-/-}$ zebrafish embryos compared to siblings (**Fig. 6, S6, S7**), which is surprising because loss of PTEN is often associated with suppression of apoptosis and enhanced cell survival (Brunet et al., 1999; Kulik, Klippel, & Weber, 1997). These responses are elicited in immortalized cell lines, or cell lines following irradiation-induced DNA damage though, which are not normal, wild-type cells or conditions. Hyper-active AKT in normal human cells initiates the release of pro-inflammatory cytokines, a hallmark of senescence-associated secretory phenotype (SASP) (Astle et al., 2012), which is thought to induce apoptosis of senescent cells (Freund, Orjalo, Desprez, & Campisi, 2010). Thus, the elevated p-AKT in *ptena*$^{-/-}$*ptenb*$^{-/-}$ zebrafish embryos may induce se-

nescence and apoptosis. However, one would expect apoptosis to follow arrested proliferation in AKT-induced senescence, whilst in *ptena*$^{-/-}$*ptenb*$^{-/-}$ zebrafish embryos enhanced apoptosis precedes arrested proliferation (*cf*. **Fig. 7** and **S6** with **Fig. 6** and **S5**).

In addition, arrested proliferation was not observed in the uncut caudal fin-folds of *ptena*$^{-/-}$*ptenb*$^{-/-}$ zebrafish embryos (**Fig. S5A, S5B**), suggesting elevated p-AKT alone is not sufficient to induce senescence, and that caudal fin-fold amputation has an additional effect that leads to arrested proliferation in amputated *ptena*$^{-/-}$*ptenb*$^{-/-}$ zebrafish embryos. In *Rxra* knock-out mouse embryos, where gastrulation defects during embryogenesis lead to cardiac defects and ultimately lethality by E15.5, apoptosis precedes reduced proliferation (Kubalak, Hutson, Scott, & Shannon, 2002). That study attributed this to upregulated transforming growth factor β (TGFβ) signalling. Identifying the consequences of *pten* knock-out on other signalling pathways implicated in caudal fin-fold regeneration may explain why apoptosis is enhanced and proliferation becomes arrested by 2dpa.

In conclusion, we demonstrate for the first time that Pten is required for embryonic zebrafish caudal fin-fold regeneration. Loss of Pten inhibits caudal fin-fold regeneration associated with reduced proliferation, enhanced apoptosis, and elevated AKT activation. Restoring Pten expression, or inhibiting PI3K activity during regenerative outgrowth rescues caudal fin-fold regeneration in zebrafish embryos lacking functional Pten protein. Pten likely functions to balance PI3K signalling to coordinate proper proliferation and apoptosis during regenerative outgrowth.

ACKNOWLEDGEMENTS

We thank Matthias Hammerschmidt for help with optimizing the whole-mount immunohistochemistry protocols. We thank Geert Geeven for batch processing the maximum intensity projections of all immunohistochemistry experiments.

REFERENCES

Astle, M. V, Hannan, K. M., Ng, P. Y., Lee, R. S., George, a J., Hsu, a K., … Pearson, R. B. (2012). AKT induces senescence in human cells via mTORC1 and p53 in the absence of DNA damage: implications for targeting mTOR during malignancy. *Oncogene*, *31*(15), 1949–1962. http://doi.org/10.1038/onc.2011.394

Brunet, A., Bonni, A., Zigmond, M. J., Lin, M. Z., Juo, P., Hu, L. S., … Greenberg, M. E. (1999). Akt Promotes Cell Survival by Phosphorylating and Inhibiting a Forkhead Transcription Factor. *Cell*, *96*, 857–868.

Burgering, B. M. T., & Coffer, P. J. (1995). Protein kinase B (c-Akt) in phosphatidylinositol-3-OH kinase signal transduction. *Nature*, *376*(6541), 599–602. Retrieved from http://dx.doi.org/10.1038/376599a0

Byrne, A. B., Walradt, T., Gardner, K. E., Hubbert, A., Reinke, V., & Hammarlund, M. (2014). Insulin/IGF1 Signaling Inhibits Age-Dependent Axon Regeneration. *Neuron*. http://doi.org/10.1016/j.neuron.2013.11.019

Chen, Z., Trotman, L. C., Shaffer, D., Lin, H.-K., Dotan, Z. A., Niki, M., … Pandolfi, P. P. (2005). Crucial role of p53-dependent cellular senescence in suppression of Pten-deficient tumorigenesis. *Nature*, *436*(7051), 725–730. http://doi.org/10.3892/ijo

Choorapoikayil, S., Kuiper, R. V., de Bruin, A., & den Hertog, J. (2012). Haploinsufficiency of the genes encoding the tumor suppressor Pten predisposes zebrafish to hemangiosarcoma. *Disease Models & Mechanisms*, *5*, 241–247. http://doi.org/10.1242/dmm.008326

Choorapoikayil, S., Weijts, B., Kers, R., de Bruin, A., & den Hertog, J. (2013). Loss of Pten promotes angiogenesis and enhanced vegfaa expression in zebrafish. *Disease Models & Mechanisms*, *6*(5), 1159–1166. http://doi.org/10.1242/dmm.012377

Cristofano, A. D., Pesce, B., Cordon-Cardo, C., Pandolfi, P. P., Di Cristofano, A., Pesce, B., … Pandolfi, P. P. (1998). Pten is essential for embryonic development and tumour suppression. *Nature Genetics*, *19*(4), 348–355. http://doi.org/10.1038/1235

Faucherre, a, Taylor, G. S., Overvoorde, J., Dixon, J. E., & Hertog, J. Den. (2008). Zebrafish pten genes have overlapping and non-redundant functions in tumorigenesis and embryonic development. *Oncogene*, *27*(8), 1079–1086. http://doi.org/10.1038/sj.onc.1210730

Freund, A., Orjalo, A. V, Desprez, P.-Y., & Campisi, J. (2010). Inflammatory Networks during Cellular Senescence: Causes and Consequences. *Trends in Molecular Medicine*, *16*(5), 238–246. http://doi.org/10.1016/j.molmed.2010.03.003

Gauron, C., Rampon, C., Bouzaffour, M., Ipendey, E., Teillon, J., Volovitch, M., & Vriz, S. (2013). Sustained production of ROS triggers compensatory proliferation and is required for regeneration to proceed. *Scientific Reports*, *3*, 2084. http://doi.org/10.1038/srep02084

Gemberling, M., Bailey, T. J., Hyde, D. R., & Poss, K. D. (2013). The zebrafish as a model for complex tissue regeneration. *Trends in Genetics*, *5*(13), 113.

Gorgoulis, V. G., & Halazonetis, T. D. (2010). Oncogene-induced senescence: The bright and dark side of the response. *Current Opinion in Cell Biology*, *22*(6), 816–827. http://doi.org/10.1016/j.ceb.2010.07.013

Hale, A. J., & den Hertog, J. (2016). Studying Protein-Tyrosine Phosphatases in Zebrafish. In R. Pulido (Ed.), *Protein Tyrosine Phosphatases: Methods and Protocols* (pp. 351–372). New York, NY: Springer New York. http://doi.org/10.1007/978-1-4939-3746-2_19

He, Z. (2010). Intrinsic control of axon regeneration. *Journal of Biomedical Research*, *24*(1), 2–5. http://doi.org/10.1016/S1674-8301(10)60002-4

Hirose, K., Shiomi, T., Hozumi, S., & Kikuchi, Y. (2014). Mechanistic target of rapamycin complex 1 signaling regulates cell proliferation, cell survival, and differentiation in regenerating zebrafish fins. *BMC Developmental Biology*, *14*, 42. http://doi.org/10.1186/s12861-014-0042-9

Ishida, T., Nakajima, T., Kudo, A., & Kawakami, A. (2010). Phosphorylation of Junb family proteins by the Jun N-terminal kinase supports tissue regeneration in zebrafish. *Developmental Biology*, *340*(2), 468–479. http://doi.org/10.1016/j.ydbio.2010.01.036

Kawakami, A., Fukazawa, T., & Takeda, H. (2004). Early fin primordia of zebrafish larvae regenerate by a similar growth control mechanism with adult regeneration. *Developmental Dynamics*, *231*(4), 693–9.

Kubalak, S. W., Hutson, D. R., Scott, K. K., & Shannon, R. A. (2002). Elevated transforming growth factor β2 enhances apoptosis and contributes to abnormal outflow tract and aortic sac development in retinoic X receptor α knockout embryos. *Development*.

Kulik, G., Klippel, A., & Weber, M. J. (1997). Antiapoptotic signalling by the insulin-like growth factor I receptor, phosphatidylinositol 3-kinase, and Akt. *Molecular and Cellular Biology*, *17*, 1595–1606.

Liu, K., Lu, Y., Lee, J. K., Samara, R., Willenberg, R., Sears-Kraxberger, I., … He, Z. (2010). PTEN deletion enhances the regenerative ability of adult corticospinal neurons. *Nature Neuroscience*, *13*(9), 1075–1081. http://doi.org/10.1038/nn.2603

Lucas, C. L., Kuehn, H. S., Zhao, F., Niemela, J. E., Deenick, E. K., Palendira, U., … Uzel, G. (2014). Dominant-activating germline mutations in the gene encoding the PI(3)K catalytic subunit p110delta result in T cell senescence and human immunodeficiency. *Nature Immunology*, *15*(1), 88–97. http://doi.org/10.1038/ni.2771

Myers, M. P., Pass, I., Batty, I. H., Van der Kaay, J., Stolarov, J. P., Hemmings, B. A., … Tonks, N. K. (1998). The lipid phosphatase activity of PTEN is critical for its tumor supressor function. *Proceedings of the National Academy of Sciences*, *95*(23), 13513–13518. http://doi.org/10.1073/pnas.95.23.13513

Nakatani, Y., Nishidate, M., Fujita, M., Kawakami, A., & Kudo, A. (2008). Migration of mesenchymal cell fated to blastema is necessary for fish fin regeneration. *Development Growth and Differentiation*, *50*(2), 71–83. http://doi.org/10.1111/j.1440-169X.2007.00977.x

Ohtake, Y., Hayat, U., & Li, S. (2015). PTEN inhibition and axon regeneration and neural repair. *Neural Regeneration Research*. http://doi.org/10.4103/1673-5374.165496

Padhi, B. K., Joly, L., Tellis, P., Smith, A., Nanjappa, P., Chevrette, M., … Akimenko, M. A. (2004). Screen for genes differentially expressed during regeneration of the zebrafish caudal fin. *Developmental Dynamics*, *231*(3), 527–541. http://doi.org/10.1002/dvdy.20153

Pfefferli, C., & Jaźwińska, A. (2015). The art of fin regeneration in zebrafish. *Regeneration*, *2*(2), 72–83. http://doi.org/10.1002/reg2.33

Poleo, G., Brown, C. W., Laforest, L., & Akimenko, M. A. (2001). Cell proliferation and movement during early fin regeneration in zebrafish. *Developmental Dynamics*, *221*(4), 380–390. http://doi.org/10.1002/dvdy.1152

Poss, K. D., Keating, M. T., & Nechiporuk, A. (2003). Tales of regeneration in zebrafish. *Developmental Dynamics*, *226*(2), 202–210. http://doi.org/10.1002/dvdy.10220

Rojas-Muñoz, A., Rajadhyksha, S., Gilmour, D., van Bebber, F., Antos, C., Rodríguez Esteban, C., Izpisúa Belmonte, J. C. (2009). ErbB2 and ErbB3 regulate amputation-induced proliferation and migration during vertebrate regeneration. *Developmental Biology*, *327*(1), 177–190. http://doi.org/10.1016/j.ydbio.2008.12.012

Shaw, R. J., & Cantley, L. C. (2006). Ras, PI(3)K and mTOR signalling controls tumour cell growth. *Nature*, *441*(7092), 424–430. http://doi.org/10.1038/nature04869

Sorrells, S., Toruno, C., Stewart, R. A., & Jette, C. (2013). Analysis of apoptosis in zebrafish embryos by whole-mount immunofluorescence to detect activated Caspase 3. *Journal of Visualized Experiments : JoVE*, *82*(82), e51060. http://doi.org/10.3791/51060

Stambolic, V., Suzuki, A., de la Pompa, J. L., Brothers, G. M., Mirtsos, C., Sasaki, T., … Mak, T. W. (1998). Negative regulation of PKB/Akt-dependent cell survival by the tumor suppressor PTEN. *Cell*, *95*(1), 29–39. http://doi.org/10.1016/S0092-8674(00)81780-8

Stumpf, M., Choorapoikayil, S., & den Hertog, J. (2015). Pten function in zebrafish: Anything but a fish story. *Methods*, *77–78*, 191–196. http://doi.org/http://dx.doi.org/10.1016/j.ymeth.2014.11.002

Stumpf, M., & Den Hertog, J. (2016). Differential requirement for pten lipid and protein phosphatase activity during zebrafish embryonic development. *PLoS ONE*, *11*(2), e0148508. http://doi.org/10.1371/journal.pone.0148508

Thisse, C., Thisse, B., Schilling, T. F., & Postlethwait, J. H. (1993). Structure of the zebrafish snail1 gene and its expression in wild-type, spadetail and no tail mutant embryos. *Development*, *119*(4), 1203–1215.

Thorimbert, V., Konig, D., Marro, J., Ruggiero, F., Jazwinska, A., König, D., … Jaźwińska, A. (2015). Bone morphogenetic protein signaling promotes morphogenesis of blood vessels, wound epidermis, and actinotrichia during fin regeneration in zebrafish. *FASEB Journal*, *29*(10), 4299–4312. http://doi.org/10.1096/fj.15-272955

Tucker, B., & Lardelli, M. (2007). A rapid apoptosis assay measuring relative acridine orange fluorescence in zebrafish embryos. *Zebrafish*, *4*(2), 113–116. http://doi.org/10.1089/zeb.2007.0508

van der Velden, Y. U., Wang, L., Zevenhoven, J., van Rooijen, E., van Lohuizen, M., Giles, R. H., … Haramis, A.-P. G. (2011). The serine-threonine kinase LKB1 is essential for survival under energetic stress in zebrafish. *Proceedings of the National Academy of Sciences of the United States of America*, *108*(11), 4358–4363. http://doi.org/10.1073/pnas.1010210108

Vara, J. Á. F., Casado, E., de Castro, J., Cejas, P., Belda-Iniesta, C., & González-Barón, M. (2004). PI3K/Akt signalling pathway and cancer. *Cancer Treatment Reviews*, *30*(2), 193–204. http://doi.org/http://dx.doi.org/10.1016/j.ctrv.2003.07.007

Westerfield, M. (2000). *The zebrafish book. A guide for the laboratory use of zebrafish (Danio rerio)* (4th ed.). Eugene: University of Oregon Press.

Yoshinari, N., Ishida, T., Kudo, A., & Kawakami, A. (2009). Gene expression and functional analysis of zebrafish larval fin fold regeneration. *Developmental Biology*, *325*(1), 71–81. http://doi.org/10.1016/j.ydbio.2008.09.028

SUPPORTING INFORMATION

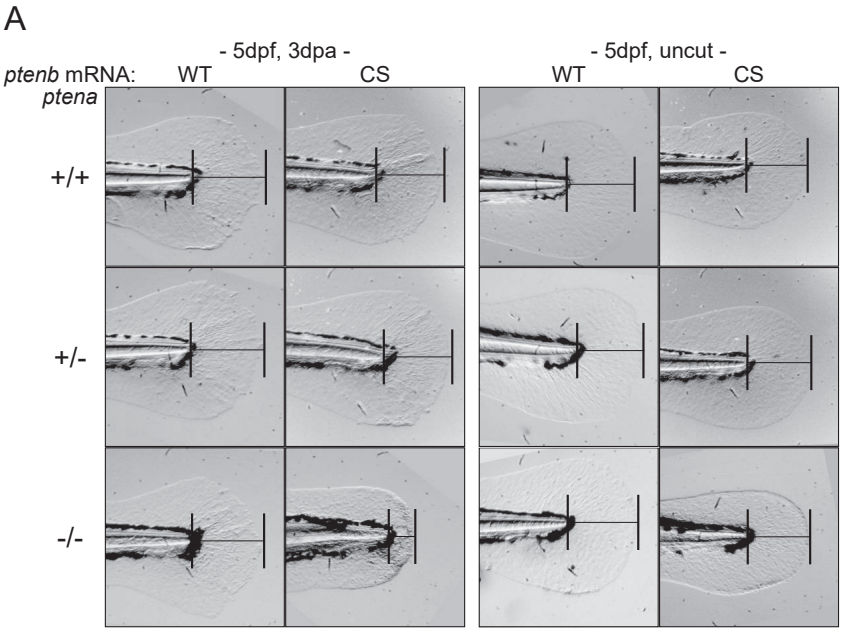

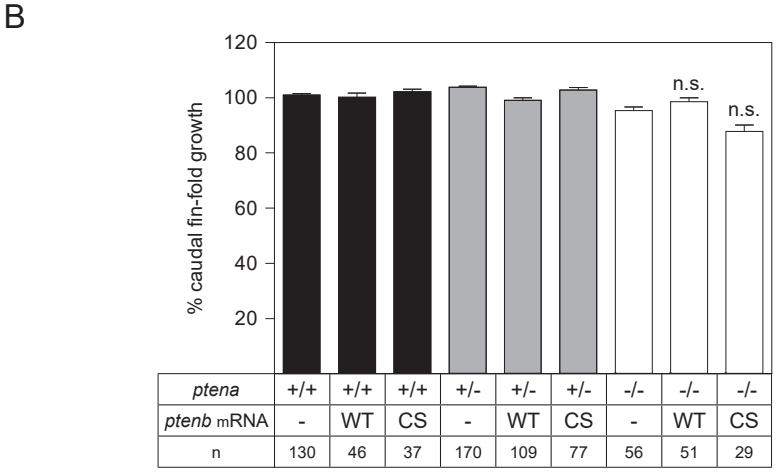

ptena	+/+	+/+	+/+	+/-	+/-	+/-	-/-	-/-	-/-
ptenb mRNA	-	WT	CS	-	WT	CS	-	WT	CS
n	130	46	37	170	109	77	56	51	29

Fig. S1. Impaired caudal fin-fold regeneration in Pten deficient embryos. Embryos from a *ptena*$^{+/-}$ *ptenb*$^{-/-}$ in-cross were micro-injected at the one-cell stage with synthetic mRNA encoding WT Ptenb (WT), catalytically inactive Ptenb-C124S (CS), or were not injected (-). At 2dpf the caudal fin-fold was amputated and regeneration was assessed after 3 days (i.e. 5dpf, 3dpa), equivalent uncut controls were included (i.e. 5dpf, uncut). All embryos were genotyped. Representative images of micro-injected embryo caudal fin-folds are shown (**A**). Uncut caudal fin-fold growth was quantified by measuring the distance from the tip of the notochord to the edge of the caudal fin-fold. The means of uncut caudal fin-fold growth are depicted relative to caudal fin growth of uncut *ptena*$^{+/+}$*ptenb*$^{-/-}$ controls. Means of micro-injected *ptena*$^{-/-}$*ptenb*$^{-/-}$ embryos were compared to non-injected *ptena*$^{-/-}$*ptenb*$^{-/-}$ embryos using a Mann-Whitney U-test. Error bars indicate standard error of the mean (**B**).

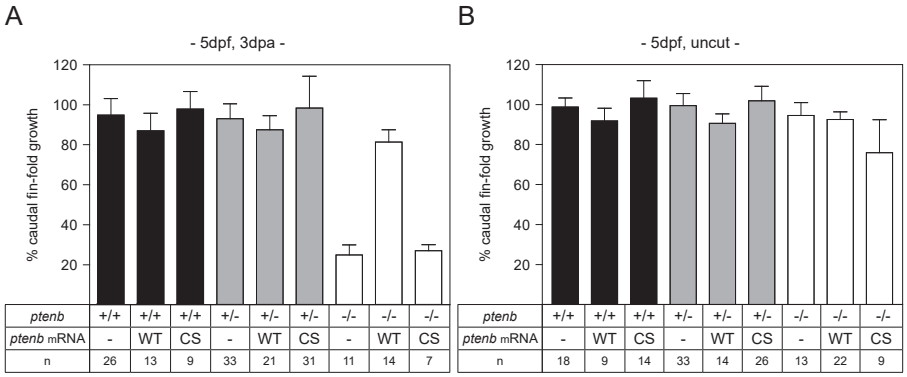

Fig. S2. Impaired caudal fin-fold regeneration in Pten deficient embryos. Embryos from a *ptena*$^{-/-}$*ptenb*$^{+/-}$ in-cross were micro-injected at the one-cell stage with synthetic mRNA encoding WT Ptenb (WT), catalytically inactive Ptenb-C124S (CS), or were not injected (-). At 2dpf the caudal fin-fold was amputated and regeneration was assessed after 3 days (i.e. 5dpf, 3dpa) (**A**), equivalent uncut controls were included (i.e. 5dpf, uncut) (**B**). All embryos were genotyped. Caudal fin growth was quantified by measuring the distance from the tip of the notochord to the edge of the caudal fin-fold. The means of caudal fin-fold growth are depicted relative to caudal fin growth of uncut *ptena*$^{-/-}$*ptenb*$^{+/+}$ controls. Error bars indicate standard error of the mean.

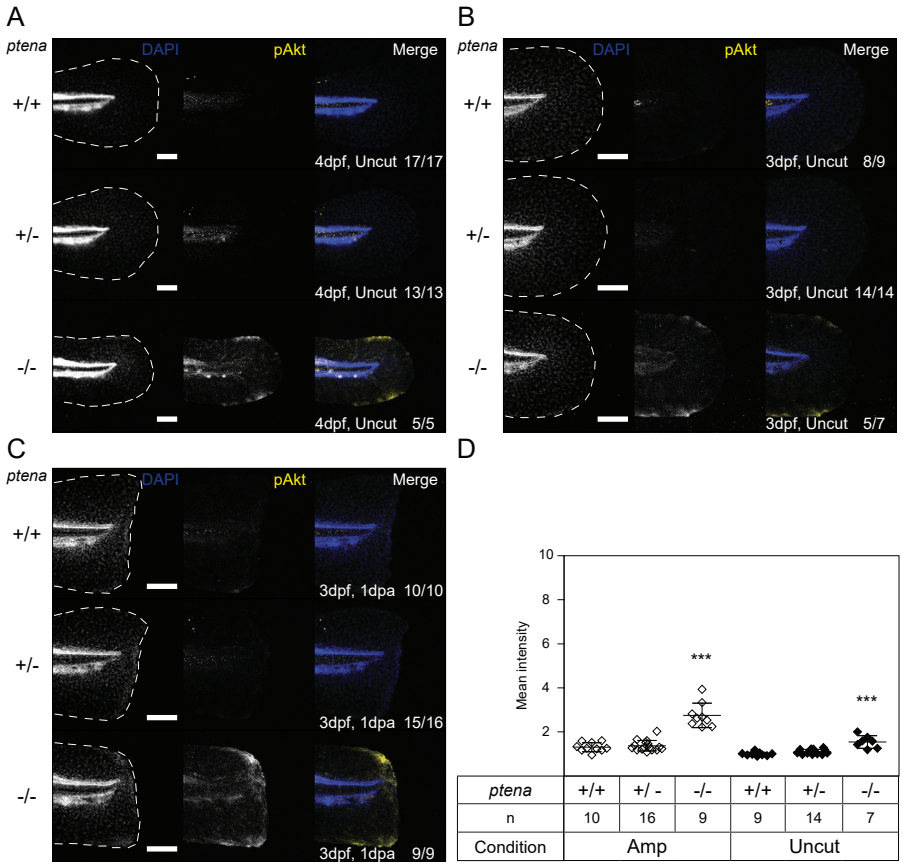

Fig. S3. Elevated p-AKT in the caudal fin-folds of Pten deficient embryos. Uncut embryos from a *ptena*$^{-/-}$*ptenb*$^{+/-}$ in-cross were fixed at 4dpf (4dpf, uncut) in parallel to the embryos depicted in **Fig. 3A** (**A**). At 2dpf the caudal fin-fold of embryos from a *ptena*$^{+/-}$*ptenb*$^{-/-}$ in-cross was amputated and allowed to regenerate. Embryos were fixed at 1dpa (i.e. 3dpf, 1dpa) (**C**), or equivalent for uncut controls (3dpf, uncut) (**B**). Embryos were subjected to whole-mount immunohistochemistry using a p-AKT-specific antibody (p-S473) (yellow). The embryos were counterstained with DAPI (blue). Maximum intensity projection images were taken of the caudal fin-folds and all embryos were genotyped. Representative images of embryo caudal fin-folds are shown, and in the left panels the edge of the fin is indicated with a dashed line. The number of embryos showing similar patterns/ total number of embryos analysed is indicated in the bottom right corner of the right panels. The scale bar represents 100µm. p-AKT immunofluorescence was quantified by mean intensity of the region between the notochord and the edge of the caudal fin-fold. Means within amputated or uncut groups are compared to *ptena*$^{+/+}$*ptenb*$^{-/-}$ embryos using a Mann-Whitney U-test. The number of embryos analysed is indicated (n). Significance: *** p<0.001; error bars represent standard deviation (**D**). Quantification of p-AKT immunofluorescence at 4dpf is depicted in **Fig. 3B**.

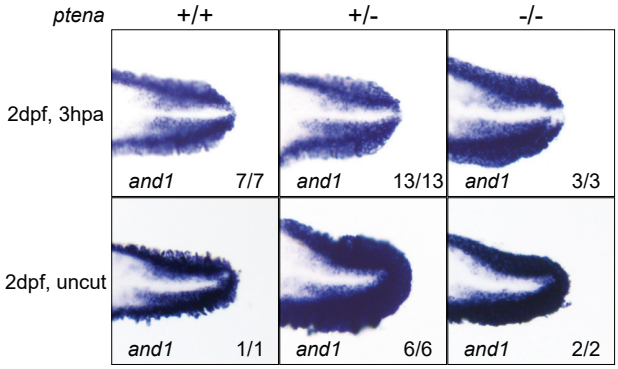

Fig. S4. *In-situ* hybridization staining of *and1* in Pten deficient embryos. At 2dpf the caudal fin-fold of embryos from a *ptena*$^{+/-}$*ptenb*$^{-/-}$ in-cross was amputated and allowed to regenerate. Embryos were fixed at 3hpa, or equivalent for uncut controls, and subjected to *in situ* hybridization for *and1*. Representative images of embryo caudal fin-folds are shown with the number of embryos/total number of embryos in the bottom right corner of each panel.

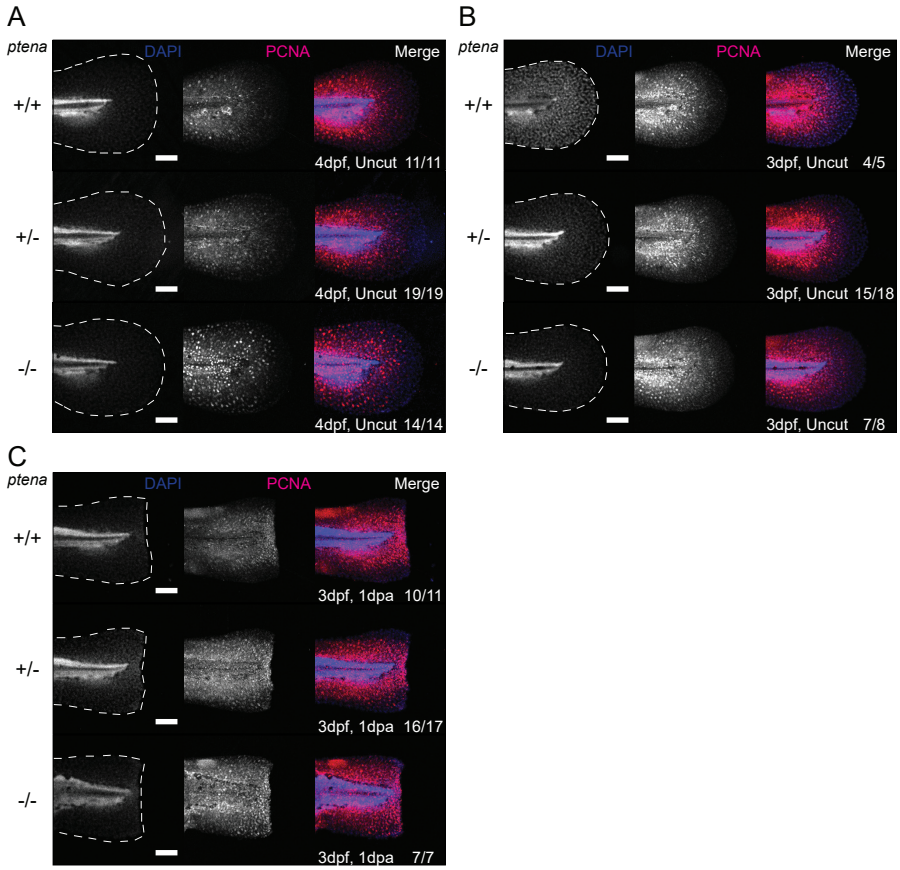

Fig. S5. Normal proliferation in the caudal fin-folds of Pten deficient embryos. Uncut embryos from a *ptena*$^{+/-}$*ptenb*$^{-/-}$ in-cross were fixed at 4dpf (4dpf, uncut) in parallel to the embryos depicted in **Fig. 6** (**A**). At 2dpf the caudal fin-fold of embryos from a *ptena*$^{+/-}$*ptenb*$^{-/-}$ in-cross was amputated and allowed to regenerate. Embryos were fixed at 1dpa (i.e. 3dpf, 1dpa) (**C**), or equivalent for uncut controls (3dpf, uncut) (**B**). Embryos were subjected to whole-mount immunohistochemistry using an antibody specific for the cell proliferation marker PCNA (red). The embryos were counter-stained with DAPI (blue). Maximum intensity projection images were taken of the caudal fin-folds and all embryos were genotyped. Representative images of embryo caudal fin-folds are shown, and in the left panels the edge of the fin-fold is indicated with a dashed line. The number of embryos showing similar patterns/ total number of embryos analysed is indicated in the bottom right corner of the right panels. The scale bar represents 100µm.

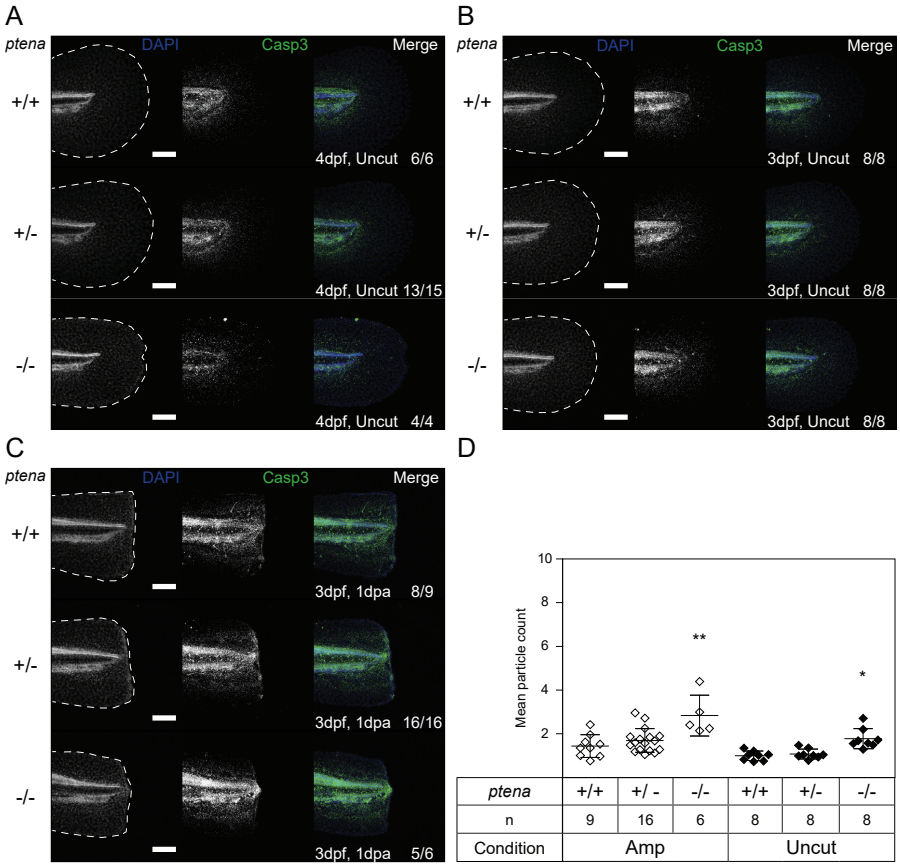

Fig. S6. Enhanced apoptosis in the caudal fin-folds of Pten deficient embryos. Uncut embryos from a *ptena*$^{+/-}$*ptenb*$^{-/-}$ in-cross were fixed at 4dpf (4dpf, uncut) in parallel to the embryos depicted in **Fig. 7A** (**A**). At 2dpf the caudal fin-fold of embryos from a *ptena*$^{+/-}$*ptenb*$^{-/-}$ in-cross was amputated and allowed to regenerate. Embryos were fixed at 1dpa (i.e. 3dpf, 1dpa) (**C**), or equivalent for uncut controls (3dpf, uncut) (**B**). Embryos were subjected to whole-mount immunohistochemistry using an antibody specific for the apoptosis marker activated Caspase-3 (green). The embryos were counterstained with DAPI (blue). Maximum intensity projection images were taken of the caudal fin-folds and all embryos were genotyped. Representative images of embryo caudal fin-folds are shown, and in the left panels the edge of the fin-fold is indicated with a dashed line. The number of embryos showing similar patterns/ total number of embryos analysed is indicated in the bottom right corner of the right panels. The scale bar represents 100µm. Caspase-3 immunofluorescence was quantified by mean particle count of the caudal fin-fold. Means within amputated or uncut groups are compared to *ptena*$^{+/+}$*ptenb*$^{-/-}$ embryos using a Mann-Whitney U-test. The number of embryos analysed is indicated (n). Significance: * $p<0.05$; ** $p<0.01$; error bars represent standard deviation (**D**). Quantification of Caspase-3 immunofluorescence at 4dpf is depicted in **Fig. 7B**.

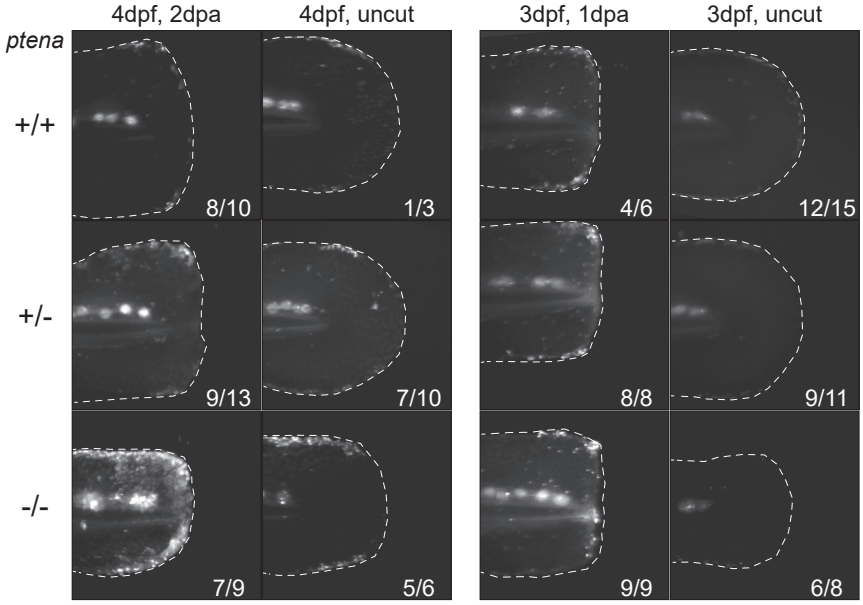

Fig. S7. Enhanced apoptosis in the caudal fin-folds of live Pten deficient embryos. At 2dpf the caudal fin-fold of embryos from a *ptena*$^{+/-}$*ptenb*$^{-/-}$ in-cross was amputated and allowed to regenerate. Embryos were stained at 2dpa (i.e. 4dpf, 2dpa) or 1dpa (i.e. 3dpf, 1dpa), or equivalent for uncut controls (i.e. 4dpf, uncut; or 3dpf, uncut), with a dye for cells undergoing apoptosis, acridine orange, for 30mins. Representative images of embryo caudal fin-folds at 4dfp and 3dpf are shown, and the edge of the fin-fold is indicated with a dashed line. The number of embryos showing similar patterns/ total number of embryos analysed is indicated in the bottom right corner of each panel.

Table S1. Primers used for amplifying *junbb* and *and1* from zebrafish embryo cDNA, and *ptena* and *ptenb* from genomic zebrafish DNA.

Primer	Sequence
and1 FWD	CAAGACAGGCCTTGAGGAAG
and1-T7 REV	TAATACGACTCACTATAGTTGGGAACTTAGTGGGATGC
junbb FWD 1	TGGGTTACGGTCACAACGAC
junbb REV 1	CAGTGTCCGTTCTCTTCCGT
BamHI-*junbb* FWD (nested 1)	ATAGGATCCTACACGACGCTGAACGCATA
junbb-EcoRI REV (nested 2)	CTCGAATTCGTGTCCGTTCTCTTCCGTCC
junbb FWD 2	TACACGACGCTGAACGCATA
junbb-T7 REV 2	TAATACGACTCACTATAGGTGTCCGTTCTCTTCCGTCC
ptena WT FWD	GAAGGTGACCAAGTTCATGCTTGGGCTTTCCAGCCGAAC
ptena KO FWD	GAAGGTCGGAGTCAACGGATTTGGGCTTTCCAGCCGAAT
ptena REV	TCAATGTTGTTTCGGTAAACACCTTCCAA
ptenb WT FWD	GAAGGTGACCAAGTTCATGCTGTTTCTTGATTCAAAGCATAAAGATCATTAC
ptenb KO FWD	GAAGGTCGGAGTCAACGGATTGTTTCTTGATTCAAAGCATAAAGATCATTAA
ptenb REV	CTGAAGTTTTTGAAACACACTTACAGGTT

Chapter 5

Differential Oxidation of Protein-Tyrosine Phosphatases during Zebrafish Caudal Fin Regeneration

Wei Wu[1*], Alexander James Hale[2,3*], Simone Lemeer[1§], and Jeroen den Hertog[2,3,§]

1. Biomolecular Mass Spectrometry and Proteomics, Bijvoet Center for Biomolecular Research and Utrecht Institute for Pharmaceutical Sciences, Utrecht University and Netherlands Proteomics Centre, Utrecht, The Netherlands
2. Hubrecht Institute – KNAW and University Medical Center Utrecht, Utrecht, the Netherlands
3. Institute Biology Leiden, Leiden University, Leiden, The Netherlands
** These authors contributed equally*
§ These authors co-directed this work

ABSTRACT

Zebrafish have the capacity to regenerate lost tissues and organs. In response to amputation of the zebrafish caudal fin, a rapid, transient increase in H_2O_2 levels was observed emanating from the wound margin, which is essential for regeneration, because quenching of reactive oxygen species blocks regeneration. We hypothesized that protein-tyrosine phosphatases (PTPs), which are susceptible to oxidation-mediated inactivation, might become oxidized in response to amputation of the caudal fin. Using the oxidized PTP-specific (ox-PTP) antibody and liquid chromatography-mass spectrometry, we identified 33 PTPs in adult zebrafish fin clips of the total of 44 PTPs that can theoretically be detected based on sequence conservation. Of these 33 PTPs, 8 were significantly more oxidized 40 min after caudal fin amputation. Surprisingly, Shp2, one of the PTPs that were oxidized in response to caudal fin amputation, was required for caudal fin regeneration. In contrast, Rptpα, which was not oxidized upon amputation, was dispensable for caudal fin regeneration. Our results demonstrate that PTPs are differentially oxidized in response to caudal fin amputation and that there is a differential requirement for PTPs in regeneration.

INTRODUCTION

Epimorphic regeneration is the perfect replacement of lost tissue, organs, or limbs. Zebrafish can fully regenerate multiple organs after injury, including the heart, retina, spinal cord, and caudal fin[1,2]. Many genes have been implicated and multiple signalling pathways have been validated to be essential for regeneration to proceed, including fibroblast growth factor (FGF), sonic hedgehog, bone morphogenetic protein, Wnt, and Notch[3,4]. However, it remains unclear how this complex process is initiated. One of the first responses following amputation of the zebrafish caudal fin is a burst of hydrogen peroxide (H_2O_2) that emanates from the wound site and extends into the tissue[5]. Inhibition of this burst of H_2O_2 impairs zebrafish caudal fin regeneration[6], demonstrating it is essential for this process.

H_2O_2 is a reactive oxygen species (ROS) that, as well as a chemoattractant, acts as a second messenger molecule to regulate intracellular signalling including mitogen activated protein kinase (MAPK), phosphoinositide-3-kinase (PI3K)/AKT, and NF-κB signal transduction[7,8]. H_2O_2 reversibly oxidizes cysteine residues that are in the thiolate anion form due to a low pKa, which results from their microenvironment. Often, the active-site cysteine of enzymes has a low pKa, which actually confers catalytic activity. Reversible oxidation of these cysteine residues temporarily activates or inactivates these enzymes[9].

Protein-tyrosine phosphatases (PTPs) constitute a family of active-site cysteine enzymes that mediate tyrosine dephosphorylation [10–12]. A total of 125 genes encoding enzymes with PTP activity have been identified in the human genome, 116 of which are cysteine-based, and constitute an enzyme superfamily divided into classical PTPs, dual-specificity PTPs, and low molecular weight PTPs[13,14]. The classical PTPs are further subdivided into receptor and non-receptor PTPs. Classical PTPs are defined by having at least one catalytic domain with a conserved signature motif (I/V)H**C**SAGXXR(S/T)G, containing the catalytic cysteine (in **bold**), which is essential for catalysing the removal of the phosphate group from phospho-tyrosine residues. The sulphur atom in the catalytic cysteine of active PTPs is in the thiolate anion form (S^-). H_2O_2 inactivates PTPs by reversibly oxidizing this sulphur atom to sulphenic acid (SOH), a labile state that rapidly rearranges to form a sulphenylamide with an adjacent nitrogen[15] or a disulphide bond with a nearby cysteine[16]. These states help protect the catalytic cysteine from further irreversible hyperoxidation to sulphinic acid (SO_2H) or sulphonic acid (SO_3H) states[17]. A monoclonal antibody (ox-PTP Ab) was raised against a hexapeptide encoding the

conserved PTP signature motif with a triply oxidized cysteine, $VHC_{SO3H}SAG$, which can be used to detect reversible and irreversible oxidation of PTPs[18,19]. The susceptibility to oxidation differs from PTP to PTP[10,20], suggesting dose-dependent specificity in ROS signalling. Mechanistically, oxidation-mediated inhibition of PTPs results in the selective amplification or attenuation of specific signalling pathways, such as FGF, PI3K/AKT, and MAPK, ultimately regulating fundamental cellular processes, including proliferation, differentiation, and cell-cell adhesion[21].

Considering the high susceptibility of PTPs to oxidation, we hypothesized that the H_2O_2 burst following zebrafish caudal fin amputation may oxidize PTPs. Using the ox-PTP-specific antibody and mass spectrometry, we detected 37 out of 52 predicted zebrafish PTP motif peptides, 8 of which were oxidized following zebrafish caudal fin amputation. We next functionally assessed the role of PTPs during regeneration. Shp2, a cytoplasmic PTP with a central role in signalling was one of the 8 oxidized PTPs. Interestingly, zebrafish mutant embryos lacking functional Shp2 displayed impaired caudal fin-fold regeneration. Zebrafish embryos lacking Rptpα, which was not oxidized upon caudal fin amputation, regenerated their caudal fin-folds normally. These results reveal differential oxidation of PTPs following caudal fin amputation *in vivo*, and suggest a differential requirement for PTPs in zebrafish caudal fin regeneration.

RESULTS

Detecting in vivo PTP oxidation following zebrafish caudal fin amputation

To investigate PTP oxidation following amputation, we isolated zebrafish caudal fin tissue by performing two sequential amputations with a 40 min interval to allow for the H_2O_2 gradient that emanates from the wound margin to form[5] (**Fig. 1**). Repeated amputation does not affect the regenerative capacity of zebrafish[22]. The first (control) and second (sample) zebrafish caudal fin clips were snap-frozen immediately following amputation and lysed in reducing or alkylating lysis buffer to detect all PTPs or oxidized PTPs, respectively (**Fig. 1**).

Under normal conditions, cells contain reduced PTPs ($PTP\text{-}S^-$) and reversibly oxidized PTPs (PTP-SOH)[11]. Reduction of all PTPs in the lysate by treatment with dithiotreitol (DTT), followed by hyperoxidation using pervanadate (PV), converts all catalytic cysteines into the sulphonic acid (SO_3H) state, allowing detection of all PTPs with the

ox-PTP-specific antibody. Reversibly oxidized PTPs can be detected by first lysing in the presence of N-ethylmaleimide (NEM), which alkylates all reduced cysteines, followed by reduction of the oxidized catalytic cysteines using DTT, and hyperoxidation using pervanadate (PV). As the reduced catalytic cysteines are protected from detection by NEM, only the catalytic cysteines that were oxidized at the time of lysis will be detected using the ox-PTP-specific antibody. Comparison of oxidized PTPs with all PTPs in a sample facilitates assessment of the extent of oxidation of the PTP family. Here, we employed protocols that we and others developed[10,18–20] to detect *in vivo* PTP oxidation following amputation of the zebrafish caudal fin using liquid chromatography mass spectrometry (LC-MS)[23] (**Fig. 1**).

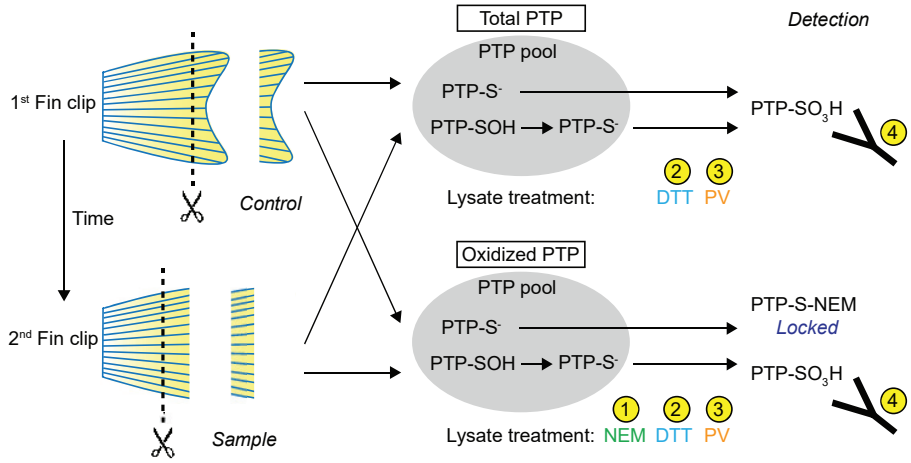

Fig. 1. Detection of total and oxidized PTPs in zebrafish caudal fins. Zebrafish caudal fin tissue was obtained by sequential amputation. The first fin clips (control) were snap-frozen immediately. The second fin clips (sample) were taken after 40 min to allow for H_2O_2 to form and oxidize proteins, and were snap-frozen immediately as well. The PTP pool in cells consists of reduced (PTP-S-) and reversibly oxidized (PTP-SOH) PTPs. Caudal fin clips were either lysed in reducing (DTT-containing) or alkylating (NEM-containing) lysis buffer to detect total and oxidized PTPs, respectively, for both control and sample caudal fin clips. As the ox-PTP antibody only binds hyperoxidized PTPs (PTP-SO_3H), a sequential reduction and oxidation process is required for detection by immunoprecipitation. **1**. NEM in the lysis buffer protects reduced PTPs from hyperoxidation. **2**. DTT reduces all oxidized PTPs to allow hyperoxidation. **3**. pervanadate (PV) hyperoxidizes all reduced PTPs to an irreversibly oxidized state (PTP-SO_3H). **4**. PTP-SO_3H PTPs are recognized by the ox-PTP-specific antibody. Immunoprecipitation allows detection by LC-MS/MS. Lysis in the absence of NEM results in detection of total PTPs. Comparison of the NEM treated first and second fin clips allows detection of the change in oxidized PTPs.

Identification of oxidized PTPs following zebrafish caudal fin amputation

We searched the zebrafish Uniprot+trEMBL database[24] for entries containing the [I/V]HCS[A/V]GXGR[S/T]G motif, and found 52 distinct PTP peptides containing this consensus motif, indicating that those may serve as the epitope for the ox-PTP antibody (**Fig. S1**). Given the tandem PTP domains in some receptor PTPs, the 52 PTP peptides represent 44 distinct PTP proteins. It is noteworthy that the zebrafish genome was duplicated early in evolution. Whilst some of the duplicated chromosomes were lost, the duplicated genes that remain have complementary or diverging expression patterns and exhibit redundant or complementary functions[25,26]. Among the zebrafish classical PTPs, 5 non-receptor PTPs and 9 receptor PTPs are duplicated, the "a" and "b" entries (**Fig. S1**). It is noteworthy that the annotation of proteins in the Uniprot+trEMBL database is incomplete and the majority of sequences submitted for zebrafish PTPs have not been reviewed or validated. The A0A1L1QZV1 and F1QWY5_CA16B entries (**Fig. S1**) actually represent Ptprr and Ptprgb, respectively, based on sequence comparison with human PTPs.

In order to unambiguously identify which PTPs are oxidized, first fin clips (control) and second fin clips (40 min) were isolated and processed as outlined in **Fig. 1**. Fin clips were isolated from 10 adult zebrafish per condition and the lysates were pooled to average out biological differences between individual fish. The experiment was performed in triplicate. Following PV treatment, fin lysates were digested with trypsin and ox-PTP peptides were immunoprecipitated by the ox-PTP-specific antibody. Immunoprecipitated peptides were subsequently analysed by LC-MS/MS. Since trypsin cleaves after the amino acids lysine and arginine, all PTP peptide sequences detected end with an arginine residue within the catalytic domain ([I/V]HCS[A/V]GXG**R**). Unambiguous identification of PTPs was thus achieved using the sequence upstream of the consensus sequence (VHCSA/VG) of every unique PTP peptide, where low sequence conservation is observed. Using this approach, we identified 37 PTP peptides containing an active-site catalytic cysteine in zebrafish caudal fin lysates (**Fig. 2a, b, Table S1**). These 37 PTP peptides are derived from 33 distinct PTP proteins, indicating that 75% (33 of 44) of all PTPs were expressed and detected in the zebrafish caudal fin. The immunoprecipitation with the ox-PTP antibody resulted in great enrichment of PTP peptides. For comparison, we analysed fin lysate by LC-MS/MS and detected 2698proteins, amongst which only 2 were PTPs. In the ox-PTP immunoprecipitates, we identified peptides derived from 124 proteins in total, 33 of which represent distinct PTPs, demonstrating the enrichment achieved by ox-PTP immunoprecipitation.

A representative spectrum obtained for the NFFSGPIVVHcSAGVGR peptide from Ptprc (CD45) is shown in **Fig. 2c**, where the peptide was almost fully sequenced with near complete y- and b-ion ladder. Representative spectra for all zebrafish PTP catalytic site peptides detected are presented in **Fig. S2.** The high quality of our data facilitated the observation of diagnostic ions in the raw MS/MS spectra and allowed us to distinguish between highly homologous PTP peptides, such as Ptpn1 and Ptpn2a (2 residue difference), or Rptpα_2 and Rptpεb_2 (single residue difference) (**Fig. S2, p1, 6, 21 and 30**). Several receptor-type PTPs contain two catalytic site cysteine motifs, representing the two PTP domains, and both PTP peptides were detected in one experiment (**Table S1**), albeit with different MS signal intensities. This is presumably due to the primary peptide sequences having different precursor ionization and MS fragmentation efficiencies.

Differences in abundance of the PTPs were assessed by comparing the spectral counts from the samples lysed in a reducing buffer of both the first and second fin clips (**Fig.1**, Total PTP) (**Table S2**). These results show large differences in abundance of distinct PTPs in zebrafish caudal fins (**Fig. 3a**). However, for the same PTP, only small differences in abundance were observed between the first and second fin clip (**Fig. 3a**).

The abundance of oxidized PTPs was assessed by analysis of samples lysed in an alkylating buffer of the first and second fin clip (**Fig. 1**, Oxidized PTP). A difference in spectral counts between the first and second fin clip represents a change in PTP oxidation upon amputation of the zebrafish caudal fin. Out of 37 PTP peptides, 8 were found significantly more oxidized in the second fin clip than in the first fin clip ($p<0.05$; **Fig. 3b**). We conclude that *in vivo* oxidation of those 8 PTPs (asterisks in **Fig. 2a**) was enhanced in response to zebrafish caudal fin amputation. As an additional control, the first and second fin clip were lysed in reducing buffer to reduce all reversibly oxidized PTPs, then treated with NEM to block all reduced cysteines and subsequently processed to detect oxidized PTPs. This control resulted in detection of background levels of PTPs in the first and second fin clips (**Table S2**), indicating that there are no triply oxidized PTPs in these lysates before processing. Moreover, these results indicate that the 8 PTPs that were detected to be oxidized in response to amputation of the zebrafish caudal fin, were all reversibly oxidized, because DTT-mediated reduction of the lysates of the second fin clip prior to processing for detection of oxidized PTPs reduced the signal to background levels. These results demonstrate that our approach effectively detected individual PTP peptides in zebrafish caudal fins as well as changes in their oxidation state following amputation.

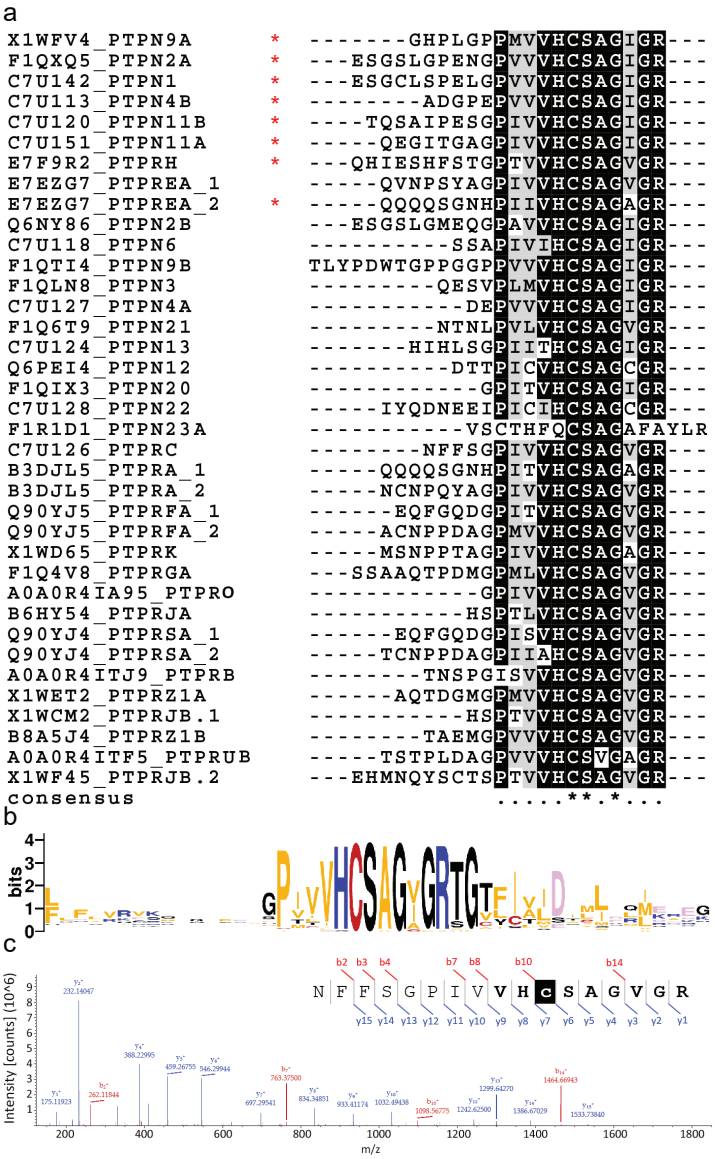

Fig. 2. Detection of PTP peptides using LC-MS/MS. Caudal fin lysates were isolated and processed as described in **Fig. 1** and LC-MS/MS was used to identify PTP peptides. (**a**) Clustal Omega alignment of 37 PTP peptides that were detected. Intensity of shading represents degree of sequence conservation. Oxidation of 8 out of 37 PTP active sites (*) was detected in the second fin clips 40min after the first fin clips. (**b**) Sequence logo obtained from 37 PTP catalytic sites and 20 flanking residues. Overall height of stack at each position indicates sequence conservation; height of symbols within the stack indicates relative frequency of each amino acid in the position. Low conservation in sequences preceding the catalytic site allows unambiguous identification of PTP species. (**c**) Representative MS/MS spectrum of a NFFSGPIVVHcSAGVGR peptide from PTPRC (CD45). Inset: peptide sequence, annotated with matched y-ions (blue) and b-ions (red). Consensus PTP catalytic site in bold; catalytic cysteine residue in white.

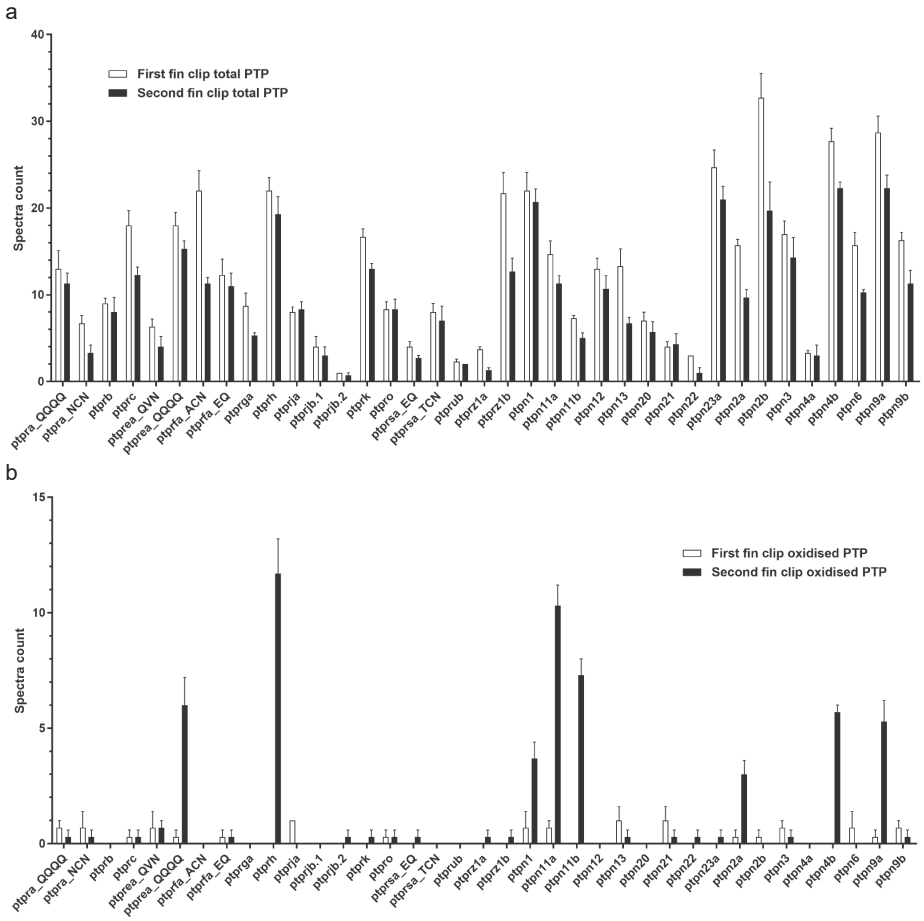

Fig. 3. Differential PTP oxidation following caudal fin amputation. (**a**) Total detectable PTP repertoire in zebrafish caudal fin clips. Spectral counts ± SE do not differ significantly between first and second fin clips (paired t-test, $p>0.05$; n=3). (**b**) Oxidized PTPs detected from first and second fin clips. Ptprea_QQQQ, Ptprh, Ptpn1, Ptpn11a, Ptpn11b, Ptpn2a, Ptpn4b and Ptpn9a are significantly more oxidized in the second fin clip compared to the first fin clip (paired t-test, $p<0.05$; n=3).

Differential requirement for PTP function in zebrafish caudal fin regeneration

Our results reveal that many PTPs are detected to be expressed in the zebrafish caudal fin, but only 8 are abundantly oxidized following caudal fin amputation. We next investigated whether PTPs have a functional role in zebrafish caudal fin regeneration. To this end, we performed caudal fin-fold regeneration assays on zebrafish embryos lacking functional Shp2 (*ptpn11a*$^{-/-}$ *ptpn11b*$^{-/-}$) or Rptpα (*ptpra*$^{-/-}$). It is noteworthy that Shp2a

and Shp2b were both abundantly oxidized following caudal fin amputation, whereas Rptpα was not oxidized under these conditions (**Fig. 2a, 3**).

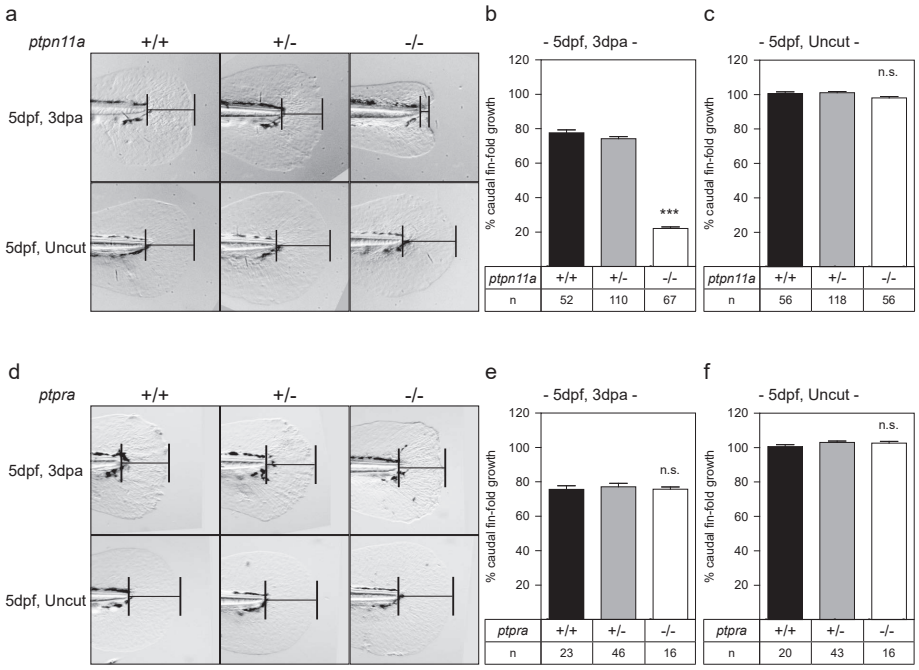

Fig. 4. Impaired caudal fin regeneration in Shp2 deficient, but not Rptpα deficient embryos. Zebrafish embryos from a *ptpn11a*$^{+/-}$*ptpn11b*$^{-/-}$ in-cross and a *ptpra*$^{+/-}$ in-cross were amputated at 2 dpf and caudal fin regeneration was assessed at 3dpa (i.e. 5dpf, 3dpa). Equivalent uncut embryos were monitored as controls (i.e. 5dpf, uncut). (a, d) Representative images of embryo caudal fins are shown. (b, c) Means of caudal fin growth of embryos lacking Shp2 (*ptpn11a*$^{-/-}$*ptpn11b*$^{-/-}$) embryos following amputation and uncut controls are depicted relative to caudal fin growth of uncut *ptpn11a*$^{+/+}$*ptpn11b*$^{-/-}$ embryos. (e, f) Means of caudal fin growth of embryos lacking Rptpα (*ptpra*$^{-/-}$) following amputation and uncut controls are depicted relative to caudal fin growth of uncut *ptpra*$^{+/+}$ embryos. Regeneration was quantified by measuring the distance from the tip of the notochord to the edge of the caudal fin as indicated. Means of amputated *ptpn11*$^{-/-}$*ptpn11b*$^{-/-}$ or *ptpra*$^{-/-}$ embryos were compared to amputated *ptpn11a*$^{+/+}$*ptpn11b*$^{+/+}$ or *ptpra*$^{+/+}$ embryos, respectively, using a Mann-Whitney U-test. Significance: *** p<0.001; n.s. not significant; error bars indicate standard error of the mean. All embryos were genotyped. Data pooled from multiple experiments.

The *ptpn11a*$^{-/-}$ *ptpn11b*$^{-/-}$ zebrafish have been previously validated and characterized[27]. Zebrafish heterozygous for Rptpα (*ptpra*$^{+/-}$) were obtained from the European Zebrafish Resource Centre (EZRC) and the (*ptpra*$^{-/-}$) offspring did not express Rptpα protein at 4 days post fertilisation (dpf) (**Fig. S3**), indicating that these are bona fide knock-outs. Both *ptpn11a*$^{-/-}$*ptpn11b*$^{-/-}$ and *ptpra*$^{-/-}$ zebrafish embryos are embryonically lethal at 6-8 dpf[27,28]. Because homozygous zebrafish adults were not viable, we inves-

tigated caudal fin-fold regeneration during embryogenesis between 2 dpf and 5 dpf. It is noteworthy that the mechanism of zebrafish embryo caudal fin-fold regeneration is identical to adult zebrafish caudal fin regeneration[29]. Normally, amputated caudal fin-folds of 2 dpf zebrafish embryos almost completely regenerate in the course of 3 days (5dpf, 3dpa). Surprisingly, *ptpn11a*$^{-/-}$*ptpn11b*$^{-/-}$ zebrafish embryos showed severely impaired regeneration of their caudal fin-folds (**Fig. 4a, b**). The normal developmental growth rate of the caudal fins was unaffected in *ptpn11a*$^{-/-}$*ptpn11b*$^{-/-}$ zebrafish embryos (**Fig. 4a, c**). In contrast, *ptpra*$^{-/-}$ zebrafish embryos regenerated their caudal fin-folds to the same extent as their siblings and no significant differences were observed in fin growth between *ptpra*$^{-/-}$ zebrafish embryos and siblings (**Fig. 4d-f**). These results show differential requirement for PTPs to facilitate caudal fin-fold regeneration in zebrafish embryos.

DISCUSSION

Our results demonstrate successful detection and identification of PTPs in zebrafish caudal fin tissue, and reversible oxidation of a subset of PTPs following caudal fin amputation (**Fig. 3, Table S2**). PTP active site peptides were efficiently immunoprecipitated and identified by LC-MS/MS. According to the Uniprot+trEMBL database, these peptides belong to 33 distinct PTPs, including 17 non-receptor and 16 receptor type PTPs, covering 75% of all theoretically observable PTPs (*cf.* **Fig. 2a, S1**). This is to our knowledge the largest repertoire of zebrafish PTPs identified in a single proteomics experiment, and serves to confirm the existence of numerous PTP species that were previously annotated only at the transcript level. As not all predicted PTP peptides may be expressed in the zebrafish caudal fin, the local coverage may be even greater.

Of the 33 PTPs that were detected in zebrafish caudal fin clips, 8 were oxidized 40 minutes after amputation, including 6 non-receptor and 2 receptor type PTPs (**Fig. 2a, 3b**): Ptpn1, Ptpn2a, Ptpn4b, Ptpn9a, Ptpn11a, Ptpn11b, Rptph, and Rptpεa. Abundance of the 8 oxidized PTP peptides and the remaining 29 PTP peptides that were identified was not significantly different between the first and second fin clips, based on semi-quantitative spectral counting (**Fig. 3a, Table S2**), indicating that the increase in spectral counts of these 8 peptides was caused by enhanced oxidation. Oxidation of these 8 PTPs was also not related to baseline PTP expression level (*cf.* **Fig. 3a, b**). In general, this indicates that not all PTPs are equally susceptible to oxidation and

that PTPs are oxidized differentially, consistent with our earlier work *in vitro*[10]. To our knowledge, our results demonstrate for the first time that differential PTP oxidation occurs in response to endogenous ROS production *in vivo*.

Interestingly, only the membrane-distal PTP domain (D2, QQQQSGNHPIIVHcSAGAGR) of Ptprεa becomes oxidized following zebrafish caudal fin amputation (**Fig. 2a, 3b**). This suggests that D2 is more sensitive to oxidation. We previously reported differential oxidation of the two catalytic domains of a close relative of Ptprεa, RPTPα. In *in vitro* experiments, the D2 domain of RPTPα is more sensitive to oxidation and appears to act as a redox sensor, regulating catalytic activity of RPTPα in an allosteric manner[19,30]. Our current results in zebrafish caudal fins suggest that Ptprεa-D2 may function in a similar manner as the redox sensor for Ptprεa.

Little is known about the role of PTPs in regeneration. The PTP superfamily member, Phosphatase and Tensin Homologue (PTEN), a lipid phosphatase, is an essential regulator of PI3K/AKT signalling and has been implicated in limiting central nervous system axon regeneration[31]. PTP type IVA 1 belongs to the phosphatase of regenerating liver (PRL)-subfamily of PTPs and was originally identified as PRL-1 because it was upregulated following liver injury and it is required for proper cell cycle progression during liver regeneration[32,33]. To date, the function of classical PTPs in regeneration had not been addressed. We performed caudal fin-fold regeneration assays on zebrafish embryos lacking either Shp2 or Rptpα. Surprisingly, zebrafish embryos lacking Shp2 (*ptpn11a*$^{-/-}$*ptpn11b*$^{-/-}$) did not regenerate their caudal fin-folds (**Fig. 4**). Yet, zebrafish embryos lacking Rptpα (*ptpra*$^{-/-}$) regenerated their caudal fin-folds normally. These results indicate that Shp2, but not Rptpα, has a specific and essential role in zebrafish embryo caudal fin-fold regeneration. The requirement for functional Shp2 in caudal fin-fold regeneration on the one hand and oxidation-mediated inactivation of Shp2 upon caudal fin amputation on the other, results in an apparent conundrum: functional Shp2 is required for caudal fin regeneration and, at the same time, Shp2 is oxidized and thus inactivated in response to zebrafish caudal fin amputation. Presumably, oxidation of Shp2 is transient. Following a lag-time, Shp2 becomes active again and exerts its essential function. However, we cannot exclude that oxidized, inactive, Shp2 has another, phosphatase-independent function in zebrafish caudal fin regeneration.

The function of oxidation of the 8 PTPs that are oxidized in response to zebrafish caudal fin regeneration remains to be determined. In general, whereas it is evident that PTPs become oxidized *in vitro*, analysis of the function of PTP oxidation *in vivo* is only recently emerging. For instance, oxidation of PTP1B and TC-PTP has a role in the

progression of type 2 diabetes mellitus[34]. PTP1B is oxidized following platelet derived growth factor stimulation[35,36], resulting in an enhanced mitogenic response, and is also transiently oxidized in response to insulin, promoting insulin receptor and leptin signalling [37]. Oxidation of TC-PTP has been reported in response to hepatic oxidative stress, an early event in type 2 diabetes progression, and exacerbates obesity and insulin resistance[38]. Both PTP1B and TC-PTP have various roles in tumour biology, metabolism, inflammation and autoimmunity, reviewed in [39–41], and their oxidation is likely important in many other processes. In immune cells, activation of the T-cell receptor results in transient ROS-induced inactivation of SHP2, activating integrin signalling and promoting T cell adhesion[42]. The cytoplasmic isoform of PTPε, cyt-PTPε[43], has an important role in maintaining osteoclast function[44], and translocates to the nucleus following oxidative stress[45]. However, the function of this translocation remains to be determined. To date, nothing is known about oxidation of Ptpn4, Ptpn9, or Rptph.

In conclusion, we used a highly sensitive and robust approach to detect and identify PTPs in zebrafish caudal fin tissue. This method facilitated the identification of the oxidation of 8 different zebrafish PTPs following zebrafish caudal fin amputation. Moreover, we provide evidence that Shp2, one of the oxidized PTPs, is essential for zebrafish caudal fin regeneration. Considering the importance of ROS signalling in various physiological processes and the susceptibility of PTPs to ROS-mediated inactivation, screening for PTP oxidation in various conditions, including wound healing, cancer, diabetes, and ageing, could identify a general role for the inactivation of PTPs in these physiological processes.

METHODS

Zebrafish husbandry

All procedures involving experimental animals were approved by the local animal experiments committee (Koninklijke Nederlandse Akademie van Weterschappen-Dier-experimenten commissie) and performed according to local guidelines and policies in compliance with national and European law. The *ptpra*$^{+/-}$ zebrafish line was purchased from EZRC (allele *ptptra*^{sa14038}, item #15584). The *ptpn11a*$^{+/-}$ *ptpn11b*$^{-/-}$ zebrafish line in the Tuebingen Long fin (TL) background was previously created by target-selected gene inactivation (TSGI), and both *ptpn11a*^{hu3459} and *ptpn11b*^{hu5920} alleles result from non-sense mutations that lead to a premature stop codon upstream of the catalytic

domain[27]. Adult *ptpra*$^{+/-}$ or *ptpn11a*$^{+/-}$ *ptpn11b*$^{-/-}$ zebrafish were in-crossed to generate *ptpra*$^{-/-}$ or *ptpn11a*$^{-/-}$*ptpn11b*$^{-/-}$ zebrafish embryos, respectively, for all experiments. Zebrafish were raised and maintained as described by Westerfield[46] under a 14 hours light/ 10 hours dark cycle at 28.5°C.

Caudal fin amputation

Adult wild-type TL zebrafish of at least 3 months old were anaesthetized in 0.6 mM Tricaine and amputated with a stainless steel surgical blade (Swann-Morton no.24). Amputated zebrafish were allowed to recover from anaesthesia in separate tanks (one individual per tank) at 28.5°C. The second amputation was performed, as the first, after 40mins or 8h of recovery on the same fin area. Fin clips were placed in individual 1.5ml tubes and snap-frozen in liquid nitrogen immediately following amputation. Zebrafish embryos were amputated as previously described [47]. Whole zebrafish embryos were lysed for genotyping at 72 hpa (5 dpf).

Protein extraction, alkylation and hyperoxidation

Snap-frozen fin clips were sonicated in lysis buffer (50 mM HEPES, 150 mM NaCl, 10% glycerol, 1% NP-40, 1x protease inhibitor (Roche), 1x phosphatase inhibitor (Roche)), supplemented with either DTT (Biorad) or NEM (Sigma-Aldrich) to create reducing or alkylating environments respectively. Alkylation and hyperoxidation of PTPs were performed as described previously[20], with the following modifications: (i) lysis buffers were degassed by bubbling 100% helium gas; (ii) zebrafish fin clips were sonicated in lysis buffer; (iii) buffer exchange before hyperoxidation was performed with 3kDa centrifugal devices to 50 mM HEPES; (iv) hyperoxidation was performed overnight.

For mass spectrometry measurements, snap-frozen amputated zebrafish caudal fin clips were divided equally into 3 conditions to measure: (1) total PTPs; (2) oxidized PTPs; or (3) control for efficiency of alkylation and baseline oxidation. In condition (1), fin clips were lysed and reduced in lysis buffer containing 10 mM DTT; in condition (2), fin clips were lysed and alkylated in lysis buffer containing 20 mM NEM for 30min, then reduced in 20 mM DTT; and in condition (3), fin clips were lysed and reduced in lysis buffer containing 10 mM DTT, alkylated in 20 mM NEM for 30min, then reduced again in 10 mM DTT. Subsequently, all three conditions were hyperoxidized with 1 mM PV (1 mM orthovanadate and 1 mM H_2O_2, mixed and left at room temperature for at least 5 min before use). Second fin clips were divided into the same 3 conditions and processed similarly. 10 fin clips per condition were used, and each of the 6 conditions,

representing one biological replicate, performed in triplicate. Protein recovery after buffer exchange was >80%, such that 400µg of fin lysate input material was obtained for each of 18 immunoprecipitations. For immunoblotting of hyperoxidized PTPs, 30 fin clips were used per condition per time point.

Immunoprecipitation of hyperoxidized PTP peptides and PTP proteins

Mouse monoclonal antibody against oxidized PTP active site (R&D Systems) was cross-linked to protein A/G-coated sepharose beads (Santa Cruz Biotechnology) with 2.5 mM disuccinimidyl suberate (Thermo Fisher Scientific) to prevent antibody co-elution. Upon elution of PTPs or PTP peptides, antibody-crosslinked beads were regenerated for sequential immunoprecipitations from the same sample, by re-using the flowthrough. In immunoprecipitations at the protein level, five sequential immunoprecipitation eluates were combined and vacuum-concentrated for immunoblotting. In PTP peptide immunoprecipitations, fin lysates were digested sequentially at 37°C in Lys C (1:100) and Trypsin (1:50) for 4 and 12 hours respectively, and diluted in 50 mM HEPES, pH 7.4. PTP peptides isolated from 5 sequential immunoprecipitations were further purified by strong cation exchange STAGE tips and analysed individually by LC-MS/MS as 5 technical replicates.

LC-MS/MS analysis and database search

Immuno-precipitated PTP peptides were separated on a 40-min reverse-phase gradient on the UHPLC 1290 system (Agilent), and analysed on an Orbitrap Q Exactive HF mass spectrometer (Thermo Scientific). Peptides were first trapped on a 2cm x 100µm Reprosil C18 pre-column (3µm) and then separated on a 50cm x 75µm Poroshell EC-C18 analytical column (2.7µm). Trapping was performed for 5min in 0.1M acetic acid (Solvent A) and elution with 80% ACN in 0.1M acetic acid (Solvent B) in gradients as follows: 13-44% solvent B in 20 min, 44-100% in 3 min and 100% for 2min, before equilibrating back to Solvent A for another 10min. Flow was passively split to 300nl/min. MS data were obtained in data-dependent acquisition mode. Full scans were acquired in the m/z range of 375-1500 at the resolution of 60,000 (m/z 400), with AGC target 3E6 and a maximum injection time of 150ms. Top 7 most intense precursor ions were selected for HCD fragmentation performed at normalized collision energy (NCE) 27%, after accumulation to target value of 1E5, also in a maximum injection time of 150ms. MS/MS acquisition was performed at a resolution of 30,000, and dynamic exclusion was set to 6.0s.

Raw spectral files were processed using MaxQuant version 1.5.3.30 and searched against the *Danio rerio* Uniprot database (version Feb 2017, including TrEMBL) using Andromeda. Cysteine carbamidomethylation was set to fixed modification, while variable modifications of methionine oxidation, cysteine hyperoxidation, as well as up to 2 missed cleavages were allowed. False discovery rate (FDR) was restricted to 1% in both protein and peptide identification.

Genotyping

All zebrafish embryos that were used in these assays were genotyped to establish *ptpra* or *ptpn11a* status. To this end, genomic zebrafish DNA was extracted through lysis of zebrafish embryos in 100µg/ml proteinase K (Sigma) diluted in SZL buffer (50 mM KCl, 2.5 mM MgCl, 10 mM Tris pH 8.3, 0.005% NP40, 0.005% Tween-20, and 10% 0.1% Gelatine). Lysis was performed by incubating at 60°C for 1 hour, followed by 95°C for 15 minutes in a thermal cycler (BioRad T100). Kompetitive Allele Specific PCR (KASP) using specific primers (**Table S2**) was carried out according to the manufacturer's instructions (LGC Group) and a PHERAstar microplate reader (BMG LABTECH) and Klustercaller software were used to identify the mutations.

Statistics

Semi-quantitative analysis of hyperoxidized PTP peptides was performed by spectral counting. Spectra obtained in five technical replicate MS runs were summed, and averaged across three biological replicates. Mean spectral count and student *t*-test statistics for difference between first and second fin clips are reported as exact two-tailed *p*-value (**Table S2**).

Histograms of whole data sets were examined to determine non-normal distribution of the data. Statistical analysis of unequal variances was obtained through a Kruskall-Wallis test. Differences between different experimental conditions were assessed for significance using a Mann-Whitney U test. Differences were considered significant when $p<0.001$, and if they satisfied a confidence interval of 95% in a Monte Carlo exact test. All tests for regenerating zebrafish embryo caudal fin-folds were performed in SPSS (IBM).

ACKNOWLEDGEMENTS

The authors thank Dr. Severine Clavier for pilot experiments to detect oxidized zebrafish PTPs in zebrafish cell lines that were at the basis of the work described here.

REFERENCES

1. Poss, K. D., Keating, M. T. & Nechiporuk, A. Tales of regeneration in zebrafish. *Dev. Dyn.* **226,** 202–210 (2003).
2. Pfefferli, C. & Jaźwińska, A. The art of fin regeneration in zebrafish. *Regeneration* **2,** 72–83 (2015).
3. Gemberling, M., Bailey, T. J., Hyde, D. R. & Poss, K. D. The zebrafish as a model for complex tissue regeneration. *Trends Genet.* **5,** 113 (2013).
4. Padhi, B. K. *et al.* Screen for genes differentially expressed during regeneration of the zebrafish caudal fin. *Dev. Dyn.* **231,** 527–541 (2004).
5. Niethammer, P., Grabher, C., Look, a T. & Mitchison, T. J. A tissue-scale gradient of hydrogen peroxide mediates rapid wound detection in zebrafish. *Nature* **459,** 996–9 (2009).
6. Yoo, S. K., Freisinger, C. M., LeBert, D. C. & Huttenlocher, A. Early redox, Src family kinase, and calcium signaling integrate wound responses and tissue regeneration in zebrafish. *J Cell Biol.* **199,** 225–34. doi: 10.1083/jcb.201203154. Epub 2012 Oct (2012).
7. Zhang, J. *et al.* ROS and ROS-Mediated Cellular Signaling. *Oxid. Med. Cell. Longev.* **2016,** (2016).
8. Reczek, C. R. & Chandel, N. S. ROS-dependent signal transduction. *Curr Opin Cell Biol* **33,** 8–13 (2015).
9. Klomsiri, C., Karplus, P. A. & Poole, L. B. Cysteine-based redox switches in enzymes. *Antioxid. Redox Signal.* **14,** 1065–77 (2011).
10. Groen, A. *et al.* Differential oxidation of protein-tyrosine phosphatases. *J Biol Chem.* **280,** 10298–304. Epub 2004 Dec 28. (2005).
11. Meng, T. C., Fukada, T. & Tonks, N. K. Reversible oxidation and inactivation of protein tyrosine phosphatases in vivo. *Mol. Cell* **9,** (2002).
12. Ostman, A. *et al.* Regulation of protein tyrosine phosphatases by reversible oxidation. *J Biochem.* **150,** 345–56 (2011).
13. Alonso, A. & Pulido, R. The extended human PTPome: A growing tyrosine phosphatase family. *FEBS J.* **283,** 1404–1429 (2016).
14. Tonks, N. K. Protein tyrosine phosphatases - From housekeeping enzymes to master regulators of signal transduction. *FEBS Journal* **280,** 346–378 (2013).
15. Salmeen, A. *et al.* Redox regulation of protein tyrosine phosphatase 1B involves a sulphenyl-amide intermediate. *Nature* **423,** 769–773 (2003).
16. Chen, C. Y., Willard, D. & Rudolph, J. Redox regulation of SH2-domain-containing protein tyrosine phosphatases by two backdoor cysteines. *Biochemistry* **48,** 1399–1409 (2009).
17. den Hertog, J., Groen, A. & van der Wijk, T. Redox regulation of protein-tyro sine phosphatases. *Arch. Biochem. Biophys.* **434,** (2005).
18. Persson, C., Kappert, K., Engström, U., Östman, A. & Sjöblom, T. An antibody-based method for monitoring in vivo oxidation of protein tyrosine phosphatases. *Methods* **35,** 37–43 (2005).
19. Persson, C. *et al.* Preferential oxidation of the second phosphatase domain of receptor-like PTP-alpha revealed by an antibody against oxidized protein tyrosine phosphatases. *Proc. Natl. Acad. Sci. U. S. A.* **101,** (2004).
20. Karisch, R. *et al.* Global proteomic assessment of the classical protein-tyrosine phosphatome and 'redoxome'. *Cell* **146,** 826–840 (2011).
21. Tonks, N. K. Protein tyrosine phosphatases: from genes, to function, to disease. *Nat Rev Mol Cell Biol* **7,** 833–846 (2006).

22. Azevedo, A. S., Grotek, B., Jacinto, A., Weidinger, G. & Saude, L. The Regenerative Capacity of the Zebrafish Caudal Fin Is Not Affected by Repeated Amputations. *PLoS One* **6,** e22820 (2011).

23. Gaspari, M. & Cuda, G. Nano LC-MS/MS: a robust setup for proteomic analysis. *Methods Mol. Biol.* **790,** 115–126 (2011).

24. The UniProt Consortium. UniProt: the universal protein knowledgebase. *Nucleic Acids Res.* **45,** D158–D169 (2017).

25. Meyer, A. & Schartl, M. Gene and genome duplications in vertebrates: the one-to-four (-to-eight in fish) rule and the evolution of novel gene functions. *Curr Opin Cell Biol* **11,** 699–704 (1999).

26. Woods, I. G. *et al.* A comparative map of the zebrafish genome. *Genome Res* **10,** 1903–1914 (2000).

27. Bonetti, M. *et al.* Distinct and overlapping functions of ptpn11 genes in zebrafish development. *PLoS One* **9,** e94884 (2014).

28. van Eekelen, M., Runtuwene, V., Overvoorde, J. & den Hertog, J. RPTPalpha and PTPepsilon signaling via Fyn/Yes and RhoA is essential for zebrafish convergence and extension cell movements during gastrulation. *Dev Biol* **340,** 626–639 (2010).

29. Kawakami, A., Fukazawa, T. & Takeda, H. Early fin primordia of zebrafish larvae regenerate by a similar growth control mechanism with adult regeneration. *Dev. Dyn.* **231,** 693–9. (2004).

30. Van Der Wijk, T., Overvoorde, J. & Den Hertog, J. H2O2-induced intermolecular disulfide bond formation between receptor protein-tyrosine phosphatases. *J. Biol. Chem.* **279,** 44355–44361 (2004).

31. Liu, K. *et al.* PTEN deletion enhances the regenerative ability of adult corticospinal neurons. *Nat. Neurosci.* **13,** 1075–1081 (2010).

32. Diamond, R. H., Cressman, D. E., Laz, T. M., Abrams, C. S. & Taub, R. PRL-1, a unique nuclear protein tyrosine phosphatase, affects cell growth. *Mol. Cell. Biol.* **14,** 3752–3762 (1994).

33. Jiao, Y. *et al.* Protein tyrosine phosphatase of liver regeneration-1 is required for normal timing of cell cycle progression during liver regeneration. *Am. J. Physiol. - Gastrointest. Liver Physiol.* **308,** G85–G91 (2015).

34. Dubé, N. & Tremblay, M. L. Involvement of the small protein tyrosine phosphatases TC-PTP and PTP1B in signal transduction and diseases: From diabetes, obesity to cell cycle, and cancer. *Biochim. Biophys. Acta - Proteins Proteomics* **1754,** 108–117 (2005).

35. Frijhoff, J. *et al.* The mitochondrial reactive oxygen species regulator p66Shc controls PDGF-induced signaling and migration through protein tyrosine phosphatase oxidation. *Free Radic. Biol. Med.* **68,** 268–277 (2014).

36. Dagnell, M. *et al.* Selective activation of oxidized PTP1B by the thioredoxin system modulates PDGF-beta receptor tyrosine kinase signaling. *Proc. Natl. Acad. Sci. U. S. A.* **110,** 13398–13403 (2013).

37. Meng, T. C., Buckley, D. A., Galic, S., Tiganis, T. & Tonks, N. K. Regulation of insulin signaling through reversible oxidation of the protein-tyrosine phosphatases TC45 and PTP1B. *J. Biol. Chem.* **279,** 37716–37725 (2004).

38. Gurzov, E. N. *et al.* Hepatic oxidative stress promotes insulin-STAT-5 signaling and obesity by inactivating protein tyrosine phosphatase N2. *Cell Metab.* **20,** 85–102 (2014).

39. Stuible, M., Doody, K. M. & Tremblay, M. L. PTP1B and TC-PTP: Regulators of transformation and tumorigenesis. *Cancer Metastasis Rev.* **27,** 215–230 (2008).

40. Yip, S. C., Saha, S. & Chernoff, J. PTP1B: A double agent in metabolism and oncogenesis. *Trends Biochem. Sci.* **35,** 442–449 (2010).

41. Chistiakov, D. A. & Chistiakova, E. I. T-cell protein tyrosine phosphatase: A role in inflammation and autoimmunity. *Int. J. Diabetes Mellit.* **2,** 114–118 (2010).

42. Kwon, J. *et al.* Receptor-stimulated oxidation of SHP-2 promotes T-cell adhesion through SLP-76-ADAP. *EMBO J.* **24,** 2331–41 (2005).

43. Elson, A. & Leder, P. Identification of a cytoplasmic, phorbol ester-inducible isoform of protein tyrosine phosphatase epsilon. *Proc Natl Acad Sci U S A* **92,** 12235–12239 (1995).

44. Chiusaroli, R. *et al.* Tyrosine Phosphatase Epsilon Is a Positive Regulator of Osteoclast Function in Vitro and In Vivo. *Mol. Biol. Cell* **15,** 234–244 (2004).

45. Kraut, J., Volohonsky, G., Toledano-Katchalski, H. & Elson, A. Nuclear Localization of Non-receptor Protein Tyrosine Phosphatase ϵ Is Regulated by Its Unique N-Terminal Domain. *Exp. Cell Res.* **281,** 182–189 (2002).

46. Westerfield, M. *The zebrafish book. A guide for the laboratory use of zebrafish (Danio rerio)*. (University of Oregon Press, 2000).

47. Hale, A. J. & den Hertog, J. in *Protein Tyrosine Phosphatases: Methods and Protocols* (ed. Pulido, R.) 351–372 (Springer New York, 2016). doi:10.1007/978-1-4939-3746-2_19

SUPPORTING INFORMATION

a

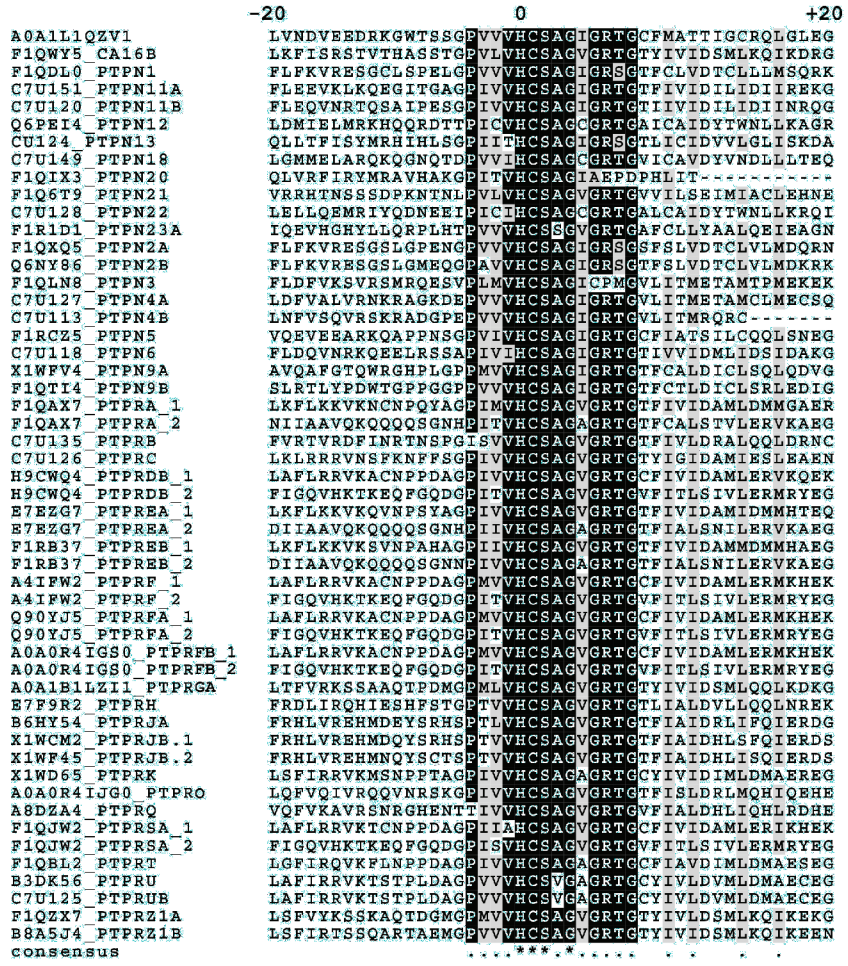

b

Fig. S1. Sequence alignments and logos of all predicted PTP peptides in the zebrafish Uniprot+trEMBL database. (**a**) Sequence alignment of 52 predicted catalytic sites ±20 flanking residues, representing 44 distinct PTPs, in the zebrafish Uniprot+trEMBL database (release Feb 2017). PTPs containing two catalytic sites are aligned as separate entries. Alignment generated with Boxshade 3.21, shading indicates sequence conservation >80%. (**b**) Sequence logo visualized with WebLogo, overall height of stack at each position indicates sequence conservation; height of symbols within the stack indicates relative frequency of each amino acid in the position.

Sup5.2 - all 36 pages

Uniprot Accession	Description	Gene name	PTP type	Sequence	Hyperoxidised cysteine	Total MS/MS count
B3DJL5_site1 (C7U129)	Ptpra protein	ptpra	Receptor	QQQQSGNHPITVHcSAGAGR	C14(hyper)	76

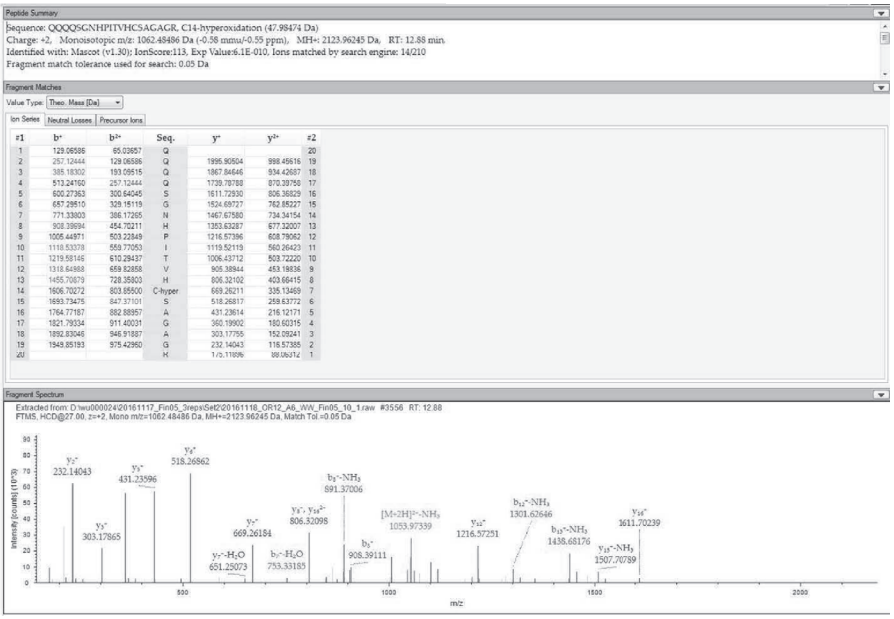

Uniprot Accession	Description	Gene name	PTP type	Sequence	Hyperoxidised cysteine	Total MS/MS count
B3DJL5_site2 (C7U129)	Ptpra protein	ptpra	Receptor	NcNPQYAGPIVVHcSAGVGR	C14(hyper)	33

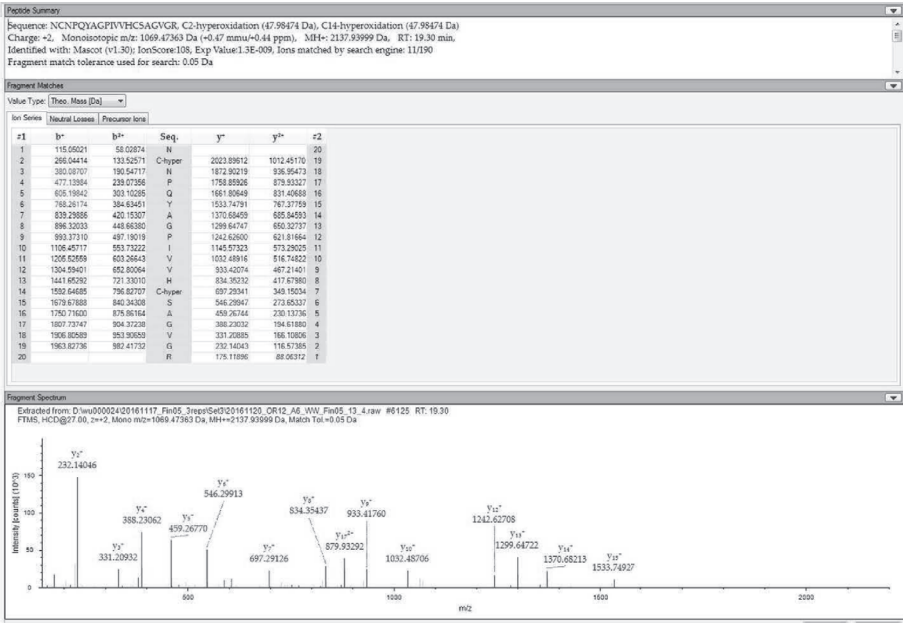

Uniprot Accession	Description	Gene name	PTP type	Sequence	Hyperoxidised cysteine	Total MS/MS count
A0A0R4ITJ9 (C7U135)	Uncharacterized protein	ptprb	Receptor	TNSPGISVVHcSAGVGR	C11(hyper)	51

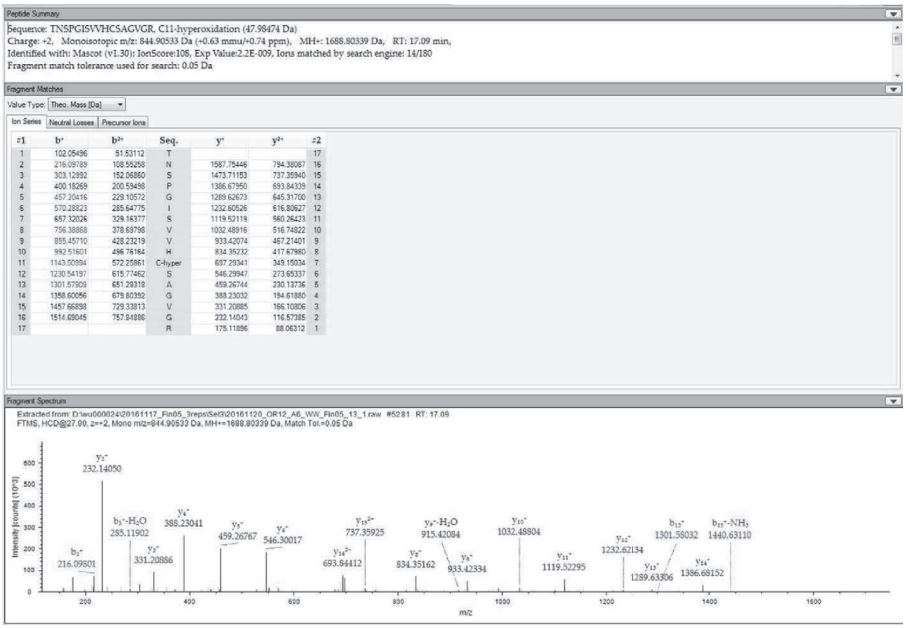

Uniprot Accession	Description	Gene name	PTP type	Sequence	Hyperoxidised cysteine	Total MS/MS count
C7U126	CD45 antigen (Fragment)	ptprc	Receptor	NFFSGPIVVHcSAGVGR	C11(hyper)	93

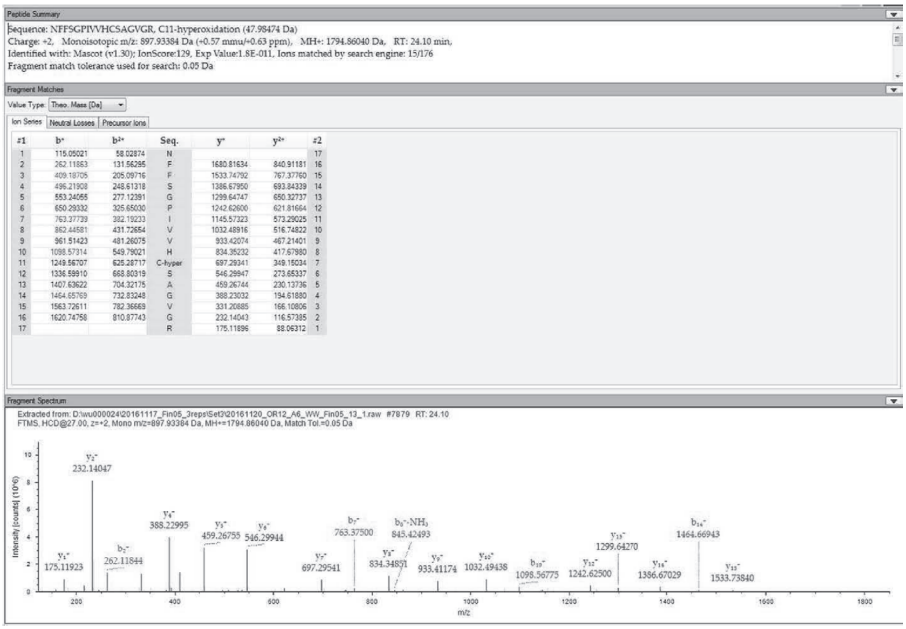

Uniprot Accession	Description	Gene name	PTP type	Sequence	Hyperoxidised cysteine	Total MS/MS count
E7EZG7_site1	Receptor-type tyrosine-protein phosphatase	ptprea	Receptor	QVNPSYAGPIV**VHcSAGVGR**	C14(hyper)	35

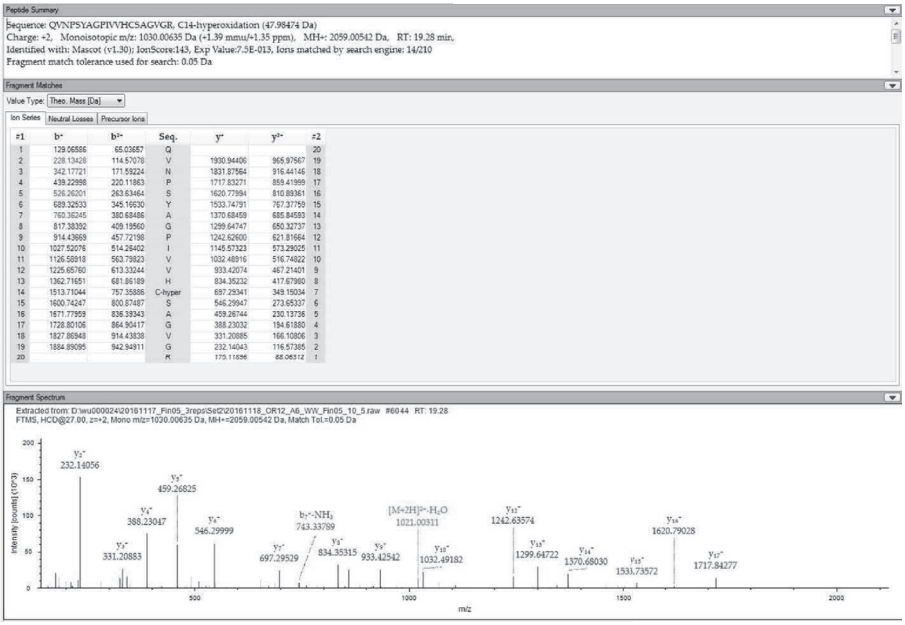

Uniprot Accession	Description	Gene name	PTP type	Sequence	Hyperoxidised cysteine	Total MS/MS count
E7EZG7_site2	Receptor-type tyrosine-protein phosphatase	ptprea	Receptor	QQQQSGNHPII**VHcSAGAGR**	C14(hyper)	119

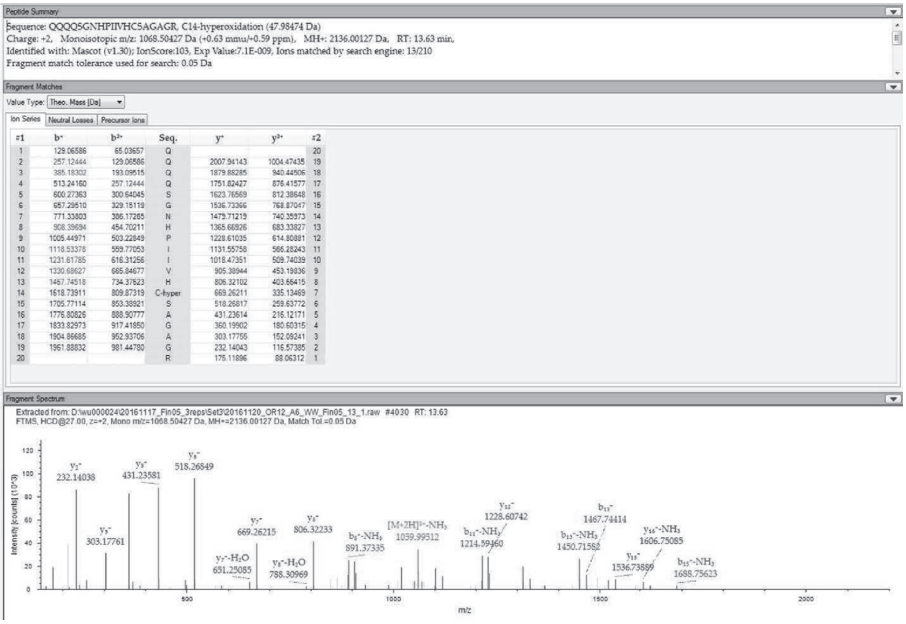

Uniprot Accession	Description	Gene name	PTP type	Sequence	Hyperoxidised cysteine	Total MS/MS count
Q90YJ5_site1	Receptor protein-tyrosine phosphatase LAR (Fragment)	ptprfa	Receptor	AcNPPDAGPMVVHcSAGVGR	C14(hyper)	100

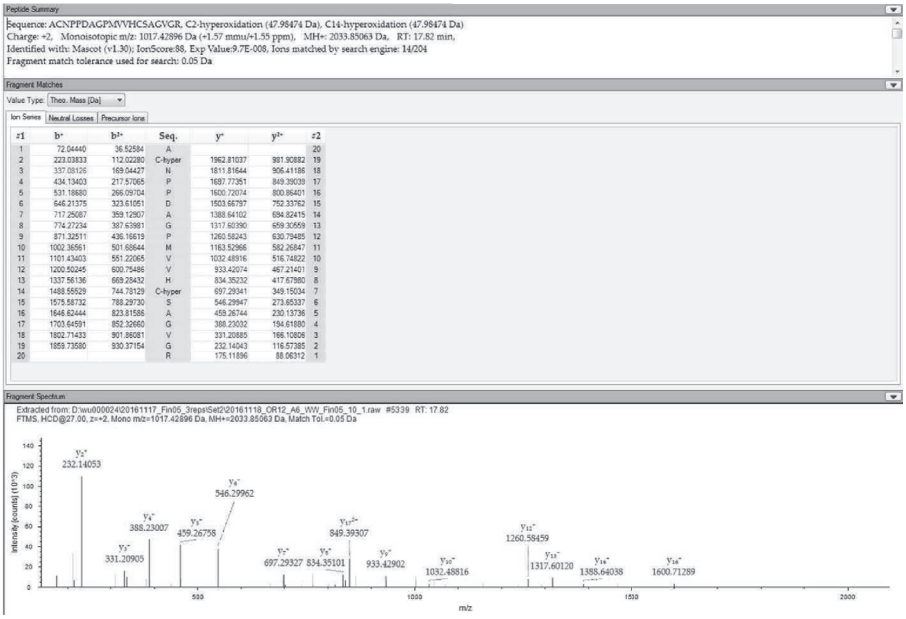

Uniprot Accession	Description	Gene name	PTP type	Sequence	Hyperoxidised cysteine	Total MS/MS count
Q90YJ5_site2	Receptor protein-tyrosine phosphatase LAR (Fragment)	ptprfa	Receptor	EQFGQDGPITVHcSAGVGR	C13(hyper)	72

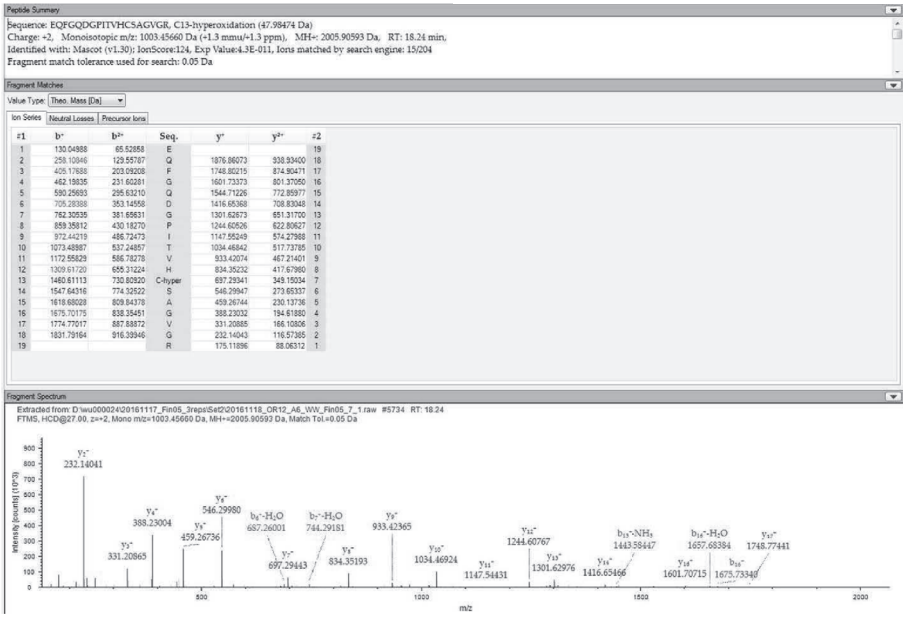

Uniprot Accession	Description	Gene name	PTP type	Sequence	Hyperoxidised cysteine	Total MS/MS count
F1Q4V8	Uncharacterized protein (Fragment)	ptprga	Receptor	SSAAQTPDMGPML**VHcSAGVGR**	C16(hyper)	42

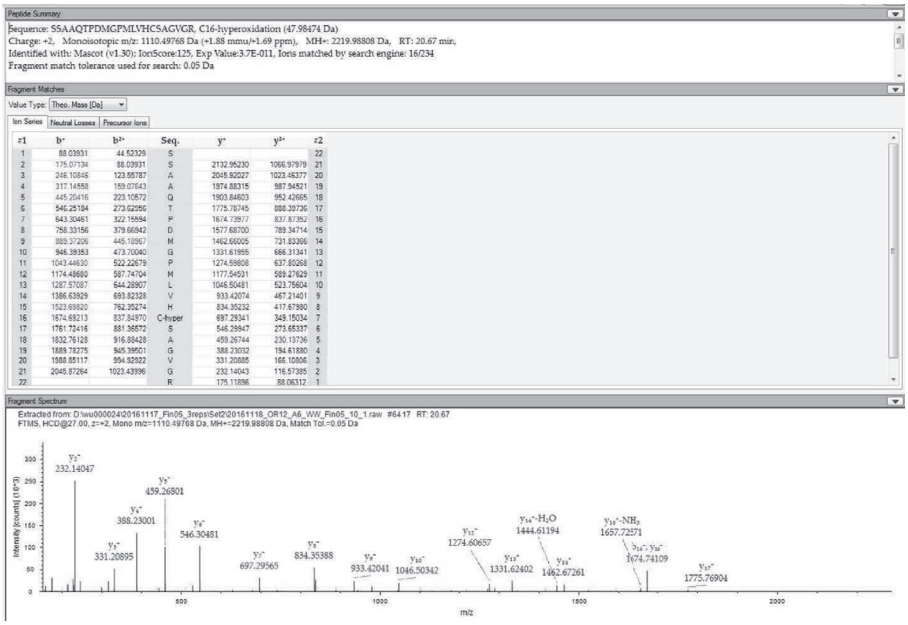

Uniprot Accession	Description	Gene name	PTP type	Sequence	Hyperoxidised cysteine	Total MS/MS count
E7F9R2	Uncharacterized protein	ptprh	Receptor	QHIESHFSTGPTV**VHcSAGVGR**	C16(hyper)	159

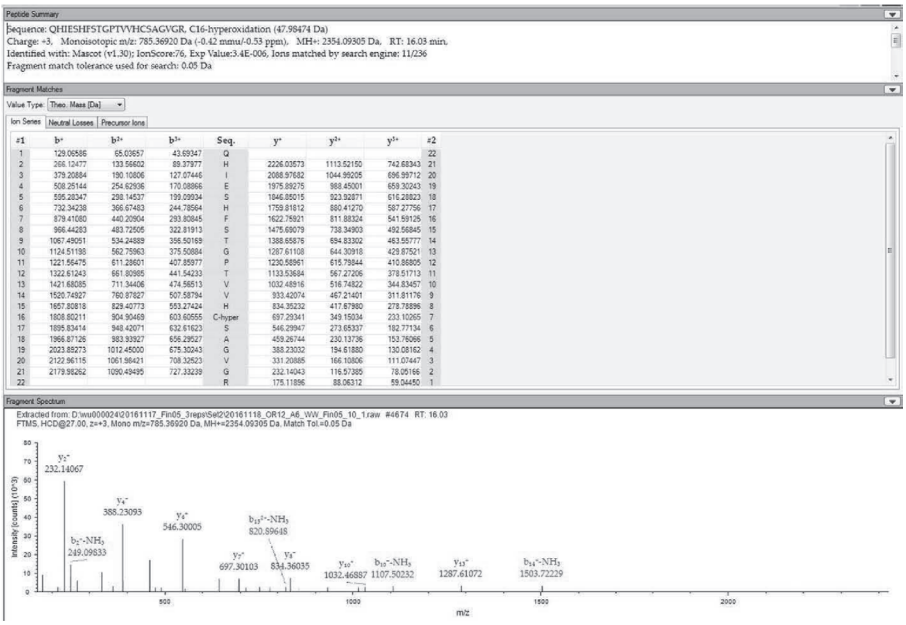

Uniprot Accession	Description	Gene name	PTP type	Sequence	Hyperoxidised cysteine	Total MS/MS count
B6HY54	Protein-tyrosine phosphatase	ptprja	Receptor	HSPTLVHcSAGVGR	C8(hyper)	52

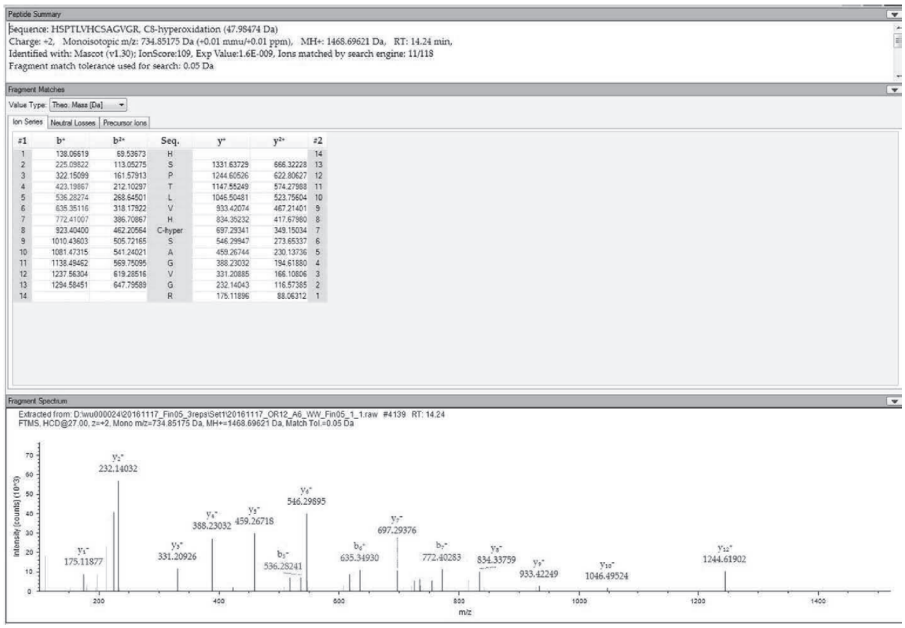

Uniprot Accession	Description	Gene name	PTP type	Sequence	Hyperoxidised cysteine	Total MS/MS count
X1WCM2	Uncharacterized protein (Fragment)	ptprjb.1	Receptor	HSPTVVHcSAGVGR	C8(hyper)	21

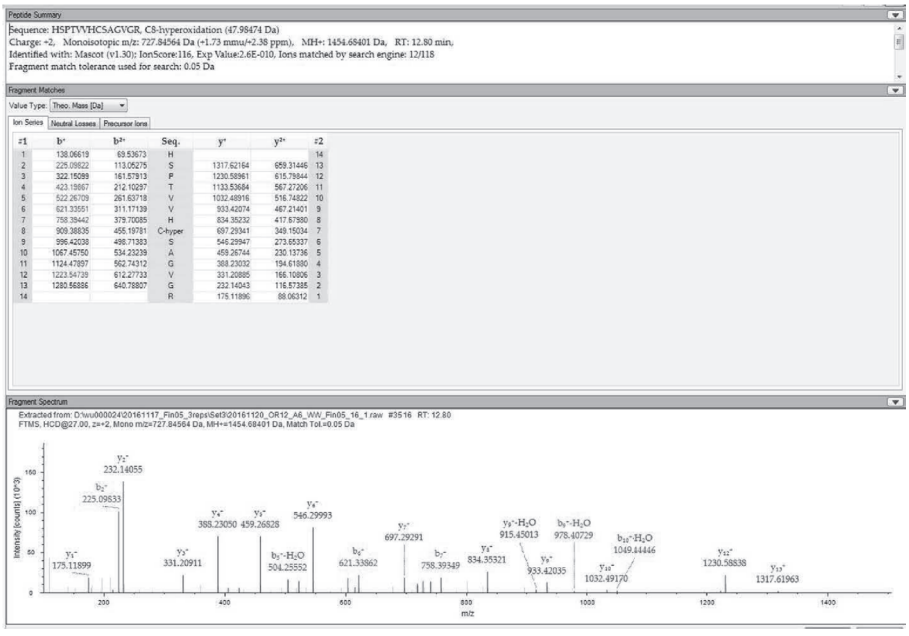

Uniprot Accession	Description	Gene name	PTP type	Sequence	Hyperoxidised cysteine	Total MS/MS count
X1WF45	Uncharacterized protein (Fragment)	ptprjb.2	Receptor	EHMNQYScTSPTVVHcSAGVGR	C16(hyper)	6

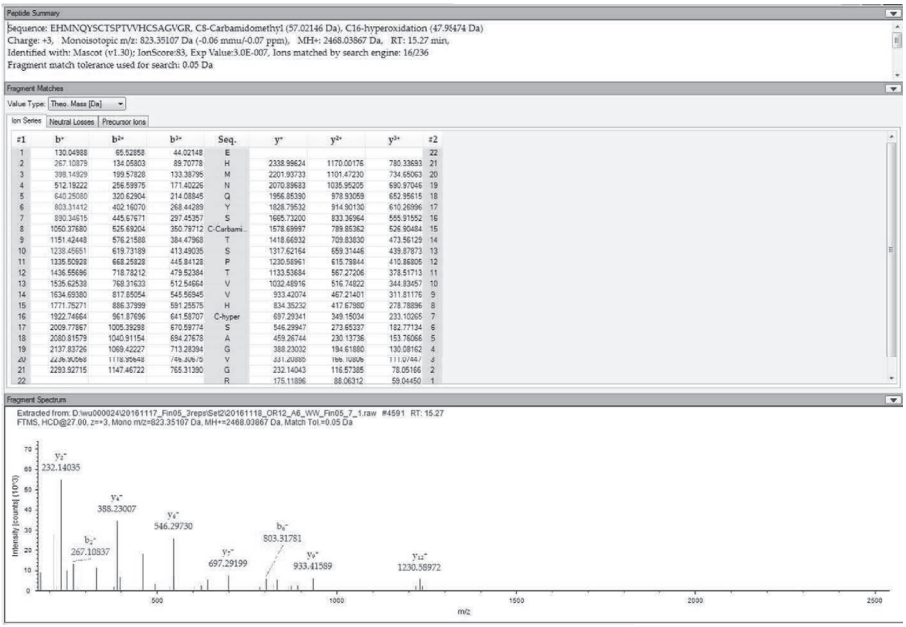

Uniprot Accession	Description	Gene name	PTP type	Sequence	Hyperoxidised cysteine	Total MS/MS count
X1WD65	Uncharacterized protein	ptprk	Receptor	MSNPPTAGPIVVHcSAGAGR	C14(hyper)	90

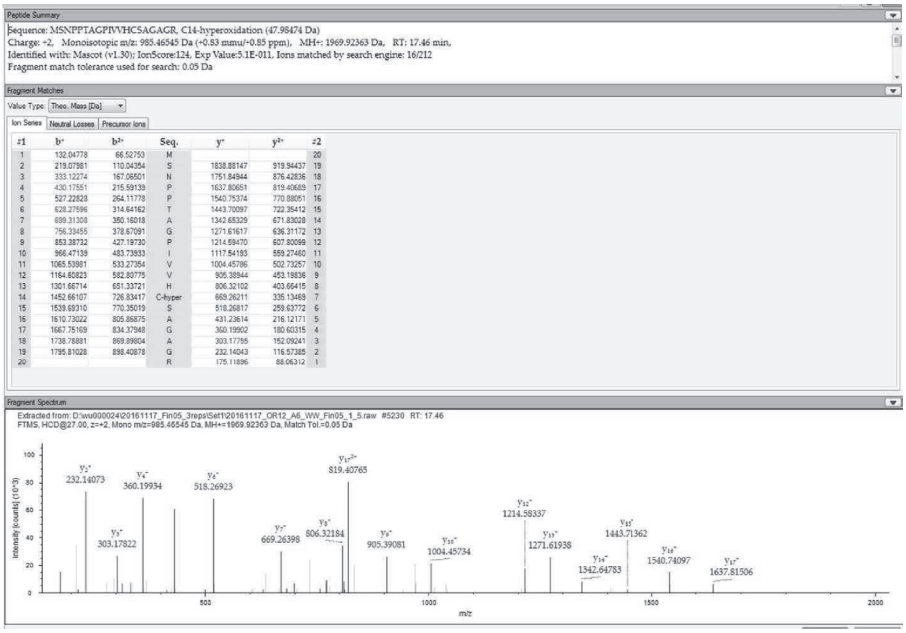

Uniprot Accession	Description	Gene name	PTP type	Sequence	Hyperoxidised cysteine	Total MS/MS count
A0A0R4IA95	Uncharacterized protein (Fragment)	ptpro	Receptor	GPIV**VHcSAGVGR**	C7(hyper)	52

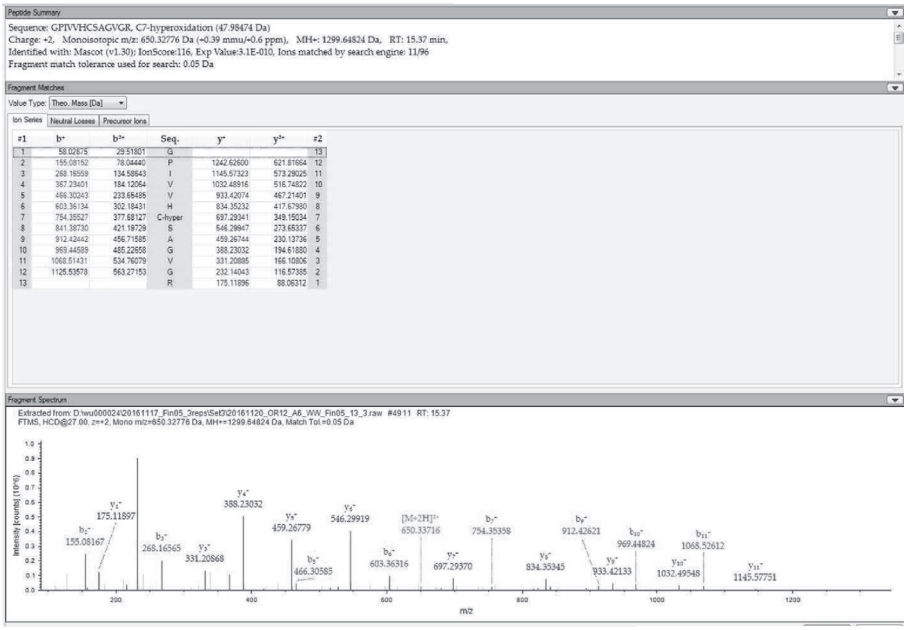

Uniprot Accession	Description	Gene name	PTP type	Sequence	Hyperoxidised cysteine	Total MS/MS count
Q90YJ4_site1	Receptor protein-tyrosine phosphatase sigma (Fragment)	ptprsa	Receptor	EQFGQDGPIS**VHcSAGVGR**	C13(hyper)	21

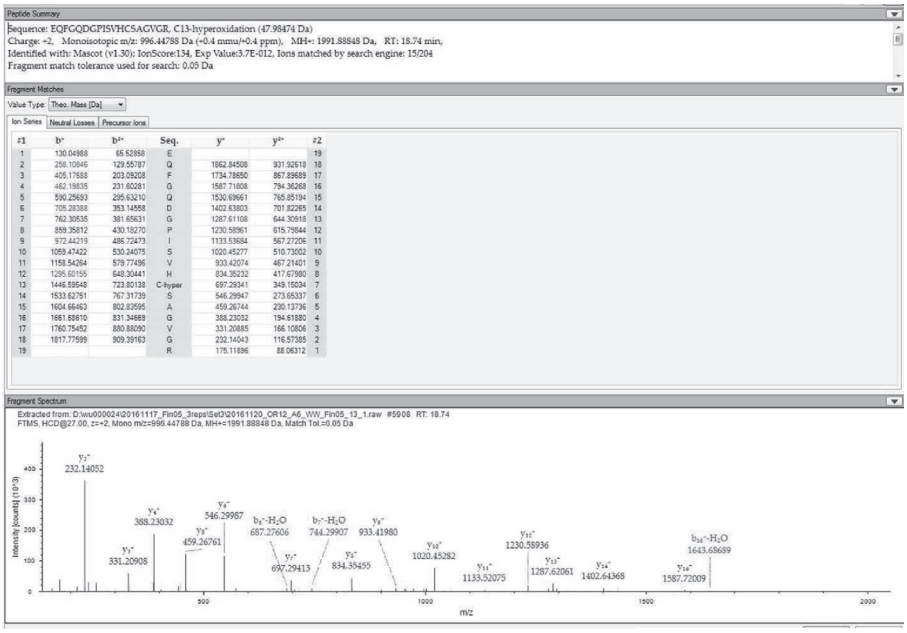

Uniprot Accession	Description	Gene name	PTP type	Sequence	Hyperoxidised cysteine	Total MS/MS count
Q90YJ4_site2	Receptor protein-tyrosine phosphatase sigma (Fragment)	ptprsa	Receptor	TcNPPDAGPIIAHcSAGVGR	C14(hyper)	45

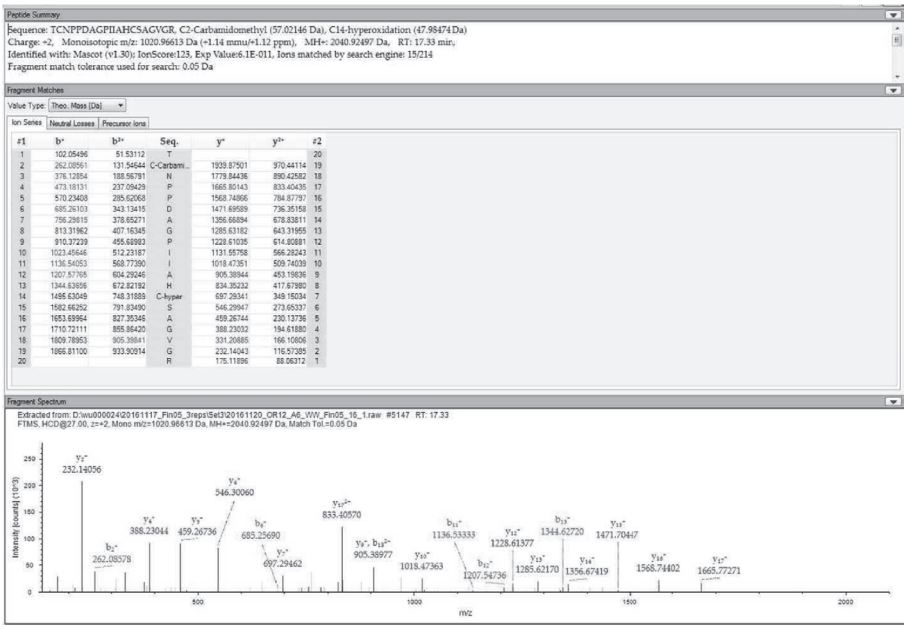

Uniprot Accession	Description	Gene name	PTP type	Sequence	Hyperoxidised cysteine	Total MS/MS count
A0A0R4ITF5 (C7U125)	Uncharacterized protein	ptprub	Receptor	TSTPLDAGPVVVHcSVGAGR	C14(hyper)	13

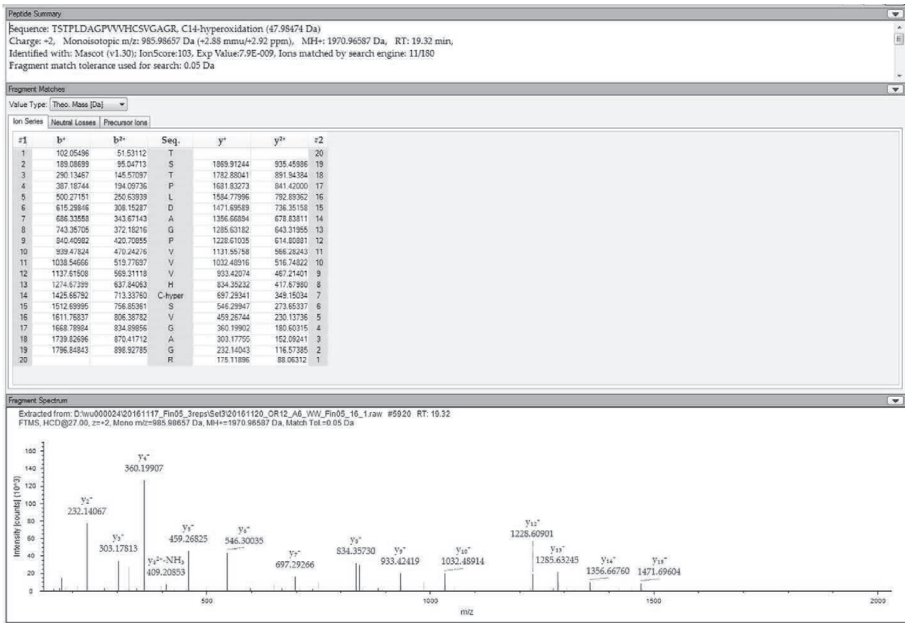

Uniprot Accession	Description	Gene name	PTP type	Sequence	Hyperoxidised cysteine	Total MS/MS count
X1WET2	Uncharacterized protein (Fragment)	ptprz1a	Receptor	AQTDGMGPMVVHcSAGVGR	C13(hyper)	16

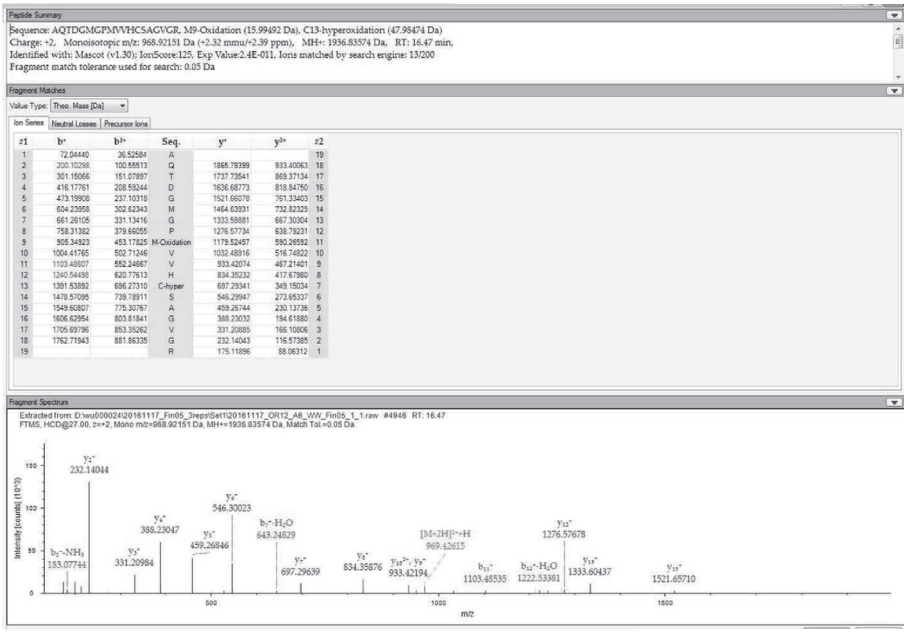

Uniprot Accession	Description	Gene name	PTP type	Sequence	Hyperoxidised cysteine	Total MS/MS count
B8A5J4	Uncharacterized protein	ptprz1b	Receptor	TAEMGPVVVHcSAGVGR	C11(hyper)	104

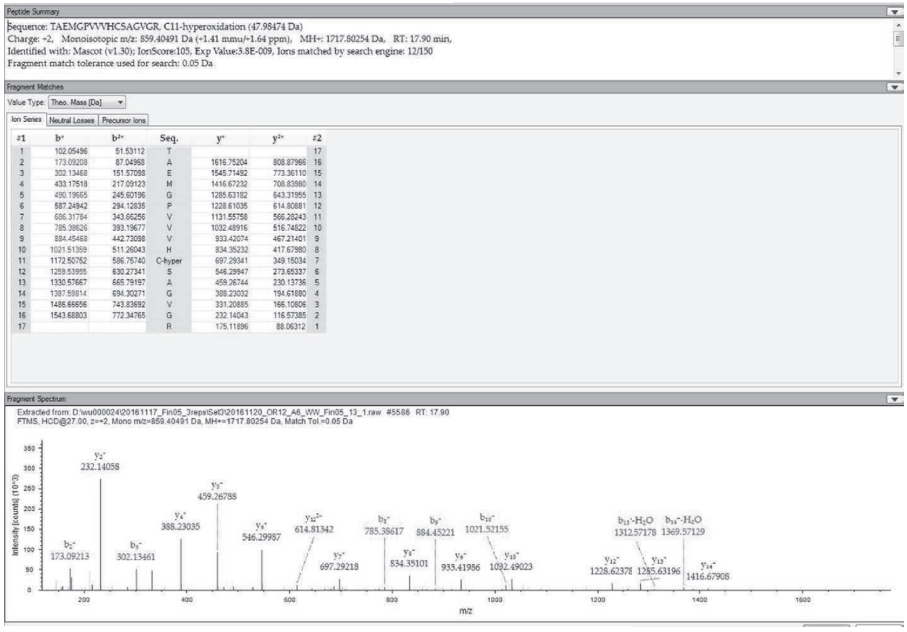

Uniprot Accession	Description	Gene name	PTP type	Sequence	Hyperoxidised cysteine	Total MS/MS count
C7U142	Protein-tyrosine phosphatase 1B (Fragment)	ptpn1	Non-receptor	ESGcLSPELGPVVVHcSAGIGR	C16(hyper)	142

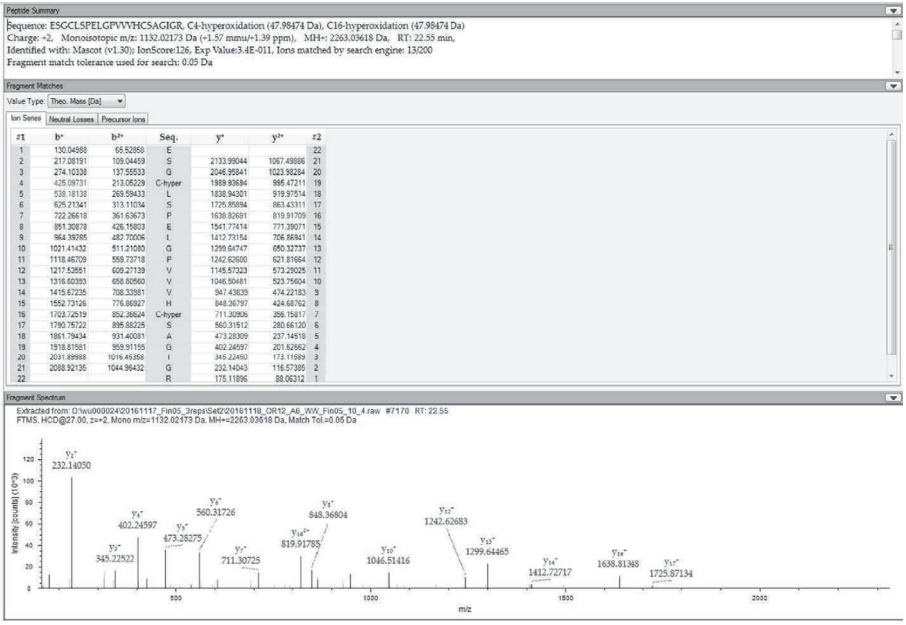

Uniprot Accession	Description	Gene name	PTP type	Sequence	Hyperoxidised cysteine	Total MS/MS count
C7U151	Protein-tyrosine phosphatase SHP-2a (Fragment)	ptpn11a	Non-receptor	QEGITGAGPIVVHcSAGIGR	C14(hyper)	112

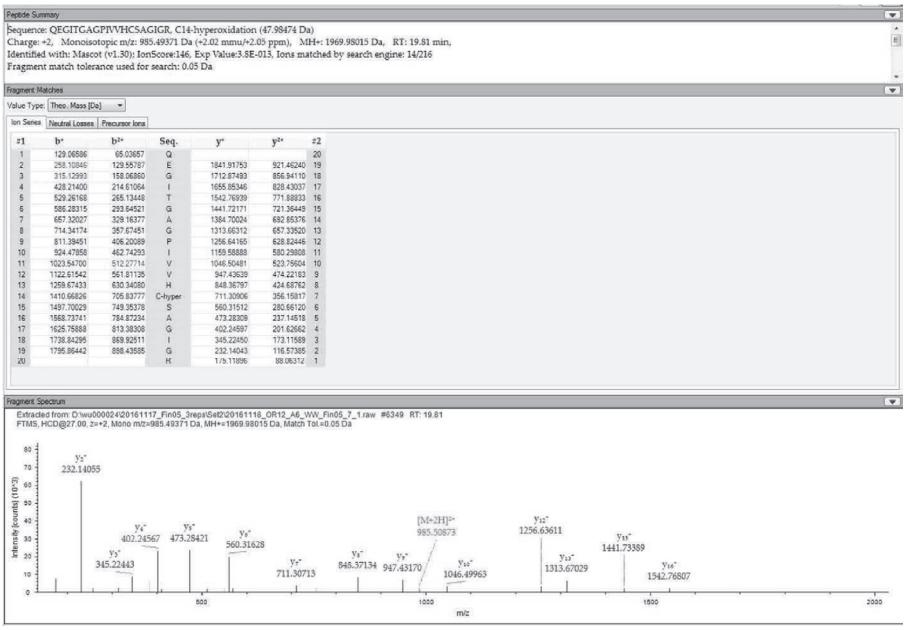

Uniprot Accession	Description	Gene name	PTP type	Sequence	Hyperoxidised cysteine	Total MS/MS count
C7U120	Protein-tyrosine phosphatase SHP-2b (Fragment)	ptpn11b	Non-receptor	TQSAIPESGPIVVHcSAGIGR	C15(hyper)	59

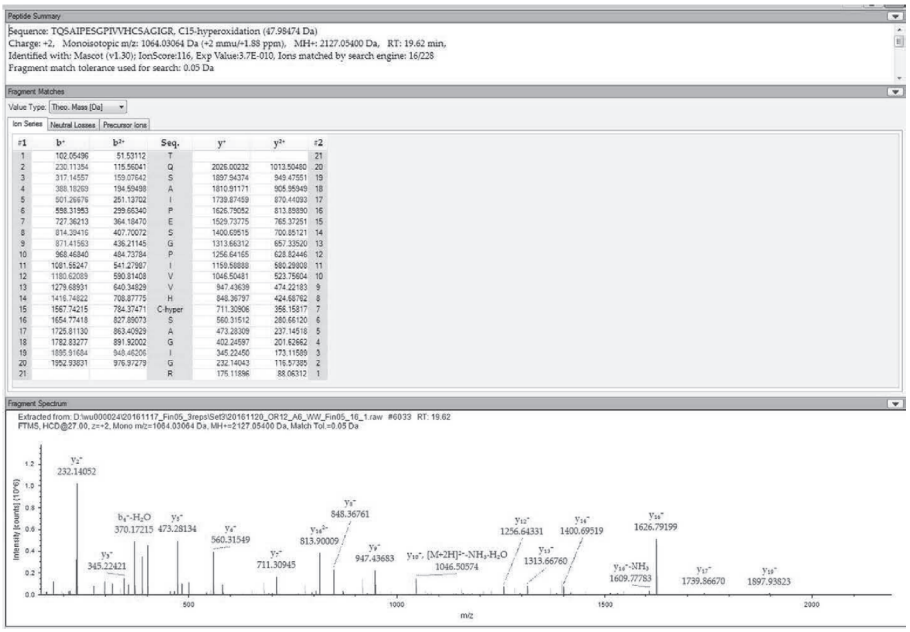

Uniprot Accession	Description	Gene name	PTP type	Sequence	Hyperoxidised cysteine	Total MS/MS count
Q6PEI4	Protein tyrosine phosphatase, non-receptor type 12	ptpn12	Non-receptor	DTTPIcVHcSAGcGR	C13(hyper)	71

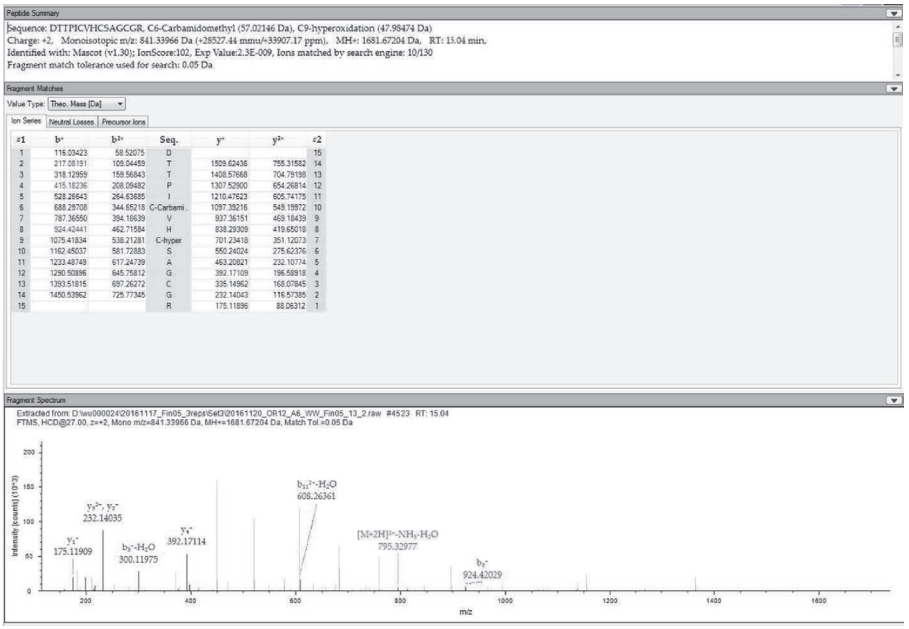

Uniprot Accession	Description	Gene name	PTP type	Sequence	Hyperoxidised cysteine	Total MS/MS count
C7U124	Protein-tyrosine phosphatase BAS (Fragment)	ptpn13	Non-receptor	HIHLSGPII**THcSAGIGR**	C12(hyper)	64

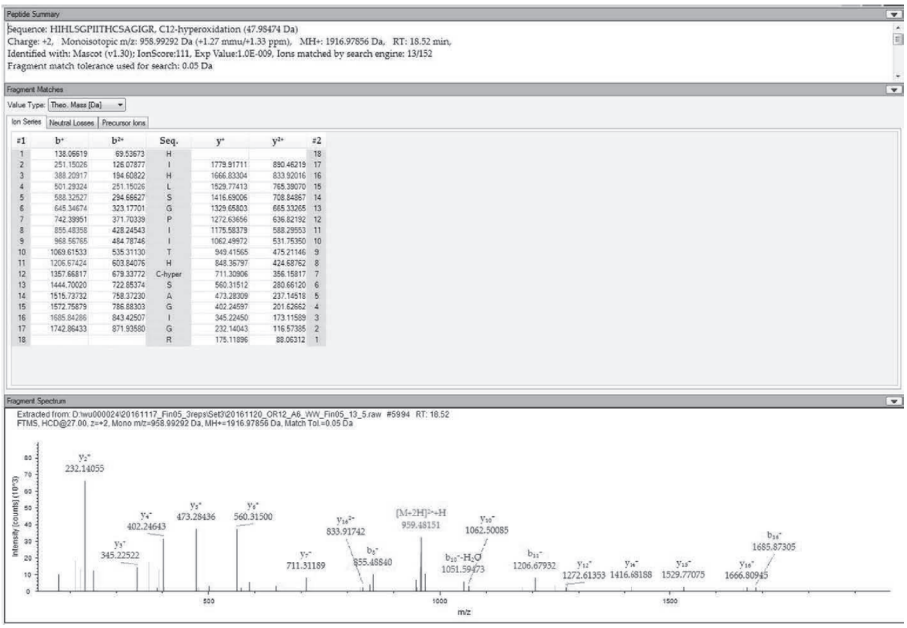

Uniprot Accession	Description	Gene name	PTP type	Sequence	Hyperoxidised cysteine	Total MS/MS count
F1QIX3	Uncharacterized protein	ptpn20	Non-receptor	GPIT**VHcSAGIGR**	C7(hyper)	38

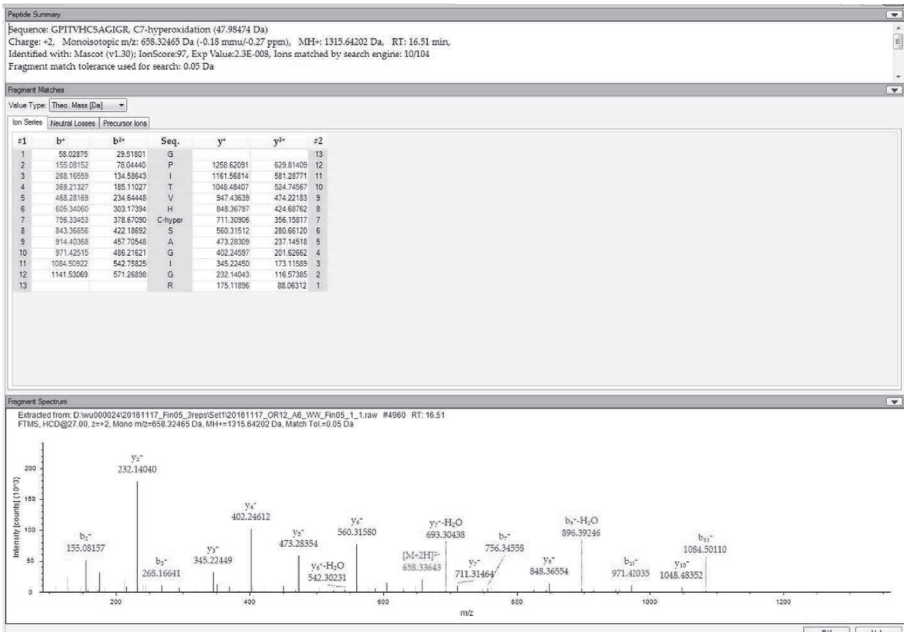

Uniprot Accession	Description	Gene name	PTP type	Sequence	Hyperoxidised cysteine	Total MS/MS count
F1Q6T9	Uncharacterized protein	ptpn21	Non-receptor	NTNLPVLVHcSAGVGR	C10(hyper)	29

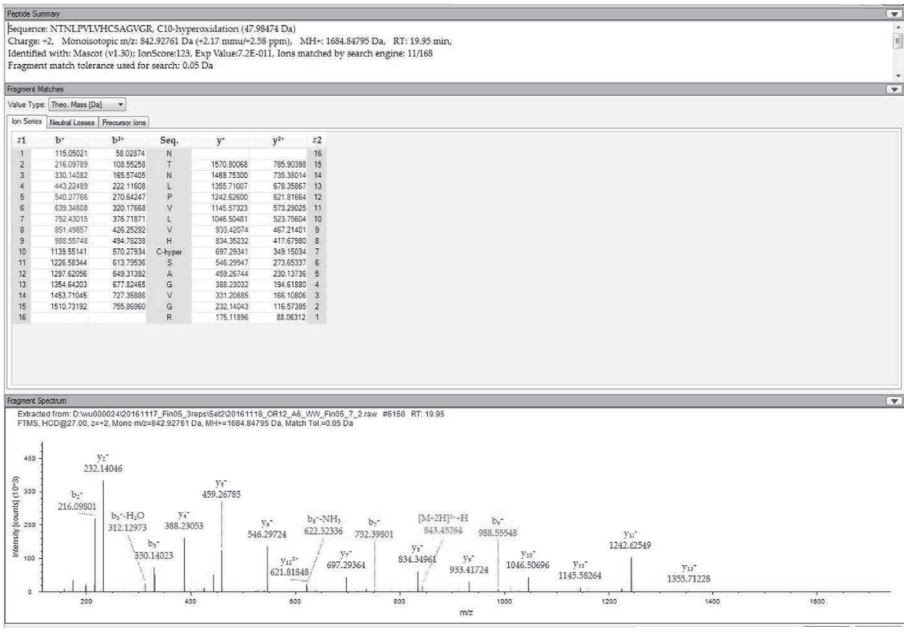

Uniprot Accession	Description	Gene name	PTP type	Sequence	Hyperoxidised cysteine	Total MS/MS count
C7U128	Protein-tyrosine phosphatase LyPTP (Fragment)	ptpn22	Non-receptor	IYQDNEEIPIcIHcSAGcGR	C18(hyper)	13

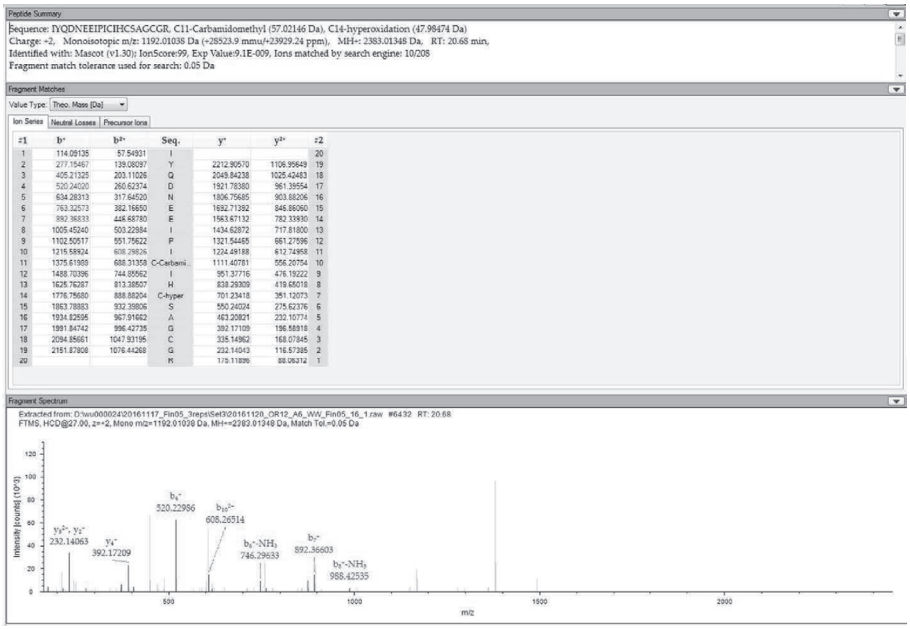

Uniprot Accession	Description	Gene name	PTP type	Sequence	Hyperoxidised cysteine	Total MS/MS count
F1R1D1	Uncharacterized protein	ptpn23a	Non-receptor	VScTHFQcSAGAFAYLR	C8(hyper)	138

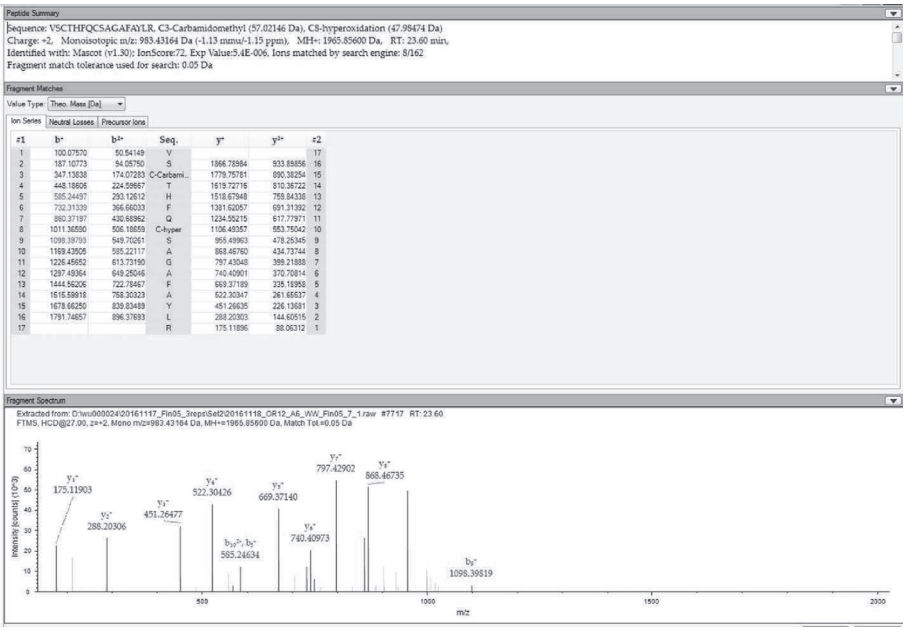

Uniprot Accession	Description	Gene name	PTP type	Sequence	Hyperoxidised cysteine	Total MS/MS count
F1QXQ5 (F1QGX6)	Tyrosine-protein phosphatase non-receptor type	ptpn2a	Non-receptor	ESGSLGPENGPVVVHcSAGIGR	C16(hyper)	86

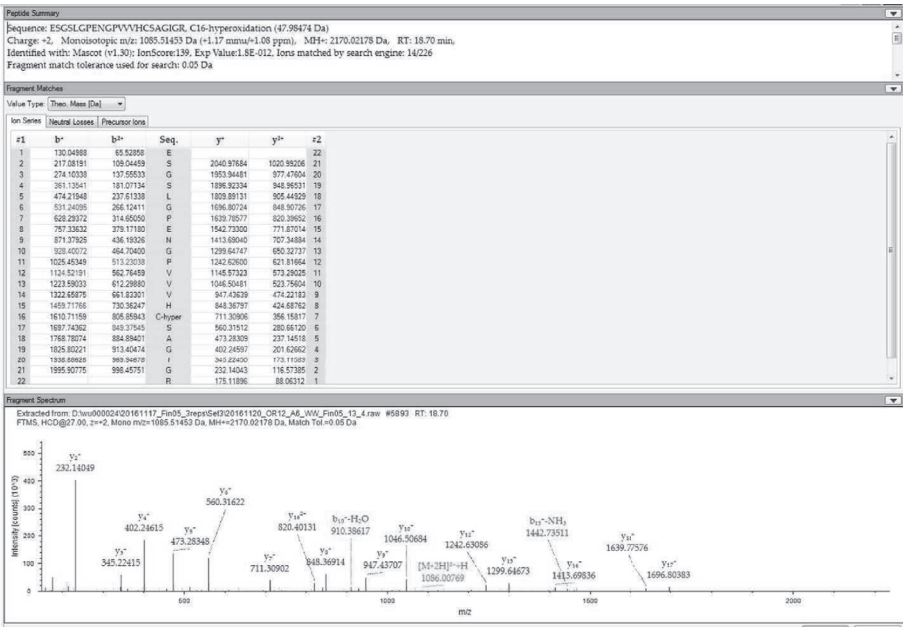

Uniprot Accession	Description	Gene name	PTP type	Sequence	Hyperoxidised cysteine	Total MS/MS count
Q6NY86	Tyrosine-protein phosphatase non-receptor type	ptpn2b	Non-receptor	ESGSLGMEQGPAVVHcSAGIGR	C16(hyper)	159

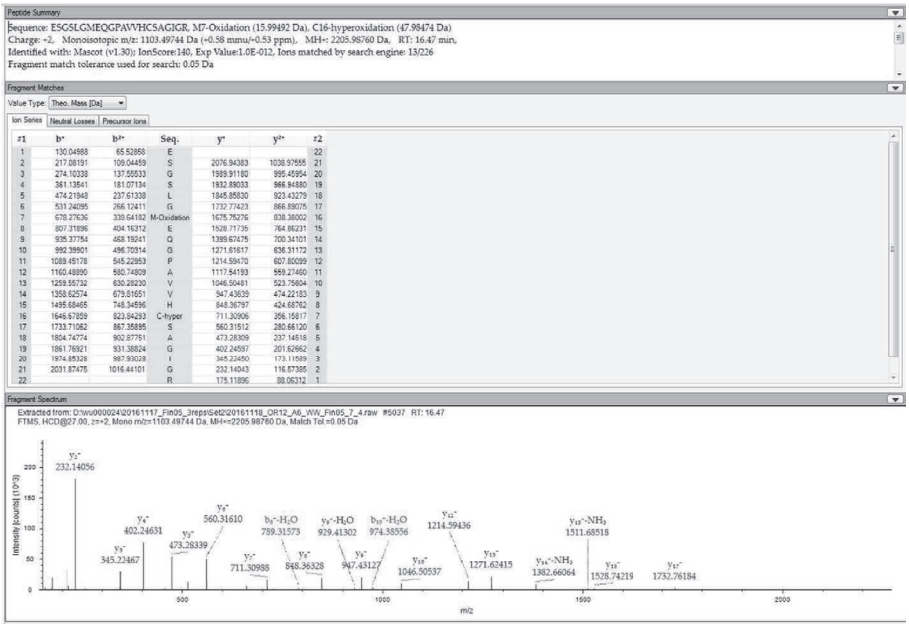

Uniprot Accession	Description	Gene name	PTP type	Sequence	Hyperoxidised cysteine	Total MS/MS count
F1QLN8	Uncharacterized protein	ptpn3	Non-receptor	QESVPLMVHcSAGIGR	C10(hyper)	97

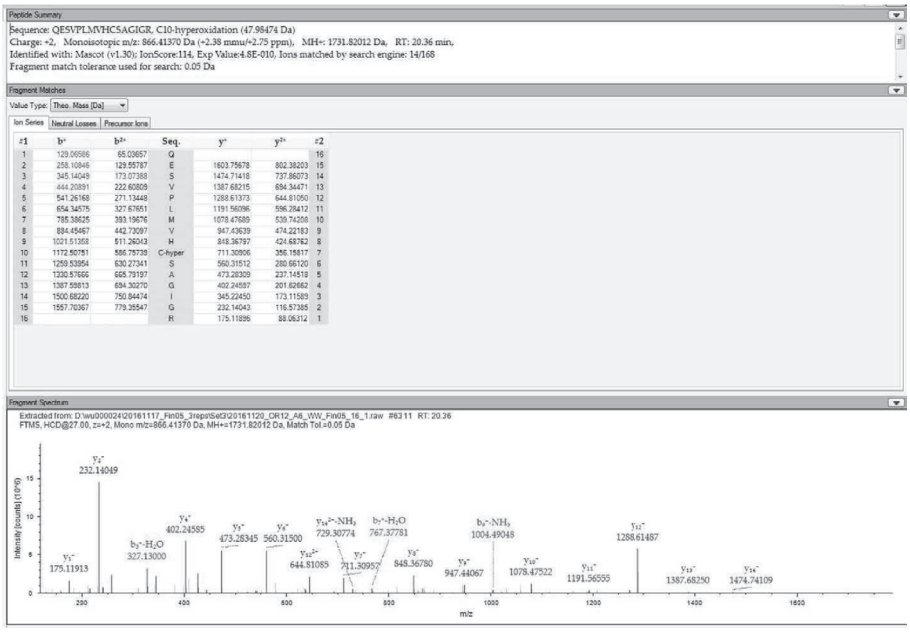

Uniprot Accession	Description	Gene name	PTP type	Sequence	Hyperoxidised cysteine	Total MS/MS count
C7U127	Protein-tyrosine phosphatase MEG1a (Fragment)	ptpn4a	Non-receptor	DEPVVVHcSAGIGR	C8(hyper)	19

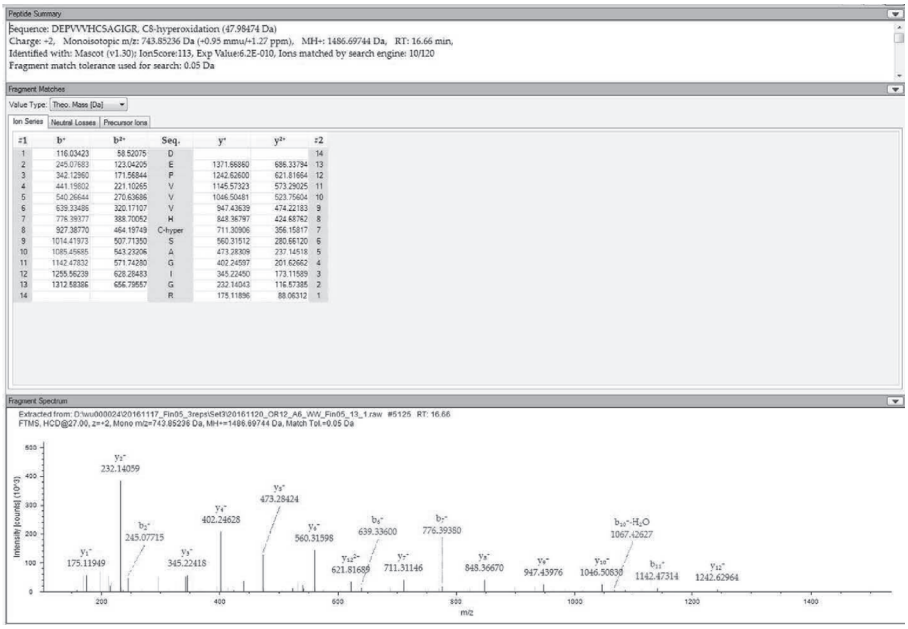

Uniprot Accession	Description	Gene name	PTP type	Sequence	Hyperoxidised cysteine	Total MS/MS count
C7U113	Protein-tyrosine phosphatase MEG1a (Fragment)	ptpn4b	Non-receptor	ADGPEPVVVHcSAGIGR	C11(hyper)	156

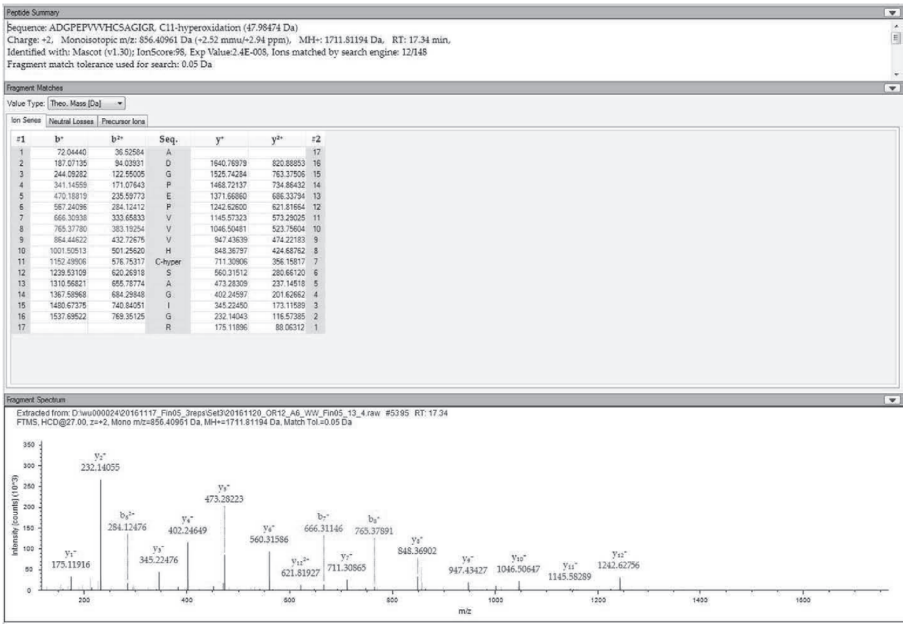

Uniprot Accession	Description	Gene name	PTP type	Sequence	Hyperoxidised cysteine	Total MS/MS count
C7U118	Protein-tyrosine phosphatase SHP-1 (Fragment)	ptpn6	Non-receptor	SSAPIVIHcSAGIGR	C9(hyper)	82

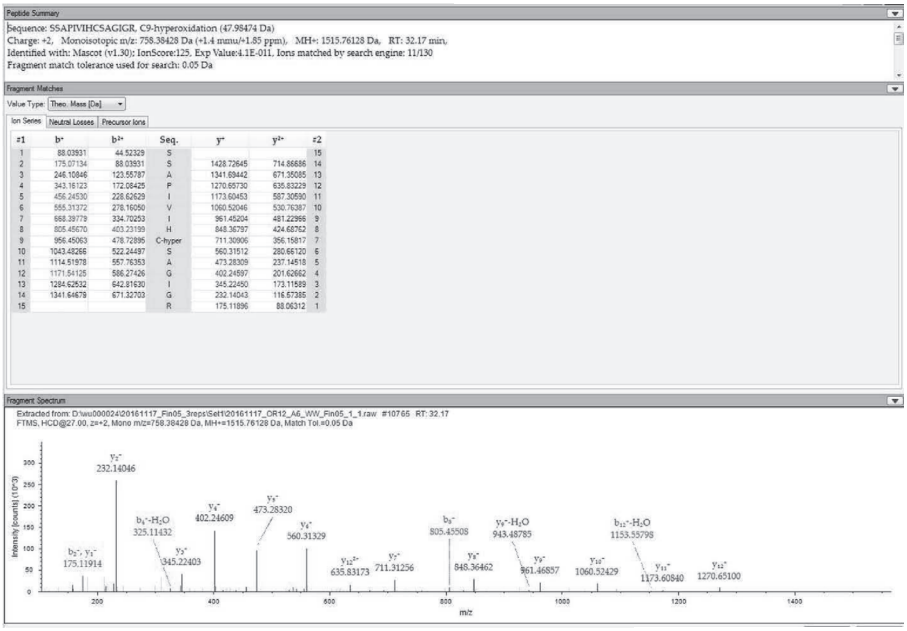

Uniprot Accession	Description	Gene name	PTP type	Sequence	Hyperoxidised cysteine	Total MS/MS count
X1WFV4	Uncharacterized protein (Fragment)	ptpn9a	Non-receptor	GHPLGPPMVVHcSAGIGR	C12(hyper)	170

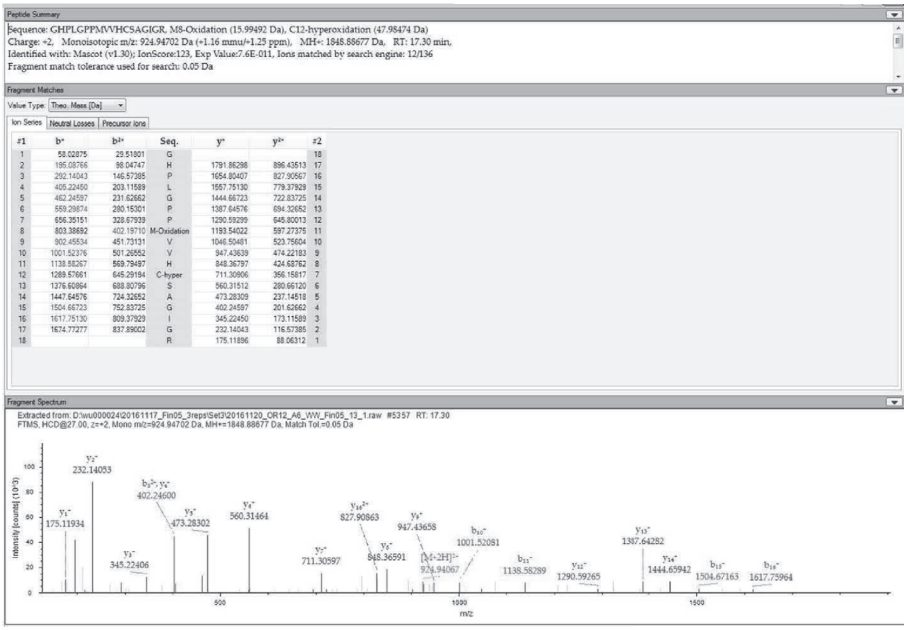

Uniprot Accession	Description	Gene name	PTP type	Sequence	Hyperoxidised cysteine	Total MS/MS count
F1QTI4	Uncharacterized protein	ptpn9b	Non-receptor	TLYPDWTGPPGGPPVVVHcSAGIGR	C19(hyper)	86

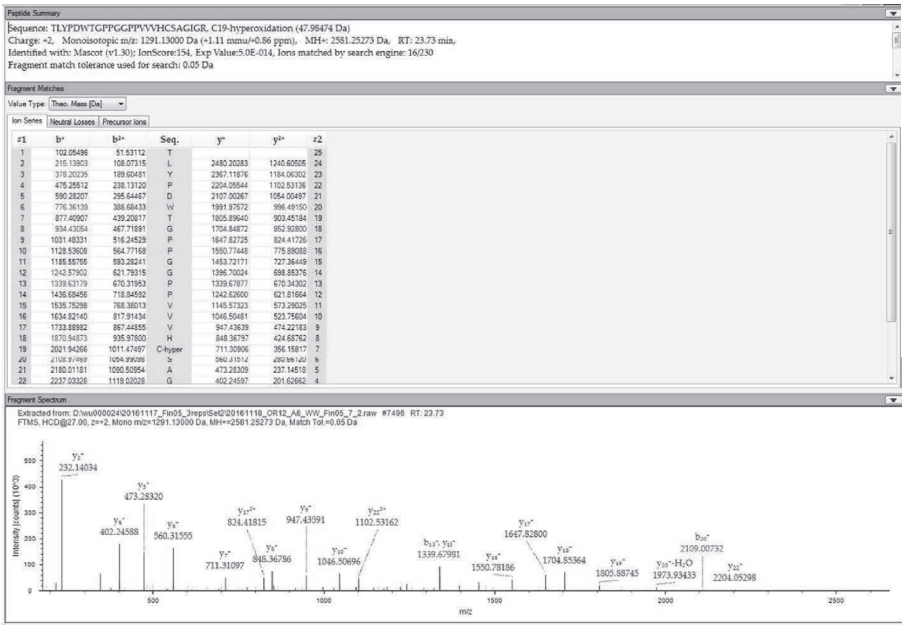

Table S1. PTP peptides detected. Conserved catalytic site sequence in blue. Position of hyper-oxidized cysteine refers to residue number within a properly cleaved tryptic peptide, without missed cleavage. Total MS/MS count is the sum of all spectra obtained from each biological replicate of PV-treated sample. Peptides oxidized in the second fin clip are highlighted in grey.

Uniprot Accession	Description	Gene name	PTP type	Sequence	Hyperoxidized cysteine	Total MS/MS count
B3DJL5_site1 (C7U129)	Ptpra protein	ptpra	Receptor	QQQQSGNHPITVHcSAGAGR	C14(hyper)	76
B3DJL5_site2 (C7U129)	Ptpra protein	ptpra	Receptor	NcNPQYAGPIVVHcSAGVGR	C14(hyper)	33
A0A0R4ITJ9 (C7U135)	Uncharacterized protein	ptprb	Receptor	TNSPGISVVHcSAGVGR	C11(hyper)	51
C7U126	CD45 antigen (Fragment)	ptprc	Receptor	NFFSGPIVVHcSAGVGR	C11(hyper)	93
E7EZG7_site1	Receptor-type tyrosine-protein phosphatase	ptprea	Receptor	QVNPSYAGPIVVHcSAGVGR	C14(hyper)	35
E7EZG7_site2	Receptor-type tyrosine-protein phosphatase	ptprea	Receptor	QQQQSGNHPIIVHcSAGAGR	C14(hyper)	119
Q90YJ5_site1	Receptor protein-tyrosine phosphatase LAR (Fragment)	ptprfa	Receptor	AcNPPDAGPMVVHcSAGVGR	C14(hyper)	100
Q90YJ5_site2	Receptor protein-tyrosine phosphatase LAR (Fragment)	ptprfa	Receptor	EQFGQDGPITVHcSAGVGR	C13(hyper)	72
F1Q4V8	Uncharacterized protein (Fragment)	ptprga	Receptor	SSAAQTPDMGPMLVHcSAGVGR	C16(hyper)	42
E7F9R2	Uncharacterized protein	ptprh	Receptor	QHIESHFSTGPTVVHcSAGVGR	C16(hyper)	159
B6HY54	Protein-tyrosine phosphatase	ptprja	Receptor	HSPTLVHcSAGVGR	C8(hyper)	52
X1WCM2	Uncharacterized protein (Fragment)	ptprjb.1	Receptor	HSPTVVHcSAGVGR	C8(hyper)	21
X1WF45	Uncharacterized protein (Fragment)	ptprjb.2	Receptor	EHMNQYScTSPTVVHcSAGVGR	C16(hyper)	6
X1WD65	Uncharacterized protein	ptprk	Receptor	MSNPPTAGPIVVHcSAGAGR	C14(hyper)	90
A0A0R4IA95	Uncharacterized protein (Fragment)	ptpro	Receptor	GPIVVHcSAGVGR	C7(hyper)	52
Q90YJ4_site1	Receptor protein-tyrosine phosphatase sigma (Fragment)	ptprsa	Receptor	EQFGQDGPISVHcSAGVGR	C13(hyper)	21
Q90YJ4_site2	Receptor protein-tyrosine phosphatase sigma (Fragment)	ptprsa	Receptor	TcNPPDAGPIIAHcSAGVGR	C14(hyper)	45
A0A0R4ITF5 (C7U125)	Uncharacterized protein	ptprub	Receptor	TSTPLDAGPVVVHcSVGAGR	C14(hyper)	13
X1WET2	Uncharacterized protein (Fragment)	ptprz1a	Receptor	AQTDGMGPMVVHcSAGVGR	C13(hyper)	16
B8A5J4	Uncharacterized protein	ptprz1b	Receptor	TAEMGPVVVHcSAGVGR	C11(hyper)	104
C7U142	Protein-tyrosine phosphatase 1B (Fragment)	ptpn1	Non-receptor	ESGcLSPELGPVVVHcSAGIGR	C16(hyper)	142
C7U151	Protein-tyrosine phosphatase SHP-2a (Fragment)	ptpn11a	Non-receptor	QEGITGAGPIVVHcSAGIGR	C14(hyper)	112
C7U120	Protein-tyrosine phosphatase SHP-2b (Fragment)	ptpn11b	Non-receptor	TQSAIPESGPIVVHcSAGIGR	C15(hyper)	59
Q6PEI4	Protein tyrosine phosphatase, non-receptor type 12	ptpn12	Non-receptor	DTTPIcVHcSAGcGR	C13(hyper)	71
C7U124	Protein-tyrosine phosphatase BAS (Fragment)	ptpn13	Non-receptor	HIHLSGPIITHcSAGIGR	C12(hyper)	64
F1QIX3	Uncharacterized protein	ptpn20	Non-receptor	GPITVHcSAGIGR	C7(hyper)	38
F1Q6T9	Uncharacterized protein	ptpn21	Non-receptor	NTNLPVLVHcSAGVGR	C10(hyper)	29
C7U128	Protein-tyrosine phosphatase LyPTP (Fragment)	ptpn22	Non-receptor	IYQDNEEIPIcIHcSAGcGR	C18(hyper)	13
F1R1D1	Uncharacterized protein	ptpn23a	Non-receptor	VScTHFQcSAGAFAYLR	C8(hyper)	138
F1QXQ5 (F1QGX6)	Tyrosine-protein phosphatase non-receptor type	ptpn2a	Non-receptor	ESGSLGPENGPVVVHcSAGIGR	C16(hyper)	86
Q6NY86	Tyrosine-protein phosphatase non-receptor type	ptpn2b	Non-receptor	ESGSLGMEQGPAVVHcSAGIGR	C16(hyper)	159
F1QLN8	Uncharacterized protein	ptpn3	Non-receptor	QESVPLMVHcSAGIGR	C10(hyper)	97
C7U127	Protein-tyrosine phosphatase MEG1a (Fragment)	ptpn4a	Non-receptor	DEPVVVHcSAGIGR	C8(hyper)	19
C7U113	Protein-tyrosine phosphatase MEG1a (Fragment)	ptpn4b	Non-receptor	ADGPEPVVVHcSAGIGR	C11(hyper)	156
C7U118	Protein-tyrosine phosphatase SHP-1 (Fragment)	ptpn6	Non-receptor	SSAPIVIHcSAGIGR	C9(hyper)	82
X1WFV4	Uncharacterized protein (Fragment)	ptpn9a	Non-receptor	GHPLGPPMVVHcSAGIGR	C12(hyper)	170
F1QTI4	Uncharacterized protein	ptpn9b	Non-receptor	TLYPDWTGPPGGPPVVVHcSAGIGR	C19(hyper)	86

Table S2. Tabulated spectra count. Mean spectra count and standard error obtained from 3 biological replicates. Peptides oxidized in second fin clip highlighted in grey. Student t-test statistics for difference between first and second fin clip reported as exact two-tailed p-value.

	First fin clip						Second fin clip							
Total MS/MS count	Mean spectra count PV	SEM PV	Mean spectra count NEM	SEM NEM	Mean spectra count Control	SEM Control	Mean spectra count PV	SEM PV	Mean spectra count NEM	SEM NEM	Mean spectra count Control	SEM Control	T.test (PV 1st clip: PV 2nd clip)	T.test (NEM 2nd clip: NEM 1st clip)
76	13.0	2.1	0.7	0.3	0.0	0.0	11.3	1.2	0.3	0.3	0.0	0.0	0.62	0.21
33	6.7	0.9	0.7	0.7	0.0	0.0	3.3	0.9	0.3	0.3	0.0	0.0	0.20	0.42
51	9.0	0.6	0.0	0.0	0.0	0.0	8.0	1.7	0.0	0.0	0.0	0.0	0.48	Not detected
93	18.0	1.7	0.3	0.3	0.0	0.0	12.3	0.9	0.3	0.3	0.0	0.0	0.14	Not detected
35	6.3	0.9	0.7	0.7	0.0	0.0	4.0	1.2	0.7	0.3	0.0	0.0	0.12	1.00
119	18.0	1.5	0.3	0.3	0.0	0.0	15.3	0.9	6.0	1.2	0.0	0.0	0.37	0.04
100	22.0	2.3	0.0	0.0	0.0	0.0	11.3	0.7	0.0	0.0	0.0	0.0	0.07	Not detected
72	12.3	1.8	0.3	0.3	0.0	0.0	11.0	1.5	0.3	0.3	0.0	0.0	0.63	Not detected
42	8.7	1.5	0.0	0.0	0.0	0.0	5.3	0.3	0.0	0.0	0.0	0.0	0.20	Not detected
159	22.0	1.5	0.0	0.0	0.0	0.0	19.3	2.0	11.7	1.5	0.0	0.0	0.38	0.02
52	8.0	0.6	1.0	0.0	0.0	0.0	8.3	0.9	0.0	0.0	0.0	0.0	0.83	Not detected
21	4.0	1.2	0.0	0.0	0.0	0.0	3.0	1.0	0.0	0.0	0.0	0.0	0.68	Not detected
6	1.0	0.0	0.0	0.0	0.0	0.0	0.7	0.3	0.3	0.3	0.0	0.0	0.42	0.42
90	16.7	0.9	0.0	0.0	0.0	0.0	13.0	0.6	0.3	0.3	0.0	0.0	0.05	0.42
52	8.3	0.9	0.3	0.3	0.0	0.0	8.3	1.2	0.3	0.3	0.0	0.0	1.00	Not detected
21	4.0	0.6	0.0	0.0	0.0	0.0	2.7	0.3	0.3	0.3	0.0	0.0	0.06	0.42
45	8.0	1.0	0.0	0.0	0.0	0.0	7.0	1.7	0.0	0.0	0.0	0.0	0.42	Not detected
13	2.3	0.3	0.0	0.0	0.0	0.0	2.0	0.0	0.0	0.0	0.0	0.0	0.42	Not detected
16	3.7	0.3	0.0	0.0	0.0	0.0	1.3	0.3	0.3	0.3	0.0	0.0	0.07	0.42
104	21.7	2.4	0.0	0.0	0.0	0.0	12.7	1.5	0.3	0.3	0.0	0.0	0.12	0.42
142	22.0	2.1	0.7	0.7	0.3	0.3	20.7	1.5	3.7	0.7	0.0	0.0	0.73	0.04
112	14.7	1.5	0.7	0.3	0.3	0.3	11.3	0.9	10.3	0.9	0.0	0.0	0.27	0.00
59	7.3	0.3	0.0	0.0	0.0	0.0	5.0	0.6	7.3	0.7	0.0	0.0	0.07	0.01
71	13.0	1.2	0.0	0.0	0.0	0.0	10.7	1.5	0.0	0.0	0.0	0.0	0.46	Not detected
64	13.3	2.0	1.0	0.6	0.0	0.0	6.7	0.7	0.3	0.3	0.0	0.0	0.12	0.53
38	7.0	1.0	0.0	0.0	0.0	0.0	5.7	1.2	0.0	0.0	0.0	0.0	0.06	Not detected
29	4.0	0.6	1.0	0.6	0.0	0.0	4.3	1.2	0.3	0.3	0.0	0.0	0.67	0.42
13	3.0	0.0	0.0	0.0	0.0	0.0	1.0	0.6	0.3	0.3	0.0	0.0	0.07	0.42
138	24.7	2.0	0.0	0.0	0.0	0.0	21.0	1.5	0.3	0.3	0.0	0.0	0.39	0.42
86	15.7	0.7	0.3	0.3	0.0	0.0	9.7	0.9	3.0	0.6	0.0	0.0	0.06	0.04
159	32.7	2.8	0.3	0.3	0.0	0.0	19.7	3.3	0.0	0.0	0.3	0.3	0.16	0.42
97	17.0	1.5	0.7	0.3	0.0	0.0	14.3	2.3	0.3	0.3	0.0	0.0	0.37	0.42
19	3.3	0.3	0.0	0.0	0.0	0.0	3.0	1.2	0.0	0.0	0.0	0.0	0.81	Not detected
156	27.7	1.5	0.0	0.0	0.0	0.0	22.3	0.7	5.7	0.3	0.0	0.0	0.09	0.00
82	15.7	1.5	0.7	0.7	0.3	0.3	10.3	0.3	0.0	0.0	0.3	0.3	0.09	0.42
170	28.7	1.9	0.3	0.3	0.0	0.0	22.3	1.5	5.3	0.9	0.0	0.0	0.18	0.01
86	16.3	0.9	0.7	0.3	0.0	0.0	11.3	1.5	0.3	0.3	0.0	0.0	0.13	0.42

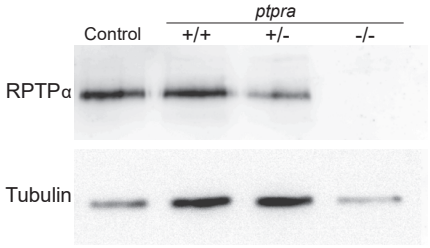

Fig. S3. Zebrafish *ptpra* knock-out embryos (*ptpra*$^{-/-}$) lack RPTPα protein. Adult zebrafish heterozygous for *ptpra* (*ptpra*$^{+/-}$) were in-crossed to generate *ptpra* knock-out embryos (*ptpra*$^{-/-}$). At 4 dpf, individual embryos were cut in half: one half lysed for protein, and the other half lysed for DNA extraction. Protein lysates of *ptpra*$^{+/+}$, *ptpra*$^{+/-}$, and *ptpra*$^{-/-}$ embryos were pooled, and 5 embryo equivalents per condition were run on an SDS-PAGE gel, immunoblotted and probed with an Rptpα-specific antibody and with tubulin to monitor equal loading. Control lane represents wild-type TL zebrafish embryos at 3 dpf.

Chapter 6

An Essential Role for Shp2-MAPK Signalling during Zebrafish Embryo Caudal Fin-Fold Regeneration

Alexander James Hale[1,2] and Jeroen den Hertog[1,2]

1. Hubrecht Institute – KNAW and University Medical Center Utrecht, Utrecht, the Netherlands
2. Institute Biology Leiden, Leiden University, Leiden, the Netherlands

ABSTRACT

Zebrafish completely regrow their caudal fins after amputation. Following injury, wound healing occurs, followed by the formation of a blastema, which produces cells to replace the lost tissue in the final phase of regenerative outgrowth. Here, we show that *ptpn11a*$^{-/-}$*ptpn11b*$^{-/-}$ zebrafish embryos, which lack functional Shp2, did not regenerate their caudal fin-folds following amputation. Rescue experiments revealed that catalytic activity and the SH2 domains, but not the two tyrosine phosphorylation sites in the C-terminal domain of Shp2a were required for caudal fin-fold regeneration. Normal expression of the blastema marker *junbb* indicated normal blastema formation in *ptpn11a*$^{-/-}$*ptpn11b*$^{-/-}$ zebrafish embryos. Cell proliferation was arrested in zebrafish embryos lacking functional Shp2, and MAPK phosphorylation was reduced. Consistent with these Shp2 results, we found that inhibition of MEK1 in wild-type zebrafish embryos inhibited caudal fin-fold regeneration and arrested cell proliferation, indicating that MAPK activation was required for regenerative outgrowth. Collectively, our results suggest an essential role for Shp2a-MAPK signalling in promoting cell proliferation during the regenerative outgrowth phase of regenerating zebrafish embryo caudal fin-folds.

INTRODUCTION

In a process termed epimorphic regeneration, zebrafish (*Danio rerio*) fully regenerate their heart, retina, spinal cord, and caudal fin after injury (1, 2). Regeneration of the zebrafish caudal fin proceeds sequentially through three distinct phases: wound healing, blastema formation, and regenerative outgrowth. The mechanism of zebrafish embryonic caudal fin-fold regeneration is the same as adult zebrafish caudal fin regeneration, though reaches completion within 72 hours, instead of within two weeks (3). Following injury, nearby cells migrate to cover the wound and form an apical epidermal cap that is essential to initiate blastema formation and regenerative outgrowth (4). Many genes have been implicated in the regenerative process (5) and multiple signalling pathways have been validated to be essential for regeneration, including fibroblast growth factor (FGF), sonic hedgehog, bone morphogenetic protein, Wnt, and Notch (6).

Src homology 2 domain containing phosphatase (SHP2) is a protein tyrosine phosphatase (PTP), encoded by the *PTPN11* gene, that dephosphorylates phosphorylated tyrosine residues of target substrates. The zebrafish genome contains two *ptpn11* genes, *ptpn11a* and *ptpn11b*, encoding Shp2a and Shp2b, respectively. Both Shp2a and Shp2b are highly homologous to human SHP2 and harbour catalytic activity. Shp2b is dispensable, but Shp2a is not, which is due to differential expression of *ptpn11a* and *ptpn11b* during early development. *Ptpn11a*$^{+/+}$*ptpn11b*$^{-/-}$ and *ptpn11a*$^{+/-}$*ptpn11b*$^{-/-}$ zebrafish are viable and fertile, yet homozygous *ptpn11a*$^{-/-}$*ptpn11b*$^{-/-}$ double knock out zebrafish are embryonically lethal from 5-7 days post fertilization (dpf) onwards (7).

SHP2 is involved in signalling initiated by various growth factors, such as epidermal growth factor (EGF), fibroblast growth factor (FGF), platelet derived growth factor (PDGF), and insulin-like growth factor 1 (IGF1) (8, 9). SHP2 has a role in promoting mitogen activated protein kinase (MAPK) signalling in response to growth factor stimulation. Yet, SHP2-mediated regulation of phosphoinositide 3-kinase (PI3K) signalling depends on the growth factor stimulus. SHP2 inhibits PI3K signalling in response to EGF, but activates PI3K signalling in response to PDGF and IGF in the same cell type (10). Hence, the effects of SHP2 on PI3K signalling are stimulus and cell-type dependent. We refer to (11) for a recent overview of SHP2 signalling.

The SHP2 protein consists of two SH2 domains, followed by a catalytically active PTP domain, and a C-terminal domain (12). SHP2, like all classical PTPs, mediates dephosphorylation of its substrates through a mechanism involving a catalytic cysteine (C460 in zebrafish Shp2a) and an assisting arginine (R466 in zebrafish) in the PTP

domain (13). SHP2 requires catalytic activity to promote MAPK and PI3K signalling, as mutation of the catalytic cysteine results in reduced downstream signalling (14, 15). Importantly, the SH2 domains and C-terminal domain of SHP2 are required for the function of SHP2 in response to growth factor stimulation. Both SH2 domains contain conserved arginine residues (R32 and R138) that are required for binding to phospho-tyrosine-containing target proteins, such as insulin receptor substrate 1 (IRS-1), PDGF receptor, and GAB1, and are essential for the function of SHP2 (16). The SH2 domains also have an ERK-independent, anti-apoptotic function, as expression of a zebrafish Shp2 mutant lacking the PTP domain and C-terminal domain rescued apoptosis induced by zebrafish Shp2 knockdown. The C-terminal SH2 domain was particularly important for this function, as full-length zebrafish Shp2a R138M failed to block apoptosis (17). The C-terminal domain of SHP2 contains serine and tyrosine phosphorylation sites, as well as a proline-rich domain, that mediate interactions with other proteins. Two tyrosines (Y542 and Y580) are particularly important, because when phosphorylated, they constitute binding sites for SH2 domain containing proteins, such as growth factor receptor-bound protein 2 (GRB2) (18, 19). Binding of GRB2 modulates the interaction of the C-terminal domain with the SH2 domains of SHP2 (20), and is required for Shp2 mediated MAPK signalling in response to EGF (21).

Collectively, the studies on the function of the domains of SHP2 show that both the SH2 and C-terminal domain potentiate, but are not definitively required for the stimulation of MAPK and PI3K signalling by the PTP domain of SHP2. Activated MAPK promotes cell proliferation, migration, and differentiation (22) and activated PI3K/AKT promotes cell cycle progression to drive cell proliferation, and enhances cell survival by inhibiting pro-apoptotic transcription factors (23). It is not surprising that SHP2 has been implicated to play a role in a plethora of cellular processes, including proliferation (24, 25), cell migration (26–28), and stem cell self-renewal and differentiation (29–32). SHP2, MAPK, and PI3K signalling are indispensable for proper embryonic development (7, 16, 33–37).

Regeneration requires cell survival, migration, proliferation and differentiation for effective wound healing and replacement of the lost tissue (4, 38, 39). MAPK activation following injury is associated with regenerative competence across species (40, 41). The need for MAPK signalling in zebrafish caudal fin regeneration has been implicated by demonstrating that inhibition of FGF receptor (FGFR) signalling (42–44) impairs regeneration. However, activation of the FGFR results in the promotion of not only MAPK, but also PI3K, Phospholipase C γ (PLCγ), and signal transducer and activator of

transcription (STAT) (45), convoluting the conclusion that MAPK signalling is required. Similarly, the requirement for activation of the EGF receptor (EGFR) family member ErbB2 for zebrafish caudal fin regeneration (46) eludes to a requirement for MAPK and PI3K signalling (47). Whereas PI3K signalling is essential for zebrafish caudal fin regeneration (38, 46), the evidence supporting a role for MAPK signalling is inconclusive. Rojas-Muñoz et al. showed that treatment of zebrafish embryos with the ErbB2/3 inhibitor PD168393 or the PI3K inhibitor LY294002 effectively blocked caudal fin regeneration, but treatment with the MEK1 inhibitor PD098059 had no effect (46). However, it has recently been shown that MAPK signalling is essential for zebrafish cardiac regeneration, as inhibition with the MEK1 inhibitor AZD6244 or expression of dominant-negative MEK1 impaired zebrafish cardiac regeneration (48). Hence, the role of SHP2 and MAPK signalling in zebrafish caudal fin regeneration remains to be determined definitively.

We investigated the role of Shp2 in zebrafish embryo caudal fin-fold regeneration using homozygous *ptpn11a*$^{-/-}$*ptpn11b*$^{-/-}$ zebrafish embryos, that lack functional Shp2 (7), and found that Shp2 is required for normal caudal fin-fold regeneration. Re-expression of wild-type Shp2a rescued regeneration, indicating that the lack of regeneration in mutant zebrafish embryos was indeed attributable to lack of functional Shp2. Rescue experiments with mutant Shp2a indicated that Shp2a catalytic activity and functional SH2 domains were required, whereas the two tyrosine residues in the C-terminus of Shp2a that are essential for certain aspects of Shp2 signalling, were dispensable for its capacity to rescue regeneration. Characterization of the regeneration defect in *ptpn11a*$^{-/-}$*ptpn11b*$^{-/-}$ zebrafish embryos by *in situ* hybridization using a *junbb*-specific probe indicated normal blastema formation. PCNA staining indicated that cell proliferation during regenerative outgrowth was reduced in *ptpn11a*$^{-/-}$*ptpn11b*$^{-/-}$ zebrafish embryos. MAPK phosphorylation was reduced in amputated caudal fin-folds of *ptpn11a*$^{-/-}$*ptpn11b*$^{-/-}$ zebrafish embryos. Pharmacological inhibition of MEK1, upstream of MAPK, in wild-type zebrafish embryos inhibited regeneration and reduced proliferation during regenerative outgrowth. The similarity with the lack of regeneration in *ptpn11a*$^{-/-}$*ptpn11b*$^{-/-}$ zebrafish embryos is consistent with Shp2a acting through MAPK in regeneration. Collectively, our results demonstrate that catalytically active Shp2a is required for zebrafish embryo caudal fin-fold regeneration and may exert its effects through activation of MAPK.

MATERIALS AND METHODS

Zebrafish husbandry

All procedures involving experimental animals were performed under licence number GZB/VVB 2041019 of the Hubrecht Institute/ Royal Academy of Arts and Sciences (Koninklijke Nederlandse Akademie van Wetenschappen, KNAW), approved by the local animal experiments committee according to local guidelines and policies in compliance with national and European law.

The *ptpn11a*$^{+/-}$*ptpn11b*$^{-/-}$ zebrafish lines in the Tuebingen Long fin (TL) background were previously created by target-selected gene inactivation (TSGI), and both *ptpn11a*^{hu3459} and *ptpn11b*^{hu5920} alleles result from non-sense mutations that lead to a premature stop codon upstream of the catalytic cysteine, C460 (7). Adult *ptpn11a*$^{+/-}$*ptpn11b*$^{-/-}$ zebrafish were in-crossed to generate *ptpn11a*$^{-/-}$*ptpn11b*$^{-/-}$ zebrafish embryos for all experiments. Zebrafish were raised and maintained as described by Westerfield (49) under a 14 hours light/ 10 hours dark cycle at 28.5°C.

mRNA synthesis and micro-injections

All constructs contain a C-terminal eGFP connected by a peptide-2a cleavage sequence (50). The constructs pCS2+-eGFP-2a-Shp2a (WT), pCS2+-eGFP-2a-Shp2a-R466M (RM), pCS2+-eGFP-2a-Shp2a-R32M-R138M (SH), and pCS2+-eGFP-2a-Shp2a-Y542F-Y580F (YF) were obtained as described (51). Sense messenger RNA (mRNA) synthesis and micro-injection into one-cell stage zebrafish embryos was performed as described (52).

Caudal fin-fold amputation

Zebrafish embryos were amputated as previously described (53), amputations were performed at 2 days post fertilisation (dpf) for all experiments. Regeneration was allowed to proceed until analysis at 3 days post amputation (dpa) or fixation at 3 hours post amputation (hpa), 1dpa or 2dpa. PD184352 (Sigma) or Dimethylsulfoxide (Sigma) was administered directly following recovery of amputated zebrafish embryos in E3 medium. Whole zebrafish embryos were lysed for genotyping or fixed in 4% paraformaldehyde (PFA), in PBS, either 3hpa for *in situ* hybridization, or at 1dpa and 2dpa for immunohistochemistry.

In situ hybridization

In situ hybridizations were performed as previously described (54), using *junbb* digoxigenin-UTP-labelled anti-sense riboprobes. Parts of *junbb* were amplified from zebrafish cDNA using specific primers (**Table S1**) and the resulting PCR products were cloned into vectors and used as DNA templates for synthesis of riboprobes. Digoxigenin-UTP-labelled anti-sense riboprobes were synthesized from *junbb* PCR product, produced using *fwd: TACACGACGCTGAACGCATA* and *rev: TAATACGACTCACTA-TAGGTGTCCGTTCTCTTCCGTCC*. Caudal fin-folds of zebrafish embryos were severed and mounted in 70% glycerol in PBS for imaging on a Zeiss Axioskop 2 Mot Plus microscope with either a Plan-NEOFLUAR 10x/0.30 or 20x/0.50 objective. The rest of the zebrafish embryo was lysed for genotyping.

Immunohistochemistry

Zebrafish embryos fixed in 4% PFA were washed in PBS 0.1% Tween-20 and antigen retrieval performed depending on the antibody used: ice-cold acetone for 20mins for PCNA; and 10mM Tris, 1mM EDTA, pH 9.0 for phospho-p44/42 MAPK (Thr202/Tyr204). Whole zebrafish embryos were incubated overnight at 4°C in mouse anti-PCNA (1:200, #M0879; DAKO Agilent Pathology Solutions), or rabbit anti-phospho-p44/42MAPK (Thr202/Tyr204) (1:100, #4370 Cell Signaling Technology). Secondary antibodies conjugated to Cy5 goat anti-mouse or goat anti-rabbit IgG were used 1:500 and 1:200 respectively (#115-175-146 and #111-175-144; Jackson ImmunoResearch). Nuclei were shown by DAPI (4',6-diamidino-2-phenylindole) staining. Caudal fin-folds of zebrafish embryos were mounted for imaging in 70% glycerol in PBS, and the rest of the zebrafish embryo was lysed for genotyping. Z-stacks (6µm step size) of the caudal fin-fold were acquired for every zebrafish embryo with a Leica Sp8 confocal microscope. ImageJ software (http://rsb.info.nih.gov./ij/) was used to generate maximum intensity (z) projections and merge channels. Quantification was performed on the original z-projections (1024 x 1024px, 300dpi) following rolling ball background subtraction with an average from 50px. Mean intensity of phospho-p44/42 MAPK (Thr202/Tyr204) (hereafter p-MAPK) was measured from the wound margin inwards using an ROI with dimensions equivalent to: h: 2.08µm (625px) and varying widths for each sample: for zebrafish embryos at 24hpa: w: 0.32µm (95px) for amputated zebrafish embryos; w: 0.75µm (225px) for uncut zebrafish embryos; for embryos at 48hpa: w: 0.82µm (246px) for amputated zebrafish embryos; w: 1.00µm (300px) for uncut zebrafish embryos.

Genotyping

All zebrafish embryos that were used in these assays were genotyped to establish *ptpn11a* status. To this end, genomic zebrafish DNA was extracted through lysis of zebrafish embryos in 100µg/ml proteinase K (Sigma) diluted in SZL buffer (50mM KCl, 2.5mM MgCl, 10mM Tris pH 8.3, 0.005% NP40, 0.005% Tween-20, and 10% 0.1% Gelatine). Lysis was performed by incubating at 60°C for 1 hour, followed by 95°C for 15 minutes in a thermal cycler (BioRad T100). The *ptpn11a*^{hu1864} allele in non-fixed tissue was analysed by Kompetitive Allele Specific PCR (KASP): primers of *ptpn11a* containing the non-sense mutations of the *ptpn11a*^{hu1864} allele (**Table S1**), were mixed with genomic zebrafish DNA and KASP master mix (LGC Group). Amplification was carried out according to the manufacturer's instructions and the resulting PCR products were analysed in a PHERAstar microplate reader (BMG LABTECH). Klustercaller software (LGC Group) was used to identify the mutations. For fixed tissue genotyping for the *ptpn11a*^{hu1864} allele was performed by nested PCR with primer sets 1-4 (**Table S1**) followed by Sanger sequencing (Macrogen Inc., Europe) to detect the mutations.

Immunoblotting

Whole cell protein extracts from human embryonic 293 T cells transfected with and overexpressing zebrafish *ptpn11a* were prepared by lysis in ice-cold buffer (25mM HEPES pH 7.4, 150mM NaCl, 0.25% deoxycholate, 1% triton X-100, 10mM MgCl2, 1mM EDTA and 10% glycerol) containing protease and phosphatase inhibitors. Samples were centrifuged at 12,000g for 20mins and the supernatant collected. Proteins were resolved in 10% SDS-PAGE gels under reducing conditions and transferred to PVDF membranes (IPVH00010, Merck Millipore). Immunoblotting was performed using anti-SHP2 (SH-PTP2 C-18, #SC-280, Santa Cruz Technology) or anti-Tubulin (#CP06, Merck Millipore) antibodies followed by horseradish peroxidase (HRP)-conjugated anti-rabbit or anti-mouse antibodies, respectively. Detection was done by enhanced chemiluminescence (#34095, Thermo Fischer Scientific).

Statistics

For analysis of caudal fin-fold lengths, histograms of whole data sets were examined to determine non-normal distribution of the data. Statistical analysis of unequal variances was obtained through a Kruskall-Wallis test. Differences between different experimental conditions were assessed for significance using a Mann-Whitney U test. Differences were considered significant when $p<0.001$, and if they satisfied

a confidence interval of 95% in a Monte Carlo exact test. All tests for regenerating caudal fin-folds were performed in SPSS (IBM). For analysis of immunohistochemistry measurements, differences between different experimental condition were assessed for significance using a Mann-Whitney U test with a confidence level set to 95%. All tests for immunohistochemistry measurements were performed in GraphPad Prism (GraphPad Software). Differences were considered significant when $p<0.05$.

RESULTS

Functional Shp2a is required for zebrafish embryo caudal fin-fold regeneration

To investigate the role of Shp2 in regeneration, homozygous *ptpn11a*$^{-/-}$*ptpn11b*$^{-/-}$ zebrafish embryos, lacking functional Shp2, were analysed for the potential to regenerate their caudal fin-fold following amputation. The caudal fin-fold of offspring from a *ptpn11a*$^{+/-}$*ptpn11b*$^{-/-}$ in-cross were amputated at 2 dpf and allowed to regenerate for 3 days. Regeneration of individual zebrafish embryos was assessed at 5 dpf (i.e. 3 days post amputation, dpa), and, subsequently, the zebrafish embryos were genotyped. In contrast to sibling *ptpn11a*$^{+/+}$*ptpn11b*$^{-/-}$ and *ptpn11a*$^{+/-}$*ptpn11b*$^{-/-}$ zebrafish embryos, which do regenerate their caudal fin-folds, regeneration of the caudal fin-fold of *ptpn11a*$^{-/-}$*ptpn11b*$^{-/-}$ zebrafish embryos is severely impaired (**Fig. 1**). Quantification of caudal fin-fold lengths, obtained by measuring the distance from the tip of the notochord to the edge of the fin-fold, were determined and are presented as percentage caudal fin-fold growth, normalized to uncut controls of *ptpn11a*$^{+/+}$*ptpn11b*$^{-/-}$ zebrafish embryos (**Fig. 1B**). Regeneration of the caudal fin-fold of *ptpn11a*$^{-/-}$*ptpn11b*$^{-/-}$ zebrafish embryos is significantly impaired, compared with sibling embryos ($p<0.001$). Normal growth rate of the caudal fin-fold of *ptpn11a*$^{-/-}$*ptpn11b*$^{-/-}$ zebrafish embryos is unaffected by the lack of functional Shp2. These results demonstrate that functional Shp2 is required for zebrafish embryo caudal fin-fold regeneration.

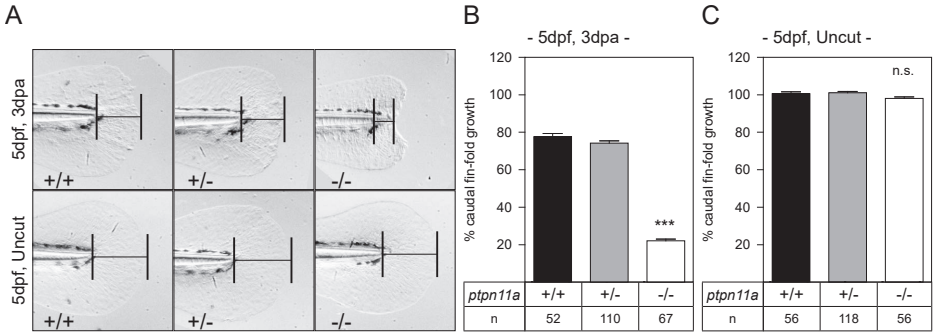

Fig. 1. Functional Shp2 is required for regeneration. Zebrafish embryos from a *ptpn11a*$^{+/-}$*ptpn11b*$^{-/-}$ in-cross were amputated at 2 dpf and caudal fin-fold regeneration was assessed at 3dpa (i.e. 5dpf, 3dpa). Equivalent uncut embryos were included as controls (i.e. 5dpf, uncut). All embryos were genotyped. (**A**) Representative images of amputated embryo caudal fin-folds at 3dpa are shown together with uncut controls for comparison. (**B**, **C**) Regeneration was quantified by measuring the distance from the tip of the notochord to the edge of the caudal fin-fold as indicated. The means of caudal fin-fold growth are depicted relative to caudal fin-fold growth of uncut *ptpn11a*$^{+/+}$*ptpn11b*$^{-/-}$ controls. Means of *ptpn11a*$^{-/-}$*ptpn11b*$^{-/-}$ embryos were compared *ptpn11a*$^{+/+}$*ptpn11b*$^{-/-}$ embryos using a Mann-Whitney U-test. Significance: *** p<0.001; n.s. not significant; error bars indicate standard error of the mean. Data pooled from multiple experiments.

Shp2a catalytic activity and the SH2 domains of Shp2a are required for zebrafish embryo caudal fin-fold regeneration

To validate that impaired regeneration in *ptpn11a*$^{-/-}$*ptpn11b*$^{-/-}$ zebrafish embryos is indeed due to the lack of functional Shp2, rescue experiments were performed. Zebrafish embryos from a *ptpn11a*$^{+/-}$*ptpn11b*$^{-/-}$ in-cross were micro-injected at the one-cell stage with synthetic mRNA encoding Shp2a, and at 2 dpf the caudal fin-fold was amputated and allowed to regenerate for 3 days. Expression of wild-type Shp2a resulted in a significant rescue (p<0.001) of regeneration in *ptpn11a*$^{-/-}$*ptpn11b*$^{-/-}$ zebrafish embryos (**Fig. 2A-B**).

The catalytic activity of SHP2 is important for the function of SHP2, although PTP-independent functions have been identified as well. The SH2 domains and the C-terminal domain of SHP2 are required for downstream signalling (17, 18, 21, 55–58). To determine which domains of Shp2a are required for caudal fin-fold regeneration, the following mutants of Shp2a were used in rescue experiments: catalytically inactive Shp2a-R466M (RM); the SH2 domain mutant Shp2a-R32M-R138M (SH), in which the essential arginine residues in both SH2 domains were mutated; and the C-terminal domain mutant Shp2a-Y542F-Y580F (YF), which lacks the two tyrosine phosphorylation sites that are important for signalling. We used the R466M mutant of Shp2a in our experiments rather than the catalytic cysteine mutant (C460S in zebrafish Shp2a), be-

cause Shp2a-C460S may trap substrates (59, 60), and thus have inadvertent dominant effects. Indeed, expression of Shp2a-C460S in wild-type zebrafish embryos induced developmental defects, and expression in *ptpn11a*$^{-/-}$*ptpn11b*$^{-/-}$ zebrafish embryos induced more severe developmental defects than non-injected Shp2 deficient zebrafish embryos (data not shown). In contrast, the Shp2a-R466M mutant is catalytically inactive and has no dominant-negative effects (17).

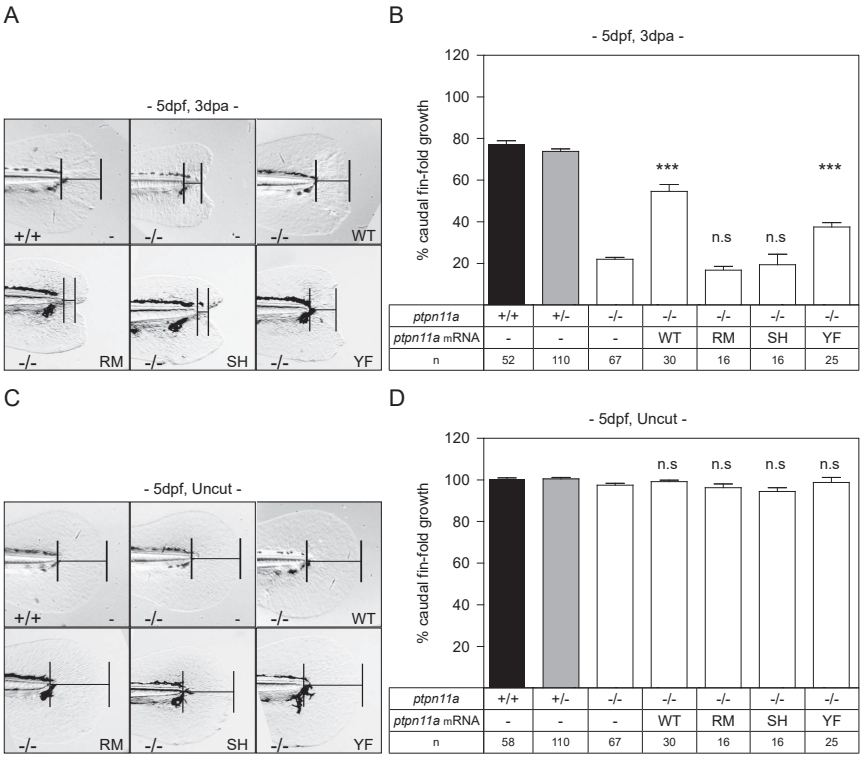

Fig. 2. The catalytic activity and SH2 domains of Shp2 are required to rescue caudal fin-fold regeneration in Shp2 deficient embryos. Embryos from a *ptpn11a*$^{+/-}$*ptpn11b*$^{-/-}$ in-cross were micro-injected at the one-cell stage with synthetic mRNA encoding wild-type Shp2a (WT), catalytically inactive Shp2a-R466M (RM), SH2 domain mutant Shp2a-R32M-R138M (SH), C-terminal tyrosines mutant Shp2a-Y542F-Y580F (YF), or were not injected (-). At 2dpf the caudal fin-fold was amputated and regeneration was assessed at 3dpa (i.e. 5dpf, 3dpa), equivalent uncut controls were included (i.e. 5dpf, uncut). All embryos were genotyped. (**A**) Representative images of amputated *ptpn11a*$^{-/-}$*ptpn11b*$^{-/-}$ embryos caudal fin-folds at 3dpa are shown together with a non-injected sibling (*ptpn11a*$^{+/+}$*ptpn11b*$^{-/-}$) for comparison. (**C**) Representative images of uncut *ptpn11a*$^{-/-}$*ptpn11b*$^{-/-}$ embryos caudal fin-folds at 3dpa. (**B**, **D**) Regeneration was quantified by measuring the distance from the tip of the notochord to the edge of the caudal fin-fold as indicated. The means of caudal fin-fold growth are depicted relative to caudal fin-fold growth of uncut *ptpn11a*$^{+/+}$*ptpn11b*$^{-/-}$ controls. Means of micro-injected amputated *ptpn11a*$^{-/-}$*ptpn11b*$^{-/-}$ embryos were compared to non-injected amputated *ptpn11a*$^{-/-}$*ptpn11b*$^{-/-}$ embryos using a Mann-Whitney U-test. Significance: *** $p<0.001$; n.s. not significant; error bars indicate standard error of the mean. Data pooled from multiple experiments.

The mRNAs encoding (mutant) Shp2a proteins also encode eGFP linked by a peptide-2a cleavage sequence, resulting in a single polypeptide that is cleaved prior to protein folding (50). At 2dpf, eGFP-positive zebrafish embryos were selected and their caudal fin-folds were amputated. Zebrafish embryos were allowed to regenerate for 3 days. Representative pictures of regenerated caudal fin-folds of *ptpn11a*$^{-/-}$*ptpn11b*$^{-/-}$ zebrafish embryos expressing mutant Shp2a protein at 3dpa are depicted (**Fig. 2A**). The equivalent uncut fin-folds (i.e. 5dpf, uncut) are all normal (**Fig. 2C**). Caudal fin-fold lengths were determined and are presented as percentage caudal fin-fold growth, normalized to uncut controls of *ptpn11a*$^{+/+}$*ptpn11b*$^{-/-}$ zebrafish embryos (**Fig. 2B, D**). In contrast to their siblings, *ptpn11a*$^{-/-}$*ptpn11b*$^{-/-}$ zebrafish embryos displayed severely impaired regeneration, which was rescued by expression of wild-type Shp2a (WT), but not by catalytically inactive Shp2a-R466M (RM). Furthermore, expression of the SH2 domain mutant of Shp2a (SH) was unable to rescue regeneration. In contrast, the mutant lacking two tyrosine phosphorylation sites in its C-terminal domain (YF) rescued regeneration of *ptpn11a*$^{-/-}$*ptpn11b*$^{-/-}$ zebrafish embryos (**Fig. 2B**). A trivial explanation for the inability of the catalytically inactive mutant of Shp2a (RM), or the SH2 domain mutant of Shp2a (SH) to rescue caudal fin-fold regeneration might be that these proteins have reduced stability. Due to low expression levels of all mutant Shp2a proteins in zebrafish embryos, it was not possible to monitor protein expression in these zebrafish embryos. However, transfection of constructs encoding the mutant Shp2a proteins in human embryonic kidney 293 T cells revealed similar expression levels of all mutant Shp2a proteins (**Fig. S1**). This suggests that the differences in ability to rescue caudal fin-fold regeneration are not due to large differences in protein expression or stability, but rather to differences in Shp2a function. Together, these results demonstrate that although the two tyrosine phosphorylation sites in the C-terminal domain are dispensable, the catalytic activity as well as the SH2 domains of Shp2 are required for zebrafish embryo caudal fin-fold regeneration.

Normal blastema formation in zebrafish embryos deficient for Shp2

Following amputation, three sequential steps can be discerned in the regeneration process: wound healing, blastema formation and regenerative outgrowth. Following wound healing, an apical epidermal cap is produced that signals for the formation of the blastema, and, thus, successful blastema formation is indicative of successful wound healing (1, 2). In the *ptpn11a*$^{-/-}$*ptpn11b*$^{-/-}$ zebrafish embryos, we assessed blastema formation at 3hpa by *in situ* hybridization using a *junbb*-specific probe, which

has previously been shown to be upregulated in the blastema (61, 62). All zebrafish embryos were subsequently genotyped. *Junbb* was clearly expressed in amputated caudal fin-folds, but not in uncut controls, and *ptpn11a*$^{-/-}$*ptpn11b*$^{-/-}$ mutant zebrafish embryos expressed *junbb* to a similar extent as their siblings following caudal fin-fold amputation (**Fig. 3**). These results indicate that blastema formation was normal in Shp2 deficient zebrafish embryos.

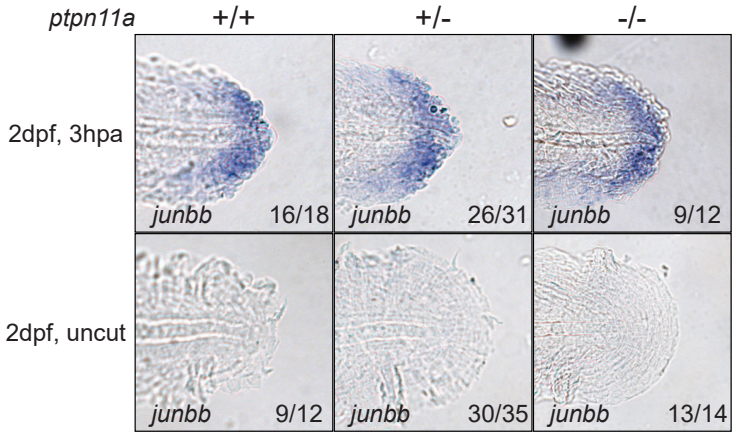

Fig. 3. Normal blastema formation in zebrafish embryos lacking functional Shp2. At 2dpf the caudal fin-folds of embryos from a *ptpn11a*$^{+/-}$*ptpn11b*$^{-/-}$ in-cross were amputated and allowed to regenerate. Embryos were fixed at 3hpa, or equivalent for uncut controls, and subjected to hybridization for *junbb*. Representative images of caudal fin-folds of genotyped embryos are shown, and the number of embryos showing similar patterns/ total number of embryos analysed is indicated in the bottom right corner of each panel.

Arrested proliferation in zebrafish embryos deficient for Shp2 during regenerative outgrowth

Proliferation is upregulated during regenerative outgrowth to generate the cells required to form and replace the lost tissue (2, 3). We analysed cell proliferation during the regenerative outgrowth stage by immunohistochemistry using an antibody specific for proliferating cell nuclear antigen (PCNA). Zebrafish embryos from a *ptpn11a*$^{+/-}$ *ptpn11b*$^{-/-}$ in-cross were fixed at 1dpa or 2dpa and subjected to whole-mount immunohistochemistry for detection of PCNA expression. All zebrafish embryos were subsequently genotyped. By 2dpa, PCNA immunofluorescence was dispersed at the edge of the amputated caudal fin-fold of *ptpn11a*$^{-/-}$*ptpn11b*$^{-/-}$ zebrafish embryos, whereas in siblings that regenerated normally, PCNA immunofluorescence was concentrated between the amputation plane and the wound margin (**Fig. 4**). Because PCNA positive

cells were predominantly concentrated in the regenerating tissue in siblings, which was absent in *ptpn11a*$^{-/-}$*ptpn11b*$^{-/-}$ zebrafish embryos, quantification of PCNA staining was not meaningful. Nevertheless, from the representative images in **Fig. 4** it is evident that proliferation was severely arrested in *ptpn11a*$^{-/-}$*ptpn11b*$^{-/-}$ zebrafish embryos at 2dpa. PCNA immunofluorescence remained low in uncut controls (**Fig. S2**). At 1dpa PCNA immunofluorescence was found between the amputation plane and the wound margin at the edge of the caudal fin-fold of siblings, whereas PCNA immunofluorescence was less pronounced in the same region of Shp2 deficient zebrafish embryos (**Fig. S2**). These results indicate that proliferation is reduced in *ptpn11a*$^{-/-}$*ptpn11b*$^{-/-}$ zebrafish embryos compared to siblings in the regenerative outgrowth phase following caudal fin-fold amputation.

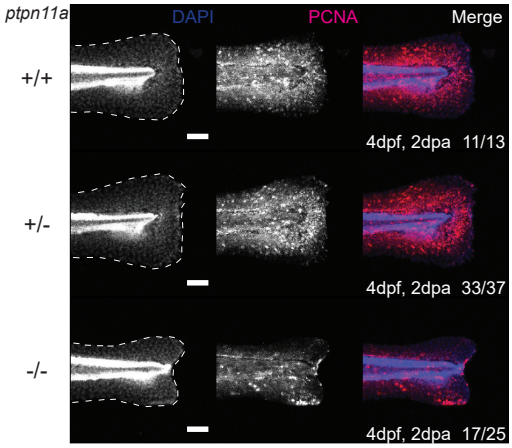

Fig. 4. Proliferation arrest at the amputated caudal fin-fold margin of Shp2 deficient embryos. At 2dpf the caudal fin-folds of embryos from a *ptpn11a*$^{+/-}$*ptpn11b*$^{-/-}$ in-cross were amputated and allowed to regenerate. Embryos were fixed at 2dpa (i.e. 4dpf, 2dpa) and subjected to whole-mount immunohistochemistry using an antibody specific for the cell proliferation marker PCNA (red). The embryos were counterstained with DAPI (blue). Maximum intensity projection images were taken of the caudal fin-folds and all embryos were genotyped. Representative images of amputated embryo caudal fin-folds are shown, and in the left panels the edge of the fin-fold is indicated with a dashed line. The number of embryos showing similar patterns/ total number of embryos analysed is indicated in the bottom right corner of the right panels. The scale bar represents 100µm. Representative pictures of equivalent uncut controls are depicted in **Fig. S2**.

Reduced MAPK signalling in zebrafish embryos deficient for Shp2

Loss of SHP2 in tissue culture cells or in knock-out mice results in reduced MAPK signalling, leading to reduced proliferation, differentiation, and developmental defects (22, 29, 30, 63–65). Furthermore, activated MAPK signalling following injury is asso-

ciated with regenerative competence across species (40, 41). To determine if loss of Shp2 affected MAPK signalling in *ptpn11a*$^{-/-}$*ptpn11b*$^{-/-}$ zebrafish embryos, we performed whole-mount immunohistochemistry using a phospho-MAPK-specific antibody (p-MAPK, phospho-p44/42 MAPK (Thr202/Tyr204)). In comparison to their siblings, *ptpn11a*$^{-/-}$*ptpn11b*$^{-/-}$ zebrafish embryos displayed significantly reduced p-MAPK levels following caudal fin-fold amputation at 4 dpf (2 dpa) as well as 3 dpf (1 dpa) (**Fig. 5, S3**). Note that p-MAPK levels were very low in the caudal fin-folds of uncut control zebrafish embryos (**Fig. S3**). These immunohistochemistry experiments indicate that MAPK signalling following caudal fin-fold amputation is reduced in zebrafish embryos lacking functional Shp2.

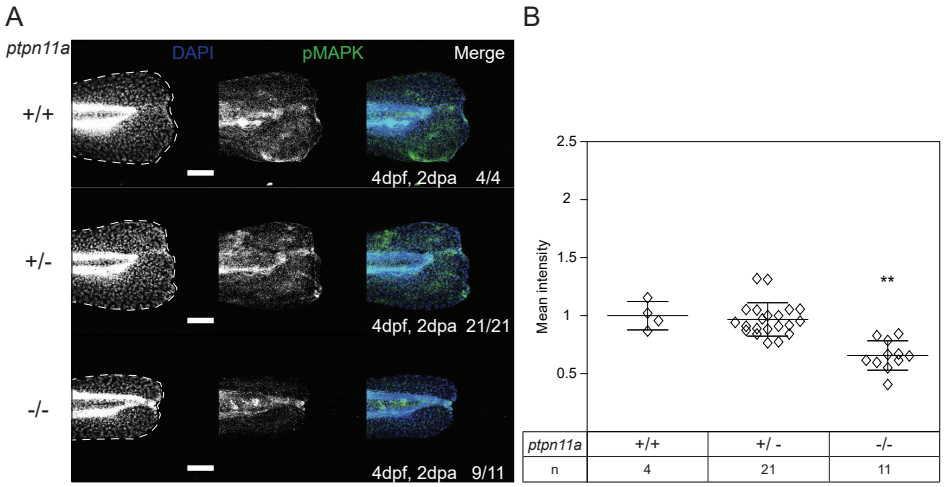

Fig. 5. Reduced p-MAPK in regenerating caudal fin-folds of Shp2 deficient embryos. At 2dpf the caudal fin-folds of embryos from a *ptpn11a*$^{+/-}$*ptpn11b*$^{-/-}$ in-cross were amputated and allowed to regenerate. Embryos were fixed at 2dpa (i.e. 4dpf, 2dpa) and subjected to whole-mount immunohistochemistry using a p-MAPK-specific antibody (Thr202/Tyr204) (green). The embryos were counterstained with DAPI (blue). Maximum intensity projection images were taken of the caudal fin-folds and all embryos were genotyped. (**A**) Representative images of amputated embryo caudal fin-folds are shown and in the left panels the edge of the fin-fold is indicated with a dashed line. The number of embryos showing similar patterns/ total number of embryos analysed is indicated in the bottom right corner of the right panels. The scale bar represents 100µm. (**B**) p-MAPK was quantified by mean intensity of the region between the notochord and the edge of the caudal fin-fold. Equivalent uncut controls were also quantified (representative pictures depicted in **Fig. S3**). Means within amputated groups are compared to *ptpn11a*$^{+/+}$*ptpn11b*$^{-/-}$ embryos using a Mann-Whitney U-test. Significance: ** $p<0.01$; error bars represent standard deviation.

Impaired caudal fin-fold regeneration and reduced cell proliferation by inhibition of MAPK signalling

To test if reduced MAPK signalling by itself is sufficient to inhibit zebrafish embryo caudal fin-fold regeneration, the caudal fin-folds of wild-type zebrafish embryos (*ptpn11a*$^{+/+}$*ptpn11b*$^{+/+}$) were amputated at 2dpf and allowed to regenerate for 3 days in the presence of 50nM MEK1 inhibitor PD184352 (also known as CI-1040) or solvent (1% DMSO) as a control. Treatment of zebrafish embryos with PD184352 significantly impaired caudal fin-fold regeneration (**Fig. 6A**). Uncut controls showed that PD184352 treatment by itself did not affect normal caudal fin-fold growth.

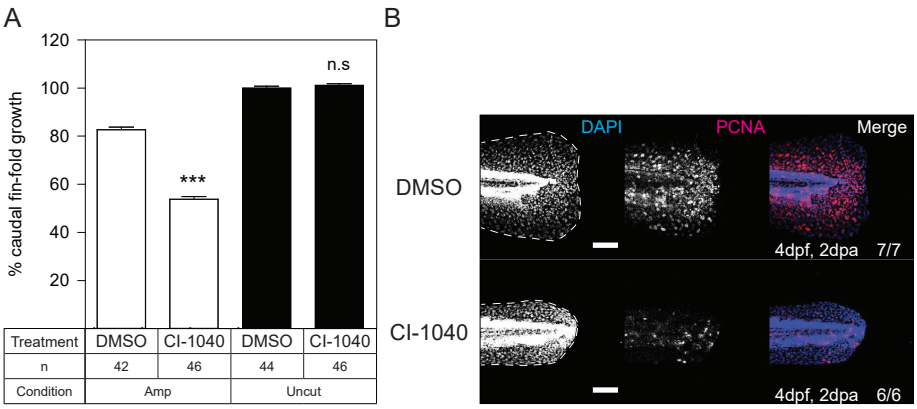

Fig. 6. Impaired regeneration and arrested cell proliferation by MAPK inhibition during caudal fin-fold regeneration. At 2dpf the caudal fin-folds of wild-type embryos were amputated and allowed to regenerate in the presence of 50nM PD184352 or 1% DMSO (solvent control). (**A**) Regeneration was quantified by measuring the distance from the tip of the notochord to the edge of the caudal fin-fold. The means of caudal fin-fold growth are depicted relative to caudal fin-fold growth of DMSO treated uncut controls. Mean of PD184352 treated amputated embryos is compared to DMSO treated amputated embryos using a Mann-Whitney U-test. The number of embryos is indicated (n). Significance: *** p<0.001; n.s. not significant; error bars indicate standard error of the mean. (**B**) Embryos were fixed at 2dpa (i.e. 4dpf, 2dpa) and subjected to whole-mount immunohistochemistry using an antibody specific for the cell proliferation marker PCNA (red). The embryos were counterstained with DAPI (blue). Maximum intensity projection images were taken of the caudal fin-folds. Representative images of amputated embryo caudal fin-folds are shown, and in the left panels the edge of the fin-fold is indicated with a dashed line. The number of embryos showing similar patterns/ total number of embryos analysed is indicated in the bottom right corner of the right panels. The scale bar represents 100µm. Representative pictures of equivalent uncut controls are depicted in **Fig. S4**.

We next investigated if the impaired regeneration of wild-type zebrafish embryos treated with PD184352 was associated with arrested cell proliferation by whole-mount immunohistochemistry for PCNA expression. At both 3dpf and 4dpf PCNA immunof-

luorescence was dispersed in zebrafish embryos treated with PD184352 compared to control zebrafish embryos treated with DMSO (**Fig. 6B, S4**). Baseline PCNA staining in the caudal fin-folds of uncut control zebrafish embryos at 3dpf and 4dpf was low, but also appeared to be reduced following PD184352 treatment (**Fig. S4**). These results demonstrate that MAPK signalling is required for normal caudal fin-fold regeneration and promotes proliferation during regenerative outgrowth.

DISCUSSION

Our results demonstrate a critical role for Shp2 in zebrafish embryo caudal fin-fold regeneration. Zebrafish embryos lacking functional Shp2 (*ptpn11a*$^{-/-}$*ptpn11b*$^{-/-}$) show severely impaired regeneration of their caudal fin-folds following amputation (**Fig. 1**). Expression of wild-type Shp2a (WT) rescues regeneration, which relies on its catalytic activity and SH2 domains (**Fig. 2**). Whilst blastema formation was normal in Shp2 deficient zebrafish embryos (**Fig. 3**), proliferation was arrested during the regenerative outgrowth phase (**Fig. 4**). We propose that the reduced p-MAPK levels in *ptpn11a*$^{-/-}$*ptpn11b*$^{-/-}$ zebrafish embryos (Fig. 5) cause impaired caudal fin-fold regeneration, which is consistent with our observation that regeneration is inhibited by MEK1 inhibition (**Fig. 6**).

As the catalytic activity of SHP2 is often paramount to regulating MAPK or PI3K signalling (14, 15), we first asked whether catalytic activity is required for zebrafish embryo caudal fin-fold regeneration. Caudal fin-fold regeneration was rescued by expressing wild-type Shp2a (WT), but not the catalytically inactive Shp2a R466M mutant (**Fig. 2A-B**), indicating that Shp2a catalytic activity is required for zebrafish embryo caudal fin-fold regeneration. As the Shp2a R466M mutant still retains functional SH2 domains, we exclude the possibility that the SH2 domains alone are sufficient for caudal fin-fold regeneration. In addition, caudal fin-fold regeneration was rescued by expressing the C-terminal domain mutant (YF), but not the SH2 domain mutant (SH), indicating that the SH2 domains are required for the function of Shp2a in zebrafish embryo caudal fin-fold regeneration, but that the two tyrosine phosphorylation sites, Y542 and Y580, in the C-terminus are not (**Fig. 2A-B**). Mutating R32 or R138 impairs the association of SHP2 with phosphorylated growth factor receptors and substrates (56), and has been shown to inhibit EGF stimulation of MAPK activation in cells (55). Thus, the inability of Shp2a-R32M-R138M to rescue caudal fin-fold regeneration suggests

that Shp2a requires recruitment or binding to a substrate for its function in caudal fin-fold regeneration. In comparison, mutating Y542 or Y580 prevents binding of SHP2 to GRB2, and reduces, but importantly does not abolish, the activation of MAPK in response to stimulation by some growth factors in tissue culture cells, suggesting that the SHP2-GRB2 interaction is dispensable in some contexts (14, 18, 58). We conclude that expression of Shp2a-Y542F-Y580F (YF) in *ptpn11a*$^{-/-}$*ptpn11b*$^{-/-}$ zebrafish embryos apparently mediated sufficient MAPK activation to rescue caudal fin-fold regeneration.

Following amputation, regeneration proceeds through wound healing, blastema formation, and then regenerative outgrowth to replace the lost tissue (1, 2). *Junbb* expression is maintained well into the initial stage of regenerative outgrowth (62), indicating that *junbb* is a definitive blastema marker. We show that the amputated caudal fin-folds of *ptpn11a*$^{-/-}$*ptpn11b*$^{-/-}$ zebrafish embryos express *junbb*, like their siblings (**Fig. 3**), indicating that both wound healing and blastema formation occur normally in the absence of Shp2. This appears to be in contrast with previous results showing that Fgfr1 signalling is required for blastema formation (43, 66). Whereas there are overlaps in FGFR1 and SHP2 signalling (45), apparently, Fgfr1 and Shp2a signalling in zebrafish differ to such an extent that blastema formation is dependent on Fgfr1, but not on Shp2. In addition to promoting MAPK signalling, SHP2 has been shown to promote or inhibit phosphoinositide 3-kinase (PI3K) signalling (10, 67). Interestingly, the symptoms that present *in vivo* as a result of loss of *ptpn11* or activating mutations of SHP2 (11) appear to be primarily due to the effect on MAPK signalling. For example, mice expressing the activating SHP2 mutant Q79R display MAPK hyperphosphorylation and congenital heart defects, whilst both these phenotypes are ameliorated in Q79R x *Erk1*$^{-/-}$ mice (68). In comparison, genetic ablation of PTPN11 in retinal cells results in reduced MAPK phosphorylation but does not affect AKT phosphorylation (64). The defects that result are also not rescued by mutating the antagonist of PI3K signalling, phosphatase and tensin homolog (PTEN), which normally increases PI3K signalling (23). However, hyper-active KRas, which has been shown to alleviate the requirement for SHP2 in the maintenance of hematopoietic stem cells (29), does rescue the retinal defects. As PI3K signalling has previously been shown to be required for blastema formation (38), and blastema formation was normal in zebrafish embryos lacking functional Shp2, we conclude that it is unlikely that Shp2 acts through PI3K signalling.

Regenerative outgrowth is characterized by proliferation and differentiation of cells to replace the lost tissue. Our results from whole-mount immunohistochemistry using

an antibody specific for PCNA, suggest that cell proliferation is arrested in the regenerating caudal fin-folds of *ptpn11a*$^{-/-}$*ptpn11b*$^{-/-}$ zebrafish embryos, compared to siblings (**Fig. 4, S2**). In addition, p-MAPK staining in *ptpn11a*$^{-/-}$*ptpn11b*$^{-/-}$ zebrafish embryos is reduced compared to siblings (**Fig. 5, S3**), suggesting the arrested proliferation is due to reduced MAPK signalling. Moreover, inhibiting MAPK signalling using an inhibitor of MEK1, upstream of MAPK, was sufficient to inhibit regeneration and arrest cell proliferation during caudal fin-fold regeneration (**Fig. 6, S4**). Our results are consistent with previous work demonstrating a requirement for Fgfr1 signalling in proliferation during zebrafish caudal fin regeneration (42, 44, 66), and reduced proliferation and regeneration in response to MEK1 inhibition during zebrafish heart regeneration (48). Recent work shows that loss of SHP2 in mice, resulting in reduced MAPK signalling and reduced proliferation, leads to impaired muscle regeneration, and this was attributed to satellite cell quiescence (69). Possibly, the loss of Shp2 in zebrafish embryo caudal fin-folds induces quiescence in dedifferentiated cells of the blastema. This would certainly be in concordance with our results showing that regenerative outgrowth was impaired, despite normal blastema formation. Collectively, our results suggest an essential role for Shp2a-MAPK signalling in promoting cell proliferation during the regenerative outgrowth phase of regenerating zebrafish embryo caudal fin-folds.

In conclusion, we demonstrate for the first time that Shp2 is required for embryonic zebrafish embryo caudal fin-fold regeneration. Loss of Shp2 inhibits zebrafish embryo caudal fin-fold regeneration associated with reduced proliferation and reduced MAPK phosphorylation. Rescue of regeneration by re-expression of Shp2a is dependent on the catalytic activity and the SH2 domains of Shp2a. Consistent with Shp2a promoting MAPK signalling, zebrafish embryo caudal fin-fold regeneration is inhibited by MEK1 inhibition, and is associated with reduced proliferation. Hence, our results suggest Shp2 is indispensable during zebrafish embryo caudal fin-fold regeneration, and is required to coordinate proper proliferation mediated by MAPK signalling during the regenerative outgrowth of the zebrafish embryo caudal fin-fold.

ACKNOWLEDGEMENTS

We thank Geert Geeven for batch processing the maximum intensity projections of all immunohistochemistry experiments.

REFERENCES

1. Pfefferli C, Jaźwińska A (2015) The art of fin regeneration in zebrafish. *Regeneration* 2(2):72–83.
2. Poss KD, Keating MT, Nechiporuk A (2003) Tales of regeneration in zebrafish. *Dev Dyn* 226(2):202–210.
3. Kawakami A, Fukazawa T, Takeda H (2004) Early fin primordia of zebrafish larvae regenerate by a similar growth control mechanism with adult regeneration. *Dev Dyn* 231(4):693–9.
4. Poleo G, Brown CW, Laforest L, Akimenko MA (2001) Cell proliferation and movement during early fin regeneration in zebrafish. *Dev Dyn* 221(4):380–390.
5. Padhi BK, et al. (2004) Screen for genes differentially expressed during regeneration of the zebrafish caudal fin. *Dev Dyn* 231(3):527–541.
6. Gemberling M, Bailey TJ, Hyde DR, Poss KD (2013) The zebrafish as a model for complex tissue regeneration. *Trends Genet* 5(13):113.
7. Bonetti M, et al. (2014) Distinct and overlapping functions of ptpn11 genes in zebrafish development. *PLoS One* 9(4):e94884.
8. Qu CK (2000) The SHP-2 tyrosine phosphatase: signaling mechanisms and biological functions. *Cell Res* 10(4):279–288.
9. Neel BG, Tonks NK (1997) Protein tyrosine phosphatases in signal transduction. *Curr Opin Cell Biol* 9(2):193–204.
10. Zhang SQ, et al. (2002) Receptor-specific regulation of phosphatidylinositol 3'-kinase activation by the protein tyrosine phosphatase Shp2. *Mol Cell Biol* 22(12):4062–4072.
11. Tajan MM, de Rocca Serra A, Valet P, Edouard T, Yart A (2015) SHP2 sails from physiology to pathology. *Eur J Med Genet* 58(10):509–525.
12. Hof P, Pluskey S, Dhe-Paganon S, Eck MJ, Shoelson SE (1998) Crystal structure of the tyrosine phosphatase SHP-2. *Cell* 92(4):441–450.
13. Kolmodin K, Aqvist J (2001) The catalytic mechanism of protein tyrosine phosphatases revisited. *FEBS Lett* 498(2–3):208–213.
14. Kontaridis MI, Liu X, Zhang L, Bennett AM (2002) Role of SHP-2 in fibroblast growth factor receptor-mediated suppression of myogenesis in C2C12 myoblasts. *Mol Cell Biol* 22(11):3875–3891.
15. Ivins Zito C, Kontaridis MI, Fornaro M, Feng G-S, Bennett AM (2004) SHP-2 regulates the phosphatidylinositide 3'-kinase/Akt pathway and suppresses caspase 3-mediated apoptosis. *J Cell Physiol* 199(2):227–236.
16. O'Reilly AM, Neel BG (1998) Structural Determinants of SHP-2 Function and Specificity in Xenopus Mesoderm Induction. *Mol Cell Biol* 18(1):161–177.
17. Stewart RA, et al. (2010) Phosphatase-dependent and -independent Functions of Shp2 in Neural Crest Cells Underlie LEOPARD Syndrome Pathogenesis. *Dev Cell* 18(5):750–762.
18. Araki T, Nawa H, Neel BG (2003) Tyrosyl phosphorylation of Shp2 is required for normal ERK activation in response to some, but not all, growth factors. *J Biol Chem* 278(43):41677–84.
19. Lu W, Gong D, Bar-Sagi D, Cole PA (2017) Site-Specific Incorporation of a Phosphotyrosine Mimetic Reveals a Role for Tyrosine Phosphorylation of SHP-2 in Cell Signaling. *Mol Cell* 8(4):759–769.
20. Sun J, et al. (2013) Antagonism between binding site affinity and conformational dynamics tunes alternative cis-interactions within Shp2. *Nat Commun* 4:2037.

21. Cunnick JM, Dorsey JF, Munoz-Antonia T, Mei L, Wu J (2000) Requirement of SHP2 binding to Grb2-associated binder-1 for mitogen-activated protein kinase activation in response to lysophosphatidic acid and epidermal growth factor. *J Biol Chem* 275(18):13842–13848.
22. Zhang W, Liu HT, Tu LIU H (2002) MAPK signal pathways in the regulation of cell proliferation in mammalian cells. *Cell Res* 12(1):9–18.
23. Vara JÁF, et al. (2004) PI3K/Akt signalling pathway and cancer. *Cancer Treat Rev* 30(2):193–204.
24. Zhu Y, et al. (2010) Control of oligodendrocyte generation and proliferation by Shp2 protein tyrosine phosphatase. *Glia* 58(12):1407–1414.
25. Aceto N, et al. (2012) Tyrosine phosphatase SHP2 promotes breast cancer progression and maintains tumor-initiating cells via activation of key transcription factors and a positive feedback signaling loop. *Nat Med* 18(4):529–537.
26. Inagaki K, et al. (2000) Roles for the protein tyrosine phosphatase SHP-2 in cytoskeletal organization, cell adhesion and cell migration revealed by overexpression of a dominant negative mutant. *Oncogene* 19(1):75–84.
27. Mañes S, et al. (1999) Concerted Activity of Tyrosine Phosphatase SHP-2 and Focal Adhesion Kinase in Regulation of Cell Motility. *Mol Cell Biol* 19(4):3125–3135.
28. Hartman ZR, Schaller MD, Agazie YM (2013) The tyrosine phosphatase SHP2 regulates focal adhesion kinase to promote EGF-induced lamellipodia persistence and cell migration. *Mol Cancer Res* 11(6):651–64.
29. Chan G, et al. (2011) Essential role for Ptpn11 in survival of hematopoietic stem and progenitor cells. *Blood* 117(16):4253–4261.
30. Ke Y, et al. (2007) Deletion of Shp2 in the brain leads to defective proliferation and differentiation in neural stem cells and early postnatal lethality. *Mol Cell Biol* 27(19):6706–17.
31. Yang W, et al. (2006) An Shp2/SFK/Ras/Erk Signaling Pathway Controls Trophoblast Stem Cell Survival. *Dev Cell* 10(3):317–327.
32. Heuberger J, et al. (2014) Shp2/MAPK signaling controls goblet/paneth cell fate decisions in the intestine. *Proc Natl Acad Sci* 111(9):3472–3477.
33. Tang TL, Freeman RM, O'Reilly AM, Neel BG, Sokol SY (1995) The SH2-containing protein-tyrosine phosphatase SH-PTP2 is required upstream of MAP kinase for early xenopus development. *Cell* 80(3):473–483.
34. Saxton TM, et al. (1997) Abnormal mesoderm patterning in mouse embryos mutant for the SH2 tyrosine phosphatase Shp-2. *EMBO J* 16(9):2352–2364.
35. Krens SFG, Spaink HP, Snaar-Jagalska BE (2006) Functions of the MAPK family in vertebrate-development. *FEBS Lett* 580(21):4984–4990.
36. Faucherre a, Taylor GS, Overvoorde J, Dixon JE, Hertog J Den (2008) Zebrafish pten genes have overlapping and non-redundant functions in tumorigenesis and embryonic development. *Oncogene* 27(8):1079–1086.
37. Cristofano AD, et al. (1998) Pten is essential for embryonic development and tumour suppression. *Nat Genet* 19(4):348–355.
38. Nakatani Y, Nishidate M, Fujita M, Kawakami A, Kudo A (2008) Migration of mesenchymal cell fated to blastema is necessary for fish fin regeneration. *Dev Growth Differ* 50(2):71–83.
39. Münch J, González-Rajal A, de la Pompa JL (2013) Notch regulates blastema proliferation and prevents differentiation during adult zebrafish fin regeneration. *Development* 140(7):1402–11.
40. Yun MH, Gates PB, Brockes JP (2014) Sustained ERK activation underlies reprogramming in regeneration-competent salamander cells and distinguishes them from their mammalian counterparts. *Stem Cell Reports* 3(1):15–23.

41. Itou J, Kawakami H, Burgoyne T, Kawakami Y (2012) Life-long preservation of the regenerative capacity in the fin and heart in zebrafish. *Biol Open* 1(8):739–746.
42. Wills AA, Kidd AR, Lepilina A, Poss KD (2008) Fgfs control homeostatic regeneration in adult zebrafish fins. *Development* 135(18):3063–3070.
43. Poss KD, et al. (2000) Roles for Fgf signaling during zebrafish fin regeneration. *Dev Biol* 222(2):347–58.
44. Lee Y, Grill S, Sanchez A, Murphy-Ryan M, Poss KD (2005) Fgf signaling instructs position-dependent growth rate during zebrafish fin regeneration. *Development* 132(23):5173–83.
45. Ornitz DM, Itoh N (2015) The Fibroblast Growth Factor signaling pathway. *Wiley Interdiscip Rev Dev Biol* 4(3):215–266.
46. Rojas-Muñoz A, et al. (2009) ErbB2 and ErbB3 regulate amputation-induced proliferation and migration during vertebrate regeneration. *Dev Biol* 327(1):177–190.
47. Oda K, Matsuoka Y, Funahashi A, Kitano H (2005) A comprehensive pathway map of epidermal growth factor receptor signaling. *Mol Syst Biol* 1:2005.0010-2005.0010.
48. Liu P, Zhong TP (2017) MAPK/ERK signalling is required for zebrafish cardiac regeneration. *Biotechnol Lett*. doi:10.1007/s10529-017-2327-0.
49. Westerfield M (2000) *The zebrafish book. A guide for the laboratory use of zebrafish (Danio rerio)* (University of Oregon Press, Eugene). 4th Ed.
50. Ryan MD, King AMQ, Thomas GP (1991) Cleavage of foot-and-mouth disease virus polyprotein is mediated by residues located within a 19 amino acid sequence. *J Gen Virol* 72(11):2727–2732.
51. Bonetti M, et al. (2014) Noonan and LEOPARD syndrome Shp2 variants induce heart displacement defects in zebrafish. *Development* 141:1961–70.
52. Stumpf M, Den Hertog J (2016) Differential requirement for pten lipid and protein phosphatase activity during zebrafish embryonic development. *PLoS One* 11(2):e0148508.
53. Hale AJ, den Hertog J (2016) Studying Protein-Tyrosine Phosphatases in Zebrafish. *Protein Tyrosine Phosphatases: Methods and Protocols*, ed Pulido R (Springer New York, New York, NY), pp 351–372.
54. Thisse C, Thisse B, Schilling TF, Postlethwait JH (1993) Structure of the zebrafish snail1 gene and its expression in wild-type, spadetail and no tail mutant embryos. *Development* 119(4):1203–1215.
55. Buonato JM, Lan IS, Lazzara MJ (2015) EGF augments TGFβ-induced epithelial-mesenchymal transition by promoting SHP2 binding to GAB1. *J Cell Sci* 6393(September):3898–3909.
56. Müller PJ, et al. (2013) Protein tyrosine phosphatase SHP2/PTPN11 mistargeting as a consequence of SH2-domain point mutations associated with Noonan Syndrome and leukemia. *J Proteomics* 84:132–147.
57. Neel BG, Gu H, Pao L (2003) The "Shp"ing news: SH2 domain-containing tyrosine phosphatases in cell signaling. *Trends Biochem Sci* 28(6):284–293.
58. Yasui N, et al. (2014) Directed network wiring identifies a key protein interaction in embryonic stem cell differentiation. *Mol Cell* 54(6):1034–1041.
59. Kolli S, Zito CI, Mossink MH, Wiemer EAC, Bennett AM (2004) The major vault protein is a novel substrate for the tyrosine phosphatase SHP-2 and scaffold protein in epidermal growth factor signaling. *J Biol Chem* 279(28):29374–29385.
60. Bunda S, et al. (2015) Inhibition of SHP2-mediated dephosphorylation of Ras suppresses oncogenesis. *Nat Commun* 6:8859.
61. Yoshinari N, Ishida T, Kudo A, Kawakami A (2009) Gene expression and functional analysis of zebrafish larval fin fold regeneration. *Dev Biol* 325(1):71–81.

62. Ishida T, Nakajima T, Kudo A, Kawakami A (2010) Phosphorylation of Junb family proteins by the Jun N-terminal kinase supports tissue regeneration in zebrafish. *Dev Biol* 340(2):468–479.

63. Yang W, et al. (2006) an shp2-erk signaling pathwy controls trophoblast stem cell survival. *Dev Cell* 10:317–327.

64. Cai Z, et al. (2011) Loss of Shp2-mediated mitogen-activated protein kinase signaling in Muller glial cells results in retinal degeneration. *Mol Cell Biol* 31(14):2973–83.

65. Zhang SQ, et al. (2004) Shp2 Regulates Src Family Kinase Activity and Ras/Erk Activation by Controlling Csk Recruitment. *Mol Cell* 13(3):341–355.

66. Shibata E, et al. (2016) Fgf signalling controls diverse aspects of fin regeneration. *Development* 143(16):2920 LP-2929.

67. Wu CJ, et al. (2001) The tyrosine phosphatase SHP-2 is required for mediating phosphatidylinositol 3-kinase/Akt activation by growth factors. *Oncogene* 20(42):6018–6025.

68. Nakamura T, et al. (2007) Mediating ERK1 / 2 signaling rescues congenital heart defects in a mouse model of Noonan syndrome. *J Clin Invest* 117(8):2–11.

69. Griger J, et al. (2017) Loss of Ptpn11 (Shp2) drives satellite cells into quiescence. *Elife* 6:e21552.

SUPPORTING INFORMATION

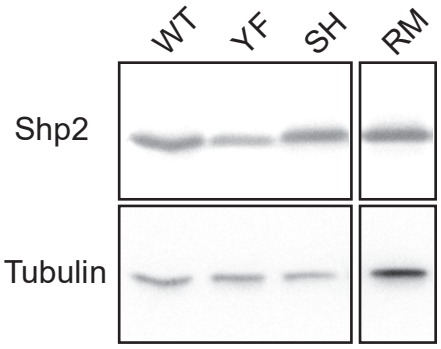

Fig. S1. Similar expression levels of *ptpn11a* mutants. Human embryonic kidney 293 T cells were transfected with CMV-promoter driven expression vector for zebrafish Shp2 mutants: Shp2a wild-type (WT); Shp2a Y542F, Y580F (YF); Shp2a R32M, R138M (SH); or Shp2a R466M (RM). Cells were lysed and the lysates run on an SDS-PAGE gel. Blots were probed using a SHP2-specific antibody and developed using enhanced chemiluminescence. Blots were stripped and re-probed for Tubulin as a loading control. All samples were loaded on the same blot, samples between SH and RM were removed as they were not relevant.

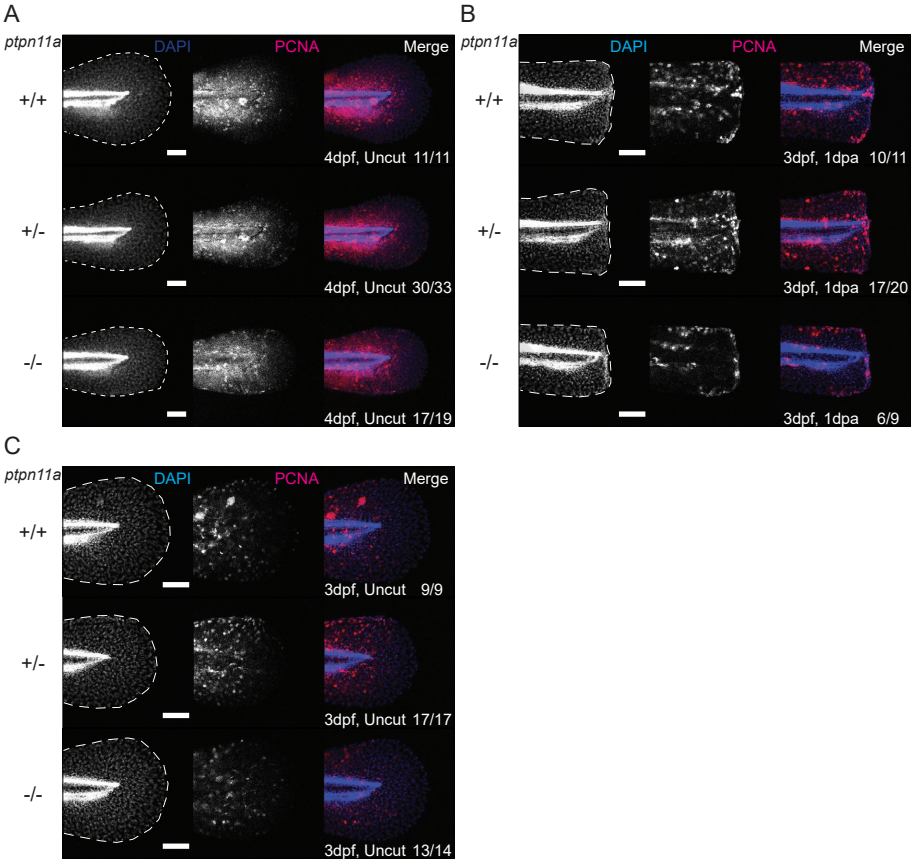

Fig. S2. Normal proliferation in uncut caudal fin-folds of Shp2 deficient embryos. Uncut embryos from a *ptpn11a*$^{+/-}$*ptpn11b*$^{-/-}$ in-cross were fixed at 4dpf (4dpf, uncut) in parallel to the embryos depicted in **Fig. 4** (**A**). At 2dpf the caudal fin-fold of embryos from a *ptpn11a*$^{+/-}$*ptpn11b*$^{-/-}$ in-cross was amputated and allowed to regenerate. Embryos were fixed at 1dpa (i.e. 3dpf, 1dpa) (**B**), or equivalent for uncut controls (3dpf, uncut) (**C**). Embryos were subjected to whole-mount immunohistochemistry using an antibody specific for the cell proliferation marker PCNA (red). The embryos were counterstained with DAPI (blue). Maximum intensity projection images were taken of the caudal fin-folds and all embryos were genotyped. Representative images of embryo caudal fin-folds are shown, and in the left panels the edge of the fin-fold is indicated with a dashed line. The number of embryos showing similar patterns/ total number of embryos analysed is indicated in the bottom right corner of the right panels. The scale bar represents 100µm.

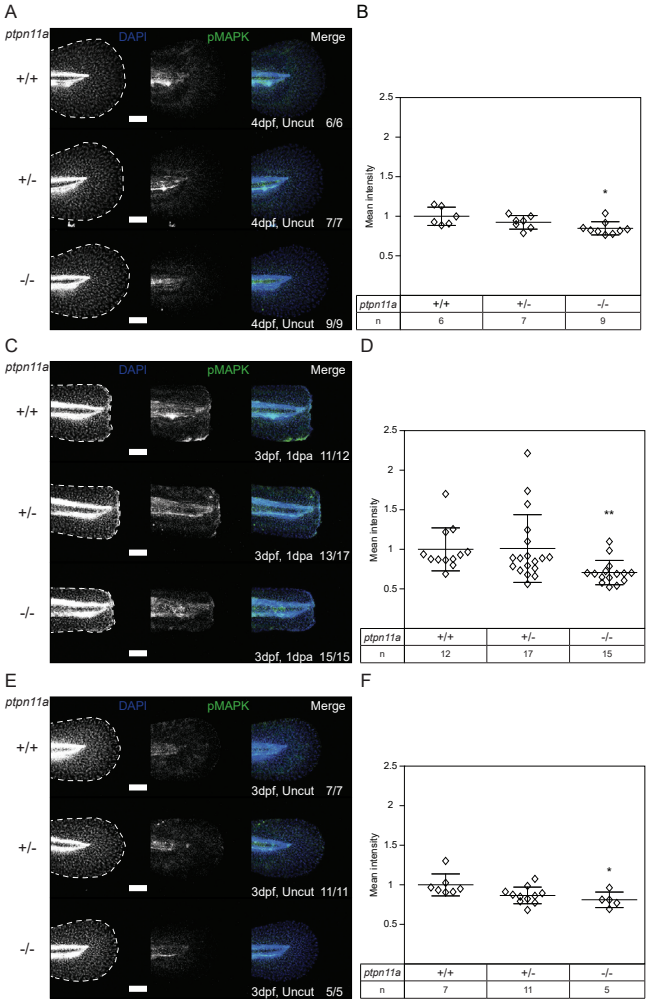

Fig. S3. Reduced p-MAPK in the caudal fin-folds of Shp2 deficient embryos. Uncut embryos from a *ptpn11a*$^{+/-}$*ptpn11b*$^{-/-}$ in-cross were fixed at 4dpf (4dpf, uncut) in parallel to the embryos depicted in **Fig. 5A** (**A**, **B**). At 2dpf the caudal fin-fold of embryos from a *ptpn11a*$^{+/-}$*ptpn11b*$^{-/-}$ in-cross was amputated and allowed to regenerate. Embryos were fixed at 1dpa (i.e. 3dpf, 1dpa) (**C**, **D**), or equivalent for uncut controls (3dpf, uncut) (**E**, **F**). Embryos were subjected to whole-mount immunohistochemistry using a p-MAPK-specific antibody (Thr202/Tyr204) (green). The embryos were counterstained with DAPI (blue). Maximum intensity projection images were taken of the caudal fin-folds and all embryos were genotyped. Representative images of embryo caudal fin-folds are shown, and in the left panels the edge of the fin-fold is indicated with a dashed line. The number of embryos showing similar patterns/ total number of embryos analysed is indicated in the bottom right corner of the right panels. The scale bar represents 100µm. p-MAPK immunofluorescence was quantified by mean intensity of the region between the notochord and the edge of the caudal fin-fold. Means within amputated or uncut groups are compared to *ptpn11a*$^{+/+}$*ptpn11b*$^{-/-}$ embryos using a Mann-Whitney U-test. The number of embryos analysed is indicated (n). Significance: ** $p<0.01$; * $p<0.05$; error bars represent standard deviation (**D**). Quantification of p-MAPK immunofluorescence at 4dpf, 2dpa is depicted in **Fig. 5B**.

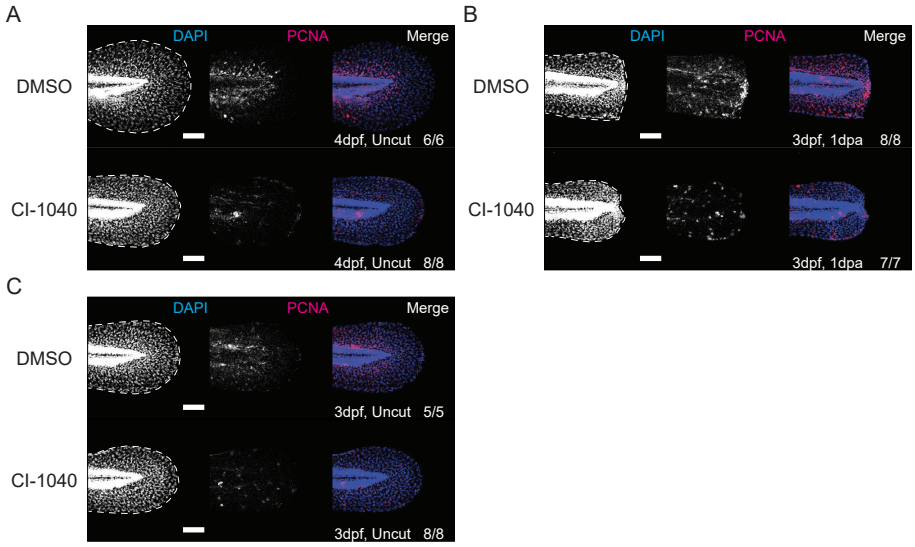

Fig. S4. Arrested proliferation in the caudal fin-folds of wild-type embryos following MAPK inhibition. Uncut wild-type embryos treated with 50nM PD184352 (CI-1040) were fixed at 4dpf (4dpf, uncut) in parallel to the embryos depicted in **Fig. 6A** (**A**). At 2dpf the caudal fin-fold of wild-type embryos was amputated and allowed to regenerate whilst incubated with 50nM PD184352 (CI-1040). Embryos were fixed at 1dpa (i.e. 3dpf, 1dpa) (**B**), or equivalent for uncut controls (3dpf, uncut) (**C**). Embryos were subjected to whole-mount immunohistochemistry using an antibody specific for the cell proliferation marker PCNA (red). The embryos were counterstained with DAPI (blue). Maximum intensity projection images were taken of the caudal fin-folds. Representative images of embryo caudal fin-folds are shown, and in the left panels the edge of the fin-fold is indicated with a dashed line. The number of embryos showing similar patterns/ total number of embryos analysed is indicated in the bottom right corner of the right panels. The scale bar represents 100µm. PCNA immunofluorescence at 4dpf, 2dpa is depicted in **Fig. 6B**.

Table S1. Primers used for amplifying *junbb* from zebrafish embryo cDNA, and *ptpn11a* from genomic zebrafish DNA.

Primer	Sequence
junbb FWD 1	TGGGTTACGGTCACAACGAC
junbb REV 1	CAGTGTCCGTTCTCTTCCGT
BamHI-*junbb* FWD (nested)	ATAGGATCCTACACGACGCTGAACGCATA
junbb-EcoRI REV (nested)	CTCGAATTCGTGTCCGTTCTCTTCCGTCC
junbb FWD 2	TACACGACGCTGAACGCATA
junbb-T7 REV 2	TAATACGACTCACTATAGGTGTCCGTTCTCTTCCGTCC
Ptpn11a WT FWD	GAAGGTGACCAAGTTCATGCTACATGGAGCATCATGGAC
Ptpn11a KO FWD	GAAGGTCGGAGTCAACGGATTACATGGAGCATCATGGAT
Ptpn11a REV	AGCTCAATGACGTCTCCGTTTTTCTCTTT
Ptpn11a FWD 1	GCGCTGTCACACACATTAAGA
Ptpn11a REV 2	TCACAGCCAATAAAGAGAAGC
Ptpn11a FWD (nested) 3	CGACCTGTATGGTGGAGAGAA
Ptpn11a REV (nested) 4	TCCCAAATTGTCATGTAAGG

Chapter 7

The Function of Shp2a during Zebrafish Embryo Caudal Fin-Fold Regeneration is Independent from the Level of Shp2a Catalytic Activity

Alexander James Hale[1,2], Jelmer Hoeksma[1], and Jeroen den Hertog[1,2]

1. Hubrecht Institute – KNAW and University Medical Center Utrecht, Utrecht, the Netherlands
2. Institute Biology Leiden, Leiden University, Leiden, The Netherlands

ABSTRACT

The production of reactive oxygen species (ROS) directly following amputation of the zebrafish embryo caudal fin-fold is essential for proper caudal fin-fold regeneration. Protein-tyrosine phosphatases (PTPs) are enzymes that dephosphorylate phosphotyrosine through a mechanism involving a catalytic cysteine, and are susceptible to reversible inactivation by ROS. Although Src homology 2 domain containing phosphatase Shp2a is oxidized following zebrafish caudal fin amputation, the catalytic activity of Shp2a is required for caudal fin-fold regeneration. Here, we show that mutation of the back-door cysteines C334 and C368 of Shp2a, which are proposed to protect the catalytic cysteine from irreversible oxidation, reduced the catalytic activity of Shp2a and enhanced the susceptibility of Shp2a to oxidation. Surprisingly, expression of these back-door cysteine mutants in *ptpn11a*$^{-/-}$*ptpn11b*$^{-/-}$ zebrafish embryos, which lack functional Shp2, rescued caudal fin-fold regeneration. As the back-door cysteine mutants of Shp2a demonstrated reduced catalytic activity, we investigated the level of Shp2a catalytic activity required for its function in zebrafish embryo caudal fin-fold regeneration by using two mutants of Shp2a, Shp2a-D61G and Shp2a-A462T, which have increased and reduced catalytic activity respectively. Interestingly, expression of Shp2a-D61G or Shp2a-A462T in *ptpn11a*$^{-/-}$*ptpn11b*$^{-/-}$ zebrafish embryos rescued caudal fin-fold regeneration to a similar extent. Collectively, our results suggest that the level of Shp2a catalytic activity does not affect the function of Shp2a in the regenerative outgrowth of the zebrafish embryo caudal fin-fold.

INTRODUCTION

Protein tyrosine phosphorylation is at the core of many essential signalling cascades, and the balance between the activity of protein tyrosine kinases and protein tyrosine phosphatases (PTPs) allows for an appropriate cellular response to stimuli (Hunter 2009). In humans, the PTP superfamily consists of 116 cysteine-based enzymes divided into three subgroups based on their structure and function: the classical PTPs, dual-specificity PTPs, and the low molecular weight PTPs (Alonso and Pulido 2016; Tonks 2013). Catalysis by all cysteine-based PTPs is mediated by a conserved cysteine in the PTP domain. The catalytic cysteine residues of PTPs are in the thiolate anion form due to a low pKa, which results from their microenvironment. Reactive oxygen species (ROS), such as H_2O_2, readily reversibly oxidize cysteine residues that are in the thiolate anion form, temporarily inactivating the catalytic activity of the PTP (Ostman et al. 2011). Mild oxidation results in conversion of the sulphur atom of the catalytic cysteine from its reduced thiolate anion form (S^-) to sulphenic acid (SOH), a labile state that rapidly rearranges to form an intra- or inter-molecular disulphide bond with a nearby cysteine or a sulphenylamide with an adjacent nitrogen (Salmeen et al. 2003). In the case of an intramolecular disulphide bond, the nearby cysteine is referred to as a "back-door cysteine" (Cumming et al. 2004; Sone et al. 1997). Rather unusually, the Src homology 2 (SH2) domain containing phosphatases SHP1 and SHP2 appear to have two back-door cysteines. Under oxidizing conditions, the catalytic cysteine is oxidized and forms a disulphide bond with one of the two back-door cysteines. However, the disulphide bond between the catalytic cysteine and one of the back-door cysteines is rapidly re-reduced, and the two backdoor cysteines form an intramolecular disulphide bond with each other to stabilize the protein under oxidizing conditions (Chen, Willard, and Rudolph 2009). The disulphide and sulphenylamide bonds are otherwise readily reduced to the catalytically active form of the PTP by endogenous glutathione and thioredoxin systems (Dagnell et al. 2013; Lee et al. 2002; Ostman et al. 2011). However, in extreme oxidizing conditions the PTPs can be hyperoxidized to form irreversible sulphinic acid (SO_2H) or sulphonic acid (SO_3H) states, permanently inactivating the PTP (Lo Conte and Carroll 2013a, 2013b).

The classical cytoplasmic PTP SHP2, encoded by the *PTPN11* gene, has two SH2 domains, a PTP domain, and a C-terminal domain (Hof et al. 1998), and is readily oxidized by ROS (Karisch et al. 2011; Meng, Fukada, and Tonks 2002). The catalytic cysteine, C459, in the PTP domain is essential for catalytic activity, and mutation to

a serine results in an inactive substrate-trapping mutant of SHP2 (Hartman, Schaller, and Agazie 2013; Kolli et al. 2004; Zhang et al. 2004). In addition, the neighbouring arginine, R465, is required for substrate binding and stabilizing the phospho-cysteine intermediate during the catalytic process (Zhang, Wang, and Dixon 1994). The crystal structure of SHP2 shows that SHP2 is in a closed conformation with the N-terminal SH2 domain folding back onto itself and interacting with residues close to the catalytic pocket. In this closed conformation, access of substrates to the catalytic site is blocked, impairing catalytic activity (Hof et al. 1998). Activation of SHP2 is facilitated by dissociation of the SH2 domains from the PTP domain, for instance by binding of the SH2 domains to phospho-tyrosine containing proteins, engendering an open conformation of SHP2, which is able to dephosphorylate its target substrates (Neel, Gu, and Pao 2003). Mutation of some key residues, such as D61 in the N-terminal SH2 domain, also results in an open conformation of SHP2 and increased catalytic activity (Darian et al. 2011). In comparison, mutations of residues close to the catalytic cysteine C459, such as R465 or A461 in the PTP domain, result in reduced catalytic activity (Keilhack et al. 2005; Stewart et al. 2010; Yu et al. 2013).

SHP2 is activated in response to growth factor stimulation, and mediates transduction of mitogen activated kinase (MAPK) and phosphatidylinositide-3-kinase (PI3K) signalling (Wu et al. 2001; Zhang, Liu, and Tu LIU 2002). SHP2 regulates a variety of cellular processes, including adipogenesis (He et al. 2013; Tao et al. 2016), haematopoiesis (Chan et al. 2011; Qu et al. 1997), and embryonic development (Bonetti, Rodriguez-Martinez, et al. 2014; Yang et al. 2006), and is mutated in a variety of human diseases (Hendriks et al. 2013). Notably, the activating D61G mutation is commonly found in patients with Noonan Syndrome (NS), whilst the inactivating A461T mutation is commonly found in patients with Noonan Syndrome with Multiple Lentigines (NSML, formerly LEOPARD syndrome). Both mutations result in aberrant MAPK signalling, leading to developmental defects (Araki et al. 2004; Jopling, van Geemen, and den Hertog 2007; Lauriol, Jaffre, and Kontaridis 2015).

ROS are able to coordinate signal transduction in multiple signalling pathways and thereby modulate cellular responses (Finkel 2011; Ray, Huang, and Tsuji 2012; Thannickal and Fanburg 2000). Moreover, ROS regulation of the activity of PTPs is evident in a variety of contexts: VE-PTP and PTP-PEST in endothelial cell migration (Frijhoff et al. 2014); PTP1B and TC-PTP in type 2 diabetes mellitus (Gurzov et al. 2014; Meng et al. 2004); and oxidation of various PTPs in cancer (Karisch et al. 2011; Liou and Storz 2010). SHP2 is oxidized following platelet derived growth factor (PDGF) stimulation,

promoting PDGF receptor signalling (Meng et al. 2002). In addition, SHP2 is associated with the linker of activated T-cells (LAT) at the plasma membrane through its SH2 domains, where it dephosphorylates associated proteins, adhesion and degranulation-promoting adapter protein (ADAP) and Vav1, to prevent T-cell adhesion. Activation of the T-cell receptor stimulates ROS production, inactivating SHP2 and enabling T-cell adhesion (Kwon et al. 2005). Therefore, SHP2 oxidation, which inactivates SHP2, appears to be induced by extracellular stimuli to promote cellular signalling and cellular responses.

Immediately following zebrafish embryo caudal fin-fold amputation, a burst of H_2O_2 emanates from the wound margin and extends into the tissue (Niethammer et al. 2009). The zebrafish genome contains two *ptpn11* genes, *ptpn11a* and *ptpn11b*, encoding Shp2a and Shp2b, respectively. Although both Shp2a and Shp2b are highly homologous to human SHP2 and harbour catalytic activity, they differ in their expression during early embryonic development, resulting in Shp2b being dispensable. Furthermore, the key residues discussed above are conserved in Shp2a (**Fig. 1A**). Whilst *ptpn11a*$^{+/+}$*ptpn11b*$^{-/-}$ and *ptpn11a*$^{+/-}$*ptpn11b*$^{-/-}$ zebrafish are viable and fertile, *ptpn11a*$^{-/-}$*ptpn11b*$^{-/-}$ double knock-out zebrafish are embryonically lethal from 5-7 days post fertilization (dpf) onwards (Bonetti, Rodriguez-Martinez, et al. 2014). The oxidation of Shp2a following caudal fin amputation (demonstrated in Chapter 5), and the requirement for a catalytically active signalling function of Shp2a during caudal fin-fold regeneration (demonstrated in Chapter 6) presents an apparent conundrum. Presumably, oxidation of Shp2a is transient and, following a lag-time, Shp2a becomes active again and exerts its essential function.

To investigate the role of Shp2a oxidation during zebrafish embryo caudal fin-fold regeneration further, we mutated the back-door cysteines of zebrafish Shp2a, C334 and C368, to a serine. We show that the catalytic activity of the back-door cysteine mutants of Shp2a, Shp2a-C334S, Shp2a C368S, and the double mutant Shp2a-C334S-C368S (2CS), *in vitro* was greatly reduced. Furthermore, immunoprecipitation of Shp2a following H_2O_2 treatment of cultured cells revealed increased reversible and irreversible oxidation of the back-door cysteine mutants of Shp2a, suggesting these mutants of Shp2a have enhanced susceptibility to oxidation. Surprisingly, expressing the back-door cysteine mutants of Shp2a in *ptpn11a*$^{-/-}$*ptpn11b*$^{-/-}$ zebrafish embryos, which normally do not regenerate their caudal fin-folds, rescued caudal fin-fold regeneration. To investigate to what extent catalytic activity of Shp2a was required for its function in caudal fin-fold regeneration, we used catalytic mutants of Shp2a with

increased (D61G) or reduced (A462T) catalytic activity. Expression of Shp2a-D61G or Shp2a-A462T rescued caudal fin-fold regeneration in *ptpn11a*$^{-/-}$*ptpn11b*$^{-/-}$ zebrafish embryos with similar efficiency, whereas catalytically inactive Shp2a-R466M did not. Collectively, our results suggest that the level of Shp2a catalytic activity does not affect its function in the regenerative outgrowth of the zebrafish embryo caudal fin-fold.

RESULTS

Back-door cysteine mutants of Shp2a have reduced catalytic activity

Mutation of the back-door cysteines in SHP1, which is highly similar to SHP2 (Pao et al. 2007), leads to irreversible oxidation of the catalytic cysteine, and mutation of C334 and C368 in Shp2a will likely have the same effect (Chen et al. 2009). We therefore created cysteine to serine mutations in either, or both, of the back-door cysteines of full-length zebrafish Shp2a, C334 and C368. N-terminal glutathione-S-transferase (GST) tagged constructs, encoding GST-Shp2a-C334S, GST-Shp2a-C368S, or GST-Shp2a-C334S-C368S (2CS), were expressed in *E. coli* bacteria and purified. We tested the catalytic activity of these zebrafish Shp2a mutant proteins in *in vitro* phosphatase assays, under reducing conditions, using para-nitrophenylphosphate (pNPP) as a chromogenic substrate. The absorbance measurements in *in vitro* phosphatase assays indicated that mutating the back-door cysteines of Shp2a reduced catalytic activity (**Fig. 1B**). Mutation of C334 or C368 reduced catalytic activity to ~50% or ~30% of wild-type GST-Shp2a (WT), respectively. The catalytic activity of the double back-door cysteine mutant of Shp2a, GST-Shp2a-2CS, was reduced to only ~20% of wild-type GST-Shp2a.

Considering the reduced activity of the back-door cysteine mutants of Shp2a, we decided to include several mutants in our study: in SHP2, the D61G mutation in the N-terminal SH2 domain results in enhanced catalytic activity, whereas the A461T mutation in the PTP domain results in reduced catalytic activity (Keilhack et al. 2005). We mutated the conserved residues in zebrafish Shp2a, D61 and A462, and tested the catalytic activity of the mutant Shp2a proteins in *in vitro* phosphatase assays under reducing conditions. As expected, the D61G mutation enhanced catalytic activity approximately 4-fold, whereas the A462T mutation reduced catalytic activity approximately 5-fold, compared to wild-type GST-Shp2a (**Fig. 1C**).

As a negative control, we included a mutant where the conserved arginine (R466 in zebrafish Shp2a) is mutated, which abolishes catalytic activity (Stewart et al. 2010).

To confirm that the R466M mutant of Shp2a has no catalytic activity, we introduced the R466M mutation in GST-Shp2a-D61G. Indeed, compared to GST-Shp2a-D61G, GST-Shp2a-D61G-R466M (RM) showed no detectable catalytic activity (**Fig. 1D**).

To exclude the possibility that the differences in catalytic activity between the different Shp2a mutants measured in *in vitro* phosphatase assays were due to differences in concentration of the purified proteins, we resolved the purified proteins on a SDS-PAGE gel. All GST-Shp2a proteins were purified and diluted to similar concentrations (**Fig. 1E**), indicating that the differences in catalytic activity were specifically due to the mutations that were introduced. Collectively, these results indicate that the catalytic activity of zebrafish Shp2a is disrupted by mutation of the back-door cysteines C334 and C368. Furthermore, as expected, mutation of D61G and A462T results in increased and reduced catalytic activity respectively, whereas mutation of R466 abolishes catalytic activity.

Back-door cysteine mutants of Shp2 are more sensitive to oxidation

Reversibly oxidized PTPs can be detected by lysing cells in the presence of iodoacetic acid (IAA), which alkylates all reduced cysteines, followed by reduction of the reversibly oxidized catalytic cysteines using dithiothreitol (DTT), and hyperoxidation using pervanadate (effectively shifting SOH to SO_3H). As the reduced catalytic cysteines are blocked by IAA, only the catalytic cysteines that were oxidized at the time of lysis (i.e. by H_2O_2 treatment) will be detected using an antibody specific for the sulphonic acid (SO_3H) state of PTPs (ox-PTP) (Persson et al. 2004, 2005). To address whether the back-door cysteine mutants of Shp2a experience enhanced sensitivity of the catalytic cysteine to oxidation, we transfected human embryonic kidney 293 T (HEK293T) cells with mammalian expression vectors encoding full-length Shp2a containing one or both back-door cysteine mutations. HEK293T cells expressing wild-type Shp2a, Shp2a-C334S, Shp2a-C368S, or Shp2a-C334S-C368S (2CS) were treated with 1mM H_2O_2 for 15 minutes and lysed in a buffer containing IAA. Shp2a was immunoprecipitated from the alkylated lysate, and the immunoprecipitates were treated with DTT, followed by pervanadate, to hyperoxidize all non-alkylated proteins for detection. Immunoblotting using the ox-PTP specific antibody revealed that H_2O_2 treatment increased oxidation in all immunoprecipitates (**Fig. 2A**). The difference in signal between H_2O_2 treated cells and untreated cells transfected with the back-door cysteine mutants of Shp2a appeared far greater than for cells transfected with wild-type Shp2a, suggesting that reversible oxidation was enhanced in Shp2a-C334S, Shp2a-C368S, and Shp2a-2CS.

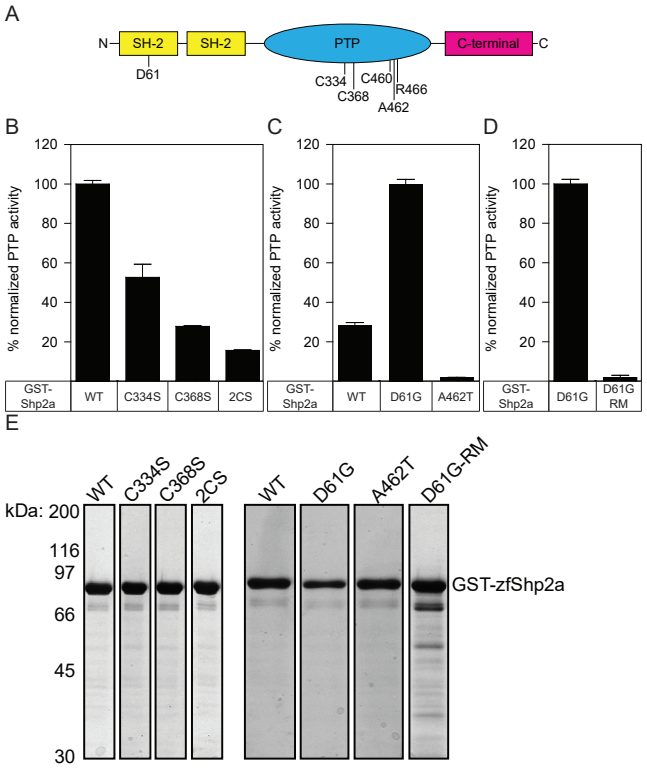

Fig. 1. Back-door cysteine mutants of zebrafish Shp2a have reduced catalytic activity. (**A**) a schematic representation of the Shp2a protein, indicating the SH2 domains (yellow), the catalytic PTP domain (blue), and the C-terminal domain (magenta). Mutation of key residues in the PTP domain results in abrogated catalytic activity. Mutation of the catalytic cysteine (C460), or the arginine assisting in the catalytic process (R466), completely abolishes catalytic activity. Mutation of D61 in the SH2 domain, associated with Noonan syndrome (NS), results in enhanced catalytic activity, whereas mutation of A462 in the PTP domain, associated with Noonan Syndrome with multiple lentigines (NSML), results in reduced catalytic activity. C460, R466 and A462 are located in the catalytic pocket of Shp2a in the PTP domain, whilst the back-door cysteines C334 and C368 are presumed to be positioned outside the catalytic pocket in the PTP domain. (**B**-**D**) catalytic activity of purified N-terminal GST tagged zebrafish Shp2a mutant fusion proteins *in vitro*. GST-Shp2a proteins were concentrated following purification, and subsequently diluted to similar levels for use in pNPP phosphatase assays. Catalytic PTP activity was measured by cleavage of the chromogenic substrate by the purified GST-Shp2a proteins under reducing conditions (in the presence of DTT), and was measured by change in absorbance at 405nm. Comparisons of catalytic activities of purified proteins within the same experiment are depicted. Percent catalytic PTP activity, representative of mean absorbance of pNPP of at least two technical repeats, is shown, normalized to that of wild-type GST-Shp2a (in **B**) or GST-Shp2a-D61G (in **C** and **D**). Error bars represent standard deviation. (**E**) Purified N-terminal GST tagged zebrafish Shp2a mutant proteins resolved on an SDS-PAGE gel. BL-21 E. coli cells were transformed with constructs encoding GST-Shp2a mutant proteins. Proteins were induced with IPTG, and isolated by lysozyme lysis, binding to GST-agarose beads, and elution with reduced glutathione. Proteins were purified by dialysis and resolved on an SDS-PAGE gel for identification by Coomassie staining. All GST-Shp2a proteins were purified and resolved for Coomassie staining on separate occasions.

Stripping and re-probing the blot revealed the differences in ox-PTP signal were not due to differences in Shp2a levels in the immunoprecipitates (**Fig. 2**). In parallel, we included Shp2a immunoprecipitates that were only treated with DTT, to examine changes in irreversibly oxidized Shp2a. Immunoblotting with the ox-PTP specific antibody revealed an increase in ox-PTP signal of Shp2a-C334S, Shp2a-C367S, or Shp2a-2CS following H_2O_2 treatment, suggesting an increase in irreversibly oxidized Shp2a following H_2O_2 treatment (**Fig. 2B**). As expected, the H_2O_2–induced difference in ox-PTP signal in wild-type Shp2a was small, suggesting that the majority of wild-type Shp2a was reversibly oxidized. Taken together, the results in **Fig. 2** suggest that the back-door cysteine mutants of Shp2a were more reversibly and irreversibly oxidized in response to H_2O_2 treatment than wild-type Shp2a.

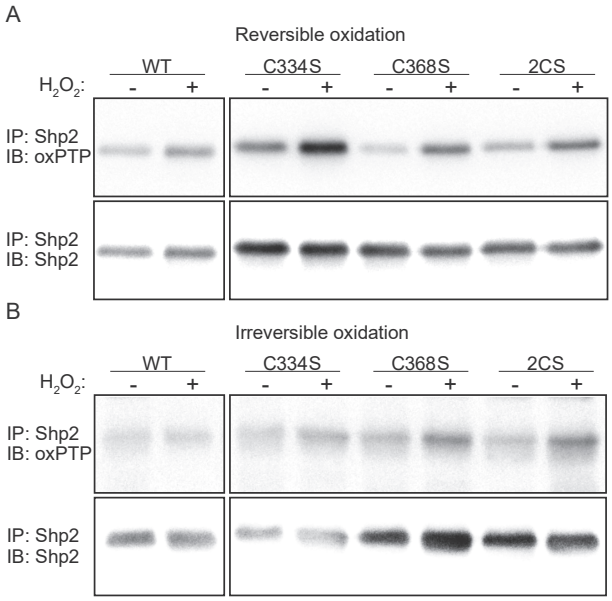

Fig. 2. Enhanced oxidation of back-door cysteine mutants of zebrafish Shp2a. HEK293T cells were transfected with plasmid vector encoding wild-type Shp2a (WT), Shp2a-C334S, Shp2a-C368S, or Shp2a-C334S-C368S (2CS). Transfected HEK293T cells were either treated with 1mM H_2O_2 (+) or an equal volume of H_2O (-) for 15 minutes prior to cell lysis. Lysis was performed on ice in buffer containing 100mM IAA, and cell lysates were immunoprecipitated with an anti-SHP2 antibody. (**A**) Shp2a immunoprecipitates were treated with DTT followed by pervanadate to convert all reversibly oxidized protein to irreversibly oxidized protein for detection (converting SOH to SO_3H). (**B**) Shp2a immunoprecipitates were treated with DTT only, to reduce all reversibly oxidized proteins and remove them from detection. Immunoblotting was performed using anti-ox-PTP and anti-SHP2 antibodies. All samples were loaded on the same blot, samples between WT and C334S were removed as they were not relevant. Blots are representative results of two repeats.

Back-door cysteine mutants of Shp2a rescue caudal fin-fold regeneration in Shp2 deficient zebrafish embryos

The enhanced oxidation of the back-door cysteine mutants of Shp2a in cells treated with H_2O_2 (**Fig. 2**) suggests that they are more susceptible to oxidation-mediated inactivation. In Chapter 5 we proposed that after its initial oxidation induced by zebrafish caudal fin amputation, Shp2a would be reduced and its activity required for regeneration of the caudal fin-fold. In Chapter 6, we demonstrate that wild-type Shp2a almost completely rescued caudal fin-fold regeneration in *ptpn11a*$^{-/-}$*ptpn11b*$^{-/-}$ zebrafish embryos, lacking functional Shp2. We hence used the back-door cysteine mutants of Shp2a to test whether changes in susceptibility to oxidation affect the ability of Shp2a mutants to rescue regeneration in zebrafish embryos lacking functional Shp2.

One-cell stage zebrafish embryos from a *ptpn11a*$^{+/-}$*ptpn11b*$^{-/-}$ in-cross were microinjected with synthetic mRNA encoding either Shp2a-C334S, Shp2a-C368S, or Shp2a-C334S-C368S (2CS). The mRNAs encoding mutant Shp2a proteins also encode eGFP linked by a peptide-2a cleavage sequence, resulting in a single polypeptide that is cleaved prior to protein folding (Ryan, King, and Thomas 1991). At 2dpf, eGFP-positive zebrafish embryos were selected and their caudal fin-folds were amputated immediately posterior to the notochord. Representative pictures of amputated fin-folds at 3 days post amputation (dpa, i.e. 5dpf, 3dpa) of *ptpn11a*$^{-/-}$*ptpn11b*$^{-/-}$ zebrafish embryos expressing mutant Shp2a protein are depicted (**Fig. 3A**). Equivalent uncut zebrafish embryo caudal fin-folds (i.e. 5dpf, Uncut) are shown in **Fig. 4A**. Caudal fin-fold lengths were determined and are presented as percentage caudal fin-fold growth, normalized to non-injected uncut controls of *ptpn11a*$^{+/+}$*ptpn11b*$^{-/-}$ zebrafish embryos (**Fig. 3B**). In contrast to their siblings, *ptpn11a*$^{-/-}$*ptpn11b*$^{-/-}$ zebrafish embryos displayed severely impaired caudal fin-fold regeneration, which, surprisingly, was rescued by expression of Shp2a-C334S, Shp2a-C368S, or Shp2a-2CS (**Fig. 3B**). We observed subtle differences in rescues between the backdoor cysteine mutants, in that Shp2a-C368S rescued to the least extent, Shp2a-C334S had an intermediate effect and Shp2a-2CS rescued regeneration of *ptpn11a*$^{-/-}$*ptpn11b*$^{-/-}$ zebrafish embryos almost completely to sibling level **(Fig. 3A, B**).

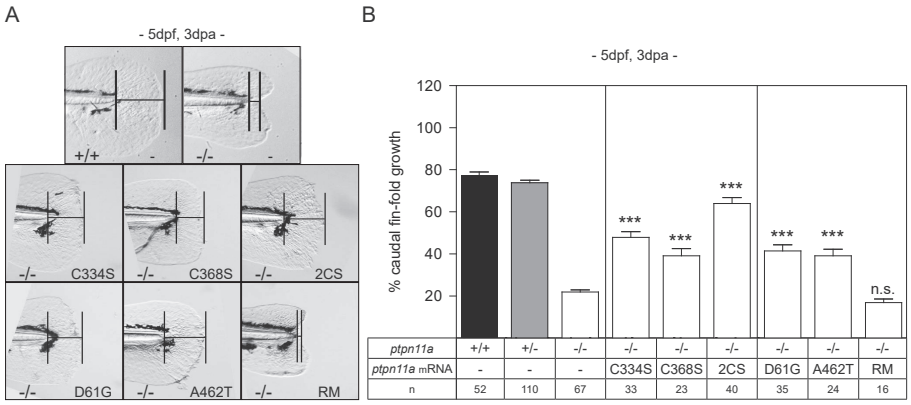

Fig. 3. Impaired caudal fin-fold regeneration in Shp2 deficient embryos is rescued by expression of Shp2a-C334S, Shp2a-C368S, or the double back-door cysteine mutant Shp2a-2CS, and by Shp2a-D61G with enhanced catalytic activity or Shp2a-A462T with reduced catalytic activity, but not by the catalytically inactive Shp2a-R466M. (**A**) Embryos from a *ptpn11a*$^{+/-}$*ptpn11b*$^{-/-}$ in-cross were micro-injected at the one-cell stage with synthetic mRNA encoding Shp2a-C334S, Shp2a-C368S, Shp2a-C334S-C368S (2CS), Shp2a-D61G, Shp2a-A462T, Shp2a-R466M (RM), or were not injected (-). At 2dpf the caudal fin-fold was amputated and regeneration was assessed at 3dpa (i.e. 5dpf, 3dpa). Equivalent uncut controls were included (i.e. 5dpf, uncut) and are shown in **Fig. 4**. All embryos were genotyped. Representative images of caudal fin-folds of non-injected embryos, and of embryos injected with Shp2a mutants are shown. (**B**) The means of caudal fin-fold growth following amputation are depicted relative to caudal fin-fold growth of uncut *ptpn11a*$^{+/+}$*ptpn11b*$^{-/-}$ controls. Means of micro-injected amputated *ptpn11a*$^{-/-}$*ptpn11b*$^{-/-}$ embryos were compared to non-injected amputated *ptpn11a*$^{-/-}$*ptpn11b*$^{-/-}$ embryos using a Mann-Whitney U-test. Significance: *** $p<0.001$; error bars indicate standard error of the mean. Data pooled from multiple experiments. Non-injected and Shp2a-R466M injected data re-used from Chapter 5 and Chapter 6, respectively, for comparison.

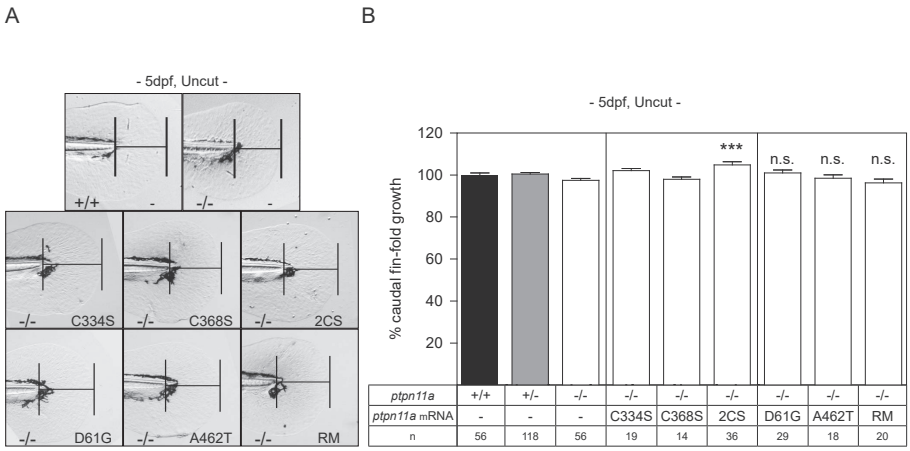

Fig. 4. Normal caudal fin-fold growth in Shp2 deficient embryos expressing Shp2a-C334S, Shp2a-C368S, the double back-door cysteine mutant Shp2a-2CS, Shp2a-D61G with enhanced catalytic activity, Shp2a-A462T with reduced catalytic activity, or the catalytically inactive Shp2a-R466M. (**A**) Embryos from a *ptpn11a*$^{+/-}$*ptpn11b*$^{-/-}$ in-cross were micro-injected at the one-cell stage with synthetic mRNA encoding Shp2a-C334S, Shp2a-C368S, Shp2a-C334S-C368S (2CS), Shp2a-D61G, Shp2a-A462T, Shp2a-R466M (RM), or were not injected (-). Caudal fin-fold length was assessed after 5 days (i.e. 5dpf, uncut). All embryos were genotyped. Representative images of caudal fin-folds of non-injected embryos, and of embryos injected with Shp2a mutants are shown. (**B**) The means of uncut caudal fin-fold growth is depicted relative to caudal fin-fold growth of uncut *ptpn11a*$^{+/+}$*ptpn11b*$^{-/-}$ controls. Means of micro-injected *ptpn11a*$^{-/-}$*ptpn11b*$^{-/-}$ embryos were compared to non-injected *ptpn11a*$^{-/-}$*ptpn11b*$^{-/-}$ embryos. Significance: *** p<0.001; n.s. not significant; error bars indicate standard error of the mean. Data pooled from multiple experiments. Non-injected and Shp2a-R466M injected data re-used from Chapter 5 and Chapter 6, respectively, for comparison.

Expression of the back-door cysteine mutants in *ptpn11a*$^{-/-}$*ptpn11b*$^{-/-}$ zebrafish embryos that were not amputated resulted in normal growth of the caudal fin-fold, with comparable lengths to non-injected zebrafish embryos and siblings (**Fig. 4B**). Furthermore, expression of Shp2a-C334S, Shp2a-C368S, or Shp2a-2CS in wild-type (*ptpn11a*$^{+/+}$*ptpn11b*$^{+/+}$) zebrafish embryos did not induce any development defects (**Fig. 5**). Due to low expression levels of all mutant Shp2a proteins in zebrafish embryos, it was not possible to monitor protein expression *in vivo*. However, transfection of constructs encoding the back-door cysteine mutant Shp2a proteins in HEK293T cells revealed similar expression levels of all mutant Shp2 proteins (**Fig. 6**). This suggests that the differences in ability to rescue caudal fin-fold regeneration are not due to differences in expression or protein stability, but rather to differences in Shp2a function. Collectively, these results suggest that the enhanced susceptibility to oxidation of the

back-door cysteine mutants of Shp2a does not impair their function *in vivo* during zebrafish embryo caudal fin-fold regeneration.
H7.5

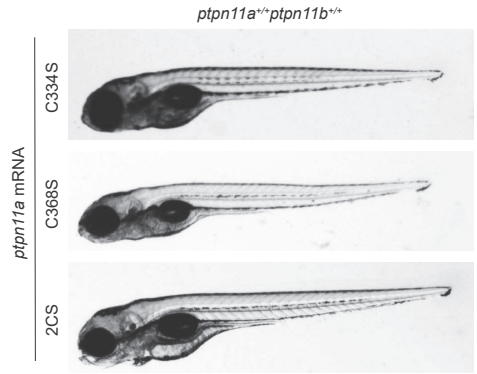

Fig. 5. No observable phenotypes in zebrafish embryos expressing the back-door cysteine mutant C334S, C368S, or C334S and C368S (2CS) of Shp2a. Wild-type (*ptpn11a*$^{+/+}$*ptpn11b*$^{+/+}$) embryos were micro-injected at the one-cell stage with synthetic mRNA encoding Shp2a C334S, Shp2a-C368S, Shp2a-C334S, C368S (2CS). Representative pictures of embryos at 5dpf are shown. Injection efficiency was checked by fluorescence microscopy with a GFP filter.

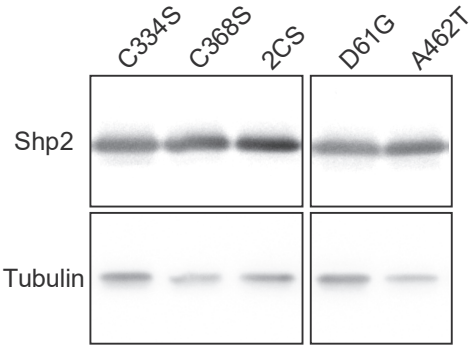

Fig. 6. Similar expression levels of Shp2a mutants. HEK293T cells were transfected with CMV-promoter driven expression vectors for mutants of Shp2a; the back-door cysteine mutants C334S, C368S, or C334S and C368S (2CS); or the catalytic mutants D61G or A462T of Shp2a. Cell lysates were resolved on an SDS-PAGE gel, and immunoblotted with anti-SHP2 and anti-Tubulin antibodies. Detection was achieved through enhanced chemiluminescence. All samples were transfected and processed in parallel.

Shp2a mutants with increased or reduced catalytic activity rescue caudal fin-fold regeneration in Shp2 deficient zebrafish embryos

The ability of the back-door cysteine mutants of Shp2a to rescue caudal fin-fold regeneration in *ptpn11a*$^{-/-}$*ptpn11b*$^{-/-}$ zebrafish embryos is also surprising considering the reduced catalytic activity observed *in vitro* (**Fig. 1B**). We hence investigated to

what extent the level of catalytic activity of Shp2a influences zebrafish embryo caudal fin-fold regeneration using Shp2a-D61G and Shp2a-A462T. We included Shp2a-R466M as a negative control, which we have previously shown does not rescue caudal fin-fold regeneration in *ptpn11a*$^{-/-}$*ptpn11b*$^{-/-}$ zebrafish embryos (Chapter 6).

One-cell stage zebrafish embryos from a *ptpn11a*$^{+/-}$*ptpn11b*$^{-/-}$ in-cross were micro-injected with synthetic mRNA encoding Shp2a-D61G, Shp2a-A462T, or Shp2a-R466M. At 2dpf, eGFP-positive zebrafish embryos were selected and their caudal fin-folds were amputated immediately posterior to the notochord. Representative pictures of amputated caudal fin-folds at 3dpa (i.e. 5dpf, 3dpa) of *ptpn11a*$^{-/-}$*ptpn11b*$^{-/-}$ embryos expressing mutant Shp2a protein are depicted (**Fig. 3A**). Equivalent uncut zebrafish embryo caudal fin-folds (i.e. 5dpf, Uncut) are shown in **Fig. 4A**. Caudal fin-fold lengths were determined and are presented as percentage caudal fin-fold growth, normalized to non-injected uncut controls of *ptpn11a*$^{+/+}$*ptpn11b*$^{-/-}$ zebrafish embryos (**Fig. 3B**). In contrast to their siblings, *ptpn11a*$^{-/-}$*ptpn11b*$^{-/-}$ zebrafish embryos displayed severely impaired regeneration, which was rescued by expression of Shp2a-D61G or Shp2a-A462T, but not the catalytically inactive Shp2a-R466M (**Fig. 3B**). Interestingly, the regenerated caudal-fin-folds of *ptpn11a*$^{-/-}$*ptpn11b*$^{-/-}$ zebrafish embryos expressing Shp2a-D61G or Shp2a-A62T appeared to be similar in length, suggesting Shp2a-D61G and Shp2a-A462T rescued caudal fin-fold regeneration to a similar extent.

Expression of Shp2a-D61G, Shp2a-A462T, or Shp2a-R466M in *ptpn11a*$^{-/-}$*ptpn11b*$^{-/-}$ zebrafish embryos that were not amputated resulted in normal growth of the caudal fin-fold, with comparable lengths to non-injected zebrafish embryos and siblings (**Fig. 4B**). Due to low expression levels of all mutant Shp2a proteins in zebrafish embryos, it was not possible to monitor protein expression *in vivo*. However, transfection of constructs encoding Shp2a-D61G or Shp2a-A462T proteins in HEK293T cells revealed similar expression levels of both Shp2a-D61G and Shp2a-A462T proteins (**Fig. 5B**). This suggests that the similarity in ability to rescue zebrafish embryo caudal fin-fold regeneration was not due to differences in expression or protein stability, and, rather, that the differences in catalytic activity of Shp2a-D61G and Shp2a-A462T does not affect their function in caudal fin-fold regeneration. Together, these results suggest that the level of catalytic activity harboured by Shp2a does not affect the extent of zebrafish embryo caudal fin-fold regeneration stimulated by Shp2a.

DISCUSSION

In summary, we created back-door cysteine mutants of Shp2a and demonstrated that these proteins have reduced catalytic activity *in vitro* (**Fig. 1B**), and enhanced susceptibility to oxidation in mammalian cells exposed to H_2O_2 (**Fig. 2**). Expression of the single (C334S or C368S) or the double (C334S-C368S, 2CS) back-door cysteine mutant of Shp2a rescued caudal fin-fold regeneration in *ptpn11a*$^{-/-}$*ptpn11b*$^{-/-}$ zebrafish embryos (**Fig. 3**). As the back-door cysteine mutants of Shp2a demonstrated reduced catalytic activity *in vitro*, we subsequently used the D61G and A462T mutants of Shp2a, which demonstrated enhanced and reduced catalytic activity *in vitro* (**Fig. 1C**), respectively, to investigate to what extent the level of catalytic activity of Shp2a determines its function in zebrafish embryo caudal fin-fold regeneration. To our surprise, expression of Shp2a-D61G or Shp2a-A462T rescued caudal fin-fold regeneration in *ptpn11a*$^{-/-}$ *ptpn11b*$^{-/-}$ zebrafish embryos to similar extents (**Fig. 3**).

Previous research demonstrated that mutation of the back-door cysteines in SHP1, which is highly similar to SHP2 (Pao et al. 2007), resulted in irreversible oxidation of the catalytic cysteine of SHP1 (Chen et al. 2009). We therefore mutated the back-door cysteines C334 and C368 in zebrafish Shp2a with the aim to investigate if this enhanced the susceptibility to irreversible oxidation of Shp2a following zebrafish embryo caudal fin-fold amputation. We thus first characterized the catalytic activity of purified N-terminally GST-tagged Shp2a-C334S, Shp2a-C368S, and Shp2a-C334S-C368S (2CS) proteins in *in vitro* phosphatase assays under reducing conditions. Mutation of C334 or C368 reduced catalytic activity of Shp2a, and mutating both back-door cysteines compounded the reduction in catalytic activity, compared to wild-type Shp2a (**Fig. 1B**). Chen et al. had previously reported that mutation of C333 in SHP2 resulted in ~90% reduction in catalytic activity compared to wild-type SHP2. Our results confirm that mutation of the back-door cysteine of Shp2a reduce catalytic activity, but that mutation of C334 results in an ~50% reduction in catalytic activity. The differences in our results could be due to our use of full-length Shp2a in *in vitro* phosphatase assays, rather than the isolated catalytic PTP domain of SHP2 tested by Chen et al. (Chen et al. 2009).

To account for the reduced activity in the back-door cysteine mutants of Shp2a in the caudal fin-fold regeneration assays that follow, we included two mutants of Shp2a in our study: Shp2a-D61G and Shp2a-A462T, which have increased and reduced catalytic activity (**Fig. 1C**), respectively, as expected (Keilhack et al. 2005). In addition, we

included Shp2a-R466M as a negative control. By introducing the R466M mutation in Shp2a-D61G, we demonstrated that mutation of R466 completely abolishes catalytic activity (**Fig. 1D**), which is consistent with previous results (Stewart et al. 2010).

The formation of an intramolecular disulphide bond between the two back-door cysteines of SHP2 in response to H_2O_2 presumably protects the catalytic cysteine from irreversible oxidation-mediated inhibition, in a similar manner to the back-door cysteines of SHP1 (Chen et al. 2009). We therefore investigated if the back-door cysteine mutants of Shp2a experienced enhanced oxidation in mammalian cells treated with H_2O_2. Treatment of HEK293T cells over-expressing zebrafish Shp2a-C334S, Shp2a-C368S, or Shp2a-C334S-C368S (2CS) with H_2O_2 induced reversible oxidation of the back-door cysteine mutants of Shp2a, and this was enhanced compared to wild-type Shp2a (**Fig. 2A**). Assessment of irreversible oxidation of Shp2a following treatment of cells with H_2O_2 indicated that irreversible oxidation of the back-door cysteine mutants of Shp2a was mildly enhanced compared to wild-type Shp2a (**Fig. 2B**). These results suggest that the back-door cysteines in Shp2a indeed protect wild-type Shp2a against irreversible oxidation. To our knowledge, the back-door cysteine mutants of Shp2a represent novel mutants with enhanced overall susceptibility to oxidation-mediated inhibition.

Previously, we demonstrated that a subset of PTPs were oxidized following the H_2O_2 burst produced by zebrafish caudal fin amputation, including Shp2a (Chapter 5). We further demonstrated zebrafish embryos deficient for Shp2 do not regenerate their caudal fin-folds, and that Shp2a requires its catalytic activity for its function in caudal fin-fold regeneration (Chapter 6). These two results present an interesting conundrum that Shp2a is oxidized following caudal fin amputation, and therefore inactivated, but its activity is required for caudal fin-fold regeneration. We used the back-door cysteine mutants of Shp2a to address this. To this end, we expressed Shp2a-C334S, Shp2a-C368S, or Shp2a-2CS in *ptpn11a*$^{-/-}$*ptpn11b*$^{-/-}$ zebrafish embryos, which normally do not regenerate, and stimulated ROS production by amputation of the caudal fin-fold at 2dpf. We expected that the back-door cysteine mutants of Shp2a would be irreversibly inactivated following the ROS produced by zebrafish embryo caudal fin-fold amputation, based on our previous results (**Fig. 2**), resulting in non-functional Shp2a and hence no rescue in caudal fin-fold regeneration. To our surprise, expression of the back-door cysteine mutants of Shp2a in *ptpn11a*$^{-/-}$*ptpn11b*$^{-/-}$ zebrafish embryos rescued caudal fin-fold regeneration (**Fig. 3**). The back-door cysteine mutants of Shp2a may experience enhanced irreversible oxidation-mediated inhibition in response

to ROS (**Fig. 2B**). Yet, a considerable proportion of Shp2a-C334S, Shp2a-C368S, and Shp2a-2CS is reversibly oxidized (**Fig. 2A**), and apparently, this is sufficient to rescue caudal fin-fold regeneration in zebrafish embryos lacking functional Shp2.

Most intracellular proteins remain reduced due to intracellular reducing systems, including the glutathione and thioredoxin systems (Lillig, Berndt, and Holmgren 2008; Lu and Holmgren 2014). Hence, the ability of the back-door cysteine mutants of Shp2a to rescue caudal fin-fold regeneration in zebrafish embryos lacking functional Shp2 suggests that the endogenous ROS produced following caudal fin-fold amputation is limited to reversible oxidation of PTPs *in vivo*. Manipulation of PTP oxidation is notoriously challenging. Resolving the crystal structure of the dual specificity PTP phosphatase and tensin homologue (PTEN) suggested that C71 was a back-door cysteine, and formed a disulphide bond with the catalytic cysteine C124 under oxidizing conditions (Cho et al. 2004; Lee et al. 2002; Leslie et al. 2003). Similar to our Shp2a back-door cysteine mutants, the C71S mutant of PTEN also displays reduced catalytic activity compared to wild-type PTEN. However, treatment of PTEN-C71S with sodium hydrosulfide (NaHS), which oxidizes wild-type PTEN even more rapidly than H_2O_2, still only induces reversible oxidation of the catalytic cysteine C124 (Greiner et al. 2013). In addition, treatment of human prostate cancer cells, over-expressing wild-type PTEN or the PTEN-C71S mutant, with H_2O_2, resulted in oxidation of wild-type PTEN, but not PTEN-C71S (Shen et al. 2015). Moreover, there was no increase in downstream AKT phosphorylation, suggesting the activity of PTEN-C71S remained unaffected, and, interestingly, that PTEN-C71S is oxidation resistant. Therefore, whilst C334 and C368 may form an intramolecular disulphide bond in response to ROS (Chen et al. 2009), this may not have any effect on the susceptibility of the catalytic cysteine to oxidation-mediated inhibition.

We also addressed the level of Shp2a catalytic activity required for its function during caudal fin-fold regeneration by expressing Shp2a-D61G and Shp2a-A462T in *ptpn11a*$^{-/-}$*ptpn11b*$^{-/-}$ zebrafish embryos, which have increased and reduced catalytic activity compared to wild-type Shp2a respectively (**Fig. 1C**). Surprisingly, expression of Shp2a D61G or Shp2a-A462T rescued the caudal fin-fold regeneration of *ptpn11a*$^{-/-}$*ptpn11b*$^{-/-}$ zebrafish embryos to a similar extent (**Fig. 3**). These results suggest that neither the enhanced catalytic activity of Shp2a-D61G, or the reduced catalytic activity of Shp2a-A462T (**Fig. 1C**) disrupts the function of Shp2a during zebrafish embryo caudal fin-fold regeneration. Furthermore, the rescue of caudal fin-fold regeneration in *ptpn11a*$^{-/-}$*ptpn11b*$^{-/-}$ zebrafish embryos by expression of Shp2a-A462T, but not Shp2a-

R466M, suggests that catalytic activity is required, but that low level Shp2a activity is sufficient for its function in caudal fin-fold regeneration.

A requirement for tight regulation of signal transduction has been demonstrated to be essential to zebrafish caudal fin regeneration for several signalling pathways (Grotek, Wehner, and Weidinger 2013; Nakatani et al. 2008; Shibata et al. 2016). Considering this, it is highly surprising that Shp2a-D61G, or Shp2a-A462T rescue the caudal fin-fold regeneration of *ptpn11a*$^{-/-}$*ptpn11b*$^{-/-}$ zebrafish embryos to a similar extent, despite extreme differences in catalytic activity. This may be due to the conformation dynamics of SHP2. Normally, SHP2 remains in the closed conformation, through interactions between the SH2 domains and the PTP domain (Hof et al. 1998). Ligation of the SH2 domains to phospho-tyrosine residues on other proteins prompts an open conformation, allowing the PTP domain to dephosphorylate substrates. "Activating" mutations, such as D61G in the N-terminal SH2 domain, disrupt the interaction between the SH2 domains and the PTP domain, and stabilize the open conformation of SHP2 (Darian et al. 2011). Recently, it has been hypothesized that whilst the SHP2 A461T mutant has reduced catalytic activity, it is also stabilized in an open conformation, allowing prolonged association with substrates that compensates for its reduced activity (Yu et al. 2013, 2014). This would certainly explain why both Shp2a-D61G and Shp2a-A462T rescue zebrafish embryo caudal fin-fold regeneration. A similar explanation may be applicable to the back-door cysteine mutants of Shp2a, because formation of an intramolecular disulphide bond, or lack thereof in the back-door cysteine mutants of Shp2a, may induce changes in protein conformation.

Collectively, our results suggest that Shp2a function entails a go/no go signal for the regenerative outgrowth of zebrafish embryo caudal fin-folds, independent of the level of Shp2a activity. Possibly, the conformation of Shp2a, rather than the level of catalytic activity has a role in its function in zebrafish embryo caudal fin-fold regeneration.

MATERIALS AND METHODS

Zebrafish husbandry

All procedures involving experimental animals were approved by the local animal experiments committee (Koninklijke Nederlandse Akademie van Weterschappen-Dierexperimenten commissie) and performed according to local guidelines and policies in compliance with national and European law. The *ptpn11a*$^{+/-}$*ptpn11b*$^{-/-}$ zebrafish lines

in the Tuebingen Long fin (TL) background were previously created by target-selected gene inactivation (TSGI), and both *ptpn11a*^{hu3459} and *ptpn11b*^{hu5920} alleles result from non-sense mutations that lead to a premature stop codon upstream of the catalytic cysteine, C460 (Bonetti, Rodriguez-Martinez, et al. 2014). Adult *ptpn11a*$^{+/-}$*ptpn11b*$^{-/-}$ zebrafish were in-crossed to generate *ptpn11a*$^{-/-}$*ptpn11b*$^{-/-}$ zebrafish embryos for all experiments. Zebrafish were raised and maintained as described by Westerfield (Westerfield 2000) under a 14 hours light/ 10 hours dark cycle at 28.5°C.

In vitro protein production and phosphatase assays

Zebrafish *ptpn11* mutant genes were cloned into a bacterial expression vector with a N-terminal Glutathione-S-transferase (GST) tag. E. coli sub-cloning competent cells (#18265-017, Invitrogen) were transformed with the constructs pGEX-ptpn11a (WT), pGEX-*ptpn11a*-C334S, pGEX-*ptpn11a*-C368S, pGEX-*ptpn11a*-C334S-C368S (2CS), pGEX-*ptpn11a*-D61G, pGEX-*ptpn11a*-A462T, or pGEX-*ptpn11a*-D61G-R466M (RM) and protein induction stimulated with 100µM isopropyl β-D-1-thiogalactopyranoside (IPTG) at 25°C overnight. Proteins were isolated by lysis of the bacterial pellet in 1mg/ml lysozyme and 10% triton X-100. The resulting supernatant was bound to GST agarose beads (#G-4510, Sigma) and washed with phosphate buffered saline (PBS). Isolated proteins were eluted from the GST agarose beads using a reduced glutathione buffer (50mM Tris, 10% glycerol, 10mM reduced glutathione), and dialyzed in Spectra/Por Dialysis membranes (#132665, Spectrum Labs) by incubating 4x 2h in PBS at 4°C. Purified proteins were concentrated in Amicon® Ultra – 0.5ml spin columns (#UFC503096, Merck Millipore). Purified proteins were diluted in 2-(N-morpholino)-ethanesulphonic acid (MES) to similar levels for use in in vitro phosphatase assays. Protein samples in MES were mixed with equal volume 2x para-nitrophenylphosphate (pNPP) mix (40mM MES, 2mM DTT, 2mM EDTA, 300mM NaCl, 20mM pNPP), and in vitro phosphatase assays performed as previously described (Lorenz 2011) with the exception that 50µl 500mM NaOH was used to stop the reaction.

Cell protein extraction and immunoblotting

Whole cell protein extracts from human embryonic kidney 293 T cells (HEK293T) cells transfected with and overexpressing zebrafish Shp2a were prepared by lysis in ice-cold buffer (25mM HEPES pH 7.4, 150mM NaCl, 0.25% deoxycholate, 1% triton X-100, 10mM MgCl2, 1mM EDTA and 10% glycerol) containing protease and phosphatase inhibitors. Samples were centrifuged at 12,000g for 20mins and the supernatant col-

lected. Total protein concentration was estimated using a detergent compatible colorimetric assay according to the manufacturer's instructions (#5000111, Bio-Rad) and all samples diluted to the same concentration. Proteins were resolved in 10% SDS-PAGE gels under reducing conditions and transferred to PVDF membranes (#IPVH00010, Merck Millipore). Immunoblotting was performed using anti-oxPTP (#MAB2844, R&D Systems Europe Ltd.) or anti-SHP2 (SH-PTP2 C-18, #SC-280, Santa Cruz Technology) antibodies followed by horseradish peroxidase (HRP)-conjugated anti-rabbit or anti-mouse antibodies (BD Pharmingen™), respectively. Detection was done by enhanced chemiluminescence (#34095, Thermo Fischer Scientific).

Alkylation, immunoprecipitation, and hyperoxidation

HEK293T were cultured in DMEM 10% fetal calf serum (FCS) and 100U/ml penicillin/streptomycin mix (#15140122, Thermo Fischer Scientific) and treated with 1mM H_2O_2 for 15mins prior to lysis in ice-cold buffer (25mM HEPES pH 7.4, 150mM NaCl, 0.25% deoxycholate, 1% triton X-100, 10mM MgCl2, 1mM EDTA and 10% glycerol), containing protease and phosphatase inhibitors, with 100mM iodoacetic acid (IAA) to achieve protein alkylation. The supernatant was collected and samples diluted to equal concentration as before. Native protein A sepharose beads (#17-0780-01, GE Healthcare) were prepared by washing in fresh ice-cold buffer (25mM HEPES pH 7.4, 150mM NaCl, 0.25% deoxycholate, 1% triton X-100, 10mM MgCl2, 1mM EDTA and 10% glycerol), containing protease and phosphatase inhibitors, with 100mM IAA. Lysates were pre-cleared by incubation with Protein A beads for 30mins at 4°C. Samples were immunoprecipitated by incubating with 0.1µg SHP2 specific antibody (SH-PTP2 C-18, #SC-280, Santa Cruz Technology)/1µl lysate and 1µl Protein A beads/40µl lysate for 2h at 4°C. Samples were rotated during all incubations steps. Protein A beads were washed between steps with HNTG (20mM HEPES pH7.5, 150mM NaCl, 10% glycerol, 0.1% Triton X-100) containing protease and phosphatase inhibitors. Samples were first treated with 10mM dithiothreitol (DTT) in fresh buffer (25mM HEPES pH 7.4, 150mM NaCl, 0.25% deoxycholate, 1% triton X-100, 10mM MgCl2, 1mM EDTA and 10% glycerol), containing protease and phosphatase inhibitors, for 15mins at room temperature, and subsequently treated with 100µM pervanadate (1 mM orthovanadate and 1 mM H_2O_2, mixed and left at room temperature for at least 5 min before use). Protein A beads were re-suspended in 2x laemmli buffer and boiled for 5-10mins. The supernatant was then resolved on 10% SDS-PAGE gels and prepared for immunoblotting as before.

mRNA synthesis and micro-injections

All constructs contain a N-terminal eGFP connected by a peptide-2a cleavage sequence (Ryan et al. 1991). The constructs pCS2+-eGFP-2a-*ptpn11a*-C334S, pCS2+-eGFP-2a-*ptpn11a*-C368S, pCS2+-eGFP-2a-*ptpn11a*-C334S-C368S (2CS), pCS2+-eGFP-2a-*ptpn11a*-D61G, and pCS2+-eGFP-2a-*ptpn11a*-A462T were obtained as described (Bonetti, Paardekooper Overman, et al. 2014). Sense messenger RNA (mRNA) synthesis and micro-injection into one-cell stage zebrafish embryos was performed as described (Stumpf and Den Hertog 2016).

Caudal fin-fold amputation

Zebrafish embryos were amputated as previously described (Hale and den Hertog 2016), amputations were performed at 2 days post fertilisation (dpf) for all experiments. Regeneration was allowed to proceed until analysis at 3 days post amputation (dpa). Whole zebrafish embryos were lysed for genotyping.

Genotyping

All zebrafish embryos that were used in these assays were genotyped to establish *ptpn11a* status. To this end, genomic zebrafish DNA was extracted through lysis of zebrafish embryos in 100µg/ml proteinase K (Sigma) diluted in SZL buffer (50mM KCl, 2.5mM MgCl, 10mM Tris pH 8.3, 0.005% NP40, 0.005% Tween-20, and 10% 0.1% Gelatine). Lysis was performed by incubating at 60°C for 1 hour, followed by 95°C for 15 minutes in a thermal cycler (BioRad T100). The *ptpn11a*^{hu1864} allele in non-fixed tissue was analysed by Kompetitive Allele Specific PCR (KASP): primers of *ptpn11a* containing the non-sense mutations of the *ptpn11a*^{hu1864} allele (*ptpn11a* WT FWD: GAAGGTGACCAAGTTCATGCTACATGGAGCATCATGGAC, *ptpn11a* KO FWD: GAAGGTCGGAGTCAACGGATTACATGGAGCATCATGGAT, *ptpn11a* REV: AGCTCAATGACGTCTCCGTTTTTCTCTTT). Primers were mixed with genomic zebrafish DNA and KASP master mix (LGC Group). Amplification was carried out according to the manufacturer's instructions and the resulting PCR products were analysed in a PHERAstar microplate reader (BMG LABTECH). Klustercaller software (LGC Group) was used to identify the mutations.

Statistics

Histograms of whole data sets were examined to determine non-normal distribution of the data. Statistical analysis of unequal variances was obtained through a Kruskall-Wallis test. Differences between different experimental conditions were assessed for

significance using a Mann-Whitney U test. Differences were considered significant when $p<0.001$, and if they satisfied a confidence interval of 95% in a Monte Carlo exact test. All tests for regenerating caudal fin-folds were performed in SPSS (IBM).

REFERENCES

Alonso, Andres and Rafael Pulido. 2016. "The Extended Human PTPome: A Growing Tyrosine Phosphatase Family." *FEBS Journal* 283(8):1404–29.

Araki, Toshiyuki et al. 2004. "Mouse Model of Noonan Syndrome Reveals Cell Type- and Gene Dosage-Dependent Effects of Ptpn11 Mutation." *Nature Medicine* 10(8):849–57.

Bonetti, Monica, Virginia Rodriguez-Martinez, et al. 2014. "Distinct and Overlapping Functions of ptpn11 Genes in Zebrafish Development." *PLoS ONE* 9(4):e94884.

Bonetti, Monica, Jeroen Paardekooper Overman, et al. 2014. "Noonan and LEOPARD Syndrome Shp2 Variants Induce Heart Displacement Defects in Zebrafish." *Development* 141:1961–70.

Chan, Gordon et al. 2011. "Essential Role for Ptpn11 in Survival of Hematopoietic Stem and Progenitor Cells." *Blood* 117(16):4253–61.

Chen, C. Y., D. Willard, and J. Rudolph. 2009. "Redox Regulation of SH2-Domain-Containing Protein Tyrosine Phosphatases by Two Backdoor Cysteines." *Biochemistry* 48(6):1399–1409.

Cho, S. H. et al. 2004. "Redox Regulation of PTEN and Protein Tyrosine Phosphatases in H(2)O(2) Mediated Cell Signaling." *FEBS Lett* 560(1–3):7–13.

Lo Conte, Mauro and Kate S. Carroll. 2013a. "The Chemistry of Thiol Oxidation and Detection." *Oxidative Stress and Redox Regulation* 1–42.

Lo Conte, Mauro and Kate S. Carroll. 2013b. "The Redox Biochemistry of Protein Sulfenylation and Sulfinylation." *The Journal of Biological Chemistry* 288(37):26480–88.

Cumming, Robert C. et al. 2004. "Protein Disulfide Bond Formation in the Cytoplasm during Oxidative Stress." *Journal of Biological Chemistry* 279(21):21749–58.

Dagnell, M. et al. 2013. "Selective Activation of Oxidized PTP1B by the Thioredoxin System Modulates PDGF-Beta Receptor Tyrosine Kinase Signaling." *Proceedings Of The National Academy Of Sciences Of The United States Of America* 110(33):13398–403.

Darian, Eva, Olgun Guvench, Bing Yu, Cheng-Kui Qu, and Alexander D. MacKerell. 2011. "Structural Mechanism Associated with Domain Opening in Gain-of-Function Mutations in SHP2 Phosphatase." *Proteins* 79(5):1573–88.

Finkel, Toren. 2011. "Signal Transduction by Reactive Oxygen Species." *The Journal of Cell Biology* 194(1):7–15.

Frijhoff, Jeroen, Markus Dagnell, Rinesh Godfrey, and Arne Ostman. 2014. "Regulation of Protein Tyrosine Phosphatase Oxidation in Cell Adhesion and Migration." *Antioxidants & Redox Signaling* 20(13):1994–2010.

Greiner, Romy et al. 2013. "Polysulfides Link H2S to Protein Thiol Oxidation." *Antioxidants & Redox Signaling* 19(15):1749–65.

Grotek, B., D. Wehner, and G. Weidinger. 2013. "Notch Signaling Coordinates Cellular Proliferation with Differentiation during Zebrafish Fin Regeneration." *Development.* 140(7):1412–23. doi: 10.1242/dev.087452. Epub 2013 Mar 5.

Gurzov, Esteban N. et al. 2014. "Hepatic Oxidative Stress Promotes Insulin-STAT-5 Signaling and Obesity by Inactivating Protein Tyrosine Phosphatase N2." *Cell Metabolism* 20(1):85–102.

Hale, Alexander James and Jeroen den Hertog. 2016. "Studying Protein-Tyrosine Phosphatases in Zebrafish." Pp. 351–72 in *Protein Tyrosine Phosphatases: Methods and Protocols*, edited by R. Pulido. New York, NY: Springer New York.

Hartman, Zachary R., Michael D. Schaller, and Yehenew M. Agazie. 2013. "The Tyrosine Phosphatase SHP2 Regulates Focal Adhesion Kinase to Promote EGF-Induced Lamellipodia Persistence and Cell Migration." *Molecular Cancer Research : MCR* 11(6):651–64.

He, Z. et al. 2013. "Nonreceptor Tyrosine Phosphatase Shp2 Promotes Adipogenesis through Inhibition of p38 MAP Kinase." *Proc Natl Acad Sci U S A* 110(1):79–88.

Hendriks, Wiljan J. a J. et al. 2013. “Protein Tyrosine Phosphatases in Health and Disease.” *FEBS J* 280(2):708–30.

Hof, Peter, Scott Pluskey, Sirano Dhe-Paganon, Michael J. Eck, and Steven E. Shoelson. 1998. “Crystal Structure of the Tyrosine Phosphatase SHP-2.” *Cell* 92(4):441–50.

Hunter, Tony. 2009. “Tyrosine Phosphorylation: Thirty Years and Counting.” *Current Opinion in Cell Biology* 21(2):140–46.

Jopling, Chris, Daphne van Geemen, and Jeroen den Hertog. 2007. “Shp2 Knockdown and Noonan/LEOPARD Mutant Shp2–Induced Gastrulation Defects.” *PLOS Genetics* 3(12):e225.

Karisch, Robert et al. 2011. “Global Proteomic Assessment of the Classical Protein-Tyrosine Phosphatome And ‘redoxome.’” *Cell* 146(5):826–40.

Keilhack, Heike, Frank S. David, Malcolm McGregor, Lewis C. Cantley, and Benjamin G. Neel. 2005. “Diverse Biochemical Properties of Shp2 Mutants: Implications for Disease Phenotypes.” *Journal of Biological Chemistry* 280(35):30984–93.

Kolli, Sivanagarani, Christina I. Zito, Marieke H. Mossink, E. A. C. Wiemer, and Anton M. Bennett. 2004. “The Major Vault Protein Is a Novel Substrate for the Tyrosine Phosphatase SHP-2 and Scaffold Protein in Epidermal Growth Factor Signaling.” *Journal of Biological Chemistry* 279(28):29374–85.

Kwon, Jaeyul et al. 2005. “Receptor-Stimulated Oxidation of SHP-2 Promotes T-Cell Adhesion through SLP-76-ADAP.” *The EMBO Journal* 24(13):2331–41.

Lauriol, Jessica, Fabrice Jaffre, and Maria I. Kontaridis. 2015. “The Role of the Protein Tyrosine Phosphatase SHP2 in Cardiac Development and Disease.” *Seminars in Cell & Developmental Biology* 0:73–81. Retrieved (http://www.ncbi.nlm.nih.gov/pmc/articles/PMC4339543/).

Lee, S. R. et al. 2002. “Reversible Inactivation of the Tumor Suppressor PTEN by H2O2.” *Journal of Biological Chemistry* 277:20336–42.

Leslie, N. R. et al. 2003. “Redox Regulation of PI 3-Kinase Signalling via Inactivation of PTEN.” *Embo Journal* 22:5501–10.

Lillig, Christopher Horst, Carsten Berndt, and Arne Holmgren. 2008. “Glutaredoxin Systems.” *Biochimica et Biophysica Acta (BBA) - General Subjects* 1780(11):1304–17.

Liou, MaGeou-Yarh and Peter Storz. 2010. *Reactive Oxygen Species in Cancer*.

Lorenz, Ulrike. 2011. “Protein Tyrosine Phosphatase Assays.” *Current Protocols in Immunology / Edited by John E. Coligan ... [et Al.]* CHAPTER:Unit-11.7.

Lu, Jun and Arne Holmgren. 2014. “The Thioredoxin Antioxidant System.” *Free Radical Biology and Medicine* 66:75–87.

Meng, T. C., T. Fukada, and N. K. Tonks. 2002. “Reversible Oxidation and Inactivation of Protein Tyrosine Phosphatases in Vivo.” *Molecular Cell* 9(2).

Meng, Tzu Ching, Deirdre A. Buckley, Sandra Galic, Tony Tiganis, and Nicholas K. Tonks. 2004. “Regulation of Insulin Signaling through Reversible Oxidation of the Protein-Tyrosine Phosphatases TC45 and PTP1B.” *Journal of Biological Chemistry* 279(36):37716–25.

Nakatani, Yuki, Masanobu Nishidate, Misato Fujita, Atsushi Kawakami, and Akira Kudo. 2008. “Migration of Mesenchymal Cell Fated to Blastema Is Necessary for Fish Fin Regeneration.” *Development Growth and Differentiation* 50(2):71–83.

Neel, Benjamin G., Haihua Gu, and Lily Pao. 2003. “The ‘Shp’ing News: SH2 Domain-Containing Tyrosine Phosphatases in Cell Signaling.” *Trends in Biochemical Sciences* 28(6):284–93.

Niethammer, Philipp, Clemens Grabher, a Thomas Look, and Timothy J. Mitchison. 2009. “A Tissue-Scale Gradient of Hydrogen Peroxide Mediates Rapid Wound Detection in Zebrafish.” *Nature* 459(7249):996–99.

Ostman, Arne et al. 2011. “Regulation of Protein Tyrosine Phosphatases by Reversible Oxidation.” *J Biochem.* 150(4):345–56.

Pao, Lily I., Karen Badour, Katherine A. Siminovitch, and Benjamin G. Neel. 2007. "Nonreceptor Protein-Tyrosine Phosphatases in Immune Cell Signaling." *Annual Review of Immunology* 25:473–523.

Persson, C. et al. 2004. "Preferential Oxidation of the Second Phosphatase Domain of Receptor-like PTP-Alpha Revealed by an Antibody against Oxidized Protein Tyrosine Phosphatases." *Proceedings of the National Academy of Sciences of the United States of America* 101(7).

Persson, Camilla, Kai Kappert, Ulla Engström, Arne Östman, and Tobias Sjöblom. 2005. "An Antibody-Based Method for Monitoring in Vivo Oxidation of Protein Tyrosine Phosphatases." *Methods* 35(1):37–43.

Qu, C. K. et al. 1997. "A Deletion Mutation in the SH2-N Domain of Shp-2 Severely Suppresses Hematopoietic Cell Development." *Molecular and Cellular Biology* 17(9):5499–5507.

Ray, P. D., B. W. Huang, and Y. Tsuji. 2012. "Reactive Oxygen Species (ROS) Homeostasis and Redox Regulation in Cellular Signaling." *Cell Signal.* 24(5):981–90. doi: 10.1016/j.cellsig.2012.01.008. Epub 2.

Ryan, Martin D., Andrew M. Q. King, and G.Paul Thomas. 1991. "Cleavage of Foot-and-Mouth Disease Virus Polyprotein Is Mediated by Residues Located within a 19 Amino Acid Sequence." *Journal of General Virology* 72(11):2727–32.

Salmeen, A. et al. 2003. "Redox Regulation of Protein Tyrosine Phosphatase 1B Involves a Sulphenyl-Amide Intermediate." *Nature* 423(6941):769–73.

Shen, Shao-Ming et al. 2015. "AIF Inhibits Tumor Metastasis by Protecting PTEN from Oxidation." *EMBO Reports* 16(11):1563–80. Retrieved (http://embor.embopress.org/content/16/11/1563.abstract).

Shibata, Eri et al. 2016. "Fgf Signalling Controls Diverse Aspects of Fin Regeneration." *Development* 143(16):2920 LP-2929.

Sone, M., S. Kishigami, T. Yoshihisa, and K. Ito. 1997. "Roles of Disulfide Bonds in Bacterial Alkaline Phosphatase." *The Journal of Biological Chemistry* 272(10):6174–78.

Stewart, Rodney A. et al. 2010. "Phosphatase-Dependent and -Independent Functions of Shp2 in Neural Crest Cells Underlie LEOPARD Syndrome Pathogenesis." *Developmental Cell* 18(5):750–62.

Stumpf, Miriam and Jeroen Den Hertog. 2016. "Differential Requirement for Pten Lipid and Protein Phosphatase Activity during Zebrafish Embryonic Development." *PLoS ONE* 11(2):e0148508.

Tao, J., L. Zheng, M. Meng, Y. Li, and Z. Lu. 2016. "Shp2 Suppresses the Adipogenic Differentiation of Preadipocyte 3T3-L1 Cells at an Early Stage." *Cell Death Discovery* 2:16051.

Thannickal, V. J. and B. L. Fanburg. 2000. "Reactive Oxygen Species in Cell Signaling." *American Journal of Physiology. Lung Cellular and Molecular Physiology* 279(6):L1005-28.

Tonks, Nicholas K. 2013. "Protein Tyrosine Phosphatases - From Housekeeping Enzymes to Master Regulators of Signal Transduction." *FEBS Journal* 280(2):346–78.

Westerfield, M. 2000. *The Zebrafish Book. A Guide for the Laboratory Use of Zebrafish (Danio Rerio)*. 4th ed. Eugene: University of Oregon Press.

Wu, C. J. et al. 2001. "The Tyrosine Phosphatase SHP-2 Is Required for Mediating Phosphatidylinositol 3-kinase/Akt Activation by Growth Factors." *Oncogene* 20(42):6018–25.

Yang, Wentian et al. 2006. "An shp2-Erk Signaling Pathwy Controls Trophoblast Stem Cell Survival." *Developmental Cell* 10:317–27.

Yu, Zhi-Hong Hong et al. 2014. "Molecular Basis of Gain-of-Function LEOPARD Syndrome-Associated SHP2 Mutations." *Biochemistry* 53(25):4136–51.

Yu, Zhi Hong et al. 2013. "Structural and Mechanistic Insights into LEOPARD Syndrome-Associated SHP2 Mutations." *Journal of Biological Chemistry* 288(15):10472–82.

Zhang, Si Qing et al. 2004. “Shp2 Regulates Src Family Kinase Activity and Ras/Erk Activation by Controlling Csk Recruitment.” *Molecular Cell* 13(3):341–55.

Zhang, Wei, Hui Tu Liu, and Hui Tu LIU. 2002. “MAPK Signal Pathways in the Regulation of Cell Proliferation in Mammalian Cells.” *Cell Research* 12(1):9–18.

Zhang, Z. Y., Y. Wang, and J. E. Dixon. 1994. “Dissecting the Catalytic Mechanism of Protein-Tyrosine Phosphatases.” *Proceedings of the National Academy of Sciences of the United States of America* 91(5):1624–27.

Chapter 8

Summarizing Discussion

Alexander James Hale[1, 2]

1. Hubrecht Institute – KNAW and University Medical Center Utrecht, Utrecht, the Netherlands
2. Institute Biology Leiden, Leiden University, Leiden, the Netherlands

Epimorphic regeneration is the complete replacement of lost tissue without scar formation. Fundamental research is challenged with understanding the process of epimorphic regeneration in organisms, such as zebrafish (*Danio rerio*), that retain a lifelong capacity for this ability. Within the last century, many advances have been made in understanding the molecular mechanisms involved in regeneration. The work described in this thesis contributes to the understanding of zebrafish caudal fin (called the "fin-fold" in zebrafish embryos) regeneration by discovering that differential oxidation of protein-tyrosine phosphatases (PTPs) is induced by caudal fin amputation. In addition, we identify that two PTPs are required for zebrafish embryo caudal fin-fold regeneration: Phosphatase and Tensin homolog (Pten), and Src homology 2 domain containing phosphatase (Shp2). Below we describe the major findings, discerning the roles of Pten and Shp2, as well as the steps of zebrafish embryo caudal fin-fold regeneration dependent on Pten and Shp2 mediated signalling.

THE TUMOUR SUPPRESSOR PTEN IS REQUIRED FOR ZEBRAFISH CAUDAL FIN REGENERATION (CHAPTER 4)

The tumour suppressor Phosphatase and Tensin homolog (PTEN) is a dual-specificity phosphatase that antagonizes phosphoinositide-3-kinase (PI3K) signalling (1). We demonstrated for the first time that loss of Pten results in impaired zebrafish embryo caudal fin-fold regeneration, indicating Pten is required for regeneration. The lack of caudal fin-fold regeneration in zebrafish embryos lacking functional Pten was associated with reduced cell proliferation, enhanced apoptosis, and elevated AKT activation during regenerative outgrowth. Restoring Pten expression or inhibiting PI3K activity during regenerative outgrowth rescued caudal fin-fold regeneration in zebrafish embryos lacking functional Pten protein. For this reason, Pten most likely has a function in balancing PI3K signalling. Thus enabling proper coordination of proliferation and apoptosis during regenerative outgrowth of the zebrafish embryo caudal fin-fold.

Loss of PTEN is known to lead to enhanced AKT signalling, promoting cell survival and proliferation in tumour cells (2). However, hyper-active AKT has been shown to induce senescence in mouse embryonic- and human-fibroblasts (3, 4), and loss of PTEN has also been shown, by enhancing p53 activity, to induce senescence in mouse and human tumour cells (4, 5). Possibly, the loss of Pten in zebrafish embryos leads to arrested cell proliferation during caudal fin-fold regeneration due to a similar induction

of cellular senescence by 2 days post-amputation (dpa). The persistence of senescent cells can have detrimental effects on tissue homeostasis (6). Moreover, inhibition of p53 activity in senescent cells has recently been shown to restore tissue homeostasis (7), supporting previous results showing that loss of PTEN induces senescence through increased p53 activity (4).

Surprisingly, we observed enhanced apoptosis in *pten* knock-out zebrafish embryos at both 1dpa and 2dpa, which is contradictory to the role AKT signalling has in enhancing cell survival (8). Furthermore, the increased apoptosis preceded the arrested cell proliferation observed at 2dpa. Apoptosis preceding reduced proliferation was also observed in mouse embryos with increased transforming growth factor β (TGFβ) signalling (9), suggesting the occurrence may not be uncommon. However, it is unclear how loss of Pten affects the order of apoptosis and proliferation, and it will be interesting to identify if the two processes are cell-type specific.

Overall, our results suggest a loss of homeostasis in caudal fin-fold regeneration of zebrafish embryos lacking functional Pten between 1dpa and 2dpa, which may lead to cellular senescence. Future research should include screening for genes that are possibly deregulated in the regenerating caudal fin-folds of zebrafish embryos lacking functional Pten. Such screenings could be achieved by performing sequencing techniques such as tomo-seq, which involves cryosectioning a zebrafish embryo and performing RNA-seq on individual sections (10), on the caudal fin-folds of zebrafish embryos lacking functional Pten and their siblings. Furthermore, useful spatial information on differences in transcription would be obtained. The identified genes could be validated by creating genetic knock-out zebrafish embryos using the new Clustered regularly interspaced short palindromic repeats (CRISPR)/CRISPR associated protein 9 (CAS9) technology, and assessing the caudal fin-fold regeneration of these knock-out zebrafish embryos. If these genes are implicated in senescence, the senescence response could be characterized by performing whole-mount immunohistochemistry for senescence markers (11) at 1dp and 2dpa.

DIFFERENTIAL OXIDATION OF PTPS DURING ZEBRAFISH CAUDAL FIN REGENERATION (CHAPTER 5)

We have detected and identified PTPs in adult zebrafish caudal fin tissue, and reversible oxidation of a subset of PTPs following caudal fin amputation. A total of 33 PTP active

site peptides were efficiently immunoprecipitated from lysates of zebrafish caudal fin clips, and identified by liquid chromatography tandem mass spectrometry (LC-MS/MS). The 33 PTP active site peptides represent 75% of all theoretically observable PTPs, and include 17 non-receptor and 16 receptor type PTPs. Furthermore, we identified the oxidation of 8 different zebrafish PTPs following caudal fin amputation: Ptpn1, Ptpn2a, Ptpn4b, Ptpn9a, Ptpn11a, Ptpn11b, Rptph, and Rptpεa.

Protein tyrosine phosphorylation regulates many cellular processes, including proliferation, differentiation, and migration, and is essential for the development and survival of eukaryotic organisms (12). Protein-tyrosine kinases (PTKs) and protein-tyrosine phosphatases (PTPs) regulate the duration of phospho-tyrosine signalling (13). Inhibition of PTPs by reactive oxygen species (ROS), thus results in maintained phospho-tyrosine signalling (14), which has consequences on cell behaviour. Yet, the study of PTP oxidation *in vivo* has been hampered by the lack of tools to detect reversibly oxidized PTPs, the complexity of distinguishing reversibly oxidized states from irreversibly oxidized states of PTPs, and the difficulty of measuring the intracellular ROS concentration to ascertain if PTPs become oxidized *in vivo* at endogenous ROS levels. Our results demonstrate a method that facilitates the identification of PTP oxidation in tissue samples, and directly implicates PTPs in zebrafish caudal fin regeneration by demonstrating that ROS produced in response to caudal fin amputation (15) induce oxidation of some, but not all, PTPs. Next, CRISPR-CAS9 technology should be used to make genetic knock-out zebrafish of the remaining 6 oxidized PTPs and investigate their role in zebrafish caudal fin regeneration. Rescue experiments, by micro-injecting synthetic mRNA encoding mutant PTP protein, could be performed on knock-out zebrafish embryos to investigate the function of each PTP.

Both inactivating and activating mutations of either PTKs or PTPs have been demonstrated to lead to aberrant tyrosine phosphorylation, which results in a plethora of developmental defects and diseases (16) and highlights the importance of balanced phospho-tyrosine signalling. We hope this method will be used by others to discover and validate the oxidation of PTPs in other tissues, including heart and tumours, and possibly in other physiological processes, such as wound healing, brain tissue of Alzheimer patients, diabetes mellitus, as well as different stages of embryonic development. Conducting such studies may reveal a differential requirement for PTPs in different contexts, and perhaps identify some PTPs as new drug targets.

Understanding and targeting PTP oxidation *in vivo* will be challenging. An example from our own findings is that zebrafish embryos lacking Shp2 (Ptpn11), which is

oxidized following caudal fin amputation, do not regenerate their caudal fin-folds. In comparison, zebrafish embryos lacking Rptpα, which is not oxidized following caudal fin amputation, regenerate their caudal fin-folds normally. These results are surprising and present a conundrum that Shp2 is inactivated, but also required for zebrafish caudal fin regeneration. We propose that Shp2 is reduced after some time following oxidation induced by zebrafish caudal fin amputation, but this will have to be validated. Although PTP oxidation could be followed over time during zebrafish caudal fin regeneration using LC-MS/MS, there would have to be some control to account for the possibility that the oxidized PTP is degraded and replaced with freshly translated reduced PTP. Instead, conformation sensing antibodies specific for reversibly oxidized PTPs (17) may illuminate the dynamics of PTP oxidation. These antibodies could be fluorescently tagged and conditionally expressed *in vivo*, or adapted to be used for whole-mount immunohistochemistry to allow for detection of oxidized PTPs at different stages of zebrafish caudal fin regeneration, as well as in response to different drug treatments.

THE ROLE OF SHP2A DURING ZEBRAFISH EMBRYO CAUDAL FIN-FOLD REGENERATION (CHAPTERS 6 AND 7)

SHP2 is a cytoplasmic PTP with two Src homology 2 (SH2) domains, a catalytic PTP domain, and a C-terminal domain (18). The PTP domain contains a conserved catalytic cysteine that dephosphorylates phospho-tyrosine substrates. The SH2 domains contain essential arginine residues required for ligation to targets. The C-terminal domain contains essential tyrosine residues implicated in receptor and substrate binding (19).

We have demonstrated that loss of Shp2 results in impaired zebrafish embryo caudal fin-fold regeneration, and that this is rescued by restoring expression of wild-type Shp2a, indicating Shp2 is normally required for zebrafish embryo caudal fin-fold regeneration. Furthermore, we have identified the aspects of Shp2a required for its function in zebrafish embryo caudal fin-fold regeneration. In zebrafish embryos lacking functional Shp2, the expression of catalytically inactive Shp2a, or Shp2a with the essential arginine residues of the SH2 domains mutated, did not rescue caudal fin-fold regeneration. In comparison, expressing Shp2a with the two essential tyrosine residues in the C-terminal domain mutated in zebrafish embryos lacking functional Shp2 protein did rescue caudal fin-fold regeneration. Hence, the catalytic activity

and the SH2 domains of Shp2a, but not the two tyrosine phosphorylation sites in the C-terminal domain, are required for the function of Shp2a during zebrafish embryo caudal fin-fold regeneration. By using whole-mount immunohistochemistry we revealed that the lack of caudal fin-fold regeneration in zebrafish embryos lacking functional Shp2 protein was associated with reduced cell proliferation and reduced mitogen activated protein kinase (MAPK) activation during regenerative outgrowth of the caudal fin-fold. Furthermore, we have shown that inhibition of the upstream MAPK kinase 1 (MEK1), which activates MAPK, following zebrafish embryo caudal fin-fold amputation, reduced cell proliferation in a similar manner. Collectively, our results strongly suggest Shp2a mediated MAPK signal transduction is required for the regenerative outgrowth of the zebrafish embryo caudal fin-fold (**Chapter 6**).

Our results of reduced MAPK activation in the caudal fin-folds of zebrafish embryos lacking functional Shp2 protein are consistent with previous studies demonstrating Shp2 mediated MAPK signalling (20–23). MAPK signalling stimulates cell proliferation, and thus zebrafish embryos lacking functional Shp2 protein experienced reduced proliferation during regenerative outgrowth of the caudal fin-fold, resulting in a lack of caudal fin-fold regeneration. Loss of SHP2 is associated with a poor response to injury (24, 25), consistent with MAPK activation following injury being associated with a regenerative competence across species (26, 27). Hence, our findings support the notion that Shp2-MAPK signalling is required for regeneration. Notably, the reason why the loss of SHP2 impairs regeneration is still under debate. For example, the loss of SHP2 in the retina of mice is shown to result in increased apoptosis following injury (24). However, no increase in apoptosis is observed in the impaired regeneration of muscle in mice following loss of SHP2 in satellite cells (25). Instead, loss of SHP2 was associated with satellite cell quiescence. In zebrafish caudal fin regeneration, cells dedifferentiate to form a blastema that will proliferate and replace the lost tissue (28, 29), and the fate of the dedifferentiated cells is lineage restricted (30). Hence, it is possible that following formation of the blastema, the loss of Shp2 induces quiescence in dedifferentiated cells. This would certainly be in concordance with our results, where we show that regenerative outgrowth was impaired in zebrafish embryos lacking functional Shp2, despite normal blastema formation (**Chapter 6**). Such quiescence phenotype may occur in all multipotent progenitors in the blastema, or may be cell-type specific.

Our findings that Shp2a is oxidized following zebrafish caudal fin amputation (**Chapter 5**) suggests that Shp2a is inactivated following caudal fin amputation. Furthermore,

oxidation-mediated inactivation of Shp2a may be necessary for zebrafish caudal fin regeneration, because production of ROS following zebrafish embryo caudal fin-fold amputation is required for caudal fin-fold regeneration (31). However, we have demonstrated that Shp2a activity is required for zebrafish embryo caudal fin-fold regeneration (**Chapter 6**), presenting the following conundrum: how is the catalytic activity of Shp2a required for regeneration when it is oxidized, and thus inactivated, following caudal fin amputation? We propose that after its initial oxidation, Shp2a is reduced to an active state to exert its function for regeneration. To test this hypothesis, we made novel back-door cysteine mutants of Shp2a. SHP2 has been proposed to have two back-door cysteines that protect the catalytic cysteine from irreversible oxidation-mediated inactivation through the formation of an intramolecular disulphide bond with each other in response to ROS (32). Mutation of these back-door cysteines may thus result in a Shp2a mutant that is permanently inactivated following amputation of the zebrafish caudal fin.

We have demonstrated that mutation of the back-door cysteines C334 or C368, or both, reduced catalytic activity, and enhanced ROS induced oxidation of Shp2a. Surprisingly though, expressing the back-door cysteine mutants of Shp2a in zebrafish embryos lacking functional Shp2 protein, rescued their caudal fin-fold regeneration. As the back-door cysteine mutants of Shp2a demonstrated reduced catalytic activity, we subsequently addressed the level of Shp2a catalytic activity required for its function in zebrafish embryo caudal fin-fold regeneration by using two mutants of Shp2a with increased and reduced catalytic activity. Interestingly, expression of Shp2a with increased (D61G) or reduced (A462T) catalytic activity in zebrafish embryos lacking functional Shp2 protein, rescued caudal fin-fold regeneration with similar efficiency. Collectively, our results suggest that the level of Shp2a catalytic activity does not affect the function of Shp2a in the regenerative outgrowth of the caudal fin-fold (**Chapter 7**).

We aimed to make novel Shp2a mutants with enhanced susceptibility to irreversible oxidation-mediated inactivation by ROS by mutating the back-door cysteines of Shp2a. Unfortunately, these back-door cysteine mutants of Shp2a remain functional during caudal fin-fold regeneration when expressed in zebrafish embryos lacking functional Shp2 (**Chapter 7**). Hence, we were unable to explain why Shp2a is oxidized following zebrafish caudal fin amputation, which should inactivate Shp2a, but the catalytic activity of Shp2a is required for zebrafish embryo caudal fin-fold regeneration. Due to the nature of the catalytic cysteine, tying catalytic activity to susceptibility to oxidation, and our limited understanding of back-door cysteines of PTPs, the field of

PTP biochemistry has limited options to manipulate PTP oxidation. Instead, further research should focus on identifying PTP oxidation at different stages of zebrafish caudal fin regeneration (as described above).

Based on our results we proposed that the regulation of Shp2a conformation is pivotal to its function during zebrafish embryo caudal fin-fold regeneration. This would explain why mutants of Shp2a with increased or reduced catalytic activity function similarly in zebrafish embryo caudal fin-fold regeneration. The A462T mutant of Shp2a, and possibly the back-door cysteine mutants of Shp2a, may be stabilized in an open conformation, allowing prolonged association with substrates and compensating for its reduced activity (33, 34). In comparison, the D61G mutant of Shp2a is proposed to have increased activity due to disruption of the interaction between the SH2 domains and the PTP domain, resulting in a permanently open conformation (35, 36). Interestingly, the ability of Shp2a mutants with low catalytic activity to remain functional during zebrafish embryo caudal fin-fold regeneration aligns with the proposal that a basal level of sustained MAPK signalling is required to maintain proliferating cells during regeneration (24, 25). The opposite, increased MAPK signalling beyond normal, appears not to be detrimental, as expression of Shp2a-D61G in zebrafish embryos lacking functional Shp2 had no more effect than expressing Shp2a-A462T. Indeed, expression of $KRas^{G12D}$, which greatly increases MAPK activation (promoting increased proliferation and migration of cells, and often leading to pancreatic neoplasms (37, 38)), in Shp2 deficient mice retina is, surprisingly, limited to rescuing retinal degeneration (24). Taken together, these results suggest that Shp2 is required in an open conformation to stimulate regenerative outgrowth, and that the level of MAPK signalling is regulated further downstream, possibly by dual specificity phosphatases (39).

The importance of balanced phospho-tyrosine signalling is evident by the plethora of developmental defects and diseases that result when either PTKs or PTPs are mutated (16). Our finding that inhibition of MAPK signalling inhibits zebrafish embryo caudal fin-fold regeneration (**Chapter 6**) demonstrates that MAPK signalling is required. However, our results in **Chapter 7**, showing that Shp2a mutants with opposite extremes in catalytic activities stimulate zebrafish embryo caudal fin-fold regeneration to a similar extent, suggest that "balanced" Shp2a activity is not crucial for zebrafish embryo caudal fin-fold regeneration. A major challenge to fully understanding the function of molecules, and hence signalling pathways, in regeneration, is manipulating their expression over time. The expression of genes fluctuates through the distinct stages of regeneration (40), and it is evident that the signalling required for regene-

ration is more complex than just upregulating or downregulating signal transduction. For example, both inhibition of Notch signalling and over-activation of Notch signalling result in impaired caudal fin regeneration (41), demonstrating that the changes in signalling are subtle and tightly regulated. Therefore, there is a need for inducible on/off systems to delineate when and for how long each gene or signalling pathway is required during regeneration. An inducible Shp2a system could be used to understand the specific moment when Shp2a function is required during zebrafish embryo caudal fin-fold regeneration. In addition, if the lack of caudal fin-fold regeneration in zebrafish embryos lacking functional Shp2 protein is due to blastema cells becoming quiescent, inducible systems could also be used to address whether the activation of Shp2, or MAPK, at 1dpa or 2dpa would re-start the regenerative outgrowth of the caudal fin-fold. Furthermore, if MAPK signalling is limited downstream of Shp2a, inducible MAPK systems could address the importance of balanced phospho-tyrosine signalling.

CONCLUSION

Overall, we show that genetic knock-out zebrafish embryos of *pten* or *ptpn11*, lacking functional Pten or Shp2 respectively, do not regenerate their caudal fins. This is attributed to the aberrant PI3K or MAPK signalling that results in zebrafish embryos lacking functional Pten or Shp2, respectively (**Chapters 4** and **6**). We make evident that amputation induces differential oxidation of PTPs in zebrafish caudal fins, and demonstrate a differential requirement for PTPs during zebrafish embryo caudal fin-fold regeneration (**Chapter 5**). We uncover that 8 PTPs are oxidized following zebrafish caudal fin amputation. Shp2a is one of the PTPs that is oxidized in the zebrafish caudal fin, but Shp2a is also required for zebrafish embryo caudal fin-fold regeneration. By expressing mutant Shp2a proteins in *ptpn11* knock-out zebrafish embryos, we investigated the role of Shp2a in caudal fin-fold regeneration. We show that Shp2a requires its catalytic activity and the function of its SH2 domains for its role in caudal fin-fold regeneration (**Chapter 6**). Shp2a does not need the tyrosine residues in its C-terminal domain, which are needed for Shp2a binding to some substrates. Our findings also reveal that the level of Shp2a catalytic activity does not determine the efficiency of zebrafish embryo caudal fin-fold regeneration (**Chapter 7**). We sought to make oxidation hypersensitive mutants of Shp2a, however these were not inactivated following zebrafish embryo caudal fin-fold amputation. Collectively, our results reveal a crucial role for Pten and

Shp2 in zebrafish caudal fin regeneration, and allow for further research to understand the importance of their dynamics during zebrafish caudal fin regeneration.

FUTURE PERSPECTIVES

We have emphasized the importance of balanced phospho-tyrosine signalling and provided numerous examples of the consequences of aberrant PTP activity in the first two chapters. Balanced phospho-tyrosine signalling is also important in zebrafish embryo caudal fin-fold regeneration, and we show that loss of *pten* or inhibition of PI3K inhibits regeneration. Furthermore, inhibition of PI3K in *pten* knock-out zebrafish embryos restored zebrafish embryo caudal fin-fold regeneration (**Chapter 4**). However, Shp2a mutants with increased and reduced catalytic activity stimulate zebrafish embryo caudal fin-fold regeneration to a similar extent (**Chapter 7**), suggesting that the regulation of phospho-tyrosine signalling occurs at multiple steps in the signalling pathway. Delineating the exact substrates and MAPK signalling pathway Shp2 is involved in will address how this "balance" is achieved. Furthermore, this will indicate which cellular processes Pten and Shp2 are involved in during the regenerative outgrowth of the zebrafish embryo caudal fin-fold.

Balanced phospho-tyrosine signalling may also regulate the duration of zebrafish caudal fin regeneration. During our studies, we always amputated adjacent to the notochord, which is the standard practice in the field of zebrafish embryo caudal fin-fold regeneration (**Chapter 3**). However, amputating only the tip of the zebrafish embryo caudal fin-fold results in regeneration that progresses over the same duration (data not shown). This is not unique to zebrafish caudal fin regeneration as the regeneration of planarian eyes also has a set duration, independent from injury size, injury type, and metabolic rate (42). Thus, regeneration of the lost tissue experiences isometric growth, where an organ grows relative to the size of the organism. In adult zebrafish caudal fins, inhibition of the serine and threonine phosphatase Calcineurin disrupts isometric growth and promotes positive allometric growth, resulting in the regenerating caudal fin growing beyond its original size (43). This was attributed to increased retinoic acid signalling, which controls the formation of the blastema, and the proliferation of the dedifferentiated cells in the blastema (44). Hence, the isometric growth of regenerating tissues may be in part due to the proliferation gradient that exists from the proximal blastema, where cells proliferate, to the differentiation

zone (45). Taking into consideration the role of PI3K and MAPK signalling in promoting proliferation, it is likely that Pten and Shp2 signalling have a role in the proliferation of cells in the blastema. Therefore, another area of interest is cell specific activity of Pten and Shp2a in different regions of the blastema. However, the molecular mechanism of the blastema is an area that requires significant leaps in understanding. For example, Notch signalling is not required for blastema formation, but when Notch signalling is enhanced the pool of proliferating cells in the blastema expands, reducing the number of cells differentiating into the lost tissue (41). Similarly, inhibition of Notch signalling causes the opposite effect. The limitation to better understanding the molecular mechanism of the blastema is the lack of the availability of mutants where protein expression can be spatio-temporally regulated at the distinct stages of regeneration. In addition, for research on the specific role of PTPs in zebrafish regeneration, there is a need for specific water-soluble inhibitors that can be applied during regeneration.

Finally, the ultimate question will be whether gains in our understanding of model organism regeneration can be translated to human wound healing. PTPs are important for the regenerative process of tissues and organs of other vertebrates. PTP1B is a negative regulator of insulin signalling (46), and *PTP1B* knock-out mice are resistant to type 2 Diabetes Mellitus (T2DM) and obesity (47). Moreover, *PTP1B* knock-out mice experience enhanced liver regeneration (48). Mouse models of T2DM, *ob/ob* mice, have impaired wound healing, which is restored when PTP1B is inhibited (49). This suggests that PTP1B negatively regulates regeneration, and that there is a differential requirement for PTPs in regeneration of the liver. This differential requirement may span across organs, and perhaps across species. Targeting PTP1B with available inhibitors (50) may be one of the steps required to unlock the regenerative capacity in human adults. As our understanding of regeneration improves, we will identify more targets and, hopefully, develop the means to attempt to induce regeneration in human adults.

REFERENCES

1. Song MS, Salmena L, Pandolfi PP (2012) The functions and regulation of the PTEN tumour suppressor. *Nat Rev Mol Cell Biol* 13(5):283–296.
2. Vara JÁF, et al. (2004) PI3K/Akt signalling pathway and cancer. *Cancer Treat Rev* 30(2):193–204.
3. Astle M V, et al. (2012) AKT induces senescence in human cells via mTORC1 and p53 in the absence of DNA damage: implications for targeting mTOR during malignancy. *Oncogene* 31(15):1949–1962.
4. Chen Z, et al. (2005) Crucial role of p53-dependent cellular senescence in suppression of Pten-deficient tumorigenesis. *Nature* 436(7051):725–730.
5. Alimonti A, et al. (2010) A novel type of cellular senescence that can be enhanced in mouse models and human tumor xenografts to suppress prostate tumorigenesis. *J Clin Invest* 120(3):681–693.
6. Freund A, Orjalo A V, Desprez P-Y, Campisi J (2010) Inflammatory Networks during Cellular Senescence: Causes and Consequences. *Trends Mol Med* 16(5):238–246.
7. Baar MP, et al. (2017) Targeted Apoptosis of Senescent Cells Restores Tissue Homeostasis in Response to Chemotoxicity and Aging. *Cell* 169(1):132–147.e16.
8. Chen WS, et al. (2001) Growth retardation and increased apoptosis in mice with homozygous disruption of the akt1 gene. *Genes Dev* 15(17):2203–2208.
9. Kubalak SW, Hutson DR, Scott KK, Shannon RA (2002) Elevated transforming growth factor β2 enhances apoptosis and contributes to abnormal outflow tract and aortic sac development in retinoic X receptor α knockout embryos. *Development* 129(3):733–746.
10. Kruse F, Junker JP, van Oudenaarden A, Bakkers J (2016) Tomo-seq: A method to obtain genome-wide expression data with spatial resolution. *Methods Cell Biol* 135:299–307.
11. Althubiti M, et al. (2014) Characterization of novel markers of senescence and their prognostic potential in cancer. *Cell Death Dis* 5:e1528.
12. Hunter T (2009) Tyrosine phosphorylation: thirty years and counting. *Curr Opin Cell Biol* 21(2):140–146.
13. Hunter T (1995) Protein kinases and phosphatases: The Yin and Yang of protein phosphorylation and signaling. *Cell* 80(2):225–236.
14. Östman A, Frijhoff J, Sandin A, Böhmer F-D (2011) Regulation of protein tyrosine phosphatases by reversible oxidation. *J Biochem* 150(4):345–56.
15. Niethammer P, Grabher C, Look a T, Mitchison TJ (2009) A tissue-scale gradient of hydrogen peroxide mediates rapid wound detection in zebrafish. *Nature* 459(7249):996–9.
16. Blume-Jensen P, Hunter T (2001) Oncogenic kinase signalling. *Nature* 411(6835):355–365.
17. Haque A, Andersen JN, Salmeen A, Barford D, Tonks NK (2011) Conformation-Sensing Antibodies Stabilize the Oxidized Form of PTP1B and Inhibit Its Phosphatase Activity. *Cell* 147(1). doi:10.1016/j.cell.2011.08.036.
18. Hof P, Pluskey S, Dhe-Paganon S, Eck MJ, Shoelson SE (1998) Crystal structure of the tyrosine phosphatase SHP-2. *Cell* 92(4):441–450.
19. Tajan MM, de Rocca Serra A, Valet P, Edouard T, Yart A (2015) SHP2 sails from physiology to pathology. *Eur J Med Genet* 58(10):509–525.
20. Cunnick JM, et al. (2002) Regulation of the mitogen-activated protein kinase signaling pathway by SHP2. *J Biol Chem* 277(11):9498–9504.
21. Heuberger J, et al. (2014) Shp2/MAPK signaling controls goblet/paneth cell fate decisions in the intestine. *Proc Natl Acad Sci* 111(9):3472–3477.
22. Yang W, et al. (2006) an shp2-erk signaling pathwy controls trophoblast stem cell survival. *Dev Cell* 10:317–327.

23. Zhang SQ, et al. (2004) Shp2 Regulates Src Family Kinase Activity and Ras/Erk Activation by Controlling Csk Recruitment. *Mol Cell* 13(3):341–355.
24. Cai Z, et al. (2011) Loss of Shp2-mediated mitogen-activated protein kinase signaling in Muller glial cells results in retinal degeneration. *Mol Cell Biol* 31(14):2973–83.
25. Griger J, et al. (2017) Loss of Ptpn11 (Shp2) drives satellite cells into quiescence. *Elife* 6:e21552.
26. Yun MH, Gates PB, Brockes JP (2014) Sustained ERK activation underlies reprogramming in regeneration-competent salamander cells and distinguishes them from their mammalian counterparts. *Stem Cell Reports* 3(1):15–23.
27. Itou J, Kawakami H, Burgoyne T, Kawakami Y (2012) Life-long preservation of the regenerative capacity in the fin and heart in zebrafish. *Biol Open* 1(8):739–746.
28. Poss KD, Keating MT, Nechiporuk A (2003) Tales of regeneration in zebrafish. *Dev Dyn* 226(2):202–210.
29. Pfefferli C, Jaźwińska A (2015) The art of fin regeneration in zebrafish. *Regeneration* 2(2):72–83.
30. Tu S, Johnson SL (2011) Fate restriction in the growing and regenerating zebrafish fin. *Dev Cell* 20(5):725–732.
31. Yoo SK, Freisinger CM, LeBert DC, Huttenlocher A (2012) Early redox, Src family kinase, and calcium signaling integrate wound responses and tissue regeneration in zebrafish. *J Cell Biol* 199(2):225–34. doi: 10.1083/jcb.201203154. Epub 2012 Oct.
32. Chen CY, Willard D, Rudolph J (2009) Redox regulation of SH2-domain-containing protein tyrosine phosphatases by two backdoor cysteines. *Biochemistry* 48(6):1399–1409.
33. Yu ZH, et al. (2013) Structural and mechanistic insights into LEOPARD syndrome-associated SHP2 mutations. *J Biol Chem* 288(15):10472–10482.
34. Yu Z-HH, et al. (2014) Molecular basis of gain-of-function LEOPARD syndrome-associated SHP2 mutations. *Biochemistry* 53(25):4136–4151.
35. Darian E, Guvench O, Yu B, Qu C-K, MacKerell AD (2011) Structural mechanism associated with domain opening in gain-of-function mutations in SHP2 phosphatase. *Proteins* 79(5):1573–1588.
36. Keilhack H, David FS, McGregor M, Cantley LC, Neel BG (2005) Diverse biochemical properties of Shp2 mutants: Implications for disease phenotypes. *J Biol Chem* 280(35):30984–30993.
37. Tuveson DA, et al. (2004) Endogenous oncogenic K-ras(G12D) stimulates proliferation and widespread neoplastic and developmental defects. *Cancer Cell* 5(4):375–387.
38. Rachagani S, et al. (2011) Activated Kras(G12D) is associated with invasion and metastasis of pancreatic cancer cells through inhibition of E-cadherin. *Br J Cancer* 104(6):1038–1048.
39. Kondoh K, Nishida E (2007) Regulation of MAP kinases by MAP kinase phosphatases. *Biochim Biophys Acta - Mol Cell Res* 1773(8):1227–1237.
40. Saxena S, et al. (2012) Proteomic Analysis of Zebrafish Caudal Fin Regeneration. *Mol Cell Proteomics* 11(6):M111.014118-M111.014118.
41. Grotek B, Wehner D, Weidinger G (2013) Notch signaling coordinates cellular proliferation with differentiation during zebrafish fin regeneration. *Development* 140(7):1412–23. doi: 10.1242/dev.087452. Epub 2013 Mar 5.
42. Deochand ME, Birkholz TR, Beane WS (2016) Temporal regulation of planarian eye regeneration. *Regeneration* 3(4):209–221.
43. Kujawski S, et al. (2014) Calcineurin Regulates Coordinated Outgrowth of Zebrafish Regenerating Fins. *Dev Cell* 28(5):573–587.

44. Blum N, Begemann G (2012) Retinoic acid signaling controls the formation, proliferation and survival of the blastema during adult zebrafish fin regeneration. *Development* 139(1):107–16. doi: 10.1242/dev.065391. Epub 2011 Nov 17.

45. Nechiporuk A, Keating MT (2002) A proliferation gradient between proximal and msxb-expressing distal blastema directs zebrafish fin regeneration. *Development* 129(11):2607–2617.

46. González-Rodríguez Á, et al. (2010) Inhibition of PTP1B restores IRS1-mediated hepatic insulin signaling in IRS2-deficient mice. *Diabetes* 59(3):588–599.

47. Cho H (2013) Protein tyrosine phosphatase 1B (PTP1B) and obesity. *Vitam Horm* 91:405–424.

48. Revuelta-Cervantes J, et al. (2011) Protein Tyrosine Phosphatase 1B (PTP1B) Deficiency Accelerates Hepatic Regeneration in Mice. *Am J Pathol* 178(4):1591–1604.

49. Zhang J, et al. (2015) Protein tyrosine phosphatase 1B impairs diabetic wound healing through vascular endothelial growth factor receptor 2 dephosphorylation. *Arterioscler Thromb Vasc Biol* 35(1):163–174.

50. Zhang S, Zhang Z-Y (2007) PTP1B as a drug target: recent developments in PTP1B inhibitor discovery. *Drug Discov Today* 12(9–10):373–381.

Appendix

SUMMARY

This thesis describes the use of zebrafish (*Danio rerio*), which have the capacity to regenerate lost tissues and organs, to study the role of protein tyrosine phosphatases (PTPs) in caudal fin regeneration. In the first three chapters, we introduce the mechanism and function of PTPs, their importance to intracellular signalling and their role in ensuring correct embryonic development, and outline the methods used to study their role in zebrafish caudal fin regeneration. These chapters provide the background for the scientific questions we pursue in the subsequent experimental chapters. Specifically, we demonstrate that both Pten and Shp2 are required for zebrafish embryo caudal fin regeneration, and that differential oxidation of PTPs during zebrafish caudal fin regeneration is evident. We also examine the molecular mechanism of Shp2a during zebrafish embryo caudal fin regeneration.

In **Chapter 1** we briefly review the structure and function of PTPs in phospho-tyrosine signalling, and how PTP activity is regulated. We introduce the process of regeneration, outlining the steps required for successful zebrafish caudal fin regeneration, and allude to the role PTPs may have in this process.

In **Chapter 2** we review the accumulating evidence highlighting the essential role PTPs have in maintaining balanced phospho-tyrosine signalling during embryonic development. We cover how the activity of one or more PTPs is instrumental in the biology of stem cell self-renewal and differentiation, gastrulation and somitogenesis, osteogenesis, and angiogenesis. We also provide examples of how PTP dysregulation, in the form of increased or reduced activity, has detrimental consequences to these processes, and hence embryonic development. The importance of balanced phospho-tyrosine signalling is evolutionary conserved, which is evident considering the numerous distinct animal models that are dependent on appropriate PTP activity. We also briefly discuss some human syndromes and diseases that are associated with aberrant PTP activity.

In **Chapter 3** we outline some of the experimental procedures used to study the role of PTPs during zebrafish caudal fin regeneration. We provide step-by-step protocols for micro-injecting synthetic messenger RNA into one-cell stage zebrafish embryos to express a protein of interest, amputating the caudal fin under anaesthesia, and lysing tissue for analysis of protein expression. We also share tips on each method collected from peers experienced in zebrafish handling and experimentation.

In **Chapter 4** we used zebrafish embryos lacking functional phosphatase and tensin homologue (Pten) protein, a tumour suppressor that acts as an antagonist of phosphoinositide 3-kinase (PI3K)/Akt signalling, to demonstrate the importance of PTPs in zebrafish caudal fin regeneration. We show that homozygous *ptena*$^{-/-}$*ptenb*$^{-/-}$ embryos, lacking functional Pten protein, do not regenerate their caudal fins following amputation. We analysed two essential and distinct steps in the regenerative process: blastema formation, and regenerative outgrowth, using *in situ* hybridization and immunohistochemistry, respectively. Although *ptena*$^{-/-}$*ptenb*$^{-/-}$ embryos do form a blastema normally, immunohistochemistry revealed arrested proliferation, increased apoptosis, and enhanced activation of Akt (activated by PI3K) during regenerative outgrowth compared to sibling embryos with functional Pten protein. Re-expression of Pten, but not the catalytically inactive mutant Pten-C124S, in *ptena*$^{-/-}$*ptenb*$^{-/-}$ embryos rescued regeneration, as did pharmacological inhibition of PI3K. Collectively, our results suggest a critical role for Pten by limiting PI3K signalling during the regenerative outgrowth phase of zebrafish embryo caudal fin regeneration.

In **Chapter 5** we uncovered differential oxidation of PTPs during caudal fin regeneration of adult zebrafish. In response to amputation of the caudal fin, a rapid and transient increase in hydrogen peroxide (H_2O_2) levels is observed emanating from the wound margin, which is essential for regeneration. We performed two sequential fin clips 40 minutes apart to extract the part of the fin that experienced the increase in H_2O_2 levels. Using an antibody specific for oxidized PTPs (ox-PTP) and liquid chromatography-mass spectrometry, we isolated and identified 33 PTPs in adult zebrafish fin clips. Of these 33 PTPs, 8 were significantly more oxidized 40 minutes after caudal fin amputation. Shp2a was one of the PTPs that was oxidized. We also provide evidence that the oxidized PTPs are important for regeneration: embryos deficient for Shp2, homozygous *ptpn11a*$^{-/-}$*ptpn11b*$^{-/-}$ embryos, did not regenerate their caudal fins; whereas embryos deficient for Rptpα, homozygous *ptpra*$^{-/-}$ embryos, which was not oxidized upon caudal fin amputation, regenerated their caudal fins normally. Our results demonstrate that PTPs are differentially oxidized in response to caudal fin amputation and suggest that there is a differential requirement for PTPs in regeneration.

In **Chapter 6** we used zebrafish embryos lacking functional Shp2 protein, a mediator of mitogen activated protein kinase (MAPK) signalling, to delineate the signalling role of Shp2a in caudal fin regeneration. Shp2a has multiple functional domains: a catalytic PTP domain, and two SH2 domains, and a C-terminal domain, for binding to different targets. We show that re-expression of Shp2a, but not the catalytically inac-

tive mutant Shp2a-R466M or the Shp2a mutant lacking the capacity to bind via its SH2 domains, rescued regeneration of homozygous *ptpn11a*$^{-/-}$*ptpn11b*$^{-/-}$ embryos following caudal fin amputation. We also show that the ability of Shp2a to bind targets through its C-terminal domain is likely not required for its function during zebrafish embryo caudal fin regeneration. By using *in situ* hybridization and immunohistochemistry, we show that *ptpn11a*$^{-/-}$*ptpn11b*$^{-/-}$ embryos formed a blastema normally, but displayed arrested proliferation and reduced activation of MAPK during regenerative outgrowth. Pharmacological inhibition of MEK, activator of MAPK, similarly inhibited regeneration and arrested proliferation during the regenerative outgrowth of zebrafish embryo caudal fins. Our results suggest a critical role for Shp2a by promoting MAPK signalling during the regenerative outgrowth phase of zebrafish embryo caudal fin regeneration.

In **Chapter 7** we mutated key residues in Shp2a to investigate the oxidation and level of catalytic activity of Shp2a required for its function during zebrafish embryo caudal fin regeneration. Shp2a is susceptible to reversible oxidation-mediated inactivation, and the two "back-door" cysteines of Shp2a are proposed to protect Shp2 from irreversible oxidation-mediated inactivation. Shp2a was oxidized following zebrafish embryo caudal fin amputation (**Chapter 5**), but its activity was also required for zebrafish embryo caudal fin regeneration (**Chapter 6**). By mutating the back-door cysteines C334 and C368 of Shp2a, we generated novel mutant Shp2a proteins that demonstrated reduced catalytic activity and enhanced susceptibility to oxidation by H_2O_2. However, expression of the back-door cysteine mutant proteins of Shp2a, rescued caudal fin regeneration in homozygous *ptpn11a*$^{-/-}$*ptpn11b*$^{-/-}$ zebrafish embryos, suggesting the back-door cysteine mutant proteins of Shp2a were not irreversibly oxidized by the H_2O_2 normally produced following caudal fin amputation. In addition, the back-door cysteine mutants of Shp2a rescued zebrafish embryo caudal fin regeneration despite reduced catalytic activity. Interestingly, Shp2a proteins carrying mutations in D61 or A462, resulting in increased or reduced catalytic activity, respectively, rescued zebrafish embryo caudal fin regeneration to similar extents. Collectively, our results suggest that Shp2a catalytic activity is required for regeneration, but that the level of Shp2a catalytic activity does not affect the function of Shp2a in zebrafish embryo caudal fin regeneration.

Finally, **Chapter 8** provides a summarizing discussion of the work presented in each of the previous experimental chapters, and the implications of our findings for future research.

NEDERLANDSE SAMENVATTING

Dit proefschrift beschrijft hoe de zebravis (*Danio rerio*), welke het vermogen bezit om verloren gegane weefsels en organen te regenereren, wordt gebruikt om de rol van tyrosine fosfatases (PTP's) in staartvinregeneratie te bestuderen. In de eerste drie hoofdstukken introduceren we het werkingsmechanisme en de functies van PTPs, hun belang voor intracellulaire signaaltransductie en hun rol in het tot stand brengen van een correcte ontwikkeling van het embryo. Daarnaast beschrijven we de methoden die gebruikt zijn om de rol van deze fosfatases in staartvinregeneratie bij zebravissen te bestuderen. Deze hoofdstukken geven de achtergrondinformatie voor de daarop volgende experimentele hoofdstukken, met daarin de wetenschappelijke vragen waarop we een antwoord hebben geprobeerd te krijgen. We laten in zebravis embryo's zien dat zowel Pten als Shp2 vereist zijn voor staartvinregeneratie en dat er overduidelijk sprake is van verschillende oxidatie niveaus van PTPs gedurende staartvinregeneratie in zebravissen. We onderzoeken ook de moleculaire werkingsmechanismen van Shp2a gedurende staartvinregeneratie in zebravis embyro's.

In **Hoofdstuk 1** bespreken we bondig de structuren van PTPs en hun functies in fosfo-tyrosine signaaltransductie, alsmede hoe PTP activiteit wordt gereguleerd. We introduceren het regeneratieproces, omschrijven de stappen die noodzakelijk zijn voor succesvolle staartvinregeneratie en zinspelen op de rol die PTPs zouden kunnen hebben in dit proces.

In **Hoofdstuk 2** behandelen we het zich opstapelende bewijs dat de onmisbare rol van PTP's in het handhaven van een gebalanceerde fosfo-tyrosine signaaltransductie gedurende embryonale ontwikkeling benadrukt. We zetten uiteen hoe de activiteit van PTP's bijdraagt aan stamcelhernieuwing en -differentiatie, gastrulatie en het vormen van de somieten, botvorming en bloedvatvorming. We geven ook voorbeelden van hoe PTP deregulatie in de vorm van verhoogde of verlaagde activiteit zeer schadelijke consequenties heeft voor bovengenoemde processen en daarmee voor de embryonale ontwikkeling in zijn geheel. Het belang van een gebalanceerde fosfo-tyrosine signaaltransductie is evolutionair geconserveerd, wat duidelijk wordt wanneer men het groot aantal verschillende diermodellen dat afhankelijk is van juiste PTP activiteit in ogenschouw neemt. We bespreken verder ook enige syndromen en ziektes welke bij mensen voorkomen en die veroorzaakt worden door afwijkende PTP activiteit.

In **Hoofdstuk 3** beschrijven we een aantal van de experimentele procedures die zijn gebruikt voor het bestuderen van de rol van PTP's in staartvinregeneratie in zebravissen.

In **Hoofdstuk 4** hebben we, om het belang van PTP's in staartvinregeneratie in zebravissen aan te tonen, zebravis embryo's gebruikt die geen werkend 'phosphatase and tensin homologue' (Pten) eiwit bezitten. Pten is een tumorsuppressor die werkt als een tegenhanger van fosfo-inositide 3-kinase (PI3K)/Akt signaaltransductie. We laten zien dat homozygote *ptena*$^{-/-}$*ptenb*$^{-/-}$ embryo's, die geen functioneel Pten eiwit hebben, na amputatie hun staartvin niet regenereren. We hebben twee essentiële en onmiskenbare stappen in het regeneratieproces geanalyseerd met behulp van *in situ* hybridisatie en immuunhistochemie: blastema formatie, ook wel kiemweefselvorming genoemd, en expansie (regeneratieve groei). Hoewel *ptena*$^{-/-}$*ptenb*$^{-/-}$ embryo's wel een normale blastema vormen, liet immuunhistochemie een blokkade in celdeling, een toename in celdood, en verhoogde Akt activiteit zien gedurende de expansiefase in vergelijking tot embryo's met functioneel Pten eiwit uit hetzelfde legsel. Het opnieuw tot expressie brengen van Pten evenals farmacologische inhibitie van PI3K redden het regeneratieproces, echter, expressie van de katalytische inactieve mutant Pten-C124S doet dit niet. Samengenomen suggereren onze bevindingen dat Pten een onmisbare rol heeft in het beperken van PI3K/Akt signaaltransductie gedurende de expansiefase van staartvinregeneratie in zebravis embryo's.

In **Hoofdstuk 5** hebben we ontdekt dat er sprake is van differentiële oxidatie van PTP's gedurende staartvinregeneratie in volwassen zebravissen. Als reactie op amputatie van de staartvin is er een snelle en voorbijgaande verhoging van het waterstofperoxide (H_2O_2) niveau bij de wondgrens waar te nemen, welke essentieel is voor regeneratie. We voerden, met een interval van 40 minuten, twee opeenvolgende vin clips uit, om precies dat deel van de vin te verzamelen dat is blootgesteld aan de verhoogde H_2O_2 niveaus. Door gebruik te maken van een antilichaam dat geoxideerde PTP's (ox-PTP) herkent en vloeistofchromatografie in combinatie met massaspectrometrie hebben we 33 PTP's uit vin clips van volwassen zebravissen geïsoleerd en geidentificeerd. Van deze 33 waren er 8 PTP's 40 minuten na amputatie significant meer geoxideerd. Shp2a was één van de PTPs die geoxideerd bleek te zijn. We leveren ook bewijs dat de geoxideerde PTP's belangrijk zijn voor regeneratie: embryo's die geen Shp2 hebben, homozygote *ptpn11a*$^{-/-}$*ptpn11b*$^{-/-}$ embryo's, regenereren hun staartvin niet, terwijl embryo's die geen Rptpα bezitten, homozygote *ptprα*$^{-/-}$ embryo's, welke niet was geoxideerd na staartvinamputatie in volwassen zebravissen, hun staartvin wel

regenereren. Onze resultaten laten zien dat PTP's in verschillende mate geoxideerd worden als reactie op staartvinamputatie en suggereren dat er verschillen zijn in de onmisbaarheid van verschillende PTP's voor regeneratie.

In **Hoofdstuk 6** hebben we zebravis embyo's zonder functioneel Shp2 eiwit gebruikt om de rol van Shp2a in de signaaltransductie in staartvinregeneratie op te helderen. Shp2 is een intermediair in 'mitogen activated protein kinase' (MAPK) signaaltransductie. Shp2a heeft meerdere eiwitdomeinen met diverse functies: een katalytisch fosfatase domein, en twee SH2 domeinen plus een C-terminaal domein voor het binden aan diverse factoren. We laten zien dat, wanneer de staartvin wordt geamputeerd, het opnieuw tot expressie brengen van Shp2a het regeneratieproces in homozygote *ptpn11a*$^{-/-}$*ptpn11b*$^{-/-}$ embryo's redt. De katalytisch inactieve mutant Shp2a-R466M en de Shp2a mutant die niet in staat is tot het binden van factoren met zijn SH2 domeinen kunnen het regeneratieproces in embryo's zonder functioneel Shp2 eiwit niet herstellen. We laten ook zien dat de capaciteit van Shp2a om factoren te binden via zijn C-terminale domein waarschijnlijk niet noodzakelijk is voor zijn functie tijdens staartvinregeneratie in zebravis embryo's. Door *in situ* hybridisatie en immuunhistochemie te gebruiken laten we zien dat *ptpn11a*$^{-/-}$*ptpn11b*$^{-/-}$ embryo's een normale blastema vormen, maar een blokkade in proliferatie en een verminderede activatie van MAPK vertonen gedurende de expansiefase. Farmacologische inhibitie van MEK, het eiwit dat MAPK activeert, belet regeneratie op vergelijkbare wijze en zorgt voor een stop in proliferatie gedurende de expansiefase. Onze resultaten duiden op een cruciale rol van Shp2a tijdens de expansiefase van staartvinregeneratie in zebravis embryo's, door middel van het bevorderen van MAPK signaaltransductie.

In **Hoofdstuk 7** hebben we belangrijke aminozuren in Shp2a gemuteerd om te onderzoeken welke mate van oxidatie en welk peil van katalytische activiteit van deze fosfatase vereist zijn voor zijn correcte functie tijdens staartvinregeneratie in zebravis embryo's. Shp2a is gevoelig voor omkeerbare inactivatie door oxidatie en er wordt gepostuleerd dat de twee "hulp" cysteïnes van Shp2a het eiwit beschermen tegen zogeheten onomkeerbare inactivatie door oxidatie. Shp2a werd geoxideerd na staartvinamputatie (**Chapter 5**), maar zijn activiteit was ook noodzakelijk voor embryonale staartvin regeneratie (**Chapter 6**). Door de hulp cysteïnes C334 en C368 van Shp2a te muteren, hebben we geheel nieuwe mutante eiwitten gegenereerd die een verminderde katalytische activiteit en een verhoogde gevoeligheid voor oxidatie door H_2O_2 bezitten. Desalniettemin herstelt het tot expressie brengen van de hulp cysteïne mutanten van Shp2a staartvin regeneratie in homozygote *ptpn11a*$^{-/-}$*ptpn11b*$^{-/-}$ em-

bryo's, wat suggereert dat de hulp cysteïne mutanten van Shp2a niet onomkeerbaar geoxideerd werden door de normale en natuurlijke hoeveelheid H_2O_2 die wordt geproduceerd na staartvinamputatie. Bovendien herstellen de hulp cysteine mutanten van Shp2a de staartvinregeneratie ondanks hun gereduceerde katalytische activiteit. Interessant is dat Shp2a eiwitten met mutaties in de aminozuren D61 en A462, welke resulteren in respectievelijk verhoogde en verlaagde katalytische activiteit, staartvinregeneratie in zebravis embryo's in gelijke mate herstellen. Gezamenlijk duiden onze resultaten erop dat Shp2a katalytische activiteit vereist is tijdens regeneratie, maar dat de mate van katalytische activiteit de functie van Shp2a in staartvinregeneratie in zebravis embryo's niet beïnvloedt.

Tenslotte biedt **Hoofdstuk 8** een samenvattende discussie van het werk dat gepresenteerd is in elk van de voorgaande experimentele hoofdstukken en beschrijft de implicaties van onze bevindingen voor toekomstig onderzoek.

LIST OF PUBLICATIONS

Hale, A. J., & den Hertog, J. (2016). Studying Protein-Tyrosine Phosphatases in Zebrafish. *Methods in Molecular Biology*, 1447, 351-72

Hale, A. J., ter Steege E., & den Hertog, J. (2017). Recent Advances in Understanding the Role of PTPs in Development and Disease. *Developmental Biology* (Accepted)

Wu W.*, Hale A. J.*, Lemeer S., & den Hertog J. (2017) Differential oxidation of protein-tyrosine phosphatases during zebrafish caudal fin regeneration. *Scientific Reports* (Accepted)

Hale A. J., Kiai A., Sikkens J., & den Hertog J. (2017) Impaired caudal fin-fold regeneration in zebrafish embryos deficient for the tumour suppressor Pten. (Under revision)

Hale A. J., & den Hertog J. (2017) An essential role for Shp2-MAPK signalling during zebrafish embryo caudal fin-fold regeneration. (Submitted)

*equal contribution

CURRICULUM VITAE

Alexander J. Hale was born on July 8th 1990 in the London borough of Hillingdon, United Kingdom. Soon after, he moved with his parents to the Netherlands, and attended primary school at the Delftsche Schoolvereeniging, in Delft, until 2000. Alex completed his secondary education, majoring in Mathematics, Chemistry, and Biology, at the British School in the Netherlands, in Voorschoten, in 2008. He moved to the United Kingdom to study Biomedical Sciences at the University of Manchester, where he graduated with an upper second (2.1) in 2011. During his research internship he investigated the role of Pim1 kinase in melanoma cell cycle progression and presented this work at the 2011 Young European Scientist Conference.

Alex moved to London, United Kingdom, for his Research Masters in Biomedical Research at Imperial College London. During this time, he researched paracrine Hedgehog signalling in pancreatic cancer cells, specifically focussing on the role of Sonic Hedgehog palmitoylation in this process, in the lab of Prof. A. Magee. Alex also researched the role of Prohibitin in prostate cancer metabolism in the labs of Prof. C. Bevan and Dr. H. Keun. Alex graduated from Imperial College London with a Distinction (1^{st}) and honours in 2012.

In November 2012 Alex moved to Utrecht and started his PhD thesis at Leiden University in the lab of Prof. J. den Hertog, working from the Hubrecht Institute. The focus of his PhD was to discover if protein-tyrosine phosphatases became oxidized following zebrafish caudal fin amputation, and to study the role of protein-tyrosine phosphatases during zebrafish caudal fin regeneration. The results of these studies are presented in this thesis.